

Analyse mathématique et contrôle optimal de lois de conservation multi-échelles : application à des populations cellulaires structurées

Peipei Shang

▶ **To cite this version:**

Peipei Shang. Analyse mathématique et contrôle optimal de lois de conservation multi-échelles : application à des populations cellulaires structurées. Equations aux dérivées partielles [math.AP]. Université Pierre et Marie Curie - Paris VI, 2012. Français. NNT : . tel-00847756

HAL Id: tel-00847756

https://theses.hal.science/tel-00847756

Submitted on 24 Jul 2013

HAL is a multi-disciplinary open access archive for the deposit and dissemination of scientific research documents, whether they are published or not. The documents may come from teaching and research institutions in France or abroad, or from public or private research centers.

L'archive ouverte pluridisciplinaire **HAL**, est destinée au dépôt et à la diffusion de documents scientifiques de niveau recherche, publiés ou non, émanant des établissements d'enseignement et de recherche français ou étrangers, des laboratoires publics ou privés.

Université Pierre et Marie Curie

U.F.R. de Mathématiques

Analyse mathématique et contrôle optimal de lois de conservation multi-échelles : application à des populations cellulaires structurées

THÈSE

présentée et soutenue publiquement le 05 Juillet 2012

pour l'obtention du diplôme de

Doctorat de l'université Pierre et Marie Curie

(spécialité mathématiques)

par

Peipei SHANG

sous la direction de Frédérique Clément et Jean-Michel Coron

devant le jury composé de

Fatiha ALABAU-BOUSSOUIRA	Examinateur
Yacine CHITOUR	Examinateur
Frédérique CLÉMENT	Directrice de thèse
Jean-Michel CORON	Directeur de thèse
Marie DOUMIC	Examinateur
Jean-Pierre PUEL	Rapporteur
Jean-Pierre RAYMOND	Examinateur
Emmanuel TRÉLAT	Examinateur

INRIA Paris-Rocquencourt **Laboratoire Jacques-Louis Lions**

Mis en page avec la classe thloria.

Remerciements

Je tiens tout d'abord à remercier mes directeurs de thèse Frédérique Clément et Jean-Michel Coron, de m'avoir proposé un sujet d'étude passionnant et de m'avoir encadrée durant ces trois années. Ils ont su me communiquer leur goût pour les mathématiques appliquées à la biologie en me faisant profiter de leur expérience et de leurs contacts, aussi bien mathématiciens que biologistes. J'ai beaucoup apprécié la liberté qu'ils m'ont laissée dans le choix des sujets à aborder, tout en étant toujours disponibles pour répondre à mes questions et m'apporter leurs aide précieuse. Je remercie le projet de grande envergure initiative Regate qui me donne financière afin que je puisse venir en France pour faire ma thèse. Je remercie Jean-Michel Coron pour me soutenir à voyager pour participer à diverses conférences.

J'adresse mes sincères remerciements à Tatsien Li de m'avoir introduit dans le domaine du contrôle et m'ont recommandé de venir en France pour ma thèse. Je remercie mon collègue Zhiqiang Wang pour son aide sur la vie et à l'étude lors de ma première venue en France.

Je remercie Fabio Ancona et Jean-Pierre Puel ont gracieusement accepté de rapporter ma thèse et je les remercie pour le temps qu'ils y ont consacré et pour les remarques bienveillantes dont ils m'ont gratifié. Je suis enfin très heureux que Fatiha Alabau-Boussouira, Yacine Chitour, Marie Doumic, Jean-Pierre Raymond et Emmanuel Trélat m'aient fait l'honneur de participer à mon jury.

J'ai eu la chance de bénéficier durant ces années de thèse de la très bonne ambiance du INRIA Paris-Rocquencourt, et je tiens à remercier mes collegues à l'INRIA : Michel, François, Patrick, Alexandre, Arnaud, Leila, Mohamed, Wen, Julien. Et plus particulierèment, je tiens a remercier mes collegues Benjamin Aymard et Pierre Gabriel qui m'ont aidée à corriger le français de ma thèse. J'ai eu la chance de bénéficier durant ces années de thèse de la très bonne ambiance du Laboratoire Jacques-Louis Lions, et je tiens à remercier mes amis et mes collegues Jixun, Malik, Jean-Philippe, Pierre, Mamadou, Mathieu, Vincent, Camille, Morgan, Marianne... avec lesquels je passe tres bons moments.

Je souhaite également remercier Martine Verneuille, Martine Girardot à l'INRIA, Florence Saidani, Salima Lounici, Mme Danielle Boulic et Mme Liliane Ruprecht à LJLL dont l'efficacité m'a permis de ne consacrer que le strict minimum de mon temps et de mes efforts à des tâches administratives.

Je ne peux bien évidemment pas manquer de saluer les membres de la communauté du contrôle avec lesquels j'ai le plaisir d'échanger lors des nombreux séminaires colloques, écoles d'été et autres trimestres IHP, ainsi et en vrac je citerais : Olivier, Sergio, Karine, Sylvain, Axel, Eduardo, Julien, Thuy, Ivonne, Khai. Je me souviendrai tous les bons moments passés à Paris, à Marseille, à Italie, à Bilbao, à Benasque...

Pour finir, je souhaite exprimer toute ma gratitude à ma famille pour m'avoir constamment soutenu pendant toutes ces années d'études.

Ce que j'aime dans les mathématiques appliquées, c'est qu'elles ont pour ambition de donner du monde des systèmes une représentation qui permette de comprendre et d'agir. Et, de toutes les représentations, la représentation mathématique, lorsqu'elle est possible, est celle qui est la plus souple et la meilleure.

Jacques-Louis Lions

Table des matières

Introduction générale **1**

1 Un modèle de système de fabrication hautement ré-entrant 1

2 Un modèle biologique de l'ovulation folliculaire 3

2.1 Présentation du modèle biologique 3

2.2 Caractère bien posé du problème 8

2.3 Problèmes de contrôle associés au modèle 8

2.4 Expériences numériques 14

3 Un modèle d'un protocole d'amplification pour les protéines mal repliées . . . 15

4 Perspectives 18

General introduction **21**

5 A model of highly re-entrant manufacturing system 21

6 A biological model of follicular ovulation 23

6.1 Presentation of the biological model 23

6.2 Well-posedness 28

6.3 Related control problems 29

6.4 Numerical observations 34

7 A model of an amplification protocol for misfolded proteins 35

8 Perspectives 38

Chapter 1
Analysis and control of a scalar conservation law

1.1 Introduction and main results 41

1.2 Preliminaries 44

1.3 Well-posedness of Cauchy problem with L^∞ data 44

1.4 Stability with respect to the initial and boundary data 49

1.5 L^p-optimal control for demand tracking problem 54

1.6 Appendix 59

1.6.1 Basic lemmas 59

1.6.2 Proof of the regularity of the weak solution 60

1.6.3 Proof of the uniqueness of the weak solution 65

Chapter 2
Cauchy problem for multiscale conservation laws

2.1 Introduction 71
2.2 Main results 74
2.3 Fixed point argument and construction of a local solution to Cauchy problem 75
2.3.1 Fixed point argument 76
2.3.2 Construction of a local solution to Cauchy problem 79
2.4 Uniqueness of the solution 90
2.5 Proof of the existence of a global solution to Cauchy problem 94
2.6 Appendix 96
2.6.1 Introduction of the model 96
2.6.2 Mathematical reformulation 98
2.6.3 Basic lemmas 100

Chapter 3
Optimal control of cell mass and maturity in a model of follicular ovulation

3.1 Introduction 103
3.2 Problem statement and introductory results 106
3.2.1 Optimal control problem 106
3.2.2 Simplifications with respect to the original model 108
3.2.3 Solution to Cauchy problem 109
3.2.4 Minimal time versus maximal maturity 110
3.3 Optimal results for finite Dirac masses 111
3.3.1 Proof of the existence of the optimal control 113
3.3.2 Pontryagin Maximum Principle 115
3.3.3 Proof of the bang-bang property of the optimal control 124
3.4 Optimal control in the PDE case 129

Chapter 4
Some numerical results

4.1 Notations and some assumptions 133
4.2 Constant control 136
4.2.1 Computation of the zero-order moment 136
4.2.2 Computation of the asymptotic maximal maturity 139
4.2.3 The behaviour of the maturity $M(t)$ when the control $u = 0$ 143
4.2.4 Results on optimal constant control 144
4.3 Bang-bang control 147

4.3.1 Some notations and possible control strategies 147
4.3.2 Optimal switching direction for bang-bang control 147
4.3.3 Optimal control 151

Chapter 5
Optimization of an Amplification Protocol for Misfolded Proteins

5.1 Introduction 157
5.2 The Eigenvalue Problem 160
5.3 Pontryagin Maximum Principle 161
5.3.1 Modified cost function 162
5.3.2 Original cost function 164

Bibliography **171**

Introduction générale

Dans cette thèse, j'ai surtout étudié le caractère bien posé pour des équations aux dérivées partielles et des problèmes de contrôle optimal. J'ai étudié les problèmes de Cauchy associés à des lois de conservation hyperboliques avec des vitesses non-locales, pour un modèle 1D (système de fabrication industrielle), puis 2D (processus de sélection folliculaire). J'ai étudié par la suite des problèmes de contrôle optimal, d'abord sur le modèle 2D, puis sur un modèle basé sur des équations differentielles ordinaires (amplification de protéines mal repliées). Dans ce qui suit, je présenterai les résultats obtenus dans l'ordre de ces trois modèles.

1 Un modèle de système de fabrication hautement ré-entrant

Une usine (ou ligne de fabrication) ré-entrante est un système de production où les produits intermédiaires repassent un grand nombre de fois sur plusieurs machines. C'est par exemple le cas dans les usines de fabrication de semi-conducteurs. Armbruster et al. ont introduit dans [5] une modélisation par des lois de conservation scalaires non linéaires avec une vitesse de propagation non-locale. Une telle description est très utile car elle donne des solutions analytiques explicites et permet aussi d'utiliser des méthodes numériques classiques et assez simples rendant bien compte de l'évolution de la fabrication dans l'usine. Dans ce modèle, la variable solution de l'équation hyperbolique est la densité $\rho(t,x)$ de produits intermédiaires à l'instant t et à l'étape $x \in [0,1]$ de la production, le cas $x = 0$ représentant le début de la ligne de production, $x = 1$ la fin et $x \in (0,1)$ les étapes intermédiaires. L'équation de conservation prend la forme

$$\rho_t(t,x) + (\rho(t,x)\lambda(x,W(t)))_x = 0, \quad t \geqslant 0, 0 \leqslant x \leqslant 1, \tag{1}$$

où

$$W(t) = \int_0^1 \rho(t,x)dx$$

est la quantité totale de produits intermédiaires dans l'usine.

Dans le chapitre 1, nous étudions ces lois de conservation scalaire. Nous supposons que la fonction de vitesse $\lambda > 0$ est continûment différentiable, i.e. $\lambda \in C^1([0,1] \times [0,\infty))$. Par

exemple, le cas particulier où

$$\lambda(x, W) = \frac{1}{1+W}$$

est introduit dans [5, 62].

Pour (1), les données supplémentaires sont

1. La donnée initiale

$$\rho(0, x) = \rho_0(x), \quad 0 \leqslant x \leqslant 1, \tag{2}$$

2. Le flux d'entrée des produits dans l'usine, ce qui suggère la condition au bord

$$\rho(t, 0)\lambda(0, W(t)) = u(t), \quad t \geqslant 0. \tag{3}$$

Motivé par des applications, un problème de contrôle naturel est le *Demand Tracking Problem (DTP)*. L'objectif du *DTP* est de minimiser la différence entre le flux réel sortant (de l'usine) $y(t) = \rho(t, 1)\lambda(1, W(t))$ et une demande donnée $y_d(t)$ sur une période de temps fixe. Un problème de contrôle alternatif est le *Backlog Problem (BP)*. L'objectif du *BP* est de minimiser la différence entre la quantité de produits qui ont quitté l'usine et la demande totale de produits sur une période de temps fixe.

Le carnet de commandes d'un système de production à un moment donné t est défini comme

$$\beta(t) = \int_0^t \rho(s, 1)\lambda(1, W(s))ds - \int_0^t y_d(s)ds.$$

Le carnet de commandes $\beta(t)$ peut être négatif ou positif, un carnet de commandes positif correspondant à une surproduction et un carnet de commandes négatif correspondant à une pénurie.

Dans le cas où λ ne dépend pas de la variable d'espace x, les auteurs de [62] ont étudié deux problèmes de contrôle précédent (*DTP* et *BP*). Ces études reposent sur des calculs d'adjoints, incorporant la loi de conservation scalaire comme une contrainte d'un problème d'optimisation non linéaire. Ils ont obtenu des résultats numériques sur ces deux problèmes fondamentaux. Cela leur a aussi permis de bien quantifier l'influence de la non-linéarité du temps de cycle sur les limites de la réactivité du système de production.

Dans [35], les auteurs ont prouvé l'existence et l'unicité de solutions au problème de Cauchy pour des données L^1 au bord et ont étudié la régularité de ces solutions. Ils ont également prouvé l'existence de contrôles optimaux qui minimise la norme L^2 de la différence entre le flux de sortie et le flux désiré. Dans [35] la vitesse non-locale λ ne dépend pas de la variable spatiale x, ce qui n'est pas réaliste pour de nombreuses situations. Dans le chapitre 1 nous généralisons les résultats de [35] au cas où λ dépend de x.

La principale difficulté de ce chapitre vient du caractère non-local de la vitesse et de sa dépendance en x . Dans [27], qui est aussi motivé en partie par [5, 62], il est aussi montré que le problème de Cauchy est bien posé pour les systèmes de loi de conservation hyperboliques avec une vitesse non-locale dans $\mathbb{R}^n$. Toutefois les méthodes utilisées dans cet article ne permettent

pas de traiter le cas où $\mathbb{R}^n$ est remplacé par $[0,1]$. Nous prouvons l'existence, l'unicité et la régularité de la solution faible au problème de Cauchy (1), (2) et (3) avec les données initiales et les conditions aux limites dans L^∞. Les démonstrations reposent sur la méthode des caractéristiques. Nous rappelons ici que dans le précédent document [35], les auteurs ont obtenu le caractère bien posé pour une donnée dans L^p $(1 \leqslant p \leqslant \infty)$. L'hypothèse L^∞ dans ce chapitre est nécessaire, avec nos méthodes, quand la fonction de vitesse λ dépend de la variable d'espace x. En utilisant l'expression implicite de la solution en terme de caractéristiques, nous avons également démontré la stabilité (la dépendance continue) à la fois de la solution et du flux sortant par rapport aux données initiales et au bord $x = 0$.

Le problème de contrôle optimal que nous étudions dans le chapitre 1 est lié au problème du *DTP*. L'objectif est de minimiser la norme L^p avec $1 \leqslant p \leqslant \infty$ de la différence entre le flux réel de sortie $y(t) = \rho(t,1)\lambda(1, W(t))$ et une demande désirée $y_d(t)$ sur une période de temps fixe. Avec l'aide de l'expression implicite de la solution faible et par des arguments de compacité, nous prouvons, toujours dans ce chapitre, l'existence de solutions à ce problème de contrôle optimal.

2 Un modèle biologique de l'ovulation folliculaire

Comme une généralisation de ce type de loi de conservation avec une vitesse non-locale, dans le cas 2D, nous nous sommes intéressés à un sujet particulier, le modèle de développement des follicules ovariens, qui traite des stratégies de reproduction. Ce modèle a été développé dans le cadre d'un projet interdisciplinaire, l'action d'envergure REGATE (REgulation of the GonAdoTropE axis : https ://www.rocq.inria.fr/sisyphe/reglo/regate.html) de l'INRIA.

2.1 Présentation du modèle biologique

Chez les femelles au mammifères, la réserve d'ovocytes disponibles au cours de la vie reproductive est constitué très tôt dans la vie. Chaque ovocyte de cette réserve est entourée d'une seule couche de cellules somatiques, le tout constituent un follicule primordial. Les follicules quittent en permanence le réserve de follicules primordiaux pour entrer dans un processus de croissance et de maturation. Les follicules ovariens sont des structures tissulaires sphéraidales abritant l'ovocyte en cours de maturation. Le processus de l'ovulation est l'aboutissement du développement folliculaire, à partir du moment où ils quittent la réserve de follicules primordiaux jusqu'au ce stade ovulatoire.

Le développement des follicules ovariens est un processus crucial pour la reproduction chez les mammifères, car sa fonction biologique est de libérer au moment de l'ovulation un (chez les espèces mono-ovulantes) ou plusieurs (chez les espèces poly-ovulantes) ovocyte(s) fécondable(s) et aptes au développement. Au cours de chaque cycle ovarien, de nombreux follicules sont en concurrence pour leur survie. Peu de follicules atteignent une taille ovulatoire,

puisque la plupart d'entre eux subissent un processus de dégénérescence, connu sous le nom d'atrésie (voir par exemple [73]). Le sort d'un follicule est déterminé par les changements se produisant dans sa population cellulaire en réponse à un contrôle hormonal provenant de l'hypophyse (voir figure 1).

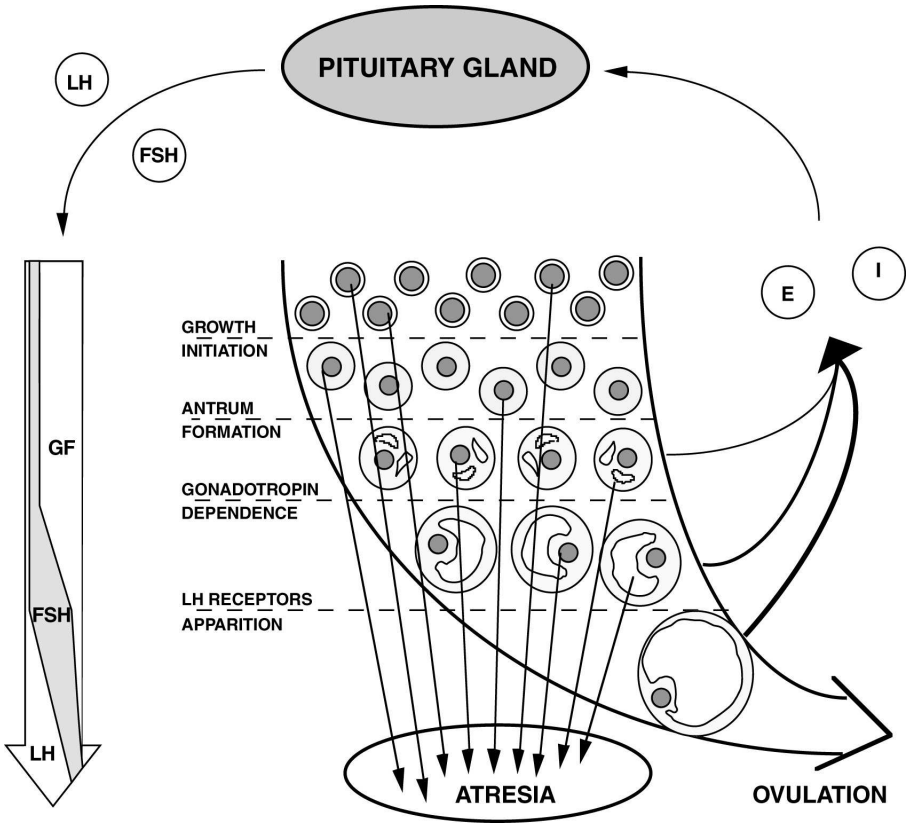


FIG. 1. Développement folliculaire terminal (Schéma repris de [20]).

La population des cellules folliculaires est composée de cellules proliférantes, de cellules différenciées et de cellules apoptotiques. Les cellules sont caractérisées par leur position au sein ou en dehors du cycle cellulaire et par leur sensibilité à l'hormone folliculo-stimulante (FSH). Cela nous amène à distinguer 3 phases cellulaires (voir figure 2). La phase 1 ($G1$) et la phase 2 (SM) correspondent à des phases de prolifération et la phase 3 (D) correspond à la phase de différenciation, qui concerne cellules ayant quitté le cycle cellulaire. En phases 1 et 3, les cellules sont sensibles à la FSH, alors qu'en phase 2 elle sont insensibles à la FSH. L'entrée de cellules en apoptose peut survenir dans les phases 1 et 3 (voir figure 2).

Un modèle mathématique, utilisant à la fois un formalisme multi-échelles et les concepts de la théorie du contrôle, a été conçu dans [45] pour décrire le processus de sélection des follicules ovariens sur une base cellulaire. Pour chaque follicule, la dynamique des populations de cellules est gouvernée par une loi de conservation, qui décrit les changements dans la distribution de l'âge des cellules et de leur maturité. Ces dynamiques sont interdépendentes et sont décrites

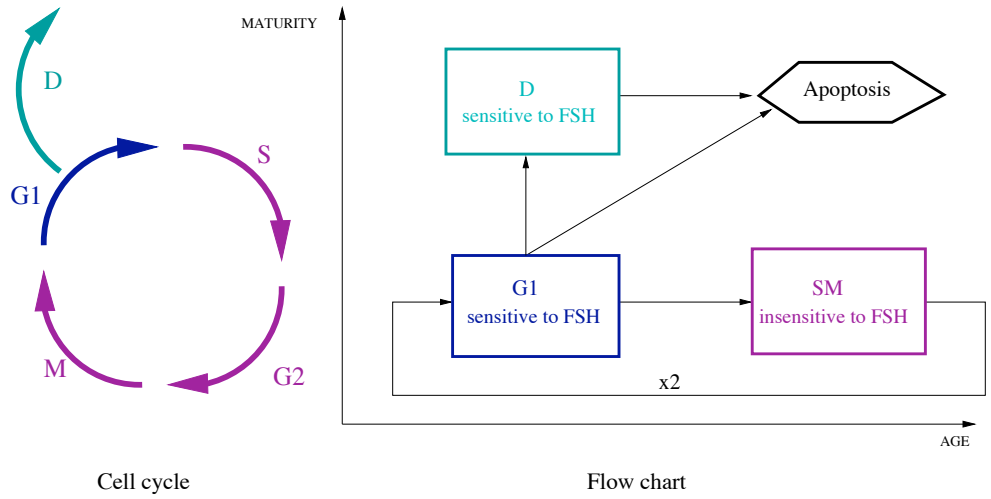


FIG. 2. Diagramme des flux cellulaires. Le cycle cellulaire correspond au parcours cyclique des phases $G1$ et SM. Quand une cellule-mère entre dans la phase $G1$ à partir de la phase SM, elle donne naissance à deux cellules-filles. La différenciation des cellules correspond à la sortie de $G1$ pour entrer en D. L'entrée de cellules en apoptose peut survenir dans les phases $G1$ et D (Schéma repris de [22]).

par un système hyperbolique couplé entre les follicules et les différentes phases cellulaires, ce qui entraîne une loi de conservation vectorielle et le couplage entre les conditions aux limites. Les fonctions de vitesse et de maturité possèdent un caractère à la fois local et non-local.

Dans ce modèle, la position d'une cellule à l'instant $t \in [0, T]$ $(T > 0)$ est définie par son âge a et sa maturité γ. L'âge des cellules a est un marqueur de la progression dans le cycle cellulaire (en phase 1 et en phase 2) ou du temps écoulé depuis la sortie du cycle cellulaire (en phase 3). La durée de la phase 1 est $a_1 > 0$ et la durée totale du cycle est a_2 (voir figure 3). La maturité γ est utilisée pour discriminer entre les cellules en cycle et les autres, par comparaison à un seuil γ_s, et pour caractériser la vulnérabilité des cellules à l'apoptose. Les phases 1, 2 et 3 correspondent aux plages de suivantes du plan âge-maturité (voir figure 3).

$$\Omega_{1,k} := [(k-1)a_2, (k-1)a_2 + a_1] \times [0, \gamma_s], \quad \Omega_{2,k} := [(k-1)a_2 + a_1, ka_2] \times [0, \gamma_s],$$
$$\Omega_{3,k} := [(k-1)a_2, ka_2] \times [\gamma_s, \gamma_m],$$

où γ_m est la valeur asymptotique maximale de la maturité qui est telle que $\gamma_m > \gamma_s$ (voir figure 3).

La population de cellules dans un follicule f est représentée par des fonctions de densité de cellules $\phi^f_{j,k}(t, a, \gamma)$ définies sur chaque phase cellulaire $Q^f_{j,k}$, qui satisfont les lois de conservation suivantes

$$\frac{\partial \phi^f_{j,k}}{\partial t} + \frac{\partial (g_f(u_f)\phi^f_{j,k})}{\partial a} + \frac{\partial (h_f(\gamma, u_f)\phi^f_{j,k})}{\partial \gamma} = -\lambda(\gamma, U)\phi^f_{j,k} \quad \text{in } Q^f_{j,k}, \tag{4}$$

avec

$$Q^f_{j,k} := \Omega_{j,k} \times [0,T], \quad f = 1, \cdots, n,$$

où $j = 1, 2, 3$ représente la phase 1, la phase 2 et la phase 3, $k = 1, \cdots, n$ et N est le nombre de cycles cellulaires consécutifs (voir figure 3).

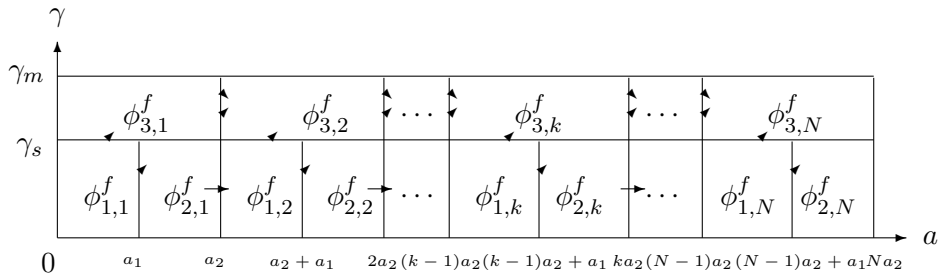


FIG. 3. Domaine de la solution dans le modèle original. Pour chaque follicule f, le domaine consiste en la suite de cycles cellulaires N. a représente l'âge de la cellule et γ désigne sa maturité. La partie supérieure du domaine correspond à la phase de différenciation et la partie inférieure à la phase de prolifération.

Définissons l'opérateur de maturité M

$$M(\varphi)(t) := \int_0^{\gamma_m} \int_0^{a_m} \gamma\varphi(t,a,\gamma)\, da d\gamma. \tag{5}$$

Alors

$$M_f(t) := \sum_{j=1}^{3}\sum_{k=1}^{N} M(\phi^f_{j,k})(t) = \sum_{j=1}^{3}\sum_{k=1}^{N} \int_0^{\gamma_m} \int_0^{a_m} \gamma\phi^f_{j,k}(t,a,\gamma)\, da d\gamma \tag{6}$$

est la maturité folliculaire globale à l'échelle folliculaire, tandis que

$$M(t) := \sum_{f=1}^{n} M_f(t) = \sum_{f=1}^{n}\sum_{j=1}^{3}\sum_{k=1}^{N} \int_0^{\gamma_m} \int_0^{a_m} \gamma\phi^f_{j,k}(t,a,\gamma)\, da d\gamma \tag{7}$$

est la maturité globale à l'échelle de l'ovaire.

De (5) à (7), a_m et γ_m sont les valeurs maximales de l'âge et de la maturité. La vitesse et le terme source sont des fonctions régulières de u_f et de U, où $U(M)$ est le contrôle global, qui peut être interprété comme le niveau de FSH plasmatique, et les $u_f(M_f, M)$ sont les contrôles locaux qui représentent les niveaux de FSH biodisponibles pour chaque follicule. Plus précisément, le contrôle global U résulte du rétro-contrôle exercé par l'ovaire sur l'hypophyse, qui module le taux de sécrétion de FSH. Ce rétro-contrôle est responsable de la réduction des niveaux de FSH, conduisant à la dégénérescence de tous les follicules, sauf de ceux qui sont sélectionnés pour l'ovulation. Le contrôle local u_f, spécifique à chaque follicule, modélise la biodisponibilité de FSH en lien avec la vascularisation folliculaire. Il est donné comme une proportion de U (voir [45]).

Dans la phase 1 et dans la phase 3, à la fois le contrôle global U et un contrôle local u_f agissent sur les vitesses de vieillissement (fonction g_f, contrôlée localement dans la phase 1), et la maturation (fonction h_f, contrôlée localement dans la phase 1 et la phase 3) ainsi que sur le terme de perte (λ taux d'apoptose, globalement contrôlé dans la phase 1 et la phase 3).

La phase 2 n'est pas contrôlée et se finit par la mitose après un délai correspondent à la durée de cette phase $a_2 - a_1$ (aucune cellule ne quitte le cycle pendant cette phase). L'augmentation de la masse cellulaire se fait par la mitose. Au moment de la mitose, une cellule mère donne naissance à deux cellules filles, ce qui se traduit par un doublement local du flux. Pour plus de détails sur le formulation des vitesses et des termes sources, on peut se référer à [22] et [43]. Les conditions initiales sont

$$\phi^f_{j,k}(0,a,\gamma) = \phi^f_{k0}(a,\gamma)|_{\Omega_{j,k}}, \qquad j = 1,2,3, \quad k = 1,\cdots,N. \tag{8}$$

Le flux sur chaque bord des domaines $\Omega_{j,k}$ est soit entrant soit sortant, ce qui correspond les conditions aux limites suivantes (voir figure 3).

Il n'y a pas de flux entrant pour la phase 1 ni pour le phase 3 dans le premier cycle cellulaire (voir figure 3), par conséquent

$$\phi^f_{1,1}(t,0,\gamma) = \phi^f_{3,1}(t,0,\gamma) = 0, \quad (t,\gamma) \in [0,T] \times [0,\gamma_s]. \tag{9}$$

La mitose se produit lorsque la cellule quitte le cycle précédent et entre dans le cycle suivant (voir figure 3), donc pour $k = 2,\cdots,N$

$$g_f(u_f)\phi^f_{1,k}(t,(k-1)a_2,\gamma) = 2\tau_{gf}\phi^f_{2,k-1}(t,(k-1)a_2,\gamma), \quad (t,\gamma) \in [0,T] \times [0,\gamma_s]. \tag{10}$$

Il n'y a pas de mitose en phase 3, d'où

$$\phi^f_{3,k}(t,(k-1)a_2,\gamma) = \phi^f_{3,k-1}(t,(k-1)a_2,\gamma), \quad (t,\gamma) \in [0,T] \times [0,\gamma_s]. \tag{11}$$

Dans le même cycle k, $k = 1,\cdots,N$, la dynamique revient à une dynamique de transport entre la phase 1 et la phase 2 (voir figure 3), donc

$$\tau_{gf}\phi^f_{2,k}(t,(k-1)a_2+a_1,\gamma) = g_f(u_f)\phi^f_{1,k}(t,(k-1)a_2+a_1,\gamma), \quad (t,\gamma) \in [0,T] \times [0,\gamma_s]. \tag{12}$$

Il n'y a pas de flux à partir du bas du domaine $\gamma = 0$ (voir figure 3), donc pour $k = 1,\cdots,N$

$$\phi^f_{1,k}(t,a,0) = 0, \quad (t,a) \in [0,T] \times [(k-1)a_2,(k-1)a_2+a_1], \tag{13}$$

$$\phi^f_{2,k}(t,a,0) = 0, \quad (t,a) \in [0,T] \times [(k-1)a_2+a_1,ka_2]. \tag{14}$$

Le seul flux entrant est celui de la phase 1 vers la phase 3, il n'y a pas de flux entrant de la phase 2 vers la phase 3, donc pour $k = 1,\cdots,N$

$$\phi^f_{3,k}(t,a,\gamma_s) = \begin{cases} \phi^f_{1,k}(t,a,\gamma_s), & (t,a) \in [0,T] \times [(k-1)a_2,(k-1)a_2+a_1], \\ 0, & (t,a) \in [0,T] \times [(k-1)a_2+a_1,ka_2]. \end{cases} \tag{15}$$

Il n'y a pas de flux entrant à partir du bord $\gamma = \gamma_m$ (voir figure 3), donc pour $k = 1,\cdots,N$

$$\phi^f_{3,k}(t,a,\gamma_m) = 0, \quad (t,a) \in [0,T] \times [(k-1)a_2,ka_2]. \tag{16}$$

2.2 Caractère bien posé du problème

Pour le problème du caractère bien posé de ce modèle biologique, les auteurs ont considéré dans [44] le cas où les valeurs de contrôle, u_f et U sont des fonctions données du temps. Les vitesses et le terme de perte sont alors $g_f(t)$, $h_f(\gamma, t)$ et $\lambda(\gamma, t)$. Ils ont traité le problème séquentiellement en utilisant les traces des solutions, qui sont bien définies pour chaque phase sur leurs frontières extérieures. A l'intérieur de chaque phase, ils ont appliqué une extension du théorème de Kruzkov [61] sur un problème avec données initiales et conditions aux bords dans L^∞ ou L^1 (voir, par exemple, [12, 80], où des solutions entropiques renormalisées sont définies pour ce type de problème). Toutefois, pour ces problèmes consécutifs, les auteurs n'ont pas pu définir la trace de la solution sur la frontière extérieur, ce qui pose un problème important pour l'étude de la phase suivante.

Par ailleurs, nous considérons ici à la fois les problèmes en boucle ouverte et en boucle fermée, c'est à dire que u_f et U sont des fonctions de M_f, M et t. Les principales difficultés pour étudier le modèle biologique proviennent du caractère non-locale de la vitesse, du couplage entre les conditions aux limites et du couplage entre les différents follicules dans le modèle. En outre, nous avons à traiter des termes source, et le problème est en 2D.

Dans le chapitre 1, le modèle de fabrication très ré-entrante n'est que 1D, n'a pas de terme source, et les vitesses sont toujours positives, tandis que dans le modèle 2D de l'ovulation folliculaire, les vitesses de maturation h_f $(f = 1, \cdots, n)$ dépendent de la valeur courante du contrôle local u_f et peut changer de signe dans la phase 3.

Dans [92], l'auteur a abordé la question du caractère bien posé pour les systèmes de loi de conservation hyperboliques avec une vitesse non-locale. Toutefois, notre méthode de preuve et même notre définition de solutions différent de celles indiquées dans [92]. Dans [92], l'auteur a utilisé le théorème de point fixe de Schauder pour prouver l'existence de la solution, tandis que notre démonstration utilise le théorème du point fixe de Banach, qui est plus utile en pratique pour calculer la solution numériquement. En outre, l'auteur a prouvé l'unicité sous des hypothèses fortes, de données initiales continûment différentiables, tandis que nous obtenons l'unicité lorsque les données initiales ne sont que dans L^∞. En utilisant le théorème du point fixe de Banach, nous avons d'abord prouvé que la maturité $\vec{M} := (M_1, \cdots, M_n)$ existe comme un point fixe d'une application à partir d'un espace de fonctions continues. On peut alors construire une solution locale au problème de Cauchy par la méthode des caractéristiques. En utilisant une estimation a priori et en progressant étape par étape, nous obtenons une solution globale. Nous prouvons également l'unicité de cette solution faible (voir le chapitre 2).

2.3 Problèmes de contrôle associés au modèle

La vitesse de vieillissement g_f commande la durée du cycle de division cellulaire. Une fois que l'âge des cellules a atteint un âge critique, l'événement de la mitose est déclenché, et

une cellule mère donne naissance à deux cellules filles, qui à leur tour entrent dans un cycle cellulaire. La vitesse de maturation contrôle le temps nécessaire pour atteindre un seuil de maturité γ_s, lorsque la cellule quitte définitivement le cycle cellulaire. Par conséquent, il y a des singularités locales dans la sous-partie du domaine où $\gamma \leqslant \gamma_s$, qui correspondent au doublement de flux en raison des événements successifs de mitose. Une fois sortée du cycle, la cellule n'est pas plus capable de contribuer à l'augmentation de la masse cellulaire folliculaire.

Le controle hormonal exercé par FSH agit directement sur les cellules folliculaires pour contrôler leur engagement vers prolifération ou la différenciation. A son tour, le rétro-contrôle hormonal exercé par l'ovaire sur l'axe hypothalamo-hypophysaire découle de la contribution pondérée de toutes les cellules réparties entre tous les follicules. Par conséquent, un processus de compétition contrôlé par FSH, se déroulant au sein de la population de follicules, est intimement lié au dynamiques cellulaires prenant place au sein d'un follicule donné.

L'ovulation est déclenchée lorsque les niveaux d'estradiol atteignent une valeur seuil M_s. Comme la sécrétion d'estradiol est liée à la maturité (voir [45]), l'instant T_s de déclenchement de l'ovulation est défini à partir de la maturité ovarienne globale

$$T_s = \min\{T | M(T) = M_s\}. \tag{17}$$

Les follicules sont alors triés en fonction de leur maturité individuelle. Les follicules ovulatoires sont ceux dont la maturité au moment T a dépassé un seuil M_{s1} tel que $M_{s1} \leqslant M_s$. Le taux d'ovulation est calculé comme

$$N_{s,s1} = \text{Card}\,\{f | M_f(T_s) \geqslant M_{s1}\}.$$

Le sort d'un follicule est déterminé par les changements qui se produisent dans sa population de cellules en réponse à un contrôle hormonal provenant de la glande hypophysaire. Seuls les follicules les plus robustes peuvent survivre dans un environnement pauvre en FSH.

Dans son ensemble, le système (4), (8) à (16) complété par le temps d'arrêt (17) définit un problème d'atteignabilité multi-échelles.

En ce qui concerne les problèmes de contrôle associés au modèle, la question est de proposer des problèmes de contrôle raisonnables du point de vue biologique et abordables du point de vue mathématique.

Un concept central à la compréhension de ces processus intriqués est celle de la gestion des ressources cellulaires des follicules, à la fois à l'échelle folliculaire (intensité de la sélection) et à l'échelle de l'ovaire (déclenchement et chronologie de l'ovulation). Il existe en effet un équilibre finement réglé entre la production de nouvelles cellules par la prolifération, qui augmente la masse totale de cellules, et la maturation des cellules, qui augmente leur contribution à la sécrétion d'estradiol.

Ce concept a déjà été étudié sur un terrain mathématique. Dans [21], l'auteur a étudié le problème du contrôle optimal des ressources des cellules folliculaires, mais pour un système à compartiments modèlerés par un EDO. La variable de contrôle principale était le taux de

sortie du cycle cellulaire, le taux instantané de transfert du compartiment de prolifération (correspondant ici à la partie inférieure du domaine où $\gamma \leqslant \gamma_s$), où les cellules se divisent à un taux constant déterminé par la durée du cycle cellulaire, vers le compartiment de différenciation, où les cellules peuvent seulement mûrir. Sous certaines hypothèses concernant le nombre initial de cellules folliculaires, en utilisant le principe de maximum de Pontryagin (PMP), l'auteur a prouvé que la stratégie optimale pour le taux de sortie du cycle cellulaire était un contrôle de type bang-bang qui consistait à commuter une seule fois entre la valeur minimale et la valeur maximale de l'intervalle de valeurs admissibles pour le contrôle. Dans le cadre plus simple des EDO, l'auteur a également examiné la mort cellulaire et le transfert possible à un compartiment d'apoptose. Comme on s'y attendait intuitivement, la stratégie optimale consiste à appliquer un taux d'apoptose minimal, ce qui justifie notre hypothèse d'une absence de perte de cellules. Puisque le taux de sortie de la cellule dans le cadre EDO est étroitement liée à la vitesse de maturation dans notre modèle EDP, ce résultat nous a encouragés à chercher des contrôles optimaux de type bang-bang.

Un autre problème de contrôle associé à la loi de conservation EDP a été étudié dans [44]. Là, les auteurs se sont concentrés sur la maturité folliculaire au moment final, dans le sens où ils ont cherché l'ensemble des conditions initiales compatibles avec l'atteinte d'une maturité seuil à un temps final fixé. Ils ont décrit les ensembles de conditions initiales microscopiques compatibles avec l'ovulation ou avec l'atrésie dans le cadre de la *backwards reachable set theory*. Etant donné que ces jeux s'intersectent en grande partie, leurs résultats illustrent l'impact de premier plan exercé par le contrôle sur la dynamique cellulaire dans le modèle.

Dans [75], qui a également été motivé par [45], l'auteur a réduit et simplifié le modèle en le reformulent en un système d'EDO couplées. L'auteur s'est focalisé sur la question du processus de sélection dans une approche de type de théorie des jeux, où un follicule joue contre tous les autres. Le modèle se prête à une analyse par la théorie des bifurcations, qui permet d'étudier la question de la sélection pour un follicule spécifique parmi toute la population. Que le follicule devienne atrétique (condamné) ou ovulatoire (sauvé) dépend de la masse cellulaire dont il dispose au moment où toutes les cellules cessent de proliférer. Toutefois, ce travail ne traite pas du cas où la commande agit directement sur les termes de vitesse.

En outre, par rapport aux problèmes étudiés en général dans la littérature, ce problème de contrôle est tout à fait différent, puisque les termes de contrôle apparaissent dans les flux. Dans la littérature, la plupart des monographies étudient le cas où les commandes sont appliquées soit à l'intérieur du domaine (voir [34]), soit sur la limite (voir [32, 39, 46, 76]). Pour le moment, nous considérons un problèmeune plus abordable qui est centrée sur la définition du contrôle optimal local u_f correspondant à une unique trajectoire ovulatoire. Cette hypothèse reste plausible dans le contexte thérapeutique de la stimulation ovarienne, qui vise à obtenir un unique follicule ovulatoire par un contrôle fin des niveaux de FSH. Dans le chapitre 3, nous considérons un problème de contrôle optimal qui consiste à maximiser la maturité ovarienne

finale au temps prévu. Nous avons fait plusieurs simplifications sur la dynamique du modèle.

A_1. Nous ne considérons qu'un seul follicule en développement, i.e. $f = 1$;

A_2. Il n'y a pas de terme de perte, i.e. $\lambda = 0$;

A_3. La vitesse de vieillissement n'est pas contrôlée, i.e. $g_f \equiv 1$;

A_4. La division cellulaire est représentée par un nouveau terme de gain;

A_5. La valeur seuil M_s peut toujours être atteinte en un temps fini.

La simplification (A_1) signifie que, dans ce problème, nous nous sommes spécialement intéressés au couplage entre les conditions nécessaires pour déclencher l'ovulation, d'une part, et le contrôle de la dynamique des cellules folliculaires, d'autre part. Nous avons considéré cette interaction indépendamment du processus de sélection des follicules, dans le sens où nous avons isolé la dynamique d'un follicule spécifique, comme si nous pouvions ignorer l'influence des autres follicules en croissance.

(A_2) à (A_4) nous permettent de simplifier la dynamique cellulaire. Dans (A_2), nous négligeons la mort cellulaire (apoptose), ce qui est tout à fait naturel si l'on considère seulement les trajectoires ovulatoires, tandis que, dans (A_3), nous considérons que l'âge cellulaire évolue comme le temps (de sorte que la durée d'un cycle cellulaire est constant et non contrôlé). En outre, le processus de division cellulaire est distribué sur les âges avec (A_4), de sorte qu'il existe un nouveau terme de gain dans le modèle à la place de la condition de transfert liée a la mitose. Même si la façon dont la prolifération cellulaire est représentée n'est pas tout à fait réaliste (pas de mitose), cela n'a aucune incidence sur la dynamique tant que la durée moyenne d'un cycle cellulaire est conservée.

Même s'il est simplifié, le problème étudié ici capte toujours la question essentielle, du compromis entre prolifération et différenciation qui caractérise le développement folliculaire terminal. D'une part, le follicule peut bénéficier d'un élargissement forte et rapide de sa population de cellules. D'autre part, cette augmentation se fait au détriment de la maturation des cellules individuelles. Ce compromis a été instancié ici comme un problème de composition de vitesses. Une vitesse de vieillissement relativement élevée tend à favoriser la production de cellules tandis qu'une vitesse de maturation relativement élevée tend à favoriser une augmentation de la maturité moyenne des cellules.

L'hypothèse (A_2) nous permet de remplacer le critère de temps minimal (17) par un critère qui consiste à maximiser la maturité ovarienne finale. On peut remarquer que dans le problème de contrôle initial, il pourrait n'y avoir aucune solution optimale sans l'hypothèse (A_5), si la maturité cible est supérieure à la maturité maximale atteignable de façon asymptotique.

Sous des hypothèses simplificatrices, nous sommes passés, pour des raisons de simplicité technique, à un problème équivalent où le temps final est fixe et le critère d'optimalité est la maturité folliculaire au moment final. Sur le plan biologique, cela signifie que pour n'importe quel temps final choisi t_1, la maturité résultante au temps final $M(t_1)$ peut être choisie à son

tour comme une cible de maturité qui serait atteinte en un temps minimal à l'instant t_1.

Nous désignons par $\rho(t,x,y)$ la fonction de densité qui satisfait la loi de conservation suivante :

$$\rho_t + \rho_x + ((a(y)+b(y)u)\rho)_y = c(y)\rho, \quad t \in (t_0,t_1),\ x>0,\ y>0, \tag{18}$$

où

$$a(y) := -y^2, \quad b(y) := c_1 y + c_2, \tag{19}$$

et

$$c(y) := \begin{cases} c_s, & \text{if } y \in [0,y_s), \\ 0, & \text{if } y \in [y_s,\infty), \end{cases} \tag{20}$$

où y_s, c_s, c_1 et c_2 sont des données constantes strictement positives.

Nous supposons qu'il n'y a pas de flux sortant, i.e.

$$\rho(t,0,y) = \rho(t,x,0) = 0, \quad \forall t \in (t_0,t_1),\ x>0,\ y>0. \tag{21}$$

L'état initial est

$$\rho(0,x,y) = \rho_0(x,y),\ x \geqslant 0,\ y \geqslant 0, \tag{22}$$

nous étudions le cas où ρ_0 est une mesure de Borel positive sur $\mathbb{R}\times\mathbb{R}$ à support compact inclus dans $[0,1]\times[0,y_s]$.

Pour toute commande $u \in L^\infty((t_0,t_1);[w,1])$ admissible, óu $0<w<1$, nous définissons la fonction de coût comme

$$J(u) := -\int_0^{+\infty}\int_0^{+\infty} y\, d\rho(t_1,x,y), \tag{23}$$

et nous voulons étudier le problème de contrôle optimal suivant :

$$\text{minimiser } J(u) \text{ pour } u \in L^\infty((t_0,t_1);[w,1]). \tag{24}$$

L'idée est d'approcher la densité par des masses de Dirac finies, nous donnons les résultats de contrôle optimal pour des masses de Dirac finies. Ensuite, nous passons à la limite pour obtenir des résultats de contrôle optimal pour le cas des EDP.

Nous choisissons les données initiales $\rho_0 \geqslant 0$ comme une combinaison linéaire d'un nombre fini de masses de Dirac. Pour $(\alpha,\beta)^{\mathrm{tr}} \in \mathbb{R}^2$, on note $\delta_{\alpha,\beta}$ la masse de Dirac en $(\alpha,\beta)^{\mathrm{tr}}$. Nous supposons que, pour un positif N donné, il existe une suite $((x_1^{k0},x_2^{k0}))_{k\in\{1,\dots,N\}}$ d'éléments de $[0,1]\times[0,y_s]$ et une suite $(x_3^{k0})_{k\in\{1,\dots,N\}}$ de nombres réels strictement positifs tels que

$$\rho_0 := \sum_{k=1}^{N} x_3^{k0}\delta_{x_1^{k0},x_2^{k0}}.$$

Nous en arrivons à considérer le problème de contrôle optimal suivant :

$$\begin{cases} \dot{x}^k = f(x^k, u), \quad u \in L^\infty((t_0, t_1); [w, 1]), \quad t \in [t_0, t_1], \\ x^k(t_0) = x^{k0}, \end{cases}$$

où

$$f(x^k, u) = \begin{pmatrix} 1 \\ a(x_2^k) + b(x_2^k)\, u \\ c(x_2^k)\, x_3^k \end{pmatrix}, \; x^k = \begin{pmatrix} x_1^k \\ x_2^k \\ x_3^k \end{pmatrix}, \; x^{k0} = \begin{pmatrix} x_1^{k0} \\ x_2^{k0} \\ x_3^{k0} \end{pmatrix}.$$

La fonction de coût devient maintenant

$$J(u) = -\int_{t_0}^{t_1} \big(a(x_2) + b(x_2)u + c(x_2)x_2\big)x_3 \, dt - x_2^0 x_3^0 \to \text{minimiser} \tag{25}$$

La principale différence entre ce problème de contrôle optimal et le problème de contrôle optimal classique [79] est que l'intégrande de la fonctionnelle J est discontinue (voir [81, 82, 83]). Cela complique considérablement l'analyse du problème de (25), en particulier, ce fait ne permet pas d'obtenir des conditions nécessaires d'optimalité en appliquant directement l'appareil standard de la théorie des problèmes d'extrêma [16, 60].

Dans [87], l'auteur a étudié le cas d'une fonctionnelle générale qui inclut à la fois la fonction caractéristique discontinue et les conditions continues. Là, l'auteur considère le problème de contrôle optimal suivant

$$\begin{cases} \dot{x} = f(x, u), \; u \in U, \; t \in [0, T], \\ x(0) \in M_0, \; x(T) \in M_1, \\ J(x, u, T) = \int_0^T (p(x, u) + q(x)\delta_M(x))\, dt \to \text{ minimiser}. \end{cases} \tag{26}$$

Ici, $x = (x_1, \cdots, x_n) \in \mathbb{R}^n$, $u = (u_1, \cdots, u_m) \in \mathbb{R}^m$, U est un ensemble convexe compact non vide de $\mathbb{R}^m$, M_0, M_1 sont des ensembles fermés non vides dans $\mathbb{R}^n$, et δ_M est une fonction caractéristique d'un ensemble fermé donné M dans $\mathbb{R}^n$. L'ensemble M est défini par une fonction scalaire $g(x)$

$$M = \{x \in \mathbb{R}^n | g(x) \leqslant 0\}.$$

Ici, f, g, p et q sont tous réguliers. Le temps final $T \geqslant 0$ du processus de contrôle est supposé libre. La classe de contrôles admissibles dans le problème (26) se compose de toutes les fonctions mesurables bornées u tel que $u(t) \in U$ pour presque tout $t \in [0, T]$. La principale méthode que l'auteur a utilisée dans [87] pour étudier le problème (26) est une méthode d'approximation [6, 8].

Une des difficultés de notre problème est que les deux intégrandes de la fonction de coût et de la dynamique sont discontinues. Nous pouvons néanmoins utiliser la méthode d'approximation comme dans [87] pour traiter notre problème de contrôle. Cette méthode consiste à approcher le problème de contrôle optimal discontinu par une suite de problèmes classiques de contrôle optimal bien choisis dépendant de contôle optimal u^* et à passer ensuite à la limite

sur le paramètre de perturbation pour les problèmes d'approximation dans les expressions des conditions nécessaires d'optimalité. Lorsque le temps prévu est assez grand (pour garantir que toutes les cellules soient entrées en phase 3) et sous certaines hypothèses sur les paramètres, en utilisant le PMP, nous donnons des résultats optimaux dans le cas où des masses de Dirac sont utilisées comme une approximation de la densité. Nous montrons que pour des masses de Dirac finies, toutes les commandes mesurables optimales sont des contrôles bang-bang avec un temps de commutation unique. Nous donnons aussi quelques illustrations numériques pour compléter nos résultats théoriques. Enfin, en passant à la limite nous avons prouvé qu'il existe un contrôle de type bang-bang avec un temps de commutation unique (voir le chapitre 3).

2.4 Expériences numériques

Dans le chapitre 4, nous revenons à une formulation plus biologique de la dynamique des cellules, nous revenons au modèle original avec des conditions aux limites discontinues (mitose). Pour que le temps final coïncide avec le moment de déclenchement de l'ovulation, nous avons supposé dans le chapitre 3 qu'il est suffisamment grand pour garantir que le processus de prolifération ait cessi. Dans cette partie numérique, nous nous sommes également intéressés au cas où le temps final n'est pas si grand, ce qui nous aide à comprendre la dynamique des cellules de manière plus approfondie.

Certaines variables observables biologiquement peuvent être obtenues à parti de la densité cellulaire dans le modèle. Le nombre total de cellules, qui peut être déterminé expérimentalement [88], est équivalent au moment d'ordre zéro de la densité :

$$M^0(t) = \sum_{f=1}^{n}\sum_{j=1}^{3}\sum_{k=1}^{N}\int_0^{\gamma_m}\int_0^{a_m}\phi_{j,k}^f(t,a,\gamma)\,da\,d\gamma.$$

Nous montrons dans le chapitre 4 comment calculer le moment d'ordre zéro en estimant combien de cycles cellulaires vont être effectués. Nous pouvons également obtenir des informations sur la répartition de la population cellulaire entre cellules proliférantes et cellules différenciés, via la fraction de croissance (GF) définie comme (voir [78])

$$GF(t) = \frac{\displaystyle\sum_{f=1}^{n}\sum_{j=1}^{2}\sum_{k=1}^{N}\int_0^{\gamma_s}\int_0^{a_m}\phi_{j,k}^f(t,a,\gamma)\,da\,d\gamma}{M^0(t)}.$$

Même s'il n'est pas simple de faire des comparaisons quantitatives, en raison à la fois des simplifications nécessaires pour étudier le problème de contrôle et de la rareté des données biologiques dynamiques, sur la, nous pouvons faire usage des principes suivants :

– La fraction de croissance diminue de façon constante au cours du développement des follicules, de sorte que nous pouvons en déduire que le temps final dans le problème devrait se produire après un temps définie comme "l'exit time" (le moment où toutes les cellules ont quitté le domaine de prolifération).

– L'information la plus fiable concerne le nombre total de cellules M^0 aux moments initiaux et finaux. Dans le cas de la brebis, le ratio d'augmentation entre $M^0(0)$ et $M^0(t_1)$ est de l'ordre de 20 à 30. Avec une fraction de croissance constante de un ($GF = 1$, pas de cellules différenciées), cette durée devrait à peu près correspondre à des cellules progressant le long de 4 à 5 cycles cellulaires (lorsque toutes les cellules se multiplient, le temps de doublement est égal à la durée du cycle cellulaire). Puis que le fraction de croissance diminue ($GF < 1$), le temps écoulé depuis le début jusqu'au temps final devrait en fait être plus long et correspondre à 6 (ou peut-être 7) cycles cellulaires (qui est cohérent avec le nombre de doublements observés dans la population).

On peut trouver un seuil pour le temps final de telle sorte que, avant ce seuil, le contrôle optimal consiste à toujours la valeur minimale de la commande admissible. Après ce seuil, la commande optimale est de appliquer toujours la valeur maximale.

Ensuite, nous étudions l'évolution de la maturité avec un contrôle de type bang-bang. Nous observons que le contrôle bang-bang est meilleur que le contrôle constant. En calculant le moment d'ordre zéro et la maturité asymptotique, nous prouvons que pour toutes les constantes $a < b$ dans l'intervalle de valeurs admissibles pour le contrôle, la direction de commutation $a \to b$ est mielleure que $b \to a$. Nous montrons enfin que pour le temps final fixe t_1, qui est déterminé par des considérations biologiques, la stratégie optimale consiste à commuter le contrôle intervenant dans la vitesse entre sa valeur minimale et sa valeur maximale, ce qui est cohérent avec le résultat que nous avons obtenu dans le chapitre 3.

3 Un modèle d'un protocole d'amplification pour les protéines mal repliées

La croissance et la fragmentation est un phénomène commun pour une population structurée. Il apparaît par exemple dans un contexte de division cellulaire ([1, 9, 10, 11, 40, 44, 48, 57, 74, 77]). Les protéines prions sont responsables de encéphalopathies spongiformes et apparaissent sous la forme d'agrégats dans des cellules infectées. Ces polymères se développent par fixation de monomères non infectieux, en les convertissant, en protéines infectieuses. D'autre part, ils augmentent leur nombre en se divisant (voir [42]).

Un outil prometteur pour concevoir un test de diagnostic est la technique de la PMCA (Protein Misfolding Cyclic Amplification) (voir [65]). Le principe de la PMCA est fondé sur "l'hypothèse purement protéique". Selon cette hypothèse largement acceptée, l'agent infectieux de la encéphalo patries spongiformes, connu sous le nom prion, consiste en une protéine mal repliée appelée PrPsc (Prion Protein scrapie). La PrPsc se réplique dans un processus d'auto-propagation, en convertissant la forme normale de la PrPc (PrPc pour protéine prion cellulaire) dans la PrPsc. La PMCA a permis de consolider l'idée d'une réplication autocatalytique de la PrPsc par polymérisation nucléé [19, 90, 91]. Dans ce modèle, la PrPsc est

considérée comme une forme polyméisée de la PrPc. Les polymères peuvent s'allonger en agrégeant des monomères PrPc, et ils peuvent se reproduirent en se divisant en fragments plus petits. La PrPc est essentiellement exprimée par les cellules du système nerveux central, en PrPsc est concentrée dans cette zone. La quantité de la PrPsc dans les tissus tels que le sang est très faible et c'est pourquoi il est très difficile de le diagnostiquer chez une personne infectée. La PMCA mime le mécanisme de nucléation/polymérisation se produisant *in vivo* dans le but d'amplifier rapidement le taux de polymères présents en faible quantité dans un échantillon infecté. Cette technique pourrait permettre de détecter la PrPsc dans les échantillons de sang par exemple. Mais pour l'instant elle n'est pas assez efficace pour le faire. Les outils mathématiques de modélisation et d'optimisation peuvent contribuer à optimiser le protocole PMCA.

Masel *et al.* [72] a proposé un modèle mathématique pour la polymerization nucléée. Nous partons de celui-ci et ajoutons un paramètre de *sonication* pour modéliser la PMCA. Dans le protocole PMCA, les monomères de PrPc sont en excès, de sorte que leur quantité varie peu pendant l'expérience. Nous supposons que cette variation est assez petite pour être négligée et la quantité de monomères est supposée être constante dans le temps. Désignons par $x_i(t)$ la densité des polymères composés de $i \in N$ protéines PrPsc au moment t. Alors l'évolution de la quantité de polymères est donnée par le système couplé d'EDOs

$$\frac{dx_i}{dt} = -r(u(t))(\tau_i x_i - \tau_{i-1}x_{i-1}) - u(t)\beta_i x_i + 2u(t)\sum_{j=i+1}^{n} \beta_j\, \kappa_{i,j}\, x_j \ , \quad 1 \leqslant i \leqslant n \ . \tag{27}$$

Les polymères de taille i se décomposent en petits agrégats avec le taux de β_i. Ce taux est modulé par le paramètre de *sonication* $u(t)$ comme un contrôle qui reflète l'intensité des ultrasons utilisés par la *sonication*. Nous écrivons ce problème sous forme matricielle

$$\begin{cases} \dot{X}(t) = M(u(t))\, X(t), & t > 0, \\ X(t=0) = X^0, \end{cases}$$

où $X(t) = (x_i(t))_{1\leqslant i\leqslant n}^{tr}$ est la distribution de polymères et $M(u) := uF + r(u)G$ avec G la matrice de croissance et F la matrice de fragmentation

$$G = \begin{pmatrix} -\tau_1 & & & & \\ \tau_1 & -\tau_2 & & & \\ & \ddots & \ddots & & \\ & & & -\tau_{n-1} & \\ & & & \tau_{n-1} & 0 \end{pmatrix}, \quad F = \begin{pmatrix} 0 & & & \\ & -\beta_2 & & (2\kappa_{ij}\beta_j)_{i<j} \\ & & \ddots & \\ & 0 & & \\ & & & -\beta_n \end{pmatrix}.$$

Les coefficients de ces matrices sont supposés être positifs

$$\forall i \in [1, n-1], \qquad \tau_i > 0 \quad \text{et} \quad \beta_{i+1} > 0.$$

Ensuite, le problème d'optimisation qui nous intéresse est de trouver un contrôle $u(t)$ qui maximise la quantité finale de PrPsc

$$\psi(X(T)) := \sum_{i=1}^{n} i\, x_i(T) \quad \rightarrow \text{maximiser} \tag{28}$$

pour un temps final de l'expérience T donné. En effet, la présence de PrPsc ne peut être détectée expérimentalement (par Western Blot, voir [65] pour plus de détails) que si cette quantité est supérieure à un seuil critique.

Lorsque r est non linéaire, l'ensemble de vitesse

$$\mathcal{V}(X) := \{(uF + r(u)G)X,\ u \in [u_{min}, u_{max}]\}$$

n'est pas convexe, et nous ne pouvons pas garantir l'existence d'un contrôle optimal. Néanmoins, nous pouvons résoudre *un problème de contrôle optimal relaxé* (voir [63] par exemple). Pour expliquer cela, nous réécrivons notre problème initial de contrôle optimal comme suit : trouver

$$(u_1^*(t), u_2^*(t)) \in \Omega := \{(u_1, u_2) \mid u_2 = r(u_1)\}$$

qui maximise $\psi(X(t))$ avec X une solution de

$$\begin{cases} \dot{X}(t) = \big(u_1(t)F + u_2(t)G\big)\, X(t), & t > 0, \\ X(0) = X^0. \end{cases}$$

Dans ce cas, le problème de contrôle relaxé consiste à trouver $(u_1^*(t), u_2^*(t))$ dans l'enveloppe convexe $H(\Omega)$ de Ω (voir figure 4), qui maximise le coût $\psi(X(T))$. Pour ce problème convexifié, l'ensemble de vitesse est donnée par l'enveloppe convexe $H(\mathcal{V}(X))$ de $\mathcal{V}(X)$ et est donc convexe. Donc, il existe un contrôle optimal (relaxé) et d'ailleurs la réponse $X^*(t)$ à ce contrôle est la limite uniforme de réponses à des contrôles classiques (voir [63]). En conséquence, il est intéressant de résoudre le problème de contrôle optimal relaxé.

Nous modifions la fonction de coût

$$\tilde{\psi}(X(T)) = \phi_1 \cdot X(T) \quad \rightarrow \text{maximiser} \tag{29}$$

Supposons que la condition initiale est donnée par

$$X(0) = V_1,$$

où V_1 et ϕ_1 sont les premiers vecteurs propres, c'est à dire que si nous supposons que $(\bar{u}_1, \bar{u}_2)$ est une paire qui maximise la valeur propre de Perron λ_1, alors (V_1, ϕ_1, λ_1) est la solution au problème valeur propre Perron

$$\begin{cases} \lambda_1 V_1 = (\bar{u}_1 F + \bar{u}_2 G)V_1, \\ \lambda_1 \phi_1 = \phi_1(\bar{u}_1 F + \bar{u}_2 G), \\ \lambda_1 > 0, \quad \phi_1 V_1 = 1. \end{cases} \tag{30}$$

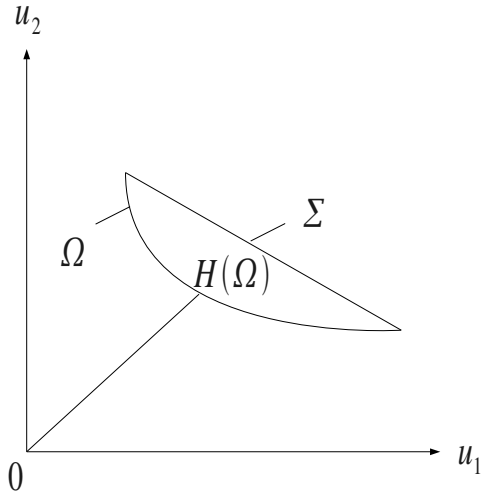


FIG. 4. L'enveloppe convexe $H(\Omega)$ de Ω dans le cas où r est décroissance et convexe.

Utilisant le PMP, nous avons prouvé que pour la fonction de coût modifiée (29), la paire de contrôle constant $(\bar{u}_1, \bar{u}_2)$ qui maximise la valeur propre de Perron est un contrôle optimal. Pour le problème de contrôle d'origine (28), nous avons prouvé que pour le cas 2D, le contrôle optimal se situe sur Σ (voir figure 4). En outre, le contrôle optimal est un contrôle de type bang-bang avec un contrôle constante qui est celui qui maximise la valeur propre de Perron. Pour le cas 3D, nous prouvons seulement que le contrôle optimal se situe sur Σ (voir figure 4).

4 Perspectives

Système de fabrication

- Pour le modèle 1D de système de fabrication, il serait également intéressant d'étudier le caractère bien posé dans le cas où les conditions aux limites et les conditions initiales sont distribuées selon une mesure de Borel réelle. Une première difficulté réside dans la façon de définir une notion correcte de solution.
- On pourait aussi considérer un terme source (possiblement non linéaire), en transformant la loi de conservation en une loi d'équilibre. L'équation de point fixe $W \to F(W)$ devient alors un peu plus compliquée, mais une borne de type Lipschitz sur la source devrait être suffire pour rendre l'application contractante.

  En outre, nous pourions faire une généralisation en prenant λ discontinue (par exemple constante par morceaux (PC) ou de variation bornée (BV)). L'existence d'une solution de ρ dans $C^0((0,T); L^1(0,1))$ peut alors être obtenue de la même manière, mais il faut aussi vérifier que $\rho(t,\cdot) \in PC(0,1)$ ou $BV(0,1)$, dès lors que ρ_0 et u sont à la fois dans un PC ou BV, respectivement. Ceci est inspiré d'un travail similaire pour le cas PC

[47].

– En ce qui concerne le problème de contrôle optimal, il serait intéressant d'étudier la dérivabilité au sens de Gàteaux de la solution ou au flux sortant par rapport aux conditions initiales ou aux conditions aux limites. Dans [26], les auteurs ont d'abord présenté un résultat rigoureux sur la dérivabilité au sens de Gàteux de la solution par rapport à l'état initial. Puis, sur la base des résultats de différentiabilité, les auteurs donnent une condition nécessaire d'optimalité. Puisque nous pouvons obtenir l'expression explicite de la solution, il est possible de calculer directement la dérivabilité au sens de Gàteaux de la solution par rapport aux conditions initiales ou aux conditions aux limites.

Modèle de l'ovulation folliculaire

– Contrôle de type bang-bang

Dans le chapitre 3, nous avons prouvé qu'il existe un contrôle de type bang-bang avec un seul temps de commutation, nous faisons la conjecture que chaque contrôle optimal est aussi un contrôle bang-bang avec un temps de commutation unique dans le cas de l'EDP. Pour traiter ce problème, on peut d'abord construire un problème auxiliaire de contrôle optimal plus régulier et prouver que, pour ce problème de contrôle régularisé, chaque commande optimale est un contrôle de type bang-bang avec un temps de commutation unique. Puis on peut passer à la limite pour prouver que, pour le problème de contrôle optimal discontinu, chaque commande optimale est un contrôle de type bang-bang.

– Cas où la vitesse de vieillissement est également contrôlable

Jusqu'à présent, nous avons fait l'hypothèse que la vitesse de vieillissement est constante, donc noncontrôlable. En fait, la vitesse de vieillissement dans la phase 1 est également sensible à FSH, et par conséquent, elle est également contrôlable. Plus précisément, il est intéressant d'étudier

$$\rho_t + g(u)\rho_x + (h(y,u)\rho)_y = c\rho.$$

Avec une vitesse de vieillissement contrôlée, nous pouvons prendre en compte le cycle cellulaire et étudier précisément les phénomènes liés à la fois à l'âge et à la maturité des cellules. Nous pourrions d'abord considérer des masses de Dirac finies comme une approximation de la densité. Nous pourrions ensuite étudier le PMP pour ce problème de contrôle optimal en dimension finie.

– Problème multi-échelles

Une question importante est de considérer le développement couplé de deux ou plusieurs follicules et le phénomène de sélection comme un problème de contrôle multi-échelles en boucle fermée. Nous pourrions d'abord considérer deux follicules avec des densités différentes au temps initial et chercher les contrôles optimaux qui maximisent la maturité globale à un moment final donné. Ensuite, cette stratégie pourrait être mise en œuvre numériquement pour prédire le destin des follicules (l'ovulation ou atrésie).

– Les essais numériques nous donnent une relation entre le temps de commutation op-

timal et la valeur de saturation de a et b du contrôle (voir section 4.3.3). Nous avons constaté que le temps de commutation optimal augmente à mesure que la valeur maximale de saturation b diminue. Il serait intéressant d'étudier cette observation sur le plan théorique.

– Dans le chapitre 2, nous utilisons le théorème du point fixe de Banach pour prouver l'existence de la solution, nous pourrions aussi l'étudier numériquement la solution approchée du problème de Cauchy.

Modèle d'un protocole d'amplification pour les protéines mal repliées

– Pour la version modifiée de la fonction coût (29) (voir section 5.3.1), nous avons prouvé le contrôle constant qui maximise les valeurs propres de Perron satisfait le PMP, mais on ne sait pas dire si c'est le seul contrôle qui satisfait le PMP.

– Nous pouvons considérer le problème de contrôle optimal lié à la fonction de coût originale (28). Dans le cas 2D, en utilisant le PMP, nous avons prouvé que la commande optimale est un contrôle de type bang-bang. En outre, le contrôle optimal est la valeur qui maximise la valeur propre de Perron. Il est toujours intéressant d'étudier le cas 3D pour voir ce qu'il en est du contrôle optimal. Pour le moment, nous savons seulement que le contrôle optimal se situe sur la frontière Σ (voir section 5.3.2). D'après les simulations numériques, il peut arriver que le contrôle optimal n'est pas un contrôle de type bang-bang. Pour toute dimension, nous faisons la conjecture que le contrôle optimal se situe sur Σ. Une idée pourrait être d'utiliser le calcul des variations pour prouver que la dérivée du coût par rapport à un $\tilde{U}(t) = \sigma U(t)$ ($\sigma > 1$) est positive.

– Nous pouvons considérer un autre problème de contrôle optimal lié à la fonction de coût originale (28) (see section 5.3.2), mais avec une contrainte sur l'état final

$$\begin{aligned} \psi(X(T)) := \sum_{i=1}^{n} i\, x_i(T) \quad &\rightarrow \text{maximiser}, \\ X(T) = CV_1, \quad &(31) \end{aligned}$$

pour une constante $C > 0$. Pour ce problème de contrôle optimal avec cette contrainte terminale, en utilisant le PMP, nous pouvons également obtenir une condition nécessaire d'optimalité. A partir de cette condition nécessaire d'optimalité, nous faisons la conjecture que chaque contrôle optimal se situe sur la frontière Σ.

General introduction

In this thesis, I have mainly studied the well-posedness of partial differential equations and optimal control problems. I have studied the Cauchy problems associated with hyperbolic conservation laws with nonlocal velocities, for a 1D model (manufacturing system) and then for a 2D model (process of follicular selection). I have then studied optimal control problems on the 2D model and on an ODE-based model (amplification of misfolded proteins). In the following, I will present the results obtained in the order of these three models.

5 A model of highly re-entrant manufacturing system

A highly re-entrant manufacturing system (or production line) is a production system which produces a large number of parts in a very large number of consecutive production steps. This is the case e.g., for a semiconductor factory. Armbruster et al. have introduced in [5] a model by nonlinear conservation laws with a nonlocal velocity. This kind of systems are very useful because it can provide explicit solutions and it benefits from efficient numerical tools for simulation. Futhermore, it describes very well the progress of the production in the factory. In this model, the mathematical variable of the hyperbolic equation is the density function $\rho(t,x)$ describing the density of products at stage $x \in [0,1]$ of the production at time t, The case where $x = 0$ represents the beginning of the production line, while $x = 1$ represents the end and $x \in (0,1)$ represents the intermidiate steps. Assuming mass conservation, the time evolution of the product density is described by the continuity equation. The equation of conservation law is the following

$$\rho_t(t,x) + (\rho(t,x)\lambda(x,W(t)))_x = 0, \quad t \geqslant 0, 0 \leqslant x \leqslant 1, \tag{32}$$

where

$$W(t) = \int_0^1 \rho(t,x)dx$$

is the total quantity of the products in the factory.

In chapter 1, we study this scalar conservation law. We assume that the velocity function $\lambda > 0$ is continuous differentiable, i.e., $\lambda \in C^1([0,1] \times [0,\infty))$. For instance, the special case

$$\lambda(x, W) = \frac{1}{1+W}$$

is considered in [5, 62].

For (32), the supplementary conditions are

1. the initial condtion
$$\rho(0, x) = \rho_0(x), \quad 0 \leqslant x \leqslant 1, \tag{33}$$
2. the influx of the products in the factory, which suggests the boundary condition
$$\rho(t, 0)\lambda(0, W(t)) = u(t), \quad t \geqslant 0. \tag{34}$$

Motivated by applications, one natural control problem is related to the *Demand Tracking Problem (DTP)*. The objective of *DTP* is to minimize the difference between the actual outflux $y(t) = \rho(t, 1)\lambda(1, W(t))$ and a given demand forecast $y_d(t)$ over a fixed time period. An alternative control problem is *Backlog Problem (BP)*. The objective of *BP* is to minimize the difference between the number of the total products that have left the factory and the number of the total demanded products over a fixed time period.

The form of production system at a given time t is defined as

$$\beta(t) = \int_0^t \rho(s, 1)\lambda(1, W(s))ds - \int_0^t y_d(s)ds.$$

The backlog $\beta(t)$ can be negative or positive, with a positive backlog corresponding to overproduction and a negative backlog corresponding to a shortage.

In the case where λ doesn't depend on the local position x, the authors in [62] studied these two prototypical control problems (*DTP* and *BP*). The method was based on the formal adjoint method for constrained optimization, incorporating the scalar conservation law as a constraint of a nonlinear optimization problem. They obtained numerical results for these two fundamental problems and discussed the influence of the nonlinearity of the cycle time on the limits of the reactivity of the production system.

In [35], the authors proved the existence and uniqueness of solutions of Cauchy problem with initial and boundary conditions given in L^1, and studied their regularity properties. They also proved the existence of optimal controls that minimizes the L^2-norm of the mismatch between the actual and a desired output signal. In [35], the nonlocal velocity λ doesn't depend on the space x, which is not natural in numerous cases. In chapter 1, we generalize the results of [35] to the case where the velocity λ depends on x.

The main difficulty of this work comes from the nonlocal velocity and dependance on x. In [27], which is also motivated in part by [5, 62], the authors also addressed well-posedness for systems of hyperbolic conservation laws with a nonlocal velocity in $\mathbb{R}^n$. However, the methods

used in this paper cannot be applied to the case where $\mathbb{R}^n$ is replaced by $[0,1]$. We proved the existence, uniqueness and regularity of the weak solution to Cauchy problem (32), (33) and (34) with initial and boundary data in L^∞. The main approach is the characteristic method. We point out here that in the previous paper [35], the authors obtained the well-posedness for L^p $(1 \leqslant p \leqslant \infty)$ data. The L^∞ assumption in this chapter is necessary since the velocity function λ depends on the space variable x. Using the implicit expression of the solution in terms of the characteristics, we also prove the stability (continuous dependence) of both the solution and the out-flux with respect to the initial and boundary data.

The optimal control problem that we study in this chapter is related to the *DTP*. The objective is to minimize the L^p-norm with $1 \leqslant p \leqslant \infty$ of the difference between the actual out-flux $y(t) = \rho(t,1)\lambda(1,W(t))$ and a given demand forecast $y_d(t)$ over a fixed time period. With the help of the implicit expression of the weak solution and by compactness arguments, we prove in this chapter the existence of solutions to this optimal control problem.

6 A biological model of follicular ovulation

As a generalization of this type of conservation law with nonlocal velocity, in 2D case, we are interested with a special subject that models the development of ovarian follicles which deals with reproductive strategies. This model has been developed in the framework of the interdisciplinary project, the INRIA large scale initiative action REGATE (REgulation of the GonAdoTropE axis : https://www.rocq.inria.fr/sisyphe/reglo/regate.html).

6.1 Presentation of the biological model

In mammals, the pool of oocytes available for a female through her reproductive life is constituted very early in life. Each oocyte of this pool is surrounded by only one layer of somatic cells, the whole making up a primordial follicle. Follicles continuously leave this pool to enter a process of growth and functional maturation. Ovarian follicles are spheroidal, tissular structures sheltering the maturing oocyte. The ovulation process is the endpoint of follicular development, the process of growth and functional maturation undergone by ovarian follicles, from the time they leave the pool of primordial follicles until ovulatory stage.

The development of ovarian follicles is a crucial process for reproduction in mammals, as its biological meaning is to release one (in mono-ovulating species) or several (in poly-ovulating species) fertilizable oocyte(s) enabled to subsequent embryo development at the time of ovulation. During each ovarian cycle, numerous follicles are in competition for their survival. Few follicles reach an ovulatory size, since most of them undergo a degeneration process, known as atresia (see for instance [73]). The fate of a follicle is determined by the changes occurring in its cell population in response to an hormonal control originating from the pituitary gland (see figure 5).

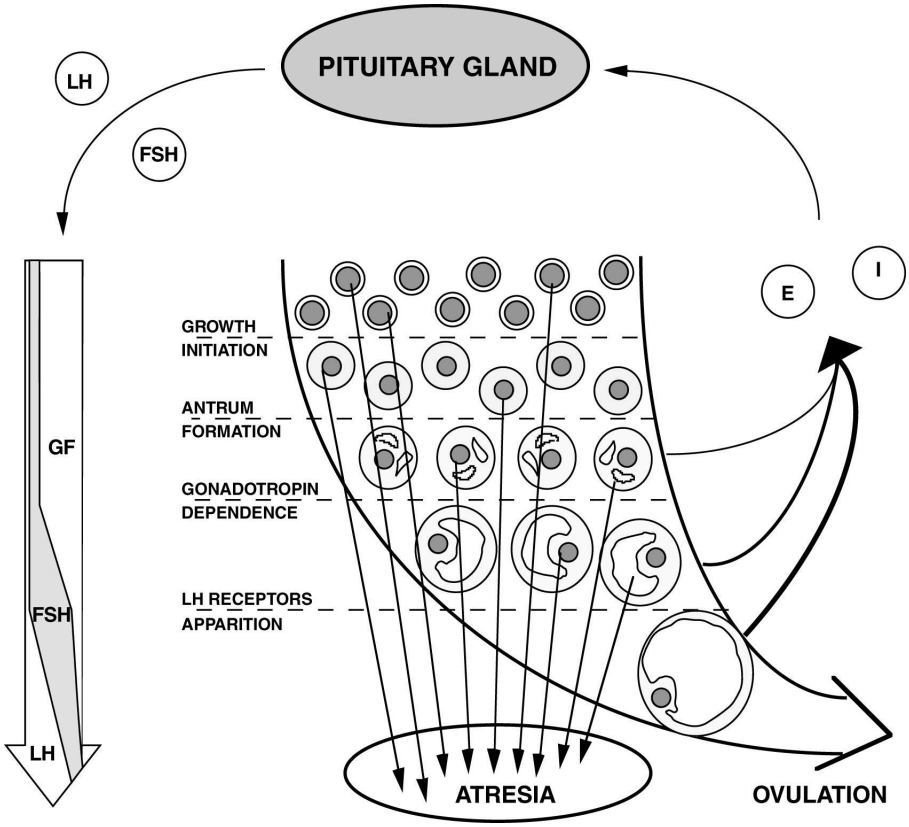


Figure 5. The illustration of terminal development of follicular ovarian (Picture retrieved from [20]).

The follicular cell population consists of proliferating, differentiated and apoptotic cells. Cells are characterized by their positions within or outside the cell cycle and by their sensitivities to the follicle stimulating hormone (FSH). This leads one to distinguish 3 cellular phases (see figure 6). Phase 1 ($G1$) and phase 2 (SM) correspond to the proliferation phases and phase 3 (D) corresponds to the differentiation phase, after the cells have exited the cell cycle. Phase 1 and phase 3 are sensitive to FSH, while phase 2 is insensitive to FSH. The apoptosis phenomena may occur in phases 1 and phase 3 (see figure 6).

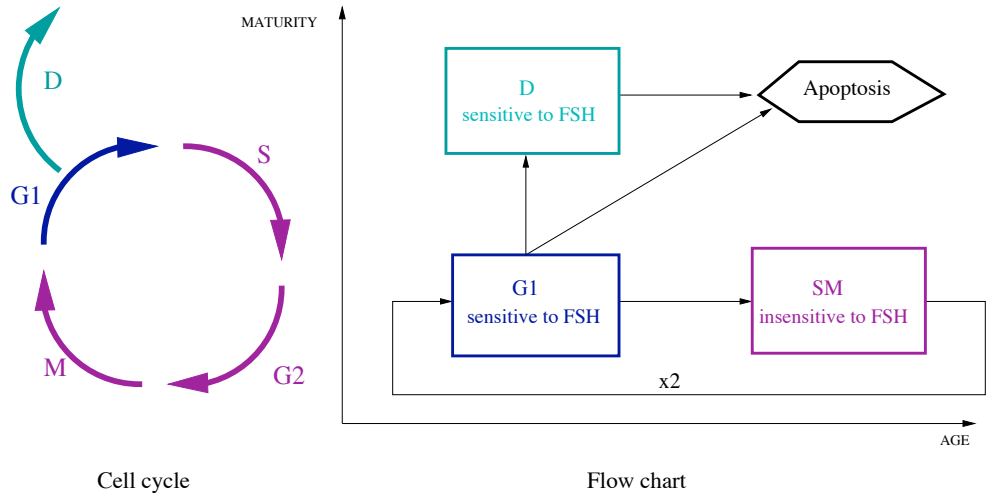


Figure 6. Cellular flow chart. One cell cycle includes $G1$ and SM phases. When a mother cell enters the $G1$ phase from the SM phase, it gives birth to two daughter cells. Differentiation of cells corresponds to the output stream of $G1$ phase to enter D phase. The apoptosis phenomena may occur in phases $G1$ and D (Picture retrieved from [22]).

A mathematical model, using both multi-scale modeling and control theory concepts, has been designed to describe the follicle selection process on a cellular basis [45]. For each follicle, the cell population dynamics is ruled by a conservation law, which describes the changes in the distribution of cell age and maturity. A control term, representing FSH signal, intervenes both in the velocity and loss terms of the conservation law. The densities interact through a coupled hyperbolic system between different follicles and cell phases, which results in a vector conservation law and coupling between boundary conditions. The maturity velocity functions possess both a local and nonlocal character.

In this model, the position of a cell at time $t \in [0, T]$ ($T > 0$) is defined by its age a and maturity γ. The cell age a is a marker of progression within the cell cycle (in phase 1 and phase 2) and evolves as time t outside the cell cycle (in phase 3). The duration of phase 1 is $a_1 > 0$ and the total cycle duration is a_2 (see figure 7). The maturity γ is used to discriminate between the cycling and non-cycling cells by comparison to a threshold γ_s and to characterize the cell vulnerability towards apoptosis. Phase 1, 2 and 3 correspond to ranges in the values

of (a, γ) in the following sets of the age-maturity plane (see figure 7)

$$\Omega_{1,k} := [(k-1)a_2, (k-1)a_2 + a_1] \times [0, \gamma_s], \quad \Omega_{2,k} := [(k-1)a_2 + a_1, ka_2] \times [0, \gamma_s],$$
$$\Omega_{3,k} := [(k-1)a_2, ka_2] \times [\gamma_s, \gamma_m],$$

where γ_m is the maximum of the maturity such that $\gamma_m > \gamma_s$ (see figure 7).

The cell population in a follicle f is represented by cell density functions $\phi^f_{j,k}(t, a, \gamma)$ defined on each cellular phase $Q^f_{j,k}$ with age a and maturity γ, which satisfy the following conservation laws

$$\frac{\partial \phi^f_{j,k}}{\partial t} + \frac{\partial (g_f(u_f)\phi^f_{j,k})}{\partial a} + \frac{\partial (h_f(\gamma, u_f)\phi^f_{j,k})}{\partial \gamma} = -\lambda(\gamma, U)\phi^f_{j,k} \quad \text{in } Q^f_{j,k}, \tag{35}$$

with

$$Q^f_{j,k} := \Omega_{j,k} \times [0, T], \quad f = 1, \cdots, n,$$

where $j = 1, 2, 3$ represents phase 1, phase 2 and phase 3, $k = 1, \cdots, N$, and N is the number of consecutive cell cycles (see figure 7).

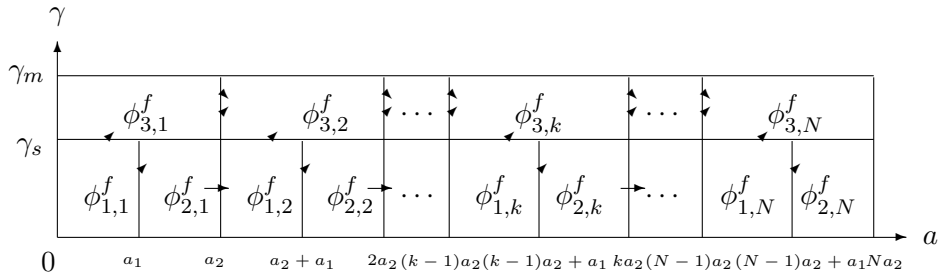


Figure 7. Domain of the solution in the original model. For each follicle f, the domain consists of the sequence of N cell cycles. a denotes the age of the cell and γ denotes its maturity. The top of the domain corresponds to the differentiation phase and the bottom to the proliferation phase.

Let us define the maturity operator M as

$$M(\varphi)(t) := \int_0^{\gamma_m} \int_0^{a_m} \gamma \varphi(t, a, \gamma)\, da d\gamma. \tag{36}$$

Then

$$M_f(t) := \sum_{j=1}^{3} \sum_{k=1}^{N} M(\phi^f_{j,k})(t) = \sum_{j=1}^{3} \sum_{k=1}^{N} \int_0^{\gamma_m} \int_0^{a_m} \gamma \phi^f_{j,k}(t, a, \gamma)\, da d\gamma \tag{37}$$

is the global follicular maturity on the follicular scale, while

$$M(t) := \sum_{f=1}^{n} M_f(t) = \sum_{f=1}^{n} \sum_{j=1}^{3} \sum_{k=1}^{N} \int_0^{\gamma_m} \int_0^{a_m} \gamma \phi^f_{j,k}(t, a, \gamma)\, da d\gamma \tag{38}$$

is the global maturity on the ovarian scale.

In (36) to (38), a_m and γ_m are maximum of age and maturity. The velocity and source terms are all smooth functions of u_f and U, where $U(M)$ is the global control that can be interpreted as the FSH plasmatic level and $u_f(M_f, M)$ is the local control that represents intrafollicular bioavailable FSH levels. More precisely, the global control U results from the ovarian feedback onto the pituitary gland and impacts the secretion of FSH. The feedback is responsible for reducing FSH release, leading to the degeneration of all but those follicles selected for ovulation. The local control u_f, specific to each follicle, accounts for the modulation in FSH bioavailability related to follicular vascularization. It is given as a proportion of U (see [45]).

In phase 1 and phase 3, both a global control U and a local control u_f act on the velocities of aging (g_f function, locally controlled in phase 1), and maturation (h_f function, locally controlled in phase 1 and phase 3) as well as on the loss term (λ apoptosis rate, globally controlled in phase 1 and phase 3). Phase 2 is uncontrolled and corresponds to completion of mitosis after a pure delay in age $a_2 - a_1$ (no cells leave the cycle here). The increase in the cell mass occurs through mitosis. At the time of mitosis, a mother cell gives birth to two daughter cells, which results in a local doubling of the flux. One can refer to [22] and [43] for more details about the velocity and source terms.

The initial conditions are given as

$$\phi^f_{j,k}(0, a, \gamma) = \phi^f_{k0}(a, \gamma)|_{\Omega_{j,k}}, \qquad j = 1, 2, 3, \quad k = 1, \cdots, N. \tag{39}$$

Each boundary segment of each $\Omega_{j,k}$ is either inward or outward (see figure 7), which suggests the following boundary conditions.

There is no influx for phase 1 and phase 3 in the first cell cycle (see figure 7), hence

$$\phi^f_{1,1}(t, 0, \gamma) = \phi^f_{3,1}(t, 0, \gamma) = 0, \quad (t, \gamma) \in [0, T] \times [0, \gamma_s]. \tag{40}$$

The mitosis happens when the cell leaves the previous cycle and goes into the next cycle (see figure 7), hence for $k = 2, \cdots, N$

$$g_f(u_f)\phi^f_{1,k}(t, (k-1)a_2, \gamma) = 2\tau_{gf}\phi^f_{2,k-1}(t, (k-1)a_2, \gamma), \quad (t, \gamma) \in [0, T] \times [0, \gamma_s]. \tag{41}$$

There is no mitosis in phase 3, hence

$$\phi^f_{3,k}(t, (k-1)a_2, \gamma) = \phi^f_{3,k-1}(t, (k-1)a_2, \gamma), \quad (t, \gamma) \in [0, T] \times [0, \gamma_s]. \tag{42}$$

In the same cycle k, $k = 1, \cdots, N$, the dynamics amounts to a transport dynamics from phase 1 to phase 2 (see figure 7), hence

$$\tau_{gf}\phi^f_{2,k}(t, (k-1)a_2 + a_1, \gamma) = g_f(u_f)\phi^f_{1,k}(t, (k-1)a_2 + a_1, \gamma), \quad (t, \gamma) \in [0, T] \times [0, \gamma_s]. \tag{43}$$

There is no influx from the bottom $\gamma = 0$ (see figure 7), hence for $k = 1, \cdots, N$

$$\phi^f_{1,k}(t, a, 0) = 0, \quad (t, a) \in [0, T] \times [(k-1)a_2, (k-1)a_2 + a_1], \tag{44}$$

$$\phi^f_{2,k}(t, a, 0) = 0, \quad (t, a) \in [0, T] \times [(k-1)a_2 + a_1, ka_2]. \tag{45}$$

There is only influx from phase 1 to phase 3, and no influx from phase 2 to phase 3 (see figure 7), hence for $k = 1, \cdots, N$

$$\phi^f_{3,k}(t, a, \gamma_s) = \begin{cases} \phi^f_{1,k}(t, a, \gamma_s), & (t, a) \in [0, T] \times [(k-1)a_2, (k-1)a_2 + a_1], \\ 0, & (t, a) \in [0, T] \times [(k-1)a_2 + a_1, ka_2]. \end{cases} \tag{46}$$

There is no influx from the above $\gamma = \gamma_m$ (see figure 7), hence for $k = 1, \cdots, N$

$$\phi^f_{3,k}(t, a, \gamma_m) = 0, \quad (t, a) \in [0, T] \times [(k-1)a_2, ka_2]. \tag{47}$$

6.2 Well-posedness

For the well-posedness of this biological model, in [44], the authors considered the case where the control values are in steady state, i.e. the u_f and U control terms are given functions of time. The velocities and loss term are then given functions $g_f(t)$, $h_f(\gamma, t)$ and $\lambda(\gamma, t)$. They tried to solve the problems in sequence when the traces of the solutions for each phase on their outward boundaries (left and upper segments) are well defined. For each phase, to solve such a problem, with L^∞ or L^1 boundary and initial values, extensions of the classical Kruzkov entropy solutions [61] to boundary value problems have been proposed (see, e.g., [12, 80], where renormalized entropy solutions are defined for this type of problem). However, for this consecutive problem, the authors encountered a problem in defining the trace of the solution on the outward boundary, in order to solve the problem in the next phase.

In contrast, we consider both closed and open loop problems, that is to say u_f and U are functions of M_f, M and t. The main difficulties to study this biological model come from the nonlocal velocity, the coupling between boundary conditions and the coupling between different follicles in the model. Additionally, we have to deal with source terms, and the problem is a 2D one.

In chapter 1, the model of the highly re-entrant manufacturing system is only 1D and does not have source terms. There, the velocities are always positive, while in the 2D model of follicular ovulation, the maturity velocities $h_f(f = 1, \cdots, n)$ depend on the current value of the local control u_f, it may change sign in phase 3.

In [92], the author addressed the question of well-posedness for systems of hyperbolic conservation laws with a nonlocal velocity. However, our method of proof and even our definition of solutions are different from the ones given in [92]. In [92], the author used the Schauder fixed point theorem to prove the existence of the solution, while our proof uses the Banach fixed point theorem, which is more useful to compute numerically the solution. Furthermore, the author proved the uniqueness under strong assumptions that the initial data is continuously differentiable, while we get the uniqueness when initial data is only in L^∞. Using contraction mapping theorem, we first prove that the maturity $\vec{M} := (M_1, \cdots, M_n)$ exists as a fixed point of a map from a continuous function space. We can then construct a local solution to the Cauchy problem by characteristic method. Using a priori estimate and

progressing step by step, we get a global solution. We also prove the uniqueness of this weak solution (see chapter 2).

6.3 Related control problems

The aging velocity g_f controls the duration of the cell division cycle. Once the cell age has reached a critical age, the mitosis event is triggered, and one mother cell gives birth to two daughter cells, which both enter a new cell cycle. The maturation velocity controls the time needed to reach a threshold maturity γ_s, when the cell exits the division cycle definitively. After the exit time, the cell is no more able to contribute to the increase in the follicular cell mass. Hence, there are local singularities in the subpart of the domain where $\gamma \leqslant \gamma_s$, that correspond to the flux doubling due to the successive mitosis events.

The hormonal control exerted by FSH acts directly on follicular cells to control their commitment towards either proliferation or differentiation. In turn, the hormonal feedback exerted by the ovary on the hypothalamo-pituitary axis ensues from the weighted contribution of all cells distributed amongst all follicles. Hence, a hormone-driven competition process, occurring within the population of simultaneously developing follicles, is intertwined with each cell dynamics process taking place within a given follicle.

Ovulation is triggered when estradiol levels reach a threshold value M_s. As estradiol secretion is related to maturity (see [45]), the ovulation time T_s is defined as

$$T_s = \min\{T | M(T) = M_s\}. \tag{48}$$

The follicles are then sorted according to their individual maturity. The ovulatory follicles are those whose maturity at time T has overpassed a threshold M_{s1} such as $M_{s1} \leqslant M_s$. The ovulation rate is computed as

$$N_{s,s1} = \text{Card}\,\{f | M_f(T_s) \geqslant M_{s1}\}.$$

The fate of a follicle is determined by the changes occurring in its cell population in response to an hormonal control originating from the pituitary gland. Only the best-fitted follicles can survive in an unfavorable, FSH-poor environment.

As a whole, system (35), (39) to (47) combined with stopping condition (48) defined a multiscale reachability problem. Concerning the related control problem, one question is to define some control problems reasonable from biological point of view and tractable from mathematical point of view.

A concept central to the understanding of these entangled processes is that of the management of follicular cell resources, both on the follicular (intensity of selection) and ovarian (triggering and chronology of ovulation) scales. There is indeed a finely tuned balance between the production of new cells through proliferation, that increases the whole cell mass, and the maturation of cells, that increases their contribution to hormone secretion.

This concept has already been investigated on a mathematical ground. In [21], the author studied a minimal time problem in a simpler ODE framework, where the proliferating and differentiated cells were respectively pooled in a proliferating and a differentiated compartment. The main control variable was the cell cycle exit rate, the instantaneous rate of transfer from the proliferation compartment (corresponding here to the bottom part of the domain where $\gamma \leqslant \gamma_s$), where the cells divided (at a constant rate determined by the duration of the cell cycle) to the differentiation compartment, where cells could only mature. Under some assumptions concerning the initial number of follicular cells, the author proved by Pontryagin Maximum Principle (PMP) that the optimal strategy is a bang-bang control, which consists in applying permanently the minimal apoptosis rate and in switching once the cell cycle exit rate from its minimal bound to its maximal one. As expected intuitively, the optimal strategy consisted in applying a minimal apoptosis rate, which substantiates our assumption of no cell loss. Since the cell exit rate in the ODE framework is closely related to the vertical (maturity) velocity here, this result encouraged us to look for bang-bang optimal control.

Another control problem associated to the PDE conservation law was investigated in [44]. There, the authors focused on the follicular maturity at final time, in the sense that they looked for the set of initial conditions compatible with reaching a threshold maturity at a fixed final time. They described the sets of microscopic initial conditions compatible with either ovulation or atresia in the framework of backwards reachable set theory. Since these sets were largely overlapping, their results illustrate the prominent impact of cell dynamics control in the model.

In [75], which was also motivated by [45], the author reduced and simplified the model into a system of coupled ODEs, based on the asymptotic properties of the original law. The author focused on the issue of the selection process in a game theory approach, where one follicle plays against all the other ones. After giving some assumptions on velocities according to biological observations, the model is amenable to analysis by bifurcation theory, that allows one to predict the issue of the selection for one specific follicle amongst the whole population. Whether the follicle becomes atretic (doomed) or ovulatory (saved) depends on the follicular cell mass reached at the time when all cells stop proliferating. However, this work did not deal directly with the control problem where the control acts directly on the velocity terms.

Compared in literature of general control problems, this control problem is quite different, since the control terms appear in the flux. While in the literature, most monographs study the case where the controls are either applied inside of the domain (see [34]) or on the boundary (see [32, 39, 46, 76]). For the moment, we consider a more tractable problem which is centered on defining the optimal local control u_f corresponding to a single ovulatory trajectory. This assumption remains bearable in the therapeutic context of mild ovarian stimulation, that aims at getting one ovulatory follicle by a finely tuned control of FSH levels. In chapter 3, we consider an optimal control problem that consists in maximizing the final maturity for a

given target time. We have made several simplifications on the model dynamics.

A_1. We consider only one developing follicle, i.e. $f = 1$;

A_2. There is no loss term anymore, i.e. $\lambda = 0$;

A_3. The age velocity is uncontrolled, i.e. $g_f \equiv 1$;

A_4. The cell division is represented by a new gain term;

A_5. The target maturity M_s can always be reached in finite time.

Simplification (A_1) means that, in this problem, we are specially interested in the coupling between the condition needed to trigger the ovulation, on the one hand, and the control of the follicular cell dynamics, on the other hand. We consider this interaction independently of the process of follicle selection, in the sense that we isolate the dynamics of one specific follicle, as if we could ignore the influence of the other growing follicles.

(A_2) to (A_4) allow us to simplify the cell dynamics. In (A_2), we neglect the cell death (apoptosis), which is quite natural when considering only ovulatory trajectories, while, in (A_3), we consider that the cell age evolves as time (so that the cell duration is constant and uncontrolled). Moreover, the cell division process is distributed over ages with (A_4), so that there is a new gain term in the model instead of the former mitosis transfer condition. Even if the way that cell proliferation is represented is less realistic (no real mitosis), this does not impact the dynamics too much as long as the average cell cycle duration is preserved.

Even if it is simplified, the problem studied here still captures the essential question of the compromise between proliferation and differentiation that characterizes terminal follicular development. On the one hand, the follicle can benefit from a strong and quick enlargement of its cell population. On the other hand, this enlargement occurs at the expense of the maturation of individual cells. This compromise was instanced here as a problem of composition of velocities. A relatively high aging velocity tends to favor cell mass production while a relatively high maturation velocity tends to favor an increase in the average cell maturity.

Assumptions (A_2) allows us to replace the minimal time criterion (48) by a criterion that consists in maximizing the final maturity. It can be noticed that in the initial control problem, there might be no optimal solution without assumption (A_5), if the target maturity is higher than the maximal asymptotic reachable maturity.

Under these simplifying assumptions, we shifted, for sake of technical simplicity, to an equivalent problem where the final time is fixed and the optimality criterion is the follicular maturity at final time. On the biological ground, this means that for any chosen final time t_1, the resulting maturity at final time $M(t_1)$ can be chosen in turn as a maturity target which would be reached in minimal time at time t_1.

We denote by $\rho(t, x, y)$ the density function which satisfies the following conservation law on a fixed time horizon:

$$\rho_t + \rho_x + ((a(y) + b(y)u)\rho)_y = c(y)\rho, \quad t \in (t_0, t_1),\, x > 0,\, y > 0, \tag{49}$$

where

$$a(y) := -y^2, \quad b(y) := c_1 y + c_2, \tag{50}$$

and

$$c(y) := \begin{cases} c_s, & \text{if } y \in [0, y_s), \\ 0, & \text{if } y \in [y_s, \infty), \end{cases} \tag{51}$$

with y_s, c_s, c_1 and c_2 given strictly positive constants.

We assume that there is no outer influx, i.e.

$$\rho(t, 0, y) = \rho(t, x, 0) = 0, \quad \forall t \in (t_0, t_1),\ x > 0,\ y > 0. \tag{52}$$

The initial condition is

$$\rho(0, x, y) = \rho_0(x, y),\ x \geqslant 0,\ y \geqslant 0, \tag{53}$$

we study the case where ρ_0 is a positive Borel measure on $\mathbb{R} \times \mathbb{R}$ with a compact support included in $[0, 1] \times [0, y_s]$.

For any admissible control $u \in L^\infty((t_0, t_1); [w, 1])$, where $0 < w < 1$, we define the cost function

$$J(u) := -\int_0^{+\infty} \int_0^{+\infty} y \, d\rho(t_1, x, y), \tag{54}$$

and we want to study the following optimal control problem:

$$\text{minimize } J(u) \text{ for } u \in L^\infty((t_0, t_1); [w, 1]). \tag{55}$$

The idea is to first approximate the density by finite Dirac masses, and give optimal control results for finite Dirac masses. Then, we pass to the limit to get optimal control results for the PDE case.

We choose the initial data $\rho_0 \geqslant 0$ as a linear combination of a finite number of Dirac masses. For $(\alpha, \beta)^{\mathrm{tr}} \in \mathbb{R}^2$, we denote by $\delta_{\alpha,\beta}$ the Dirac mass at $(\alpha, \beta)^{\mathrm{tr}}$. We assume that, for some positive integer N, there exist a sequence $((x_1^{k0}, x_2^{k0}))_{k \in \{1,\dots,N\}}$ of elements in $[0, 1] \times [0, y_s]$ and a sequence $(x_3^{k0})_{k \in \{1,\dots,N\}}$ of strictly positive real numbers such that

$$\rho_0 := \sum_{k=1}^{N} x_3^{k0} \delta_{x_1^{k0}, x_2^{k0}}.$$

We arrive to consider the following optimal control problem:

$$\begin{cases} \dot{x}^k = f(x^k, u), \quad u \in L^\infty((t_0, t_1); [w, 1]), \quad t \in [t_0, t_1], \\ x^k(t_0) = x^{k0}, \end{cases}$$

where

$$f(x^k, u) = \begin{pmatrix} 1 \\ a(x_2^k) + b(x_2^k)\, u \\ c(x_2^k)\, x_3^k \end{pmatrix}, \ x^k = \begin{pmatrix} x_1^k \\ x_2^k \\ x_3^k \end{pmatrix}, \ x^{k0} = \begin{pmatrix} x_1^{k0} \\ x_2^{k0} \\ x_3^{k0} \end{pmatrix}.$$

The cost function now becomes

$$J(u) = -\int_{t_0}^{t_1} \big(a(x_2) + b(x_2)u + c(x_2)x_2\big)x_3\,dt - x_2^0 x_3^0 \to \text{minimize} \tag{56}$$

The main difference between this optimal control problem and the classical optimal control problem [79] is that the integrand of the functional J is discontinuous (see [81, 82, 83]). This fact considerably complicates the analysis of problem (56), in particular, this fact does not allow one to derive necessary optimality conditions by applying directly the standard apparatus of the theory of extremal problems [16, 60].

In [87], the author studied the case of a general functional that includes both the discontinuous characteristic function and continuous terms. There, the author consider the following optimal control problem

$$\begin{cases} \dot{x} = f(x,u),\ u \in U,\ t \in [0,T], \\ x(0) \in M_0,\ x(T) \in M_1, \\ J(x,u,T) = \int_0^T (p(x,u) + q(x)\delta_M(x))\,dt \to \text{ minimize}. \end{cases} \tag{57}$$

Here, $x = (x_1, \cdots, x_n) \in \mathbb{R}^n$, $u = (u_1, \cdots, u_m) \in \mathbb{R}^m$, U is a nonempty convex compact set in $\mathbb{R}^m$, M_0 and M_1 are nonempty closed sets in $\mathbb{R}^n$, and δ_M is the characteristic function of a given closed set M in $\mathbb{R}^n$. The set M is defined by a scalar function $g(x)$

$$M = \{x \in \mathbb{R}^n | g(x) \leqslant 0\}.$$

Here, f, g, p and q are all smooth enough. The final time $T \geqslant 0$ of the control process is assumed to be free. The class of admissible controls in problem (57) consists of all measurable bounded functions u such that $u(t) \in U$ for almost every $t \in [0,T]$. The main method the author used in [87] to study problem (57) is an approximation method [6, 8].

One of the difficulties of our problem is that both the integrand of the cost function and the dynamics are discontinuous. However, we can nevertheless use the same approximation method as in [87] to tackle with our control problem. This method consists in approximating the original discontinuous optimal control problem by a sequence of well chosen classical optimal control problems depending on optimal control u^* and then passing to the limit with respect to the perturbation parameter in the relations of the necessary optimality conditions for the approximating problems. When the target time is large enough (to guarantee that all the cells will exit to phase 3) and under some assumptions on the parameters, after applying PMP, we give some optimal results in the case where Dirac masses are used as a rough approximation of the density. We have proved that for finite Dirac masses, every optimal control is bang-bang control with one single switching time. We also give some numerical illustrations to complete our theoretical results. Finally, we go back to the original PDE formulation of the model. By passing to the limit, we have proved that there exists an optimal bang-bang control with one single switching time (see chapter 3).

6.4 Numerical observations

In chapter 4, we go back to the very original model with discontinuous mitosis boundary conditions. To make the final time coincide with the ovulation time, we assumed in chapter 3 that it is large enough to guarantee that all cells will stop proliferating. In the numerical study part, we are also interested in the case where the final time is not so large, which helps us to understand the cell dynamics in more depth.

Some biologically observable variables can be derived from the cell density in the model. The total cell number, that can be counted on dissected follicles [88], is equivalent to the zero-order moment of the density:

$$M^0(t) = \sum_{f=1}^{n} \sum_{j=1}^{3} \sum_{k=1}^{N} \int_0^{\gamma_m} \int_0^{a_m} \phi_{j,k}^f(t, a, \gamma)\, da\, d\gamma.$$

We show in chapter 4 how to compute the zero order moment by judging how many cycles the cells will progress. We can also get information on how the cell population is divided into proliferating cells and differentiated ones, through what is known as the growth fraction (GF) defined as (see [78])

$$GF(t) = \frac{\displaystyle\sum_{f=1}^{n} \sum_{j=1}^{2} \sum_{k=1}^{N} \int_0^{\gamma_s} \int_0^{a_m} \phi_{j,k}^f(t, a, \gamma)\, da\, d\gamma}{M^0(t)}.$$

Even if it is not straightforward, due to both the simplifications needed to study the control problem and the scarcity of kinetic biological data, to make quantitative comparisons, we can make use of the following principles:

- The growth fraction decreases steadily in the course of terminal follicle development, so that we can deduce that the final time in the problem is expected to occur after the exit time (the time when every cells have exited the proliferation domain).
- The most reliable information concerns the total cell number M^0 at initial and final times. In the case of the ewe, the ratio of increase between $M^0(0)$ and $M^0(t_1)$ can be targeted to a range of 20 to 30. With a constant growth fraction of one ($GF = 1$, no differentiated cells), this duration would roughly correspond to the cells progressing through 4 to 5 cell cycles (when all cells are proliferating, the doubling time equals the cell cycle duration). Since the growth fraction decreases ($GF < 1$), the time elapsed from the beginning to the final time is expected to be longer: a duration equivalent to 6 (or possibly 7) cell cycles (which is consistent with the number of doublings observed in the population).

We found there is a threshold for the target time such that, before this threshold, the optimal control is to give always minimal value of the admissible control. After this threshold, the optimal control is to give always the maximal value of control.

Then we study the evolution of the maturity with bang-bang control. We observe that bang-bang control is better than constant control. By computing the zero-order moment and asymptotic maturity, we prove that for any constants $a < b$ in admissible control, the switching direction $a \to b$ is better than $b \to a$. We finally prove that for fixed target time t_1, which is determined by biological considerations, the optimal strategy consists in switching the maturity velocity from its minimal bound to its maximal bound, which coincides with the result we obtained in chapter 3.

7 A model of an amplification protocol for misfolded proteins

Growth and fragmentation is a common phenomenon for a structured population. It arises for instance in a context of cell division ([1, 9, 10, 11, 40, 44, 48, 57, 74, 77]). The prion's proteins are responsible of spongiform encephalopaties and appear in the form of aggregates in infected cells. Such polymers grow attaching non infectious monomers and converting them into infectious ones. On the other hand, they increase their number by splitting (see [42]).

A promising tool to design a diagnosis test is the protein misfolded cyclic amplification (PMCA) technique [65]. The PMCA principle is based on the "protein-only hypothesis". According to this widely accepted hypothesis, the infectious agent of TSE, known as prions, may consist in misfolded proteins called PrPsc (for Prion Protein scrapie). The PrPsc replicates in a self-propagating process, by converting the normal form of PrPc (called PrPc for Prion Protein cellular) into PrPsc. The PMCA enabled to consolidate the idea of an autocatalytic replication of PrPsc by nucleated polymerization [19, 90, 91]. In this model, PrPsc is considered to be a polymeric form of PrPc. Polymers can lengthen by addition of PrPc monomers, and they can replicate by splitting into smaller fragments. The PrPc is mainly expressed by the cells of the central nervous system, so PrPsc concentrates in this zone. The amount of PrPsc in tissues like blood is very small and this is why it is very difficult to diagnose an infected individual. The PMCA mimics the nucleation/polymerization mechanism occurring *in vivo* with the aim to quickly amplify polymers present in minute amount in an infected sample. This technique could allow to detect PrPsc in samples of blood for instance. But for now it is not efficient enough to do so. Mathematical modelling and optimization tools can help to optimize the PMCA protocol.

Masel *et al.* [72] proposed a mathematical model for the nucleated polymerziation. We start from it and introduce a *sonication* parameter to model the PMCA. In the PMCA protocol, the monomers of PrPc are in large excess, so their quantity varies little during the experiment. We assume that this variation is small enough to be neglected and the quantity of monomers is supposed to be constant in time. Let us denote by $x_i(t)$ the density of polymers composed of $i \in \mathbb{N}$ PrPsc proteins at time t. Then the evolution of the quantity of polymers

is given by the coupled system of ODEs

$$\frac{dx_i}{dt} = -r(u(t))(\tau_i x_i - \tau_{i-1}x_{i-1}) - u(t)\beta_i x_i + 2u(t)\sum_{j=i+1}^{n} \beta_j\, \kappa_{i,j}\, x_j\ , \quad \text{for } 1 \leqslant i \leqslant n\ . \quad (58)$$

The polymers of size i split into smaller aggregates with the rate β_i. This rate is modulated by the *sonication* parameter $u(t)$ as a control which reflects the intensity of ultrasounds *sonication*. We write this problem under a matrix form

$$\begin{cases} \dot{X}(t) = M(u(t))\, X(t), & t > 0, \\ X(t=0) = X^0, \end{cases}$$

where $X(t) = (x_i(t))_{1\leqslant i\leqslant n}^{tr}$ is the size-distribution of polymers and $M(u) := uF + r(u)G$ with G the growth matrix and F the fragmentation matrix as

$$G = \begin{pmatrix} -\tau_1 & & & & \\ \tau_1 & -\tau_2 & & & \\ & \ddots & \ddots & & \\ & & & \tau_{n-2} & -\tau_{n-1} \\ & & & & \tau_{n-1} \quad 0 \end{pmatrix}, \quad F = \begin{pmatrix} 0 & & & \\ & -\beta_2 & & (2\kappa_{ij}\beta_j)_{i<j} \\ & & \ddots & \\ & 0 & & \\ & & & -\beta_n \end{pmatrix}.$$

The coefficients of these matrices are assumed to be positive

$$\forall i \in [1, n-1], \qquad \tau_i > 0 \quad \text{and} \quad \beta_{i+1} > 0.$$

Then the optimization problem we are interested in is to find a control $u(t)$ that maximizes the final quantity of PrPsc

$$\psi(X(T)) := \sum_{i=1}^{n} i\, x_i(T) \quad \to \text{maximize} \quad (59)$$

for a given final time of experiment T. Indeed the presence of PrPsc can be detected experimentally (by Western Blot, see [65] for more details) only if this quantity is greater than a critical threshold.

When r is nonlinear, the velocity set

$$\mathcal{V}(X) := \{(uF + r(u)G)X,\ u \in [u_{min}, u_{max}]\}$$

is not convex, and we cannot ensure the existence of an optimal control. Nevertheless, we can solve a so-called *optimal relaxed control problem* (see [63] for instance). To explain this, we rewrite our original optimal control problem as follows: find

$$(u_1^*(t), u_2^*(t)) \in \Omega := \{(u_1, u_2) \mid u_2 = r(u_1)\}$$

which maximizes $\psi(X(T))$ with X solution to

$$\begin{cases} \dot{X}(t) = \big(u_1(t)F + u_2(t)G\big)\, X(t), \qquad t > 0, \\ X(0) = X^0. \end{cases}$$

In this case, the relaxed control problem consists in finding $(u_1^*(t), u_2^*(t))$ in the convex hull $H(\Omega)$ of Ω (see figure 8), which maximizes the payoff $\psi(X(T))$. For this convexified problem, the velocity set is given by the convex hull $H(\mathcal{V}(X))$ of $\mathcal{V}(X)$ and is thus convex. So there exists an optimal (relaxed) control and moreover the response $X^*(t)$ to this control is the uniform limit of responses to classical controls (see [63]). As a consequence, it is of interest to solve the optimal relaxed control problem.

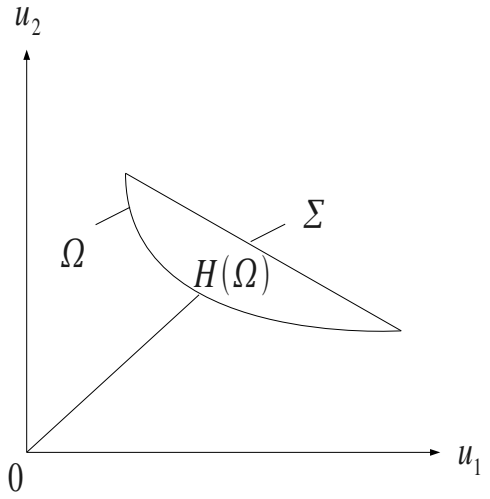


Figure 8. The convex hull $H(\Omega)$ of Ω in the case where r is decreasing and convex.

We modify the cost function as

$$\tilde{\psi}(X(T)) = \phi_1 \cdot X(T) \quad \rightarrow \text{maximize} \tag{60}$$

Suppose that the initial condition is given by

$$X(0) = V_1,$$

where V_1 and ϕ_1 is the first eigenvector, i.e. if we assume that $(\bar{u}_1, \bar{u}_2)$ is a pair which maximizes the Perron eigenvalue λ_1, then (V_1, ϕ_1, λ_1) is solution to the Perron eigenvalue problem

$$\begin{cases} \lambda_1 V_1 = (\bar{u}_1 F + \bar{u}_2 G)V_1, \\ \lambda_1 \phi_1 = \phi_1(\bar{u}_1 F + \bar{u}_2 G), \\ \lambda_1 > 0, \quad \phi_1 V_1 = 1. \end{cases} \tag{61}$$

Using PMP, we have proved that with the modified cost function (60), the constant control pair $(\bar{u}_1, \bar{u}_2)$ that maximizes the Perron eigenvalue is an optimal control to (60). For the original control problem (59), we have proved that for 2D case, the optimal control lies on Σ (see figure 8). Furthermore, the optimal control is bang-bang control with a constant control as the one that maximizes the Perron eigenvalue. For 3D case, we only prove that the optimal control lies on Σ (see figure 8).

8 Perspectives

The manufacturing system

- For 1D model of manufacturing system, it is also interesting to study the well-posedness in the case where the initial and the boundary conditions are distributed over a real Borel measure. A first difficulty lies in how to define a proper notion of solution.

- We may also consider a (possily nonlinear) source term (turning the conservation law into a balance law). The fixed point equation $W \to F(W)$ then becomes a bit more complicated, but a Lipschitz-bound on the source should be enough to make this map contractive.

  Moreover, we are interested in a further generalization of the work by taking λ discontinuous (for instance piecewise constant (PC) or bounded variation (BV)). The existence of solution ρ in $C^0((0,T); L^1(0,1))$ can then be obtained in the same way, but we should also verify $\rho(t,\cdot) \in PC(0,1)$ or $BV(0,1)$, provided that ρ_0 and u are both in PC or BV, respectively. This is inspired from a work [47] for the PC case.

- Concerning the optimal control problem, it is interesting to study the Gâteaux differentiability of the solution or the outflux with respect to initial or boundary conditions. In [26], the authors first present a rigorous result on the Gâteaux differentiability of the solution with respect to the initial condition. Then, based on the differentiability results, the authors state a necessary optimality condition. Since we can get explicit expression of the solution, it is feasible to compute directly the Gâteaux differentiability of the solution with respect to initial or boundary conditions.

The model of follicular ovulation

- Bang-bang control

  In chapter 3, we have proved that there exists an optimal bang-bang control with one single switching time, we conjecture that every optimal control is a bang-bang control with one single switching time for our PDE case. To handle this problem, we may first construct an auxiliary smooth optimal control problem and prove that for this smooth control problem, every optimal control is bang-bang control with one single switching

time. Then we can pass to the limit to prove that for discontinuous optimal control problem, every optimal control is bang-bang control.

- The case where the age velocity is also controllable

  Since now, we made assumption that the ageing velocity is constant, which is uncontrollable. Actually, the ageing velocity in phase 1 is also sensitive to FSH, hence it is also controllable. More precisely, it is interesting to study

  $$\rho_t + g(u)\rho_x + (h(y,u)\rho)_y = c\rho.$$

  With the controlled ageing velocity, we can account for the cell cycle and study precisely the phenomena related to both the age and the maturity of the cells. We can first consider finite Dirac masses as an approximation of the density. Then we can study PMP for this finite dimensional optimal control problem.

- Multiscale problem

  An important question is to consider the coupled development of two or more follicles as a closed loop multiscale problem of selection. We could first consider two follicles with different densities at initial time and search for optimal controls that maximize the global maturity at a final given time. Then this strategy could be to implement through numerical computation to predict the fate of the follicles (ovulation or atresia).

- Numerical observations give us the relation between optimal switching time and the saturating value a and b (see section 4.3.3). We found that the optimal switching time is increasing as the maximal saturating value b is decreasing. It is still interesting to study this phenomena theoretically.

- In chapter 2, we use Banach fixed point theorem to prove the existence of the solution, which can be used to compute the solution to the Cauchy problem numerically.

The model of an amplification protocol for misfolded proteins

- For the modified version of cost function (60) (see section 5.3.1), we have proved the constant control that maximizes the Perron eigenvalue satisfies PMP. It is still unknown whether this is the only control that satisfies PMP.

- We consider the optimal control problem with the original cost function (59). For 2D case, using PMP, we have proved that the optimal control is bang-bang control, furthermore, the optimal control is the value that maximizes the Perron eigenvalue. It is still interesting to study 3D case to see what is the optimal control. For the moment, we can only get that the optimal control lies on the boundary Σ (see section 5.3.2). According to numerical simulation, it may happen that the optimal control is not a bang-bang control. For any dimension, we conjecture that the optimal control lies on

Σ. An idea could be to use calculus of variation to prove that the derivative of the cost with respect to a variation $\tilde{U}(t) = \sigma U(t)$ ($\sigma > 1$) is positive.

- We consider another related optimal control problem with the original cost function (59) (see section 5.3.2), but together with a terminal constraint

$$\begin{aligned} \psi(X(T)) := \sum_{i=1}^{n} i\, x_i(T) \quad &\rightarrow \text{maximize}, \\ X(T) = CV_1, \quad & \end{aligned} \tag{62}$$

for a constant $C > 0$. For this optimal control problem with terminal constraint, using PMP, we can also derive a necessary optimality condition. From this necessary optimality condition, we conjecture that every optimal control lies on the line Σ.

Chapter 1

Analysis and control of a scalar conservation law modeling a highly re-entrant manufacturing system

In this chapter, we study a scalar conservation law that models a highly re-entrant manufacturing system as encountered in semi-conductor production. As a generalization of [35], the velocity function possesses both the local and nonlocal character. We prove the existence and uniqueness of the weak solution to the Cauchy problem with initial and boundary data in L^∞. We also obtain the stability (continuous dependence) of both the solution and the out-flux with respect to the initial and boundary data. Finally, we prove the existence of an optimal control that minimizes, in the L^p-sense with $1 \leqslant p \leqslant \infty$, the difference between the actual out-flux and a forecast demand over a fixed time period. This article has appeared in Journal of Differential Equations (see [86]).

1.1 Introduction and main results

We study the scalar conservation law

$$\rho_t(t,x) + (\rho(t,x)\lambda(x,W(t)))_x = 0, \quad t \geq 0, 0 \leqslant x \leqslant 1, \tag{1.1}$$

where

$$W(t) = \int_0^1 \rho(t,x)dx$$

is the total quantity of the products. We assume that the velocity function $\lambda > 0$ is continuous differentiable, i.e., $\lambda \in C^1([0,1] \times [0,\infty))$, in the whole chapter. For instance, we recall that the special case of

$$\lambda(x,W) = \frac{1}{1+W}$$

was used in [5, 62].

This work is motivated by problems arising in the control of semiconductor manufacturing systems which are characterized by their highly re-entrant feature. This character is, in

particular, described in terms of the velocity function λ in the model: it is a function of the total mass $W(t)$ (the integral of the density ρ). As a generalization of [35] (in which $\lambda = \lambda(W(t))$), here we assume that the velocity λ varies also with respect to the local position x, as can be naturally encountered in practice. These phenomena also appear in some biological models (modeling the development of ovarian follicles, see [44, 45]).

In the manufacturing system, with a given initial data

$$\rho(0, x) = \rho_0(x), \quad 0 \leqslant x \leqslant 1, \tag{1.2}$$

the natural control input is the in-flux, which suggests the boundary condition

$$\rho(t, 0)\lambda(0, W(t)) = u(t), \quad t \geq 0. \tag{1.3}$$

Motivated by applications, one natural control problem is related to the *Demand Tracking Problem (DTP)*. The objective of *DTP* is to minimize the difference between the actual out-flux $y(t) = \rho(t, 1)\lambda(1, W(t))$ and a given demand forecast $y_d(t)$ over a fixed time period. An alternative control problem is *Backlog Problem (BP)*. The objective of *BP* is to minimize the difference between the number of the total products that have left the factory and the number of the total demanded products over a fixed time period. The backlog of a production system at a given time t is defined as

$$\beta(t) = \int_0^t \rho(s, 1)\lambda(1, W(s))ds - \int_0^t y_d(s)ds.$$

The backlog $\beta(t)$ can be negative or positive, with a positive backlog corresponding to over-production and a negative backlog corresponding to a shortage.

Partial differential equation models for such manufacturing systems are motivated by the very high volume (number of parts manufactured per unit time) and the very large number of consecutive production steps. They are popular due to their superior analytic properties and the availability of efficient numerical tools for simulation. For more detailed discussions, see e.g. [4, 5, 58, 62]. In many aspects these models are quite similar to those of traffic flows [25] and pedestrian flows [27, 28, 37].

The hyperbolic conservation laws and related control problems have been widely studied for a long time. The fundamental problems include the existence, uniqueness, regularity and continuous dependence of solutions, controllability, asymptotic stabilization, existence and uniqueness of optimal controls. For the well-posedness problems, we refer to the works [13, 14, 64, 71] (and the references therein) in the content of weak solutions to systems (including scalar case) in conservation laws, and [66, 70] in the content of classical solutions to general quasi-linear hyperbolic systems. For the controllability of linear hyperbolic systems, one can see the important survey [84]. The controllability of nonlinear hyperbolic equations (or systems) are studied in [30, 33, 50, 55, 59, 67, 68, 89], while the attainable set and asymptotic stabilization of conservation laws can be found in [2, 3]. In particular, [31] provides

a comprehensive survey of controllability and stabilization in partial differential equations that also includes nonlinear conservation laws.

We prove the existence, uniqueness and regularity of the weak solution to Cauchy problem (1.1), (1.2) and (1.3) with initial and boundary data in L^∞. The main approach is the characteristic method. We point out here that in the previous paper [35], the authors obtained the well-posedness for L^p $(1 \leqslant p < \infty)$ data. The L^∞ assumption in this work is due to the fact that the velocity function λ depends on the space variable x. Using the implicit expression of the solution in terms of the characteristics, we also prove the stability (continuous dependence) of both the solution and the out-flux with respect to the initial and boundary data. The stability property guarantees that a small perturbation to the initial and (or) boundary data produces also only a small perturbation to the solution and the out-flux.

The optimal control problem that we study is related to the *Demand Tracking Problem*. This problem is motivated by [35] and originally inspired by [62]. The objective is to minimize the L^p-norm with $1 \leqslant p \leqslant \infty$ of the difference between the actual out-flux $y(t) = \rho(t,1)\lambda(1, W(t))$ and a given demand forecast $y_d(t)$ over a fixed time period. With the help of the implicit expression of the weak solution and by compactness arguments, we prove the existence of solutions to this optimal control problem.

The main difficulty comes from the nonlocal velocity in the model. A related manuscript [27], which is also motivated in part by [5, 62], addressed well-posedness for systems of hyperbolic conservation laws with a nonlocal velocity in $\mathbb{R}^n$. The authors studied the Cauchy problem in the whole space $\mathbb{R}^n$ without considering any boundary conditions and they also gave a necessary condition for the possible optimal controls. However, the method of proof and even the definition of solutions are different from ours. Another scalar conservation law with nonlocal velocity is to model sedimentation of particles in a dilute fluid suspension, see [93] for the well-posedness of the Cauchy problem. In this model, the nonlocal velocity is due to a convolution of the unknown function with a symmetric smoothing kernel. There are also some other 1D models with nonlocal velocity, either in divergence form or not, which are related to the 3D Navier-Stokes equations or the Euler equations in the vorticity formulation. Nevertheless, the nonlocal character in these models comes from a singular integral of the unknown function (see [38] and the references therein, especially [29]).

First in section 1.2 some basic notations and assumptions are given. Next in section 1.3 we prove the existence and uniqueness of the weak solution to Cauchy problem (1.1), (1.2) and (1.3) with initial data $\rho_0 \in L^\infty(0,1)$ and boundary data $u \in L^\infty(0,T)$. Some remarks on the regularity of the weak solution to the Cauchy problem are also given in section 1.3. In section 1.4 we establish the stability of the weak solution and the out-flux with respect to the initial and boundary data. Then in section 1.5, we prove the existence of the solution to the optimal control problem of minimizing the L^p-norm $(1 \leqslant p \leqslant \infty)$ of the difference between the actual and any desired (forecast) out-flux. Finally in the appendix, we give two basic lemmas and the proofs of Lemmas 1.3.1-1.3.2 that are used in section 1.3.

1.2 Preliminaries

First we introduce some notations which will be used in the whole chapter:

$$
\begin{aligned}
&L^\infty_+(0,1) := \{f \in L^\infty(0,1)\colon f \text{ is nonnegative almost everywhere}\},\\
&L^\infty_+(0,T) := \{f \in L^\infty(0,T)\colon f \text{ is nonnegative almost everywhere}\},\\
&\|\rho_0\|_{L^\infty} := \|\rho_0\|_{L^\infty(0,1)} := \operatorname*{ess\,sup}_{x\in(0,1)} |\rho_0(x)|,\\
&\|u\|_{L^\infty} := \|u\|_{L^\infty(0,T)} := \operatorname*{ess\,sup}_{t\in(0,T)} |u(t)|
\end{aligned}
$$

and

$$M := \|u\|_{L^1(0,T)} + \|\rho_0\|_{L^1(0,1)}, \tag{1.4}$$

$$\overline{\lambda}(M) := \inf_{(x,W)\in[0,1]\times[0,M]} \lambda(x,W) > 0, \tag{1.5}$$

$$\|\lambda\|_{C^0} := \|\lambda\|_{C^0([0,1]\times[0,M])} := \sup_{(x,W)\in[0,1]\times[0,M]} |\lambda(x,W)|, \tag{1.6}$$

$$\|\lambda_x\|_{C^0} := \|\lambda_x\|_{C^0([0,1]\times[0,M])} := \sup_{(x,W)\in[0,1]\times[0,M]} |\lambda_x(x,W)|, \tag{1.7}$$

$$\|\lambda_W\|_{C^0} := \|\lambda_W\|_{C^0([0,1]\times[0,M])} := \sup_{(x,W)\in[0,1]\times[0,M]} |\lambda_W(x,W)|. \tag{1.8}$$

We also define the characteristic curve $\xi = \xi(s;t,x)$, which passes through the point (t,x), by the solution to the ordinary differential equation

$$\frac{d\xi}{ds} = \lambda(\xi(s), W(s)), \quad \xi(t) = x, \tag{1.9}$$

where W is a continuous function. The existence and uniqueness of the solution to (1.9) is guaranteed by the assumption that $\lambda \in C^1([0,1]\times[0,\infty))$ with $|W(s)| \leqslant M$ for all s. The characteristic curve ξ is frequently used afterward and it is precisely illustrated in different situations.

1.3 Well-posedness of Cauchy problem with L^∞ data

First we recall, from [31, section 2.1], the usual definition of a weak solution to Cauchy problem (1.1), (1.2) and (1.3).

Definition 1.3.1. Let $T > 0$, $\rho_0 \in L^\infty(0,1)$ and $u \in L^\infty(0,T)$ be given. A weak solution of Cauchy problem (1.1), (1.2) and (1.3) is a function $\rho \in C^0([0,T]; L^1(0,1)) \cap L^\infty((0,T)\times(0,1))$ such that, for every $\tau \in [0,T]$ and every $\varphi \in C^1([0,\tau]\times[0,1])$ with

$$\varphi(\tau,x) = 0,\ \forall x \in [0,1] \quad \text{and} \quad \varphi(t,1) = 0,\ \forall t \in [0,\tau],$$

one has

$$\int_0^\tau \int_0^1 \rho(t,x)(\varphi_t(t,x)+\lambda(x,W(t))\varphi_x(t,x))dxdt + \int_0^\tau u(t)\varphi(t,0)dt + \int_0^1 \rho_0(x)\varphi(0,x)dx = 0.$$

Theorem 1.3.1. *Let $T>0$, $\rho_0 \in L^\infty_+(0,1)$ and $u \in L^\infty_+(0,T)$ be given, then Cauchy problem (1.1), (1.2) and (1.3) admits a unique weak solution $\rho \in C^0([0,T];L^1(0,1)) \cap L^\infty((0,T)\times(0,1))$, which is nonnegative almost everywhere in $[0,T]\times[0,1]$. Moreover, the weak solution ρ even belongs to $C^0([0,T];L^p(0,1))$ for all $p \in [1,\infty)$.*

Proof. Our proof is partly inspired from [33]. We first prove the existence of weak solution for small time: there exists a small $\delta \in (0,T]$ such that Cauchy problem (1.1), (1.2) and (1.3) has a weak solution $\rho \in C^0([0,\delta];L^1(0,1)) \cap L^\infty((0,\delta)\times(0,1))$. The idea is first to prove that the total mass $W(t)$ exists as a fixed point of a map $W \mapsto F(W)$, and then to construct a (unique) solution to the Cauchy problem.

Let

$$\Omega_{\delta,M} := \Big\{ W \in C^0([0,\delta]) \colon \|W\|_{C^0[0,\delta]} := \sup_{0\leqslant t\leqslant \delta} |W(t)| \leqslant M \Big\}, \tag{1.10}$$

where the constant M is given by (1.4).

For any small $\delta > 0$, we define a map $F : \Omega_{\delta,M} \to C^0([0,\delta])$, $W \mapsto F(W)$, as

$$F(W)(t) := \int_0^t u(\alpha)d\alpha + \int_0^{1-\int_0^t \lambda(\xi_1(\theta),W(\theta))d\theta} \rho_0(\beta)d\beta, \quad \forall t \in [0,\delta], \tag{1.11}$$

where ξ_1 (see figure 1.1 or figure 1.2) represents the characteristic curve passing through $(t,1)$ which is defined by

$$\frac{d\xi_1}{ds} = \lambda(\xi_1(s),W(s)), \quad \xi_1(t) = 1. \tag{1.12}$$

Here we remark that the formulation of $F(W)$ is induced by solving the corresponding *linear Cauchy problem* (1.1), (1.2) and (1.3) in which $W(\cdot) \in \Omega_{\delta,M}$ is known. It is obvious that F maps into $\Omega_{\delta,M}$ itself if

$$0 < \delta \leqslant \min\Big\{ \frac{1}{\|\lambda\|_{C^0}}, T \Big\}.$$

Now we prove that, if δ is small enough, F is a contraction mapping on $\Omega_{\delta,M}$ with respect to the C^0 norm. Let $W, \overline{W} \in \Omega_{\delta,M}$ and for any fixed $t \in [0,T]$, we define $\overline{\xi}_1$ by

$$\frac{d\overline{\xi}_1}{ds} = \lambda(\overline{\xi}_1(s),\overline{W}(s)), \quad \overline{\xi}_1(t) = 1.$$

Then, we have for every $t \in [0,\delta]$ that

$$\begin{aligned}
|F(\overline{W})(t) - F(W)(t)| &= \Big| \int_{1-\int_0^t \lambda(\xi_1(\theta),W(\theta))d\theta}^{1-\int_0^t \lambda(\overline{\xi}_1(\theta),\overline{W}(\theta))d\theta} \rho_0(\beta)d\beta \Big| \\
&\leqslant \|\rho_0\|_{L^\infty} \cdot \Big| \int_0^t (\lambda(\overline{\xi}_1(\theta),\overline{W}(\theta)) - \lambda(\xi_1(\theta),W(\theta)))d\theta \Big| \\
&\leqslant t\|\rho_0\|_{L^\infty} \cdot \Big(\|\lambda_x\|_{C^0}\|\overline{\xi}_1 - \xi_1\|_{C^0([0,t])} + \|\lambda_W\|_{C^0}\|\overline{W} - W\|_{C^0([0,\delta])} \Big).
\end{aligned}$$

By the definitions of ξ_1 and $\overline{\xi}_1$, we obtain

$$\begin{aligned}
&\|\overline{\xi}_1-\xi_1\|_{C^0([0,t])}=\sup_{0\leqslant\theta\leqslant t}|\overline{\xi}_1(\theta)-\xi_1(\theta)|\\
&=\sup_{0\leqslant\theta\leqslant t}\Big|\int_\theta^t(\lambda(\overline{\xi}_1(\sigma),\overline{W}(\sigma))-\lambda(\xi_1(\sigma),W(\sigma)))d\sigma\Big|\\
&\leqslant t\|\lambda_x\|_{C^0}\|\overline{\xi}_1-\xi_1\|_{C^0([0,t])}+t\|\lambda_W\|_{C^0}\|\overline{W}-W\|_{C^0([0,\delta])},
\end{aligned}$$

thus

$$\|\overline{\xi}_1-\xi_1\|_{C^0([0,t])}\leqslant\frac{t\|\lambda_W\|_{C^0}}{1-t\|\lambda_x\|_{C^0}}\cdot\|\overline{W}-W\|_{C^0([0,\delta])}. \tag{1.13}$$

Therefore,

$$|F(\overline{W})(t)-F(W)(t)|\leqslant\frac{t\|\rho_0\|_{L^\infty}\|\lambda_W\|_{C^0}}{1-t\|\lambda_x\|_{C^0}}\cdot\|\overline{W}-W\|_{C^0([0,\delta])},\quad\forall t\in[0,\delta].$$

Let δ be such that

$$0<\delta\leqslant\min\Big\{\frac{1}{2\|\lambda_x\|_{C^0}},\frac{1}{4\|\rho_0\|_{L^\infty}\|\lambda_W\|_{C^0}},\frac{1}{\|\lambda\|_{C^0}},T\Big\}, \tag{1.14}$$

then

$$\|F(\overline{W})-F(W)\|_{C^0([0,\delta])}\leqslant\frac{1}{2}\|\overline{W}-W\|_{C^0([0,\delta])}.$$

By means of the contraction mapping principle, there exists a unique fixed point $W=F(W)$ in $\Omega_{\delta,M}$:

$$W(t)=F(W)(t)=\int_0^t u(\alpha)d\alpha+\int_0^{1-\int_0^t\lambda(\xi_1(\theta),W(\theta))d\theta}\rho_0(\beta)d\beta,\quad\forall t\in[0,\delta].$$

Moreover, W is Lipschitz continuous:

$$W(t)=W(0)+\int_0^t W'(s)ds,$$

with

$$W'(t)=u(t)-\lambda(\xi_1(t),W(t))\rho_0(1-\int_0^t\lambda(\xi_1(\theta),W(\theta))d\theta),\quad a.e.\ t\in[0,\delta],$$

and thus

$$\|W'\|_{L^\infty(0,\delta)}\leqslant\|u\|_{L^\infty}+\|\lambda\|_{C^0}\|\rho_0\|_{L^\infty}. \tag{1.15}$$

Now we define the characteristic curve ξ_2 which passes through the origin (see figure 1.1 and figure 1.2) by

$$\frac{d\xi_2}{ds}=\lambda(\xi_2(s),W(s)),\quad\xi_2(0)=0. \tag{1.16}$$

And then for any fixed $t\in[0,\delta]$, we define the characteristic curves ξ_3,ξ_4 (see figure 1.1 and figure 1.2) which pass through (t,x) by

$$\frac{d\xi_3}{ds}=\lambda(\xi_3(s),W(s)),\quad\xi_3(t)=x,\quad\text{for } x\in[0,\xi_2(t)]. \tag{1.17}$$

$$\frac{d\xi_4}{ds}=\lambda(\xi_4(s),W(s)),\quad\xi_4(t)=x,\quad\text{for } x\in[\xi_2(t),1]. \tag{1.18}$$

From the uniqueness of the solution to the ordinary differential equation, we know that there exist $\alpha \in [0,\delta]$ and $\beta \in [0,1]$ such that

$$\xi_3(\alpha) = 0 \quad \text{and} \quad \xi_4(0) = \beta. \tag{1.19}$$

Now we define a function ρ by

$$\rho(t,x) := \begin{cases} \dfrac{u(\alpha)}{\lambda(0,W(\alpha))}\, e^{-\int_\alpha^t \lambda_x(\xi_3(\theta),W(\theta))d\theta}, & 0 \leqslant x \leqslant \xi_2(t), 0 \leqslant t \leqslant \delta, \\ \rho_0(\beta)\, e^{-\int_0^t \lambda_x(\xi_4(\theta),W(\theta))d\theta}, & 0 \leqslant \xi_2(t) \leqslant x, 0 \leqslant t \leqslant \delta, \end{cases} \tag{1.20}$$

which is obviously nonnegative almost everywhere in $(0,\delta)\times(0,1)$. Using the following two lemmas, we can prove that ρ defined by (1.20) is the unique weak solution to the Cauchy problem (1.1), (1.2) and (1.3).

Lemma 1.3.1. *The function ρ defined by* (1.20) *is a weak solution to Cauchy problem* (1.1), (1.2) *and* (1.3). *Moreover, the weak solution ρ even belongs to $C^0([0,\delta];L^p(0,1))$ for all $p \in [1,\infty)$ and the following two estimates hold for all $t \in [0,\delta]$:*

$$0 \leqslant W(t) = \|\rho(t,\cdot)\|_{L^1(0,1)} \leqslant M, \tag{1.21}$$

$$\|\rho(t,\cdot)\|_{L^\infty(0,1)} \leqslant e^{T\|\lambda_x\|_{C^0}} \cdot \max\left\{\|\rho_0\|_{L^\infty}, \frac{\|u\|_{L^\infty}}{\overline{\lambda}(M)}\right\}. \tag{1.22}$$

Lemma 1.3.2. *The weak solution to Cauchy problem* (1.1), (1.2) *and* (1.3) *is unique.*

We leave the proofs of Lemma 1.3.1 and Lemma 1.3.2 in the appendix.

Now we suppose that we have solved Cauchy problem (1.1), (1.2) and (1.3) to the moment $\tau \in (0,T)$ with the weak solution $\rho \in C^0([0,\tau];L^p(0,1)) \cap L^\infty((0,\tau)\times(0,1))$. Similar to Lemma 1.3.1 and Lemma 1.3.2, we know that this weak solution is given by

$$\rho(t,x) = \begin{cases} \rho_0(\beta)\, e^{-\int_0^t \lambda_x(\xi_4(\theta),W(\theta))d\theta}, & \text{if } 0 \leqslant \xi_2(t) \leqslant x \leqslant 1, 0 \leqslant t \leqslant \tau, \\ \dfrac{u(\alpha)}{\lambda(0,W(\alpha))}\, e^{-\int_\alpha^t \lambda_x(\xi_3(\theta),W(\theta))d\theta}, & \text{else.} \end{cases}$$

Moreover, the two uniform a priori estimates (1.21) and (1.22) hold for all $t \in [0,\tau]$. Hence we can choose $\delta \in (0,T)$ independent of τ such that (1.14) holds. Applying Lemma 1.3.1 and Lemma 1.3.2 again, the weak solution $\rho \in C^0([0,\tau];L^p(0,1))$, as well as estimates (1.21) and (1.22), is extended to the time interval $[\tau,\tau+\delta]\cap[\tau,T]$. Step by step, we finally have a unique global weak solution $\rho \in C^0([0,T];L^p(0,1)) \cap L^\infty((0,T)\times(0,1))$. This finishes the proof of Theorem 1.3.1. □

Remark 1.3.1. Let ρ be the weak solution in Theorem 1.3.1 and $W \in C^0([0,T])$ be the total mass function: $W(t) = \int_0^1 \rho(t,x)dx$. Let ξ_1,ξ_2,ξ_3,ξ_4 and α,β be defined by (1.12), (1.16), (1.17), (1.18) and (1.19), respectively. It follows from our proof of Theorem 1.3.1 that (see figure 1.3, figure 1.4 and figure 1.5)

$$\rho(t,x) = \begin{cases} \rho_0(\beta)\, e^{-\int_0^t \lambda_x(\xi_4(\theta),W(\theta))d\theta}, & \text{if } 0 \leqslant \xi_2(t) \leqslant x \leqslant 1, 0 \leqslant t \leqslant T, \\ \dfrac{u(\alpha)}{\lambda(0,W(\alpha))}\, e^{-\int_\alpha^t \lambda_x(\xi_3(\theta),W(\theta))d\theta}, & \text{else.} \end{cases} \tag{1.23}$$

and the following estimate holds:

$$\|\rho(t,\cdot)\|_{L^\infty(0,1)} \leqslant e^{T\|\lambda_x\|_{C^0}} \cdot \max\Big\{\|\rho_0\|_{L^\infty}, \frac{\|u\|_{L^\infty}}{\overline{\lambda}(M)}\Big\}, \quad \forall t \in [0,T]. \tag{1.24}$$

Moreover, $W(t)$ can be expressed as (see figure 1.5)

$$W(t) = \begin{cases} \displaystyle\int_0^t u(\alpha)d\alpha + \int_0^{1-\int_0^t \lambda(\xi_1(\theta),W(\theta))d\theta} \rho_0(\beta)d\beta, & 0 \leqslant t \leqslant \xi_2^{-1}(1), \\ \displaystyle\int_{\xi_1^{-1}(0)}^t u(\alpha)d\alpha, & \xi_2^{-1}(1) \leqslant t \leqslant T, \end{cases} \tag{1.25}$$

which implies again that

$$0 \leqslant W(t) = \|\rho(t,\cdot)\|_{L^1(0,1)} \leqslant M, \quad \forall t \in [0,T]. \tag{1.26}$$

Finally, W is Lipschitz continuous:

$$W(t) = W(0) + \int_0^t W'(s)ds,$$

where (see figure 1.5)

$$W'(t) = \begin{cases} u(t) - \lambda(\xi_1(t),W(t))\rho_0(1 - \displaystyle\int_0^t \lambda(\xi_1(\theta),W(\theta))d\theta), & a.e.\ t \in [0,\xi_2^{-1}(1)], \\ u(t) - u(\xi_1^{-1}(0))\dfrac{\lambda(1,W(t))}{\lambda(0,W(\xi_1^{-1}(0)))}\, e^{-\int_{\xi_1^{-1}(0)}^t \lambda_x(\xi_1(\theta),W(\theta))\,d\theta}, & a.e.\ t \in [\xi_2^{-1}(1),T]. \end{cases}$$

and

$$\|W'\|_{L^\infty(0,T)} \leqslant \|u\|_{L^\infty} + \|\lambda\|_{C^0} \cdot \max\Big\{\|\rho_0\|_{L^\infty}, \frac{\|u\|_{L^\infty}}{\overline{\lambda}(M)}\, e^{T\|\lambda_x\|_{C^0}}\Big\} < \infty. \tag{1.27}$$

Remark 1.3.2. (Hidden regularity) From the definition of the weak solution, we can expect $\rho \in L^\infty((0,T)\times(0,1)) = L^\infty(0,1;L^\infty(0,T))$. In fact, under the assumptions of Theorem 1.3.1, we have the hidden regularity that $\rho \in C^0([0,1];L^p(0,T))$ for all $p \in [1,\infty)$ so that the function $t \mapsto \rho(t,x) \in L^p(0,T)$ is well defined for every fixed $x \in [0,1]$. Moreover, the following estimate holds:

$$\|\rho(\cdot,x)\|_{L^\infty(0,T)} \leqslant e^{T\|\lambda_x\|_{C^0}} \cdot \max\Big\{\|\rho_0\|_{L^\infty}, \frac{\|u\|_{L^\infty}}{\overline{\lambda}(M)}\Big\}, \quad \forall x \in [0,1]. \tag{1.28}$$

The proof of the hidden regularity is quite similar to our proof of $\rho \in C^0([0,T];L^p(0,1))$ by means of the implicit expressions (1.23) for ρ and (1.25) for $W(t)$ (see also (1.27) when T is large).

Remark 1.3.3. If $\rho_0 \in C^0([0,1])$ and $u \in C^0([0,T])$ are nonnegative and the C^0 compatibility condition is satisfied at the origin:

$$\frac{u(0)}{\lambda(0,W(0))} - \rho_0(0) = 0,$$

where $W(0) = \int_0^1 \rho_0(x)dx$, then Cauchy problem (1.1), (1.2) and (1.3) admits a unique nonnegative solution $\rho \in C^0([0,T]\times[0,1])$. If, furthermore, $\rho_0 \in C^1([0,1])$ and $u \in C^1([0,T])$ are nonnegative and the C^1 compatibility conditions are satisfied at the origin:

$$\begin{cases} \dfrac{u(0)}{\lambda(0,W(0))} - \rho_0(0) = 0, \\ \dfrac{u'(0)\lambda(0,W(0)) - u(0)\lambda_W(0,W(0))W'(0)}{|\lambda(0,W(0))|^2} + \lambda(0,W(0))\rho_0'(0) + \lambda_x(0,W(0))\rho_0(0) = 0, \end{cases}$$

where $W(0) = \int_0^1 \rho_0(x)dx$ and $W'(0) = u(0) - \rho_0(1)\lambda(1,W(0))$, then Cauchy problem (1.1), (1.2) and (1.3) admits a unique nonnegative classical solution $\rho \in C^1([0,T]\times[0,1])$.

1.4 Stability with respect to the initial and boundary data

In this section, we study the stability (or continuous dependence) of both the solution ρ itself and the out-flux y with respect to ρ_0 and u. That is to say: if the initial and boundary data are slightly perturbed, are the solution ρ and the out-flux y *also slightly perturbed*?

Let $\overline{\rho}$ be the weak solution to the Cauchy problem with the perturbed initial and boundary conditions

$$\begin{cases} \overline{\rho}_t(t,x) + (\overline{\rho}(t,x)\lambda(x,\overline{W}(t)))_x = 0, & t \geq 0, 0 \leqslant x \leqslant 1, \\ \overline{\rho}(0,x) = \overline{\rho}_0(x), & 0 \leqslant x \leqslant 1, \\ \overline{\rho}(t,0)\lambda(0,\overline{W}(t)) = \overline{u}(t), & 0 \leqslant t \leqslant T, \end{cases} \tag{1.29}$$

where $\overline{W}(t) := \int_0^1 \overline{\rho}(t,x)dx$. We denote that $\overline{y}(t) := \overline{\rho}(1,t)\lambda(1,\overline{W}(t))$. We also define the corresponding characteristics with respect to the perturbed solution $\overline{\rho}$: $\overline{\xi}_1$ (as (1.12)), $\overline{\xi}_2$ (as (1.16)), $(\overline{\xi}_3, \overline{\alpha})$ (as (1.17) and (1.19)) and $(\overline{\xi}_4, \overline{\beta})$ (as (1.18) and (1.19)), respectively.

First we have the following theorem on the stability of the weak solution ρ.

Theorem 1.4.1. *For any $\varepsilon > 0$, $p \in [1,\infty)$ and any $K > 0$ such that*

$$\|\rho_0\|_{L^\infty(0,1)} + \|u\|_{L^\infty(0,T)} \leqslant K, \quad \|\overline{\rho}_0\|_{L^\infty(0,1)} + \|\overline{u}\|_{L^\infty(0,T)} \leqslant K, \tag{1.30}$$

there exists $\eta = \eta(\varepsilon,p,K,T) > 0$ small enough such that, if

$$\|\overline{\rho}_0 - \rho_0\|_{L^p(0,1)} + \|\overline{u} - u\|_{L^p(0,T)} < \eta, \tag{1.31}$$

then

$$\|\overline{\rho}(t,\cdot) - \rho(t,\cdot)\|_{L^p(0,1)} < \varepsilon, \quad \forall t \in [0,T]. \tag{1.32}$$

Proof. Solving Cauchy problem (1.29), we know from (1.26) and (1.30) that

$$0 \leqslant \overline{W}(t) \leqslant \|\overline{\rho}_0\|_{L^1(0,1)} + \|\overline{u}\|_{L^1(0,T)} \leqslant \overline{K}, \quad \forall t \in [0,T], \tag{1.33}$$

where

$$\overline{K} := K \cdot \max\{1,T\}. \tag{1.34}$$

Replacing M by $\overline{K}$ in the definitions of $\overline{\lambda}(M)$ and $\|\lambda\|_{C^0}, \|\lambda_x\|_{C^0}, \|\lambda_W\|_{C^0}$ (see section 1.2), we introduce some new notations as $\overline{\lambda}(\overline{K})$ and (still) $\|\lambda\|_{C^0}, \|\lambda_x\|_{C^0}, \|\lambda_W\|_{C^0}$ in this section.

We first prove the stability of the weak solution for small time. Let δ be chosen by (1.14). For any fixed $t \in [0, \delta]$, we suppose that $\xi_2(t) \leqslant \overline{\xi}_2(t)$ (if $\xi_2(t) \geq \overline{\xi}_2(t)$, we can change the status of $\xi_2(t)$ and $\overline{\xi}_2(t)$, then in a similar way, we can obtain the same estimate (1.46)). In order to estimate $\|\overline{\rho}(t,\cdot) - \rho(t,\cdot)\|_{L^p(0,1)}$ for $p \in [1, \infty)$, we need to estimate $\int_0^{\xi_2(t)} |\overline{\rho}(t,x) - \rho(t,x)|^p dx$, $\int_{\xi_2(t)}^{\overline{\xi}_2(t)} |\overline{\rho}(t,x) - \rho(t,x)|^p dx$ and $\int_{\overline{\xi}_2(t)}^1 |\overline{\rho}(t,x) - \rho(t,x)|^p dx$, successively.

For almost every $x \in [0, \xi_2(t)]$, we know from Remark 1.3.1 that (see figure 1.6)

$$
\begin{aligned}
&|\overline{\rho}(t,x) - \rho(t,x)| \\
&= \Big| \frac{\overline{u}(\overline{\alpha})}{\lambda(0, \overline{W}(\overline{\alpha}))} e^{-\int_{\overline{\alpha}}^t \lambda_x(\overline{\xi}_3(\theta), \overline{W}(\theta))\, d\theta} - \frac{u(\alpha)}{\lambda(0, W(\alpha))} e^{-\int_{\alpha}^t \lambda_x(\xi_3(\theta), W(\theta))\, d\theta} \Big| \\
&\leqslant \frac{|\overline{u}(\overline{\alpha}) - u(\alpha)|}{\lambda(0, \overline{W}(\overline{\alpha}))} e^{-\int_{\overline{\alpha}}^t \lambda_x(\overline{\xi}_3(\theta), \overline{W}(\theta))\, d\theta} + \Big| \frac{u(\alpha)}{\lambda(0, \overline{W}(\overline{\alpha}))} - \frac{u(\alpha)}{\lambda(0, W(\alpha))} \Big| e^{-\int_{\overline{\alpha}}^t \lambda_x(\overline{\xi}_3(\theta), \overline{W}(\theta))\, d\theta} \\
&\quad + \frac{|u(\alpha)|}{\lambda(0, W(\alpha))} \Big| e^{-\int_{\overline{\alpha}}^t \lambda_x(\overline{\xi}_3(\theta), \overline{W}(\theta))\, d\theta} - e^{-\int_{\alpha}^t \lambda_x(\xi_3(\theta), W(\theta))\, d\theta} \Big| \\
&\leqslant C|\overline{u}(\overline{\alpha}) - u(\alpha)| + C|u(\alpha)||\overline{W}(\overline{\alpha}) - W(\alpha)| \\
&\quad + C|u(\alpha)| \Big| \int_{\overline{\alpha}}^t \lambda_x(\overline{\xi}_3(\theta), \overline{W}(\theta))\, d\theta - \int_{\alpha}^t \lambda_x(\xi_3(\theta), W(\theta))\, d\theta \Big|.
\end{aligned}
$$

Here and hereafter in this section, we denote by C various constants which do not depend on $t, x, \rho, \overline{\rho}$ but may depend on p and $\overline{K}$.

For the given $u \in L^\infty(0,T)$, let $\{u_n\}_{n=1}^\infty \subset C^1([0,T])$ be such that $u_n \to u$ in $L^p(0,T)$. And for the given $\lambda \in C^1([0,1] \times [0,\infty))$, let $\{v_n\}_{n=1}^\infty \subset C^1([0,1] \times [0, \overline{K}])$ be such that $v_n \to \lambda_x$ in $C^0([0,1] \times [0, \overline{K}])$. Using sequences $\{u_n\}_{n=1}^\infty$, $\{v_n\}_{n=1}^\infty$ and (1.15), we obtain for almost every $x \in [0, \xi_2(t)]$ that

$$
\begin{aligned}
&|\overline{\rho}(t,x) - \rho(t,x)| \\
&\leqslant C|\overline{u}(\overline{\alpha}) - u(\overline{\alpha})| + C|u_n(\overline{\alpha}) - u(\overline{\alpha})| + C|u_n(\alpha) - u(\alpha)| \\
&\quad + C|u_n(\overline{\alpha}) - u_n(\alpha)| + C|\overline{W}(\overline{\alpha}) - W(\overline{\alpha})| + C|W(\overline{\alpha}) - W(\alpha)| \\
&\quad + C|u(\alpha)| \int_{\overline{\alpha}}^t |v_n(\overline{\xi}_3(\theta), \overline{W}(\theta)) - \lambda_x(\overline{\xi}_3(\theta), \overline{W}(\theta))|\, d\theta \\
&\quad + C|u(\alpha)| \int_{\alpha}^t |v_n(\xi_3(\theta), W(\theta)) - \lambda_x(\xi_3(\theta), W(\theta))|\, d\theta \\
&\quad + C|u(\alpha)| \Big| \int_{\overline{\alpha}}^t v_n(\overline{\xi}_3(\theta), \overline{W}(\theta))\, d\theta - \int_{\alpha}^t v_n(\xi_3(\theta), W(\theta))\, d\theta \Big| \\
&\leqslant C|\overline{u}(\overline{\alpha}) - u(\overline{\alpha})| + C|u_n(\overline{\alpha}) - u(\overline{\alpha})| + C|u_n(\alpha) - u(\alpha)| \\
&\quad + C|u(\alpha)| \|v_n - \lambda_x\|_{C^0([0,1] \times [0, \overline{K}])} + C_n|\overline{\alpha} - \alpha| + C_n|u(\alpha)||\overline{\alpha} - \alpha| \\
&\quad + C_n|u(\alpha)| \|\overline{\xi}_3 - \xi_3\|_{C^0([\overline{\alpha}, t])} + C_n|u(\alpha)| \|\overline{W} - W\|_{C^0([0,\delta])}.
\end{aligned} \tag{1.35}
$$

Here and hereafter in this section, we denote by C_n various constants which do not depend on $t, x, \rho, \overline{\rho}$ but may depend on $p, \overline{K}$ and n (the index of the corresponding sequences, e.g.

$\{u_n\}_{n=1}^{\infty}$, $\{v_n\}_{n=1}^{\infty}$ and so on).

A similar estimate as (1.13) gives us

$$\|\overline{\xi}_3 - \xi_3\|_{C^0([\overline{\alpha},t])} \leqslant \frac{t\|\lambda_W\|_{C^0}}{1 - t\|\lambda_x\|_{C^0}} \cdot \|\overline{W} - W\|_{C^0([0,\delta])}. \tag{1.36}$$

From the fact that

$$\overline{\xi}_3(t) = \int_{\overline{\alpha}}^{t} \lambda(\overline{\xi}_3(\theta), \overline{W}(\theta))\, d\theta = x = \xi_3(t) = \int_{\alpha}^{t} \lambda(\xi_3(\theta), W(\theta))\, d\theta$$

and the definition of $\overline{\lambda}(\overline{K})$, we get also that

$$\begin{aligned}
|\overline{\alpha} - \alpha| &\leqslant \frac{1}{\overline{\lambda}(\overline{K})} \int_{\alpha}^{\overline{\alpha}} \lambda(\xi_3(\theta), W(\theta))\, d\theta \\
&= \frac{1}{\overline{\lambda}(\overline{K})} \int_{\overline{\alpha}}^{t} (\lambda(\overline{\xi}_3(\theta), \overline{W}(\theta)) - \lambda(\xi_3(\theta), W(\theta)))\, d\theta \\
&\leqslant \frac{1}{\overline{\lambda}(\overline{K})} \Big(t\|\lambda_x\|_{C^0} \|\overline{\xi}_3 - \xi_3\|_{C^0([\overline{\alpha},t])} + t\|\lambda_W\|_{C^0} \|\overline{W} - W\|_{C^0([0,\delta])} \Big) \\
&\leqslant \frac{t\|\lambda_W\|_{C^0}}{\overline{\lambda}(\overline{K})(1 - t\|\lambda_x\|_{C^0})} \cdot \|\overline{W} - W\|_{C^0([0,\delta])}.
\end{aligned} \tag{1.37}$$

On the other hand, by (1.25) and Hölder inequality, we have for every $t \in [0, \delta]$ that

$$\begin{aligned}
&|\overline{W}(t) - W(t)| \\
&= \Big| \int_0^t (\overline{u}(\sigma) - u(\sigma)) d\sigma + \int_0^{1 - \int_0^t \lambda(\overline{\xi}_1(\theta), \overline{W}(\theta))\, d\theta} \overline{\rho}_0(\sigma)\, d\sigma - \int_0^{1 - \int_0^t \lambda(\xi_1(\theta), W(\theta))\, d\theta} \rho_0(\sigma)\, d\sigma \Big| \\
&\leqslant \delta^{\frac{1}{q}} \|\overline{u} - u\|_{L^p(0,T)} + \|\overline{\rho}_0 - \rho_0\|_{L^p(0,1)} + \|\rho_0\|_{L^\infty} \int_0^t |\lambda(\overline{\xi}_1(\theta), \overline{W}(\theta)) - \lambda(\xi_1(\theta), W(\theta))|\, d\theta \\
&\leqslant \delta^{\frac{1}{q}} \|\overline{u} - u\|_{L^p(0,T)} + \|\overline{\rho}_0 - \rho_0\|_{L^p(0,1)} \\
&\quad + \delta \|\rho_0\|_{L^\infty} (\|\lambda_x\|_{C^0} \|\overline{\xi}_1 - \xi_1\|_{C^0([0,t])} + \|\lambda_W\|_{C^0} \|\overline{W} - W\|_{C^0([0,\delta])}),
\end{aligned}$$

where q satisfies $\frac{1}{p} + \frac{1}{q} = 1$. By the definitions of ξ_1 and $\overline{\xi}_1$, we still have (1.13), thus

$$\begin{aligned}
\|\overline{W} - W\|_{C^0([0,\delta])} &= \sup_{t \in [0,\delta]} |\overline{W}(t) - W(t)| \\
&\leqslant \frac{1 - \delta\|\lambda_x\|_{C^0}}{1 - \delta(\|\lambda_x\|_{C^0} + \|\rho_0\|_{L^\infty}\|\lambda_W\|_{C^0})} \cdot (\delta^{\frac{1}{q}} \|\overline{u} - u\|_{L^p(0,T)} + \|\overline{\rho}_0 - \rho_0\|_{L^p(0,1)}).
\end{aligned}$$

and furthermore, from the choice (1.14) of δ,

$$\|\overline{W} - W\|_{C^0([0,\delta])} \leqslant C\|\overline{u} - u\|_{L^p(0,T)} + C\|\overline{\rho}_0 - \rho_0\|_{L^p(0,1)}. \tag{1.38}$$

Therefore, combining (1.35), (1.36), (1.37) and (1.38) all together and using (1.62) in Lemma 1.6.1, we obtain easily that

$$\begin{aligned}
&\int_0^{\xi_2(t)} |\overline{\rho}(t,x) - \rho(t,x)|^p dx \\
&\leqslant C\|u_n - u\|^p_{L^p(0,T)} + C\|v_n - \lambda_x\|^p_{C^0([0,1]\times[0,\overline{K}])} \\
&\quad + C_n\|\overline{u} - u\|^p_{L^p(0,T)} + C_n\|\overline{\rho}_0 - \rho_0\|^p_{L^p(0,1)}.
\end{aligned} \tag{1.39}$$

For almost every $x \in [\overline{\xi}_2(t), 1]$, we know from Remark 1.3.1 that (see figure 1.7)

$$\begin{aligned}
&|\overline{\rho}(t,x) - \rho(t,x)| = \Big|\overline{\rho}_0(\overline{\beta}) e^{-\int_0^t \lambda_x(\overline{\xi}_4(\theta),\overline{W}(\theta))\,d\theta} - \rho_0(\beta) e^{-\int_0^t \lambda_x(\xi_4(\theta),W(\theta))\,d\theta}\Big| \\
&\leqslant |\overline{\rho}_0(\overline{\beta}) - \rho_0(\beta)| e^{-\int_0^t \lambda_x(\overline{\xi}_4(\theta),\overline{W}(\theta))\,d\theta} + |\rho_0(\beta)|\Big| e^{-\int_0^t \lambda_x(\overline{\xi}_4(\theta),\overline{W}(\theta))\,d\theta} - e^{-\int_0^t \lambda_x(\xi_4(\theta),W(\theta))\,d\theta}\Big| \\
&\leqslant C|\overline{\rho}_0(\overline{\beta}) - \rho_0(\overline{\beta})| + C|\rho_0(\overline{\beta}) - \rho_0(\beta)| \\
&\quad + C|\rho_0(\beta)|\Big| \int_0^t (\lambda_x(\overline{\xi}_4(\theta),\overline{W}(\theta)) - \lambda_x(\xi_4(\theta),W(\theta)))\,d\theta\Big|.
\end{aligned}$$

For the given $\rho_0 \in L^\infty(0,1)$, we let $\{\rho_0^n\}_{n=1}^\infty \subset C^1([0,1])$ be such that $\rho_0^n \to \rho_0$ in $L^p(0,1)$. With the help of sequences $\{\rho_0^n\}_{n=1}^\infty$, $\{v_n\}_{n=1}^\infty$, we obtain for almost every $x \in [\overline{\xi}_2(t), 1]$ that

$$\begin{aligned}
&|\overline{\rho}(t,x) - \rho(t,x)| \\
&\leqslant C|\overline{\rho}_0(\overline{\beta}) - \rho_0(\overline{\beta})| + C|\rho_0^n(\overline{\beta}) - \rho_0(\overline{\beta})| + C|\rho_0^n(\beta) - \rho_0(\beta)| + C|\rho_0^n(\overline{\beta}) - \rho_0^n(\beta)| \\
&\quad + C|\rho_0(\beta)| \int_0^t |v_n(\overline{\xi}_4(\theta),\overline{W}(\theta)) - \lambda_x(\overline{\xi}_4(\theta),\overline{W}(\theta))|\,d\theta \\
&\quad + C|\rho_0(\beta)| \int_0^t |v_n(\xi_4(\theta),W(\theta)) - \lambda_x(\xi_4(\theta),W(\theta))|\,d\theta \\
&\quad + C|\rho_0(\beta)| \int_0^t |v_n(\overline{\xi}_4(\theta),\overline{W}(\theta)) - v_n(\xi_4(\theta),W(\theta))|\,d\theta \\
&\leqslant C|\overline{\rho}_0(\overline{\beta}) - \rho_0(\overline{\beta})| + C|\rho_0^n(\overline{\beta}) - \rho_0(\overline{\beta})| + C|\rho_0^n(\beta) - \rho_0(\beta)| + C|\rho_0(\beta)|\|v_n - \lambda_x\|_{C^0([0,1]\times[0,\overline{K}])} \\
&\quad + C_n|\overline{\beta} - \beta| + C_n|\rho_0(\beta)|\|\overline{\xi}_4 - \xi_4\|_{C^0([0,t])} + C_n|\rho_0(\beta)|\|\overline{W} - W\|_{C^0([0,\delta])}. \qquad (1.40)
\end{aligned}$$

Similar to (1.13), we have

$$\|\overline{\xi}_4 - \xi_4\|_{C^0([0,t])} \leqslant \frac{t\|\lambda_W\|_{C^0}}{1 - t\|\lambda_x\|_{C^0}} \cdot \|\overline{W} - W\|_{C^0([0,\delta])}, \qquad (1.41)$$

and in particular,

$$|\overline{\beta} - \beta| = |\overline{\xi}_4(0) - \xi_4(0)| \leqslant \frac{t\|\lambda_W\|_{C^0}}{1 - t\|\lambda_x\|_{C^0}} \cdot \|\overline{W} - W\|_{C^0([0,\delta])}. \qquad (1.42)$$

Therefore, by the choice (1.14) of δ, together with estimates (1.38), (1.40), (1.41), (1.42) and (1.64) in Lemma 1.6.2, we get immediately that

$$\begin{aligned}
&\int_{\overline{\xi}_2(t)}^1 |\overline{\rho}(t,x) - \rho(t,x)|^p dx \\
&\leqslant C\|\rho_0^n - \rho_0\|_{L^p(0,1)}^p + C\|v_n - \lambda_x\|_{C^0([0,1]\times[0,\overline{K}])}^p \\
&\quad + C_n\|\overline{u} - u\|_{L^p(0,T)}^p + C_n\|\overline{\rho}_0 - \rho_0\|_{L^p(0,1)}^p. \qquad (1.43)
\end{aligned}$$

Now it is left to estimate $\int_{\xi_2(t)}^{\overline{\xi}_2(t)} |\overline{\rho}(t,x) - \rho(t,x)|^p dx$ (see figure 1.8). Since we have also

$$\|\overline{\xi}_2 - \xi_2\|_{C^0([0,t])} \leqslant \frac{t\|\lambda_W\|_{L^\infty}}{1 - t\|\lambda_x\|_{L^\infty}} \cdot \|\overline{W} - W\|_{C^0([0,\delta])}, \qquad (1.44)$$

which is similar to the estimate of (1.13), then by (1.24) and (1.38), we get

$$\begin{aligned}&\int_{\xi_2(t)}^{\overline{\xi}_2(t)} |\overline{\rho}(t,x)-\rho(t,x)|^p dx \leqslant C|\xi_2(t)-\overline{\xi}_2(t)| \leqslant C\|\overline{W}-W\|_{C^0([0,\delta])}\\ &\leqslant C\|\overline{u}-u\|_{L^\infty(0,T)} + C\|\overline{\rho}_0-\rho_0\|_{L^\infty(0,1)}. \end{aligned} \tag{1.45}$$

Summarizing the three estimates (1.39),(1.43) and (1.45), finally we prove for any fixed $t\in[0,\delta]$ with δ satisfying (1.14) that

$$\begin{aligned}&\|\overline{\rho}(t,\cdot)-\rho(t,\cdot)\|^p_{L^p(0,1)}\\ &\leqslant C\|\rho_0^n-\rho_0\|^p_{L^p(0,1)} + C\|u_n-u\|^p_{L^p(0,T)} + C\|v_n-\lambda_x\|^p_{C^0([0,1]\times[0,\overline{K}])} + C\|\overline{u}-u\|_{L^\infty(0,T)}\\ &\quad + C\|\overline{\rho}_0-\rho_0\|_{L^\infty(0,1)} + C_n\|\overline{u}-u\|^p_{L^p(0,T)} + C_n\|\overline{\rho}_0-\rho_0\|^p_{L^p(0,1)}. \end{aligned} \tag{1.46}$$

Now if we take n large enough and then η in (1.31) small enough, the right-hand side of (1.46) can be smaller than any given constant $\varepsilon>0$.

In order to obtain the global stability (1.32) from (1.46), it suffices, according to (1.14), to prove uniform a priori estimates for $\|\rho(t,\cdot)\|_{L^1(0,1)}$, $\|\rho(t,\cdot)\|_{L^\infty(0,1)}$, $\|\overline{\rho}(t,\cdot)\|_{L^1(0,1)}$, and $\|\overline{\rho}(t,\cdot)\|_{L^\infty(0,1)}$. In fact the desired a priori estimates are available by Remark 1.3.1 (see estimates (1.24) and (1.26)), hence we finally reach (1.32). This finishes the proof of Theorem 1.4.1.

□

We also have the stability on the out-flux y.

Theorem 1.4.2. *For any $\varepsilon>0$, $p\in[1,\infty)$ and any K such that* (1.30) *holds, there exists $\eta=\eta(\varepsilon,p,K,T)>0$ small enough such that, if* (1.31) *holds, then*

$$\|\overline{y}-y\|_{L^p(0,T)}<\varepsilon. \tag{1.47}$$

Proof. First, we prove $\|\overline{y}-y\|_{L^p(0,\delta)}<\varepsilon$ for δ small. Let δ be such that (1.14) holds. By Remark 1.3.1, we have for almost every $t\in[0,\delta]$ that (see figure 1.9)

$$\begin{aligned}&|\overline{y}(t)-y(t)|\\ &= |\overline{\rho}(t,1)\lambda(1,\overline{W}(t)) - \rho(t,1)\lambda(1,W(t))|\\ &\leqslant C|\overline{\rho}(t,1)-\rho(t,1)| + C|\rho(t,1)|\|\overline{W}-W\|_{C^0([0,\delta])}\\ &= C\Big|\overline{\rho}_0(\overline{\xi}_1(0))e^{-\int_0^t \lambda_x(\overline{\xi}_1(\theta),\overline{W}(\theta))d\theta} - \rho_0(\xi_1(0))e^{-\int_0^t \lambda_x(\xi_1(\theta),W(\theta))d\theta}\Big|\\ &\quad + C|\rho(t,1)|\|\overline{W}-W\|_{C^0([0,\delta])}\\ &\leqslant C|\overline{\rho}_0(\overline{\xi}_1(0))-\rho_0(\xi_1(0))| + C|\rho(t,1)|\|\overline{W}-W\|_{C^0([0,\delta])}\\ &\quad + C|\rho_0(\xi_1(0))|\Big|\int_0^t (\lambda_x(\overline{\xi}_1(\theta),\overline{W}(\theta)) - \lambda_x(\xi_1(\theta),W(\theta)))d\theta\Big|. \end{aligned}$$

Then using sequences $\{\rho_0^n\}_{n=1}^{\infty}$, $\{v_n\}_{n=1}^{\infty}$, we obtain

$$
\begin{aligned}
&|\overline{y}(t)-y(t)|\\
&\leqslant C|\overline{\rho}_0(\overline{\xi}_1(0))-\rho_0(\overline{\xi}_1(0))|+C|\rho_0^n(\overline{\xi}_1(0))-\rho_0(\overline{\xi}_1(0))|+C|\rho_0^n(\xi_1(0))-\rho_0(\xi_1(0))|\\
&\quad+C|\rho_0^n(\overline{\xi}_1(0))-\rho_0^n(\xi_1(0))|+C|\rho(t,1)|\|\overline{W}-W\|_{C^0([0,\delta])}\\
&\quad+C|\rho_0(\xi_1(0))|\int_0^t|v_n(\overline{\xi}_1(\theta),\overline{W}(\theta))-v_n(\xi_1(\theta),W(\theta))|d\theta\\
&\quad+C|\rho_0(\xi_1(0))|\int_0^t|v_n(\overline{\xi}_1(\theta),\overline{W}(\theta))-\lambda_x(\overline{\xi}_1(\theta),\overline{W}(\theta))|d\theta\\
&\quad+C|\rho_0(\xi_1(0))|\int_0^t|v_n(\xi_1(\theta),W(\theta))-\lambda_x(\xi_1(\theta),W(\theta))|d\theta,\\
&\leqslant C|\overline{\rho}_0(\overline{\xi}_1(0))-\rho_0(\overline{\xi}_1(0))|+C|\rho_0^n(\overline{\xi}_1(0))-\rho_0(\overline{\xi}_1(0))|\\
&\quad+C|\rho_0^n(\xi_1(0))-\rho_0(\xi_1(0))|+C|\rho_0(\xi_1(0))|\|v_n-\lambda_x\|_{C^0([0,1]\times[0,\overline{K}])}\\
&\quad+C_n|\rho_0(\xi_1(0))|\|\overline{\xi}_1-\xi_1\|_{C^0([0,t])}+C_n|\rho_0(\xi_1(0))|\|\overline{W}-W\|_{C^0([0,\delta])},
\end{aligned}
$$

which results in

$$
\begin{aligned}
&\int_0^{\delta}|\overline{y}(t)-y(t)|^p\,dt\\
&\leqslant C\|\rho_0^n-\rho_0\|_{L^p(0,1)}^p+C\|v_n-\lambda_x\|_{C^0([0,1]\times[0,\overline{K}])}^p+C_n\|\overline{\rho}_0-\rho_0\|_{L^p(0,1)}^p+C_n\|\overline{u}-u\|_{L^p(0,T)}^p
\end{aligned}
$$

with the help of (1.13), (1.38) and (1.63) (when $(t,x)=(t,1)$) in Lemma 1.6.2. Obviously, $\|\overline{y}-y\|_{L^p(0,\delta)}<\varepsilon$ holds if we let n large enough and then $\eta>0$ in (1.31) small enough.

In a same way, we can prove for every $\tau\in[0,T-\delta]$ by applying Theorem 1.4.1 that

$$
\|\overline{y}-y\|_{L^p(\tau,\tau+\delta)}<\varepsilon
$$

if δ satisfies (1.14) (independent of τ). Step by step, we finally prove (1.47).

□

1.5 L^p-optimal control for demand tracking problem

Let $T>0$ and $\rho_0\in L^{\infty}_{+}(0,1)$ be given. According to Theorem 1.3.1, for every $u\in L^{\infty}_{+}(0,T)$, Cauchy problem (1.1), (1.2) and (1.3) admits a unique weak solution $\rho\in L^{\infty}((0,T)\times(0,1))\cap C^0([0,T],L^p(0,1))\cap C^0([0,1],L^p(0,T))$ for all $p\in[1,\infty)$.

For any fixed given demand $y_d\in L^{\infty}(0,T)$, initial data $\rho_0\in L^{\infty}_{+}(0,1)$ and p with $1\leqslant p\leqslant\infty$, we define a cost functional on $L^{\infty}_{+}(0,T)$ by

$$
J_p(u):=\|u\|_{L^{\infty}(0,T)}+\|y-y_d\|_{L^p(0,T)},\quad u\in L^{\infty}_{+}(0,T),
$$

where $y(t):=\rho(t,1)\lambda(1,W(t))$ is the out-flux corresponding to the in-flux $u\in L^{\infty}_{+}(0,T)$ and initial data ρ_0. This cost functional is motivated by [35, 62] and the existence of the solution to this optimal control problem is obtained by the following theorem.

Theorem 1.5.1. *The infimum of the functional J_p in $L^\infty_+(0,T)$ with $1 \leqslant p \leqslant \infty$ is achieved, i.e., there exists $u^\infty \in L^\infty_+(0,T)$ such that*

$$J_p(u^\infty) = \inf_{u \in L^\infty_+(0,T)} J_p(u).$$

Proof. Let $\{u^n\}_{n=1}^\infty \subset L^\infty_+(0,T)$ be a minimizing sequence of the functional J_p, i.e.

$$\lim_{n\to\infty} J_p(u^n) = \inf_{u \in L^\infty_+(0,T)} J_p(u).$$

Then we have

$$\|u^n\|_{L^\infty(0,T)} + \|y^n\|_{L^p(0,T)} \leqslant C, \quad \forall n \in \mathbb{Z}^+. \tag{1.48}$$

Moreover, by (1.28), we know that

$$\|y^n\|_{L^\infty(0,T)} \leqslant C, \quad \forall n \in \mathbb{Z}^+. \tag{1.49}$$

Here and hereafter in this section, we denote by C various constants which do not depend on n (the index of the sequences, e.g. $\{u^n\}_{n=1}^\infty$, $\{y^n\}_{n=1}^\infty$ and so on). The boundedness of $u^n \subset L^\infty_+(0,T)$ implies that there exists $u^\infty \in L^\infty_+(0,T)$ and a subsequence of $\{u^{n_k}\}_{k=1}^\infty$ such that $u^{n_k} \overset{*}{\rightharpoonup} u^\infty$ in $L^\infty_+(0,T)$. For simplicity, we still denote the subsequence as $\{u^n\}_{n=1}^\infty$. And we let

$$\widetilde{M} := \|\rho_0\|_{L^1(0,1)} + \max\{\sup_{n\in\mathbb{Z}^+} \|u^n\|_{L^1(0,T)}, \|u^\infty\|_{L^1(0,T)}\} < \infty. \tag{1.50}$$

Let ρ^n be the weak solution to the Cauchy problem

$$\begin{cases} \rho^n_t(t,x) + (\rho^n(t,x)\lambda(x, W^n(t)))_x = 0, & t \geq 0, 0 \leqslant x \leqslant 1, \\ \rho^n(0,x) = \rho_0(x), & 0 \leqslant x \leqslant 1, \\ \rho^n(t,0)\lambda(0, W^n(t)) = u^n(t), & 0 \leqslant t \leqslant T, \end{cases}$$

where $W^n(t) := \int_0^1 \rho^n(t,x)dx$. Then for any fixed $t \in [0,T]$, we define ξ^n_1 by

$$\frac{d\xi^n_1}{ds} = \lambda(\xi^n_1(s), W^n(s)), \quad \xi^n_1(t) = 1$$

and define ξ^n_2 by

$$\frac{d\xi^n_2}{ds} = \lambda(\xi^n_2(s), W^n(s)), \quad \xi^n_2(0) = 0.$$

Thanks to (1.48), we know from (1.25) and (1.27) that

$$\|W^n\|_{W^{1,\infty}(0,T)} \leqslant C, \quad \forall n \in \mathbb{Z}^+, \tag{1.51}$$

Then it follows from Arzelà-Ascoli Theorem that there exists $\overline{W}^\infty \in C^0([0,T])$ and a subsequence $\{W^{n_l}\}_{l=1}^\infty$ such that $W^{n_l} \to \overline{W}^\infty$ in $C^0([0,T])$. Now we choose the corresponding subsequence $\{u^{n_l}\}_{l=1}^\infty$ and again, denote it as $\{u^n\}_{n=1}^\infty$. Thus we have $u^n \overset{*}{\rightharpoonup} u^\infty$ in $L^\infty_+(0,T)$ and $W^n \to \overline{W}^\infty$ in $C^0([0,T])$.

In view of (1.25), (1.50) and (1.51), there exists a small $\delta > 0$ depending only on $\widetilde{M}$ and independent of n, such that

$$W^n(t) = \int_0^t u^n(\alpha)d\alpha + \int_0^{1-\int_0^t \lambda(\xi_1^n(\theta),W^n(\theta))d\theta} \rho_0(\beta)d\beta, \quad \forall t \in [0,\delta]. \tag{1.52}$$

For any fixed $t \in [0,T]$, we define $\overline{\xi}_1^\infty$ by

$$\frac{d\overline{\xi}_1^\infty}{ds} = \lambda(\overline{\xi}_1^\infty(s), \overline{W}^\infty(s)), \quad \overline{\xi}_1^\infty(t) = 1 \text{ for any fixed } \ t \in [0,T],$$

and define $\overline{\xi}_2^\infty$ by

$$\frac{d\overline{\xi}_2^\infty}{ds} = \lambda(\overline{\xi}_2^\infty(s), \overline{W}^\infty(s)), \quad \overline{\xi}_2^\infty(0) = 0.$$

Obviously, $W^n \to \overline{W}^\infty$ in $C^0([0,T])$ implies that for any $t \in [0,\delta]$, $\xi_1^n \to \overline{\xi}_1^\infty$ in $C^1([0,t])$ and $\xi_2^n \to \overline{\xi}_2^\infty$ in $C^1([0,T])$. Thus by passing to the limit $n \to \infty$ in (1.52), we obtain

$$\overline{W}^\infty(t) = \int_0^t u^\infty(\alpha)d\alpha + \int_0^{1-\int_0^t \lambda(\overline{\xi}_1^\infty(\theta),\overline{W}^\infty(\theta))d\theta} \rho_0(\beta)d\beta, \quad \forall t \in [0,\delta]. \tag{1.53}$$

Let ρ^∞ be the weak solution to the Cauchy problem

$$\begin{cases} \rho_t^\infty(t,x) + (\rho^\infty(t,x)\lambda(x,W^\infty(t)))_x = 0, & t \geq 0, 0 \leqslant x \leqslant 1, \\ \rho^\infty(0,x) = \rho_0(x), & 0 \leqslant x \leqslant 1, \\ \rho^\infty(t,0)\lambda(0,W^\infty(t)) = u^\infty(t), & 0 \leqslant t \leqslant T, \end{cases}$$

where $W^\infty(t) := \int_0^1 \rho^\infty(t,x)dx$. For any fixed $t \in [0,T]$, we define ξ_1^∞ by

$$\frac{d\xi_1^\infty}{ds} = \lambda(\xi_1^\infty(s), W^\infty(s)), \quad \xi_1^\infty(t) = 1$$

and define ξ_2^∞ by

$$\frac{d\xi_2^\infty}{ds} = \lambda(\xi_2^\infty(s), W^\infty(s)), \quad \xi_2^\infty(0) = 0.$$

Let $\delta > 0$ be small enough so that

$$W^\infty(t) = \int_0^t u^\infty(\alpha)d\alpha + \int_0^{1-\int_0^t \lambda(\xi_1^\infty(\theta),W^\infty(\theta))d\theta} \rho_0(\beta)d\beta, \quad \forall t \in [0,\delta]. \tag{1.54}$$

We know from the proof of Theorem 1.3.1 that $W = F(W)$ has a unique fixed point in $\Omega_{\delta,\widetilde{M}}$ (replacing M by $\widetilde{M}$ in (1.10)). This implies from (1.53) and (1.54) that $W^\infty(t) \equiv \overline{W}^\infty(t)$ on $[0,\delta]$, hence for any fixed $t \in [0,\delta]$, $\xi_1^\infty(s) \equiv \overline{\xi}_1^\infty(s), \xi_2^\infty(s) \equiv \overline{\xi}_2^\infty(s)$ on $[0,t]$. Moreover, with the help of (1.14), there exists $\delta_0 > 0$ independent of $\tau \in (0,T)$ such that if $W^\infty(\tau) = \overline{W}^\infty(\tau)$ then $W^\infty(t) \equiv \overline{W}^\infty(t)$ on $[\tau, \tau+\delta_0] \cap [\tau, T]$. Hence we have $W^n \to W^\infty$ in $C^0([0,T])$ and furthermore $\xi_1^n \to \xi_1^\infty$ uniformly and $\xi_2^n \to \xi_2^\infty$ in $C^1([0,T])$.

Next we prove that $y^n(t) = \rho^n(t,1)\lambda(1,W^n(t))$ converges to $y^\infty(t) = \rho^\infty(t,1)\lambda(1,W^\infty(t))$ weakly-$*$ in $L^\infty(0,T)$. Thanks to (1.49), it suffices to prove that for any $g \in C^1([0,T])$,

$$\lim_{n\to\infty} \int_0^T (y^n(t) - y^\infty(t))g(t)dt = 0. \tag{1.55}$$

In fact, for any $g \in L^1(0,T)$, there exists a sequence $\{g^k\}_{k=1}^{\infty} \subset C^1([0,T])$ such that $g^k \to g$ in $L^1(0,T)$, hence we get from (1.49) that

$$\begin{aligned}
&\Big|\int_0^T (y^n(t) - y^\infty(t))g(t)dt\Big| \\
\leqslant &\Big|\int_0^T (y^n(t) - y^\infty(t))(g(t) - g^k(t))dt\Big| + \Big|\int_0^T (y^n(t) - y^\infty(t))g^k(t)dt\Big| \\
\leqslant &C\|g^k - g\|_{L^1(0,T)} + \Big|\int_0^T (y^n(t) - y^\infty(t))g^k(t)dt\Big|.
\end{aligned}$$

This simply shows that in order to prove $y^n \overset{*}{\rightharpoonup} y^\infty$ in $L^\infty(0,T)$, it is sufficient to prove (1.55) for all $g \in C^1([0,T])$.

Case 1. $\xi_2^\infty(T) < 1$.

$$\begin{aligned}
&\Big|\int_0^T (y^n(t) - y^\infty(t))g(t)dt\Big| \\
= &\Big|\int_0^T \Big(\rho_0(\xi_1^n(0)))\lambda(1, W^n(t))\, e^{-\int_0^t \lambda_x(\xi_1^n(\theta), W^n(\theta))d\theta} \\
&\qquad - \rho_0(\xi_1^\infty(0))\lambda(1, W^\infty(t))\, e^{-\int_0^t \lambda_x(\xi_1^\infty(\theta), W^\infty(\theta))d\theta}\Big) g(t)dt\Big|.
\end{aligned}$$

Let $\{\rho_0^k\}_{k=1}^{\infty} \subset C^1([0,1])$ be such that $\rho_0^k \to \rho_0$ in $L^1(0,1)$, then by (1.23), (1.51) and (1.63) (when $(t,x) = (t,1)$) in Lemma 1.6.2, we have

$$\begin{aligned}
&\Big|\int_0^T (y^n(t) - y^\infty(t))g(t)dt\Big| \\
\leqslant &\int_0^T |\rho_0^k(\xi_1^n(0)) - \rho_0(\xi_1^n(0))|\lambda(1, W^n(t))\, e^{-\int_0^t \lambda_x(\xi_1^n(\theta), W^n(\theta))d\theta}|g(t)|dt \\
&+ \int_0^T |\rho_0^k(\xi_1^\infty(0)) - \rho_0(\xi_1^\infty(0))|\lambda(1, W^\infty(t))\, e^{-\int_0^t \lambda_x(\xi_1^\infty(\theta), W^\infty(\theta))d\theta}|g(t)|dt \\
&+ \int_0^T \Big|\rho_0^k(\xi_1^n(0))\lambda(1, W^n(t))\, e^{-\int_0^t \lambda_x(\xi_1^n(\theta), W^n(\theta))d\theta} \\
&\qquad - \rho_0^k(\xi_1^\infty(0))\lambda(1, W^\infty(t))\, e^{-\int_0^t \lambda_x(\xi_1^\infty(\theta), W^\infty(\theta))d\theta}\Big||g(t)|dt \\
\leqslant &C\|\rho_0^k - \rho_0\|_{L^1(0,1)} + C_k\|W^n - W^\infty\|_{C^0([0,T])} + C_k\int_0^T |\xi_1^n(0) - \xi_1^\infty(0)||g(t)|dt \\
&+ C_k\int_0^T \Big|\int_0^t (\lambda_x(\xi_1^n(\theta), W^n(\theta)) - \lambda_x(\xi_1^\infty(\theta), W^\infty(\theta)))d\theta\Big||g(t)|dt
\end{aligned} \tag{1.56}$$

where C_k is a constant depending on ρ_0^k. Noting the fact that $\rho_0^k \to \rho_0$ in $L^1(0,1)$ and $\xi_1^n \to \xi_1^\infty$, $W^n \to W^\infty$ uniformly, by Lebesgue dominated convergence theorem, we let k large enough first and then n large enough, so that the right hand side of (1.56) can be arbitrarily small. This concludes (1.55) for the case of $\xi_2^\infty(T) < 1$.

Case 2. $\xi_2^\infty(T)=1$, *i.e.,* $T=(\xi_2^\infty)^{-1}(1)$. For every $\tau\in[0,T)$, we have

$$\begin{aligned}&\Big|\int_0^T (y^n(t)-y^\infty(t))g(t)dt\Big|\\ =&\Big|\int_0^\tau (y^n(t)-y^\infty(t))g(t)dt+\int_\tau^T (y^n(t)-y^\infty(t))g(t)dt\Big|\\ \leqslant&\Big|\int_0^\tau (y^n(t)-y^\infty(t))g(t)dt\Big|+C(T-\tau)^{\frac12}.\end{aligned}\tag{1.57}$$

Since it is known from Case 1 that for every $\tau\in[0,T)$, $|\int_0^\tau (y^n(t)-y^\infty(t))g(t)dt|\to 0$ as $n\to\infty$, one has (1.55) for $T=(\xi_2^\infty)^{-1}(1)$ by letting $\tau\to T$ in (1.57) .

Case 3. $\xi_2^\infty(T)>1$. Now we have

$$\int_0^T (y^n(t)-y^\infty(t))g(t)dt=\Big(\int_0^{(\xi_2^\infty)^{-1}(1)}+\int_{(\xi_2^\infty)^{-1}(1)}^T\Big)(y^n(t)-y^\infty(t))g(t)dt.$$

Using the result in Case 2, we need only to prove that $|\int_{(\xi_2^\infty)^{-1}(1)}^T (y^n(t)-y^\infty(t))g(t)dt|\to 0$.

For any fixed $\alpha\in[0,T]$, we define $\widetilde{\xi}_1^n,\widetilde{\xi}_1^\infty$ by

$$\begin{aligned}&\frac{d\widetilde{\xi}_1^n}{ds}=\lambda(\widetilde{\xi}_1^n(s),W^n(s)),\quad \widetilde{\xi}_1^n(\alpha)=0,\\ &\frac{d\widetilde{\xi}_1^\infty}{ds}=\lambda(\widetilde{\xi}_1^\infty(s),W^\infty(s)),\quad \widetilde{\xi}_1^\infty(\alpha)=0.\end{aligned}$$

And we know from $W^n\to W^\infty$ in $C^0([0,T])$ that $\widetilde{\xi}_1^n\to\widetilde{\xi}_1^\infty$ and $(\widetilde{\xi}_1^n)^{-1}\to(\widetilde{\xi}_1^\infty)^{-1}$ uniformly.

Then we get from (1.23) that

$$\begin{aligned}&\Big|\int_{(\xi_2^\infty)^{-1}(1)}^T (y^n(t)-y^\infty(t))g(t)dt\Big|\\ =&\Big|\int_{(\xi_2^\infty)^{-1}(1)}^T (\rho^n(t,1)\lambda(1,W^n(t))-\rho^\infty(t,1)\lambda(1,W^\infty(t)))g(t)dt\Big|\\ =&\Big|\int_{(\xi_2^\infty)^{-1}(1)}^T \Big(\frac{u^n(\alpha^n)\lambda(1,W^n(t))}{\lambda(0,W^n(\alpha^n))}\,e^{-\int_{\alpha^n}^t \lambda_x(\xi_1^n(\theta),W^n(\theta))d\theta}\\ &\qquad-\frac{u^\infty(\alpha^\infty)\lambda(1,W^\infty(t))}{\lambda(0,W^\infty(\alpha^\infty))}\,e^{-\int_{\alpha^\infty}^t \lambda_x(\xi_1^\infty(\theta),W^\infty(\theta))d\theta}\Big)g(t)dt\Big|,\end{aligned}$$

where $\alpha^n=(\xi_1^n)^{-1}(0),\alpha^\infty=(\xi_1^\infty)^{-1}(0)$ are determined by

$$1-\int_{\alpha^n}^t \lambda(\xi_1^n(\theta),W^n(\theta))d\theta=1-\int_{\alpha^\infty}^t \lambda(\xi_1^\infty(\theta),W^\infty(\theta))d\theta=0,\tag{1.58}$$

and thus by (1.61) (when $(t,x)=(t,1)$) in Lemma 1.6.1,

$$\frac{d\alpha^n}{dt}=\frac{\lambda(1,W^n(t))}{\lambda(0,W^n(\alpha^n))}\,e^{-\int_{\alpha^n}^t \lambda_x(\xi_1^n(\theta),W^n(\theta))d\theta},\tag{1.59}$$

$$\frac{d\alpha^\infty}{dt}=\frac{\lambda(1,W^\infty(t))}{\lambda(0,W^\infty(\alpha^\infty))}\,e^{-\int_{\alpha^\infty}^t \lambda_x(\xi_1^\infty(\theta),W^\infty(\theta))d\theta}.\tag{1.60}$$

Let (τ^n,τ^∞) be the value of (α^n,α^∞) when $t=T$ in (1.58), and let (η^n,η^∞) be the value of (α^n,α^∞) when $t=(\xi_2^\infty)^{-1}(1)$ in (1.58). Since $W^n\to W^\infty$, $\xi_1^n\to\xi_1^\infty$ uniformly, then

$\tau^n \to \tau^\infty$, $\eta^n \to \eta^\infty$ and $\alpha^n \to \alpha^\infty$ uniformly. Hence, by (1.59)-(1.60) and using the facts that $u^n \overset{*}{\rightharpoonup} u^\infty$ and $\widetilde{\xi}_1^n \to \widetilde{\xi}_1^\infty, (\widetilde{\xi}_1^n)^{-1} \to (\widetilde{\xi}_1^\infty)^{-1}$ uniformly, we obtain

$$
\begin{aligned}
&\Big| \int_{(\xi_2^\infty)^{-1}(1)}^{T} (y^n(t) - y^\infty(t)) g(t) dt \Big| \\
&= \Big| \int_{\eta^n}^{\tau^n} u^n(\alpha^n) g(t) d\alpha^n - \int_{\eta^\infty}^{\tau^\infty} u^\infty(\alpha^\infty) g(t) d\alpha^\infty \Big| \\
&\leqslant C|\eta^n - \eta^\infty| + C|\tau^n - \tau^\infty| + \int_{\eta^\infty}^{\tau^\infty} \Big| u^n(\alpha) g((\widetilde{\xi}_1^n)^{-1}(1)) - u^\infty(\alpha) g((\widetilde{\xi}_1^\infty)^{-1}(1)) \Big| d\alpha \\
&\leqslant C|\eta^n - \eta^\infty| + C|\tau^n - \tau^\infty| + C \int_{\eta^\infty}^{\tau^\infty} |g((\widetilde{\xi}_1^n)^{-1}(1)) - g((\widetilde{\xi}_1^\infty)^{-1}(1))| d\alpha \\
&\quad + \int_{\eta^\infty}^{\tau^\infty} |u^n(\alpha) - u^\infty(\alpha)| |g((\widetilde{\xi}_1^\infty)^{-1}(1))| d\alpha \\
&\quad \longrightarrow 0, \qquad \text{as} \quad n \to \infty.
\end{aligned}
$$

This concludes the proof of (1.55) for the case $\xi_2^\infty(T) > 1$.

Obviously, $y^n \overset{*}{\rightharpoonup} y^\infty$ in $L^\infty(0,T)$ implies that $y^n \rightharpoonup y^\infty$ in $L^p(0,T)$ for all $p \in [1,\infty)$. As a result,

$$
\begin{aligned}
J_p(u^\infty) &= \|u^\infty\|_{L^\infty(0,T)} + \|y^\infty - y_d\|_{L^p(0,T)} \\
&\leqslant \liminf_{n\to\infty} \|u^n\|_{L^\infty(0,T)} + \liminf_{n\to\infty} \|y^n - y_d\|_{L^p(0,T)} \\
&\leqslant \liminf_{n\to\infty} J_p(u^n) = \lim_{n\to\infty} J_p(u^n) = \inf_{u \in L_+^\infty(0,T)} J_p(u).
\end{aligned}
$$

This shows u^∞ is a minimizer of $J_p(u)$ in $L_+^\infty(0,T)$. □

1.6 Appendix

1.6.1 Basic lemmas

The following two lemmas are used to prove the existence of weak solution to Cauchy problem (1.1), (1.2) and (1.3), when changing variables in certain integrals (see section 1.6.2). We recall some assumptions that are given: $\lambda > 0$, $\lambda \in C^1([0,1] \times [0,\infty))$, $W \in \Omega_{\delta,M}$ (see (1.10) for definition).

Lemma 1.6.1. *Let ξ_3 be the characteristic (see (1.17) for definition) which passes through the point (t,x) and intersects the t-axis at the point $(\alpha,0)$. Then we have*

$$
\frac{\partial \alpha}{\partial t} = \frac{\lambda(x, W(t))}{\lambda(0, W(\alpha))} \, e^{-\int_\alpha^t \lambda_x(\xi_3(\theta), W(\theta)) d\theta}, \tag{1.61}
$$

$$
\frac{\partial \alpha}{\partial x} = -\frac{1}{\lambda(0, W(\alpha))} \, e^{-\int_\alpha^t \lambda_x(\xi_3(\theta), W(\theta)) d\theta}. \tag{1.62}
$$

Lemma 1.6.2. *Let ξ_4 be the characteristic (see (1.18) for definition) which passes through the point (t,x) and intersects the x-axis at the point $(0,\beta)$. Then we have*

$$\frac{\partial \beta}{\partial t} = -\lambda(x, w(t)) \cdot e^{-\int_0^t \lambda_x(\xi_4(\theta), W(\theta))d\theta}, \tag{1.63}$$

$$\frac{\partial \beta}{\partial x} = e^{-\int_0^t \lambda_x(\xi_4(\theta), W(\theta))d\theta}. \tag{1.64}$$

The proofs of Lemma 1.6.1 and Lemma 1.6.2 are trivial and they can be found in [70].

The next lemma is useful to prove a uniqueness result (section 1.3, Lemma 1.3.2) for Cauchy problem (1.1), (1.2) and (1.3).

Lemma 1.6.3. *If $\rho \in C^0([0,T]; L^1(0,1)) \cap L^\infty((0,T)\times(0,1))$ is a weak solution to Cauchy problem (1.1), (1.2) and (1.3), then for every $t \in [0,T]$ and every $\varphi \in C^1([0,t]\times[0,1])$ such that*

$$\varphi(\tau, 1) = 0, \quad \forall \tau \in [0,t],$$

one has

$$\int_0^t \int_0^1 \rho(\tau,x)(\varphi_\tau(\tau,x) + \lambda(x, W(\tau))\varphi_x(\tau,x))dxd\tau + \int_0^t u(\tau)\varphi(\tau,0)d\tau \\ - \int_0^1 \rho(t,x)\varphi(t,x)dx + \int_0^1 \rho_0(x)\varphi(0,x)dx = 0.$$

The proof of Lemma 1.6.3 is the same as the proof of Lemma 2.2 in [35, section 2.2].

1.6.2 Proof of the regularity of the weak solution

In this section, let us prove Lemma 1.3.1. First we recall some notations M, $\overline{\lambda}(M)$, $\|\lambda\|_{C^0}$, $\|\lambda_x\|_{C^0}$, $\|\lambda_W\|_{C^0}$ which are defined in section 1.2. And the characteristic curves ξ_1, ξ_2, ξ_3, ξ_4 are defined by (1.12), (1.16), (1.17), (1.18), respectively.

By definition (1.20), it is easy to see that $\rho \in L^\infty((0,\delta)\times(0,1))$ and that estimates (1.21) and (1.22) hold. Next we prove that the function defined by (1.20) belongs to $C^0([0,\delta]; L^p(0,1))$ for all $p \in [1,\infty)$, i.e., for every $\widetilde{t}, t \in [0,\delta]$ with $\widetilde{t} \geq t$, we need to prove

$$\|\rho(\widetilde{t},\cdot) - \rho(t,\cdot)\|_{L^p(0,1)} \to 0, \quad \text{as} \quad |\widetilde{t} - t| \to 0$$

for all $p \in [1,\infty)$. In order to do that, we estimate $\int_0^{\xi_2(t)} |\rho(\widetilde{t},x) - \rho(t,x)|^p dx$, $\int_{\xi_2(\widetilde{t})}^1 |\rho(\widetilde{t},x) - \rho(t,x)|^p dx$ and $\int_{\xi_2(t)}^{\xi_2(\widetilde{t})} |\rho(\widetilde{t},x) - \rho(t,x)|^p dx$, successively.

For almost every $x \in [0, \xi_2(t)]$, by (1.20) and noting $W \in \Omega_{\delta,M}$ (see (1.10) for definition),

we know (see figure 1.10)

$$
\begin{aligned}
&|\rho(\widetilde{t},x)-\rho(t,x)|\\
&=\Big|\frac{u(\widetilde{\alpha})}{\lambda(0,W(\widetilde{\alpha}))}\,e^{-\int_{\widetilde{\alpha}}^{\widetilde{t}}\lambda_x(\widetilde{\xi}_3(\theta),W(\theta))d\theta}-\frac{u(\alpha)}{\lambda(0,W(\alpha))}\,e^{-\int_{\alpha}^{t}\lambda_x(\xi_3(\theta),W(\theta))d\theta}\Big|\\
&\leqslant\frac{|u(\widetilde{\alpha})-u(\alpha)|}{\lambda(0,W(\widetilde{\alpha}))}\,e^{-\int_{\widetilde{\alpha}}^{\widetilde{t}}\lambda_x(\widetilde{\xi}_3(\theta),W(\theta))d\theta}\\
&\quad+\Big|\frac{u(\alpha)}{\lambda(0,W(\widetilde{\alpha}))}-\frac{u(\alpha)}{\lambda(0,W(\alpha))}\Big|\,e^{-\int_{\widetilde{\alpha}}^{\widetilde{t}}\lambda_x(\widetilde{\xi}_3(\theta),W(\theta))d\theta}\\
&\quad+\frac{u(\alpha)}{\lambda(0,W(\alpha))}\,e^{-\int_{\widetilde{\alpha}}^{\widetilde{t}}\lambda_x(\widetilde{\xi}_3(\theta),W(\theta))d\theta}-e^{-\int_{\alpha}^{t}\lambda_x(\xi_3(\theta),W(\theta))d\theta}\Big|\\
&\leqslant C|u(\widetilde{\alpha})-u(\alpha)|+C|u(\alpha)||W(\widetilde{\alpha})-W(\alpha)|\\
&\quad+C|u(\alpha)|\Big|\int_{\widetilde{\alpha}}^{\widetilde{t}}\lambda_x(\widetilde{\xi}_3(\theta),W(\theta))d\theta-\int_{\alpha}^{t}\lambda_x(\xi_3(\theta),W(\theta))d\theta\Big|,
\end{aligned}
$$

where $\widetilde{\xi}_3$ denotes the characteristic curve passing through $(\widetilde{t},x)$:

$$
\frac{d\widetilde{\xi}_3}{ds}=\lambda(\widetilde{\xi}_3(s),W(s)),\quad \widetilde{\xi}_3(\widetilde{t})=x
$$

and it intersects t-axis at $(\widetilde{\alpha},0)$: $\widetilde{\xi}_3(\widetilde{\alpha})=0$. Here and hereafter in the appendix, we denote by C various constants which do not depend on $x,t,\widetilde{t}$.

For the given $u\in L^\infty(0,T)$, we let $\{u_n\}_{n=1}^\infty\subset C^1([0,T])$ be such that $u_n\to u$ in $L^p(0,T)$. And for the given $\lambda\in C^1([0,1]\times[0,\infty))$, we let $\{v_n\}_{n=1}^\infty\subset C^1([0,1]\times[0,M])$ be such that $v_n\to\lambda_x$ in $C^0([0,1]\times[0,M])$. Using the sequences $\{u_n\}_{n=1}^\infty$, $\{v_n\}_{n=1}^\infty$ and noting (1.15), we have for almost every $x\in[0,\xi_2(t)]$ that

$$
\begin{aligned}
&|\rho(\widetilde{t},x)-\rho(t,x)|\\
&\leqslant C|u(\widetilde{\alpha})-u(\alpha)|+C|u(\alpha)||W(\widetilde{\alpha})-W(\alpha)|\\
&\quad+C|u(\alpha)|\Big|\int_{\widetilde{\alpha}}^{\widetilde{t}}\lambda_x(\widetilde{\xi}_3(\theta),W(\theta))d\theta-\int_{\alpha}^{t}\lambda_x(\xi_3(\theta),W(\theta))d\theta\Big|\\
&\leqslant C|u^n(\widetilde{\alpha})-u(\widetilde{\alpha})|+C|u^n(\alpha)-u(\alpha)|+C|u^n(\widetilde{\alpha})-u^n(\alpha)|+C|u(\alpha)||W(\widetilde{\alpha})-W(\alpha)|\\
&\quad+C|u(\alpha)|\int_{\widetilde{\alpha}}^{\widetilde{t}}|v_n(\widetilde{\xi}_3(\theta),W(\theta))-\lambda_x(\widetilde{\xi}_3(\theta),W(\theta))|d\theta\\
&\quad+C|u(\alpha)|\int_{\alpha}^{t}|v_n(\xi_3(\theta),W(\theta))-\lambda_x(\xi_3(\theta),W(\theta))|d\theta\\
&\quad+C|u(\alpha)|\Big|\int_{\widetilde{\alpha}}^{\widetilde{t}}v_n(\widetilde{\xi}_3(\theta),W(\theta))d\theta-\int_{\alpha}^{t}v_n(\xi_3(\theta),W(\theta))d\theta\Big|\\
&\leqslant C|u^n(\widetilde{\alpha})-u(\widetilde{\alpha})|+C|u^n(\alpha)-u(\alpha)|+C|u(\alpha)|\|v_n-\lambda_x\|_{C^0([0,1]\times[0,M])}+C_n|\widetilde{\alpha}-\alpha|\\
&\quad+C_n|u(\alpha)||\widetilde{t}-t|+C_n|u(\alpha)||\widetilde{\alpha}-\alpha|+C_n|u(\alpha)|\|\widetilde{\xi}_3-\xi_3\|_{C^0([\widetilde{\alpha},t])}.
\end{aligned}
\tag{1.65}
$$

Here and hereafter, we denote by C_n various constants which do not depend on $x,t,\widetilde{t}$ but may depend on n (the index of the corresponding approximating sequences, e.g. $\{u_n\}_{n=1}^\infty$, $\{v_n\}_{n=1}^\infty$ and so on).

By the definitions of $\widetilde{\xi}_3, \xi_3$ and (1.14), we derive

$$\begin{aligned}|\widetilde{\xi}_3(s)-\xi_3(s)| &= \Big|\int_s^{\widetilde{t}} \lambda(\widetilde{\xi}_3(\theta),W(\theta))d\theta - \int_s^t \lambda(\xi_3(\theta),W(\theta))d\theta\Big| \\ &\leqslant C|\widetilde{t}-t| + \delta\|\lambda_x\|_{C^0}\|\widetilde{\xi}_3-\xi_3\|_{C^0([\widetilde{\alpha},t])}, \quad \forall s\in[\widetilde{\alpha},t],\end{aligned}$$

and furthermore

$$\|\widetilde{\xi}_3-\xi_3\|_{C^0([\widetilde{\alpha},t])} \leqslant C|\widetilde{t}-t|. \tag{1.66}$$

Meanwhile, from the fact that

$$\widetilde{\xi}_3(\widetilde{t}\,) = \int_{\widetilde{\alpha}}^{\widetilde{t}} \lambda(\widetilde{\xi}_3(\theta),W(\theta))d\theta = x = \xi_3(t) = \int_\alpha^t \lambda(\xi_3(\theta),W(\theta))d\theta,$$

and definition (1.5) of $\overline{\lambda}(M)$, we get

$$\begin{aligned}|\widetilde{\alpha}-\alpha| &\leqslant \frac{1}{\overline{\lambda}(M)}\Big|\int_\alpha^{\widetilde{\alpha}} \lambda(\xi_3(\theta),W(\theta))d\theta\Big| \\ &= \frac{1}{\overline{\lambda}(M)}\Big|\int_{\widetilde{\alpha}}^t (\lambda(\widetilde{\xi}_3(\theta),W(\theta))-\lambda(\xi_3(\theta),W(\theta)))d\theta + \int_t^{\widetilde{t}} \lambda(\widetilde{\xi}_3(\theta),W(\theta))d\theta\Big| \\ &\leqslant C\|\widetilde{\xi}_3-\xi_3\|_{C^0([\widetilde{\alpha},t])} + C|\widetilde{t}-t| \\ &\leqslant C|\widetilde{t}-t|. \end{aligned} \tag{1.67}$$

Therefore, we get easily from (1.65), (1.66), (1.67) and (1.62) in Lemma 1.6.1, that

$$\begin{aligned}&\int_0^{\xi_2(t)} |\rho(\widetilde{t},x)-\rho(t,x)|^p dx \\ &\leqslant C\|u_n-u\|^p_{L^p(0,T)} + C\|v_n-\lambda_x\|^p_{C^0([0,1]\times[0,M])} + C_n|\widetilde{t}-t|^p.\end{aligned} \tag{1.68}$$

For almost every $x\in[\xi_2(\widetilde{t}\,),1]$, by definition (1.20) of ρ, we have (see figure 1.11)

$$\begin{aligned}&|\rho(\widetilde{t},x)-\rho(t,x)| \\ &= \Big|\rho_0(\widetilde{\beta})\, e^{-\int_0^{\widetilde{t}} \lambda_x(\widetilde{\xi}_4(\theta),W(\theta))d\theta} - \rho_0(\beta)\, e^{-\int_0^t \lambda_x(\xi_4(\theta),W(\theta))d\theta}\Big| \\ &\leqslant |\rho_0(\widetilde{\beta})-\rho_0(\beta)|\, e^{-\int_0^{\widetilde{t}} \lambda_x(\widetilde{\xi}_4(\theta),W(\theta))d\theta} + |\rho_0(\beta)|\Big|e^{-\int_0^{\widetilde{t}} \lambda_x(\widetilde{\xi}_4(\theta),W(\theta))d\theta} - e^{-\int_0^t \lambda_x(\xi_4(\theta),W(\theta))d\theta}\Big| \\ &\leqslant C|\rho_0(\widetilde{\beta})-\rho_0(\beta)| + C|\rho_0(\beta)|\Big|\int_0^{\widetilde{t}} \lambda_x(\widetilde{\xi}_4(\theta),W(\theta))d\theta - \int_0^t \lambda_x(\xi_4(\theta),W(\theta))d\theta\Big|,\end{aligned}$$

where the characteristic curve $\widetilde{\xi}_4$ passing through $(\widetilde{t},x)$ is defined by

$$\frac{d\widetilde{\xi}_4}{ds} = \lambda(\widetilde{\xi}_4(s),W(s)), \quad \widetilde{\xi}_4(\widetilde{t}\,) = x,$$

and it intersects x-axis at $(0,\widetilde{\beta})$: $\widetilde{\xi}_4(0)=\widetilde{\beta}$.

For the given $\rho_0 \in L^\infty(0,1)$, we let $\{\rho_0^n\}_{n=1}^\infty \subset C^1([0,1])$ be such that $\rho_0^n \to \rho_0$ in $L^p(0,1)$. Using sequences $\{\rho_0^n\}_{n=1}^\infty$ and $\{v_n\}_{n=1}^\infty$, we obtain for almost every $x \in [\xi_2(\widetilde{t}),1]$ that

$$\begin{aligned}
&|\rho(\widetilde{t},x)-\rho(t,x)|\\
\leqslant\ & C|\rho_0^n(\widetilde{\beta})-\rho_0(\widetilde{\beta})|+C|\rho_0^n(\beta)-\rho_0(\beta)|+C|\rho_0^n(\widetilde{\beta})-\rho_0^n(\beta)|+C|\rho_0(\beta)|\|v_n-\lambda_x\|_{C^0([0,1]\times[0,M])}\\
&+C|\rho_0(\beta)|\Big|\int_0^{\widetilde{t}} v_n(\widetilde{\xi}_4(\theta),W(\theta))d\theta-\int_0^t v_n(\xi_4(\theta),W(\theta))d\theta\Big|\\
\leqslant\ & C|\rho_0^n(\widetilde{\beta})-\rho_0(\widetilde{\beta})|+C|\rho_0^n(\beta)-\rho_0(\beta)|+C|\rho_0(\beta)|\|v_n-\lambda_x\|_{C^0([0,1]\times[0,M])}\\
&+C_n|\widetilde{\beta}-\beta|+C_n|\rho_0(\beta)||\widetilde{t}-t|+C_n|\rho_0(\beta)|\|\widetilde{\xi}_4-\xi_4\|_{C^0([0,t])}. \qquad (1.69)
\end{aligned}$$

By the definitions of $\widetilde{\xi}_4, \xi_4$, we have

$$\|\widetilde{\xi}_4-\xi_4\|_{C^0([0,t])} \leqslant C|\widetilde{t}-t|, \qquad (1.70)$$

which is similar to (1.66). In particular,

$$|\widetilde{\beta}-\beta| = |\widetilde{\xi}_4(0)-\xi_4(0)| \leqslant C|\widetilde{t}-t|. \qquad (1.71)$$

Therefore, we get easily from (1.69), (1.70), (1.71) and (1.64) in Lemma 1.6.2 that

$$\begin{aligned}
&\int_{\xi_2(\widetilde{t})}^1 |\rho(\widetilde{t},x)-\rho(t,x)|^p dx\\
\leqslant\ & C\|\rho_0^n-\rho_0\|_{L^p(0,1)}^p + C\|v_n-\lambda_x\|_{C^0([0,1]\times[0,M])}^p + C_n|\widetilde{t}-t|^p. \qquad (1.72)
\end{aligned}$$

Finally, we turn to estimate $\int_{\xi_2(t)}^{\xi_2(\widetilde{t})} |\rho(\widetilde{t},x)-\rho(t,x)|^p dx$ (see figure 1.12). By (1.22) and definition of ξ_2, we get that

$$\int_{\xi_2(t)}^{\xi_2(\widetilde{t})} |\rho(\widetilde{t},x)-\rho(t,x)|^p dx \leqslant C|\xi_2(\widetilde{t})-\xi_2(t)| \leqslant C|\widetilde{t}-t|. \qquad (1.73)$$

Summarizing estimates (1.68), (1.72) and (1.73), we find that for every $p \in [1,\infty)$,

$$\begin{aligned}
&\|\rho(\widetilde{t},\cdot)-\rho(t,\cdot)\|_{L^p(0,1)}^p\\
\leqslant\ & C\|u_n-u\|_{L^p(0,T)}^p + C\|\rho_0^n-\rho_0\|_{L^p(0,1)}^p + C\|v_n-\lambda_x\|_{C^0([0,1]\times[0,M])}^p\\
&+C_n|\widetilde{t}-t|^p + C|\widetilde{t}-t|. \qquad (1.74)
\end{aligned}$$

Therefore by Lebesque dominated convergence theorem, letting n large enough and then $|\widetilde{t}-t|$ small enough, the right hand side of (1.74) can be arbitrarily small. This proves that the function ρ defined by (1.20) belongs to $C^0([0,\delta];L^p(0,1))$ for all $p \in [1,\infty)$.

Finally, we prove that ρ defined by (1.20) is indeed a weak solution to Cauchy problem (1.1), (1.2) and (1.3). Let $\tau \in [0,\delta]$. For any $\varphi \in C^1([0,\tau]\times[0,1])$ with $\varphi(\tau,x) \equiv 0$ and

$\varphi(t,1)\equiv 0$, we have

$$\begin{aligned}A&:=\int_0^\tau\int_0^1 \rho(t,x)(\varphi_t(t,x)+\lambda(x,W(t))\varphi_x(t,x))dxdt\\&=\int_0^\tau\int_0^{\xi_2(t)}\frac{u(\alpha)}{\lambda(0,W(\alpha))}\,e^{-\int_\alpha^t\lambda_x(\xi_3(\theta),W(\theta))d\theta}\cdot(\varphi_t(t,x)+\lambda(x,W(t))\varphi_x(t,x))dxdt\\&\quad+\int_0^\tau\int_{\xi_2(t)}^1\rho_0(\beta)\,e^{-\int_0^t\lambda_x(\xi_4(\theta),W(\theta))d\theta}\cdot(\varphi_t(t,x)+\lambda(x,W(t))\varphi_x(t,x))dxdt.\end{aligned}$$

By (1.62) in Lemma 1.6.1 and (1.64) in Lemma 1.6.2, we obtain

$$\begin{aligned}A&=\int_0^\tau\int_0^t u(\alpha)(\varphi_t(t,\xi_3(t))+\lambda(\xi_3(t),W(t))\varphi_x(t,\xi_3(t))d\alpha dt\\&\quad+\int_0^\tau\int_0^{1-\int_0^t\lambda(\xi_1(\theta),W(\theta))d\theta}\rho_0(\beta)(\varphi_t(t,\xi_4(t))+\lambda(\xi_4(t),W(t))\varphi_x(t,\xi_4(t)))d\beta dt\\&=\int_0^\tau\int_0^t u(\alpha)\frac{d\varphi(t,\xi_3(t))}{dt}d\alpha dt+\int_0^\tau\int_0^{1-\int_0^t\lambda(\xi_1(\theta),W(\theta))d\theta}\rho_0(\beta)\frac{d\varphi(t,\xi_4(t))}{dt}d\beta dt.\end{aligned}$$

Hence by changing the order of integral, we get

$$A=\int_0^\tau\int_\alpha^\tau u(\alpha)\frac{d\varphi(t,\xi_3(t))}{dt}dtd\alpha+\Big(\int_0^{f(\tau)}\int_0^\tau+\int_{f(\tau)}^1\int_0^{f^{-1}(\beta)}\Big)\rho_0(\beta)\frac{d\varphi(t,\xi_4(t))}{dt}dtd\beta,$$

where

$$f(t):=1-\int_0^t\lambda(\xi_1(\theta),W(\theta))d\theta$$

represents the coordinate that the characteristic curve ξ_1 intersects with x-axis and $f^{-1}(\beta)$ represents the time when the characteristic curve starting from $(0,\beta)$ arrives at the boundary $x=1$. Consequently, for any $\beta\in[f(\tau),1]$, ξ_1 and ξ_4 are identical to each other since they pass through the same point $(0,\beta)$, so we get immediately that

$$\xi_4(f^{-1}(\beta))=\xi_1(f^{-1}(\beta))=1.$$

and finally that

$$\begin{aligned}A&=\int_0^\tau u(\alpha)(\varphi(\tau,\xi_3(\tau))-\varphi(\alpha,\xi_3(\alpha)))d\alpha+\int_0^{f(\tau)}\rho_0(\beta)(\varphi(\tau,\xi_4(\tau))-\varphi(0,\xi_4(0)))d\beta\\&\quad+\int_{f(\tau)}^1\rho_0(\beta)(\varphi(f^{-1}(\beta),\xi_4(f^{-1}(\beta)))-\varphi(0,\xi_4(0)))d\beta\\&=-\int_0^\tau u(\alpha)\varphi(\alpha,0)d\alpha-\int_0^{f(\tau)}\rho_0(\beta)\varphi(0,\beta)d\beta-\int_{f(\tau)}^1\rho_0(\beta)\varphi(0,\beta)d\beta\\&=-\int_0^\tau u(\alpha)\varphi(\alpha,0)d\alpha-\int_0^1\rho_0(\beta)\varphi(0,\beta)d\beta.\end{aligned}$$

This proves that ρ given by (1.23) is indeed a weak solution to Cauchy problem (1.1), (1.2) and (1.3).

1.6.3 Proof of the uniqueness of the weak solution

In this section, we prove Lemma 1.3.2. Let us assume that $\overline{\rho} \in C^0([0,\delta];L^1(0,1)) \cap L^\infty((0,\delta)\times(0,1))$ is a weak solution to Cauchy problem (1.1), (1.2) and (1.3). Here δ is such that (1.14) holds. Then by Lemma 1.6.3, for any fixed $t \in [0,\delta]$ and $\varphi \in C^1([0,t]\times[0,1])$ with $\varphi(\tau,1) \equiv 0$ for $\tau \in [0,t]$,

$$\int_0^t \int_0^1 \overline{\rho}(\tau,x)(\varphi_\tau(\tau,x) + \lambda(x,\overline{W}(\tau))\varphi_x(\tau,x))dxd\tau + \int_0^t u(\tau)\varphi(\tau,0)d\tau - \int_0^1 \overline{\rho}(t,x)\varphi(t,x)dx + \int_0^1 \rho_0(x)\varphi(0,x)dx = 0. \quad (1.75)$$

where $\overline{W}(\tau) := \int_0^1 \overline{\rho}(\tau,x)\,dx$.

Let $\psi_0 \in C_0^1(0,1)$, then we choose the test function as the solution to the following *backward linear* Cauchy problem

$$\begin{cases} \psi_\tau + \lambda(x,\overline{W}(\tau))\psi_x = 0, & 0 \leqslant \tau \leqslant t,\ 0 \leqslant x \leqslant 1, \\ \psi(t,x) = \psi_0(x), & 0 \leqslant x \leqslant 1, \\ \psi(\tau,1) = 0, & 0 \leqslant \tau \leqslant t. \end{cases}$$

For any fixed $t \in [0,\delta]$, we define the characteristic curves $\overline{\xi}_1, \overline{\xi}_2, \overline{\xi}_3, \overline{\xi}_4$ by

$$\begin{aligned} &\frac{d\overline{\xi}_1}{ds} = \lambda(\overline{\xi}_1(s),\overline{W}(s)), \quad \overline{\xi}_1(t) = 1, \\ &\frac{d\overline{\xi}_2}{ds} = \lambda(\overline{\xi}_2(s),\overline{W}(s)), \quad \overline{\xi}_2(0) = 0, \\ &\frac{d\overline{\xi}_3}{ds} = \lambda(\overline{\xi}_3(s),\overline{W}(s)), \quad \overline{\xi}_3(t) = x, \quad \text{for } x \in [0,\overline{\xi}_2(t)], \\ &\frac{d\overline{\xi}_4}{ds} = \lambda(\overline{\xi}_4(s),\overline{W}(s)), \quad \overline{\xi}_4(t) = x, \quad \text{for } x \in [\overline{\xi}_2(t),1], \end{aligned}$$

It is easy to see that there exist $\overline{\alpha} \in [0,t]$ and $\overline{\beta} \in [0,1]$ such that

$$\overline{\xi}_3(\overline{\alpha}) = 0 \quad \text{and} \quad \overline{\xi}_4(0) = \overline{\beta}.$$

In view of (1.75), we compute

$$\begin{aligned} \int_0^1 \overline{\rho}(t,x)\psi_0(x)\,dx &= \int_0^t u(\tau)\psi(\tau,0)\,d\tau + \int_0^1 \rho_0(x)\psi(0,x)\,dx \\ &= \int_0^t u(\overline{\alpha})\psi(\overline{\alpha},0)\,d\overline{\alpha} + \int_0^1 \rho_0(\overline{\beta})\psi(0,\overline{\beta})\,d\overline{\beta} \\ &= \int_0^t u(\overline{\alpha})\psi_0(x)\,d\overline{\alpha} + \int_0^{1-\int_0^t \lambda(\overline{\xi}_1(\theta),\overline{W}(\theta))\,d\theta} \rho_0(\overline{\beta})\psi_0(x)\,d\overline{\beta}. \end{aligned} \quad (1.76)$$

By the definitions of $\overline{\alpha},\overline{\beta}$ and similar to (1.62) and (1.64), we have

$$\frac{\partial\overline{\alpha}}{\partial x} = \frac{-1}{\lambda(0,\overline{W}(\overline{\alpha}))} e^{-\int_{\overline{\alpha}}^t \lambda_x(\overline{\xi}_3(\theta),\overline{W}(\theta))\,d\theta} \quad \text{and} \quad \frac{\partial\overline{\beta}}{\partial x} = e^{-\int_0^t \lambda_x(\overline{\xi}_4(\theta),\overline{W}(\theta))\,d\theta}.$$

Thus, (1.76) is rewritten as

$$\begin{aligned}&\int_0^1 \overline{\rho}(t,x)\psi_0(x)\,dx\\ &= \int_0^{\overline{\xi}_2(t)} \frac{u(\overline{\alpha})}{\lambda(0,\overline{W}(\overline{\alpha}))} e^{-\int_{\overline{\alpha}}^t \lambda_x(\overline{\xi}_3(\theta),\overline{W}(\theta))\,d\theta}\psi_0(x)\,dx + \int_{\overline{\xi}_2(t)}^1 \rho_0(\overline{\beta}) e^{-\int_0^t \lambda_x(\overline{\xi}_4(\theta),\overline{W}(\theta))\,d\theta}\psi_0(x)\,dx.\end{aligned}$$

Since $\psi_0 \in C_0^1(0,1)$ and $t \in [0,\delta]$ are both arbitrary, we obtain in $C^0([0,\delta];L^1(0,1)) \cap L^\infty((0,\delta)\times(0,1))$ that

$$\overline{\rho}(t,x) = \begin{cases} \dfrac{u(\overline{\alpha})}{\lambda(0,\overline{W}(\overline{\alpha}))}\, e^{-\int_{\overline{\alpha}}^t \lambda_x(\overline{\xi}_3(\theta),\overline{W}(\theta))d\theta}, & 0 \leqslant x \leqslant \overline{\xi}_2(t) \leqslant 1, 0 \leqslant t \leqslant \delta, \\ \rho_0(\overline{\beta})\, e^{-\int_0^t \lambda_x(\overline{\xi}_4(\theta),\overline{W}(\theta))d\theta}, & 0 \leqslant \overline{\xi}_2(t) \leqslant x \leqslant 1, 0 \leqslant t \leqslant \delta, \end{cases} \tag{1.77}$$

which hence gives

$$\begin{aligned}\overline{W}(t) &= \int_0^1 \overline{\rho}(t,x)\,dx\\ &= \int_0^t u(\overline{\alpha})d\overline{\alpha} + \int_0^{1-\int_0^t \lambda(\overline{\xi}_1(\theta),\overline{W}(\theta))d\theta} \rho_0(\overline{\beta})d\overline{\beta} = F(\overline{W})(t), \quad \forall t \in [0,\delta].\end{aligned}$$

By (1.14), we claim that $\overline{W} \in \Omega_{\delta,M}$ and then $\overline{W} \equiv W$ since W is the unique fixed point of the map $W \mapsto F(W)$ in $\Omega_{\delta,M}$. Consequently, we have $\overline{\xi}_i \equiv \xi_i$ $(i = 1,2,3,4)$ and $\overline{\alpha} = \alpha, \overline{\beta} = \beta$. Finally, by comparing (1.20) and (1.77), we obtain $\overline{\rho} \equiv \rho$. This gives us the uniqueness of the weak solution for small time.

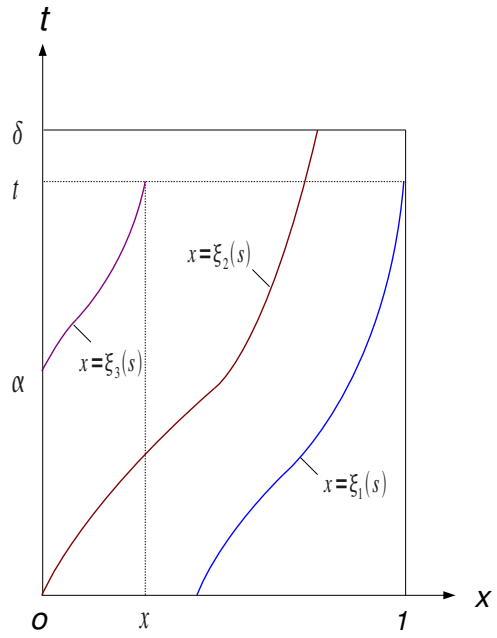


Figure 1.1. Characteristics ξ_1, ξ_2 and ξ_3

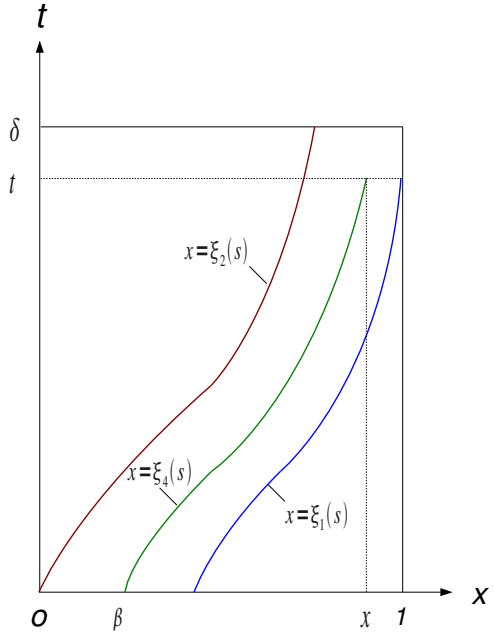


Figure 1.2. Characteristics ξ_1, ξ_2 and ξ_4

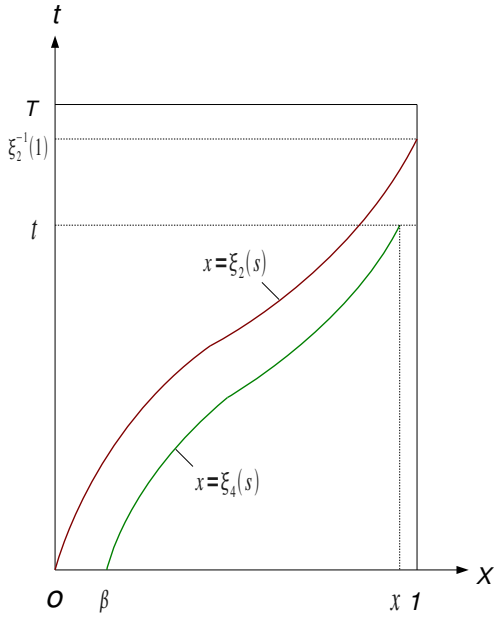


Figure 1.3. Case $0 \leqslant \xi_2(t) \leqslant x$, $0 \leqslant t \leqslant \xi_2^{-1}(1)$

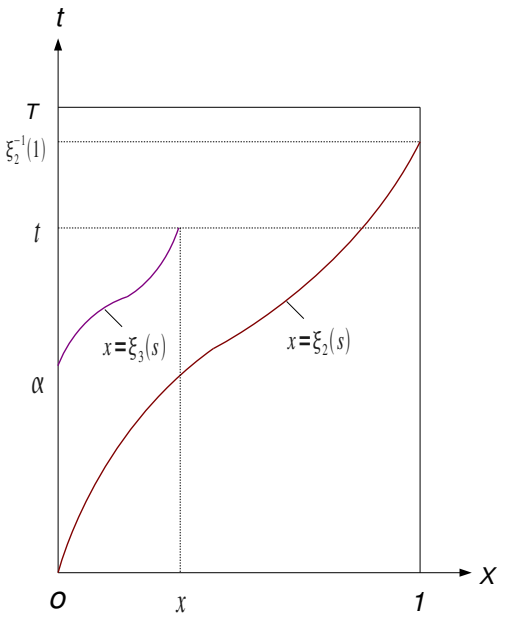


Figure 1.4. Case $0 \leqslant x \leqslant \xi_2(t)$, $0 \leqslant t \leqslant \xi_2^{-1}(1)$

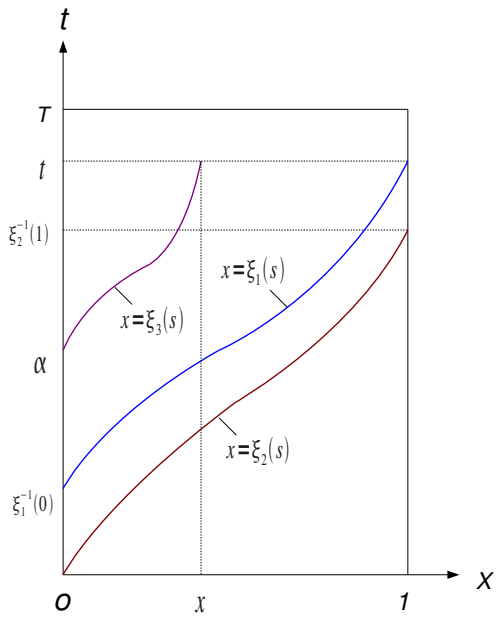


Figure 1.5. Case $0 \leqslant x \leqslant 1$, $\xi_2^{-1}(1) \leqslant t \leqslant T$

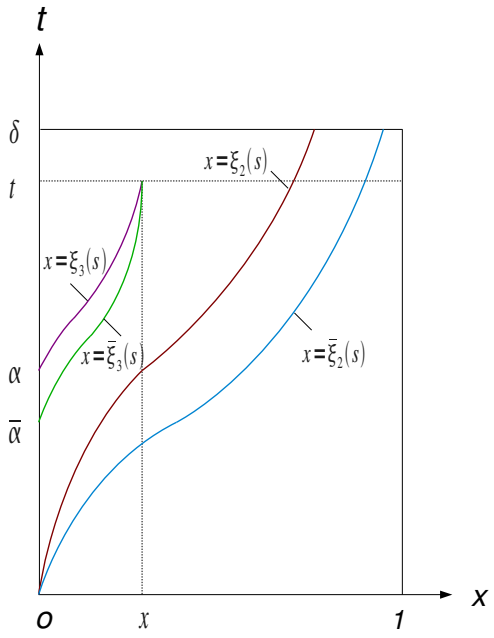


Figure 1.6. Estimate for $x \in [0, \xi_2(t)]$

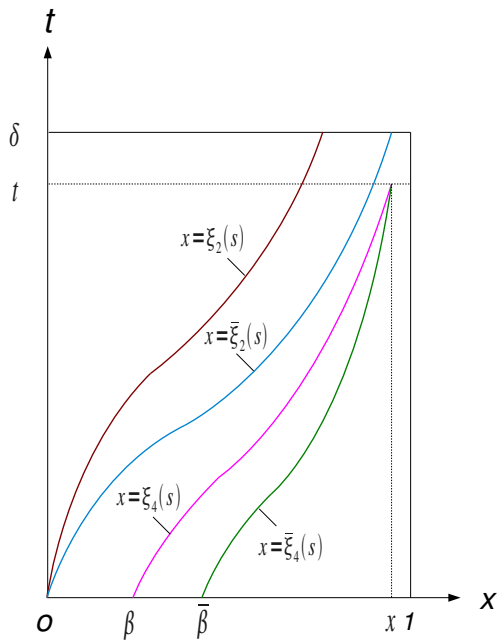


Figure 1.7. Estimate for $x \in [\bar{\xi}_2(t), 1]$

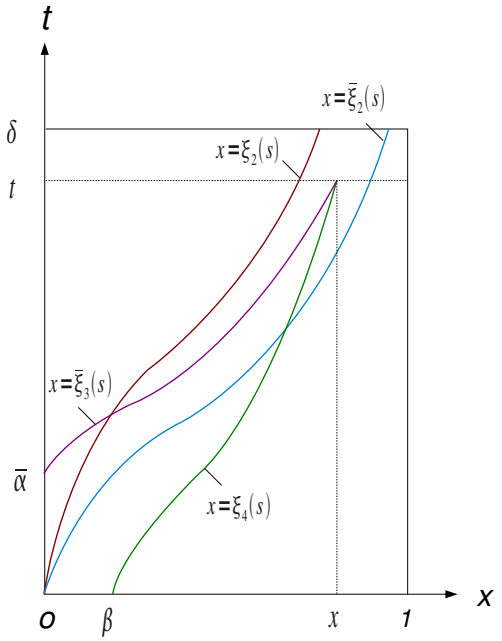


Figure 1.8. Estimate for $x \in [\xi_2(t), \bar{\xi}_2(t)]$

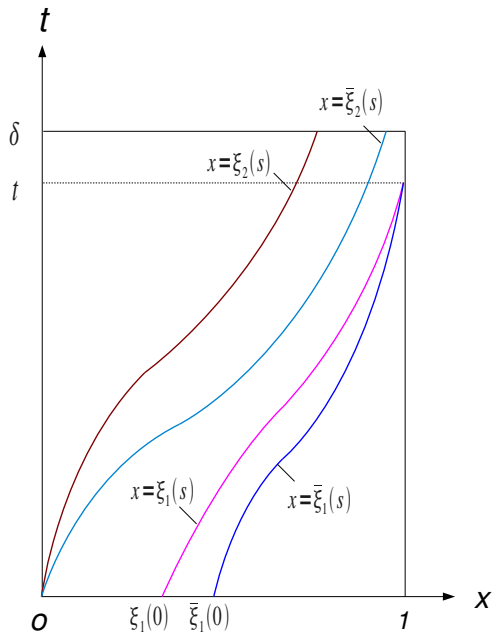


Figure 1.9. Estimate of $|\overline{y} - y|$ for $t \in [0, \delta]$

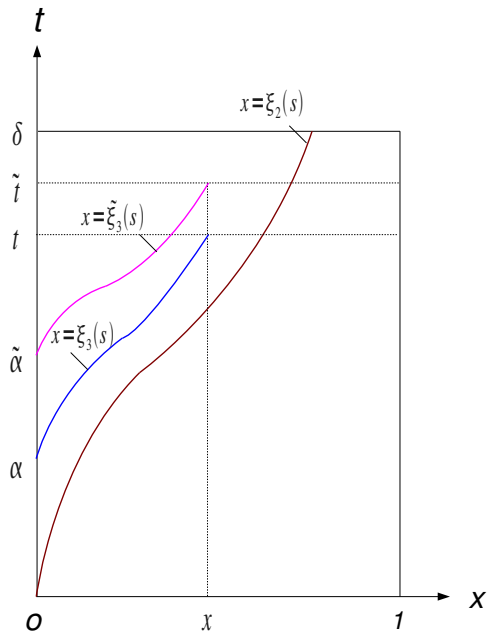


Figure 1.10. Estimate for $x \in [0, \xi_2(t)]$

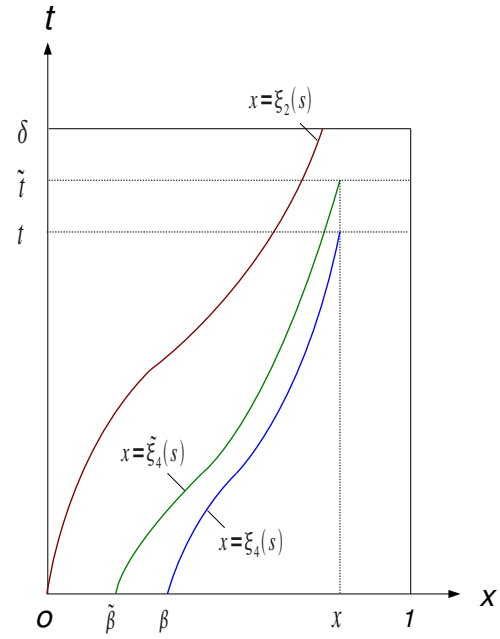


Figure 1.11. Estimate for $x \in [\xi_2(\widetilde{t}), 1]$

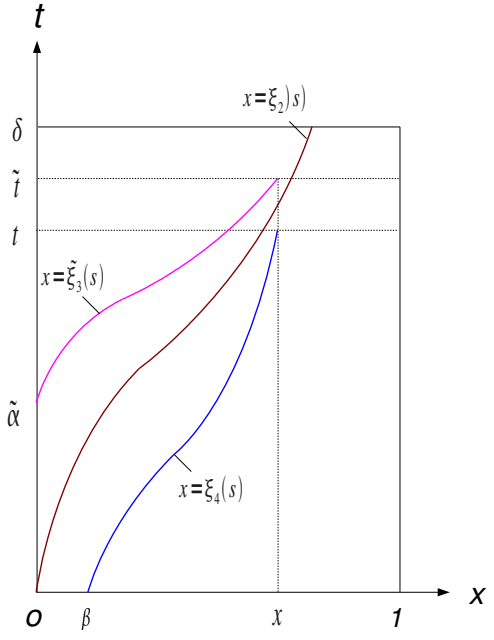


Figure 1.12. Estimate for $x \in [\xi_2(t), \xi_2(\widetilde{t})]$

Chapter 2

Cauchy problem for multiscale conservation laws: application to structured cell populations

This work is motivated by another conservation law which is now in 2D. More specifically, we study a vector conservation law that models the growth and selection of ovarian follicles. A 2D conservation law describes the age and maturity structuration of the follicular cell populations. The densities interact through a coupled hyperbolic system between different follicles and cell phases, which results in a vector conservation law and coupling between boundary conditions. The maturity velocity functions possess both a local and nonlocal character. We prove the existence and uniqueness of the weak solution to Cauchy problem with bounded initial and boundary data. This chapter has been the matter submitted for publication (see [85]).

2.1 Introduction

We consider an ovary containing a cohort of n follicles, i.e. $f = 1, \cdots, n$ and cells in each follicle progress along N cell cycles. We denote by x the age of the cells and y the maturity. After reformulation (see section 2.6.2), for each follicle f, the cell density $\vec{\phi}_f$ satisfies the following conservation law (see 2.6.1 for details)

$$\vec{\phi}_{ft}(t,x,y)+(A_f\vec{\phi}_f(t,x,y))_x+(B_f\vec{\phi}_f(t,x,y))_y=C\vec{\phi}_f(t,x,y),\ t\geqslant 0,\ (x,y)\in[0,1]^2, \quad (2.1)$$

where $\vec{\phi}_f = (\overline{\phi}_1^f, \cdots, \overline{\phi}_N^f,\ \widehat{\phi}_1^f, \cdots, \widehat{\phi}_N^f,\ \widetilde{\phi}_1^f, \cdots, \widetilde{\phi}_N^f)^{tr}$, and

$$
\begin{aligned}
A_f &:= \text{diag}\ \{\overbrace{\overline{g}_f, \cdots, \overline{g}_f}^{N},\ \overbrace{\tau_{gf}, \cdots, \tau_{gf}}^{N},\ \overbrace{\frac{\tau_{gf}}{2}, \cdots, \frac{\tau_{gf}}{2}}^{N}\},\\
B_f &:= \text{diag}\ \{\overbrace{\overline{h}_f, \cdots, \overline{h}_f}^{N},\ \overbrace{0, \cdots, 0}^{N},\ \overbrace{\widetilde{h}_f, \cdots, \widetilde{h}_f}^{N}\},\\
C &:= -\text{diag}\ \{\overbrace{\overline{\lambda}, \cdots, \overline{\lambda}}^{N},\ \overbrace{0, \cdots, 0}^{N},\ \overbrace{\widetilde{\lambda}, \cdots, \widetilde{\lambda}}^{N}\}.
\end{aligned}
$$

Correspondingly, A_f denotes the age velocity, B_f denotes the maturity velocity. They depend not only on the maturity of each individual follicle but also on the global maturity of the whole ovary. C denotes the source terms, it depends only on the global maturity of the whole ovary. Here τ_{gf} are positive constants corresponding to each follicle f, $\overline{g}_f = \overline{g}_f(u_f) \in C^1([0,\infty))$, $\overline{h}_f = \overline{h}_f(y, u_f)$, $\widetilde{h}_f = \widetilde{h}_f(y, u_f)$, $\overline{\lambda} = \overline{\lambda}(y, U)$ and $\widetilde{\lambda} = \widetilde{\lambda}(y, U)$ all belong to $C^1([0,1]\times[0,\infty))$ (see section 2.6.2 for the expressions in detail). u_f depends on both local maturity on the follicular scale and global maturity on the ovarian scale, i.e. $u_f = u_f(M_f(t), M(t), t)$, where the M_f function is the maturity on the follicular scale given by

$$
\begin{aligned}
M_f(t) :=& \sum_{k=1}^{N} \int_0^1 \int_0^1 \gamma_s^2 y \overline{\phi}_k^f(t,x,y)\, dx\, dy + \sum_{k=1}^{N} \int_0^1 \int_0^1 \gamma_s^2 y \widehat{\phi}_k^f(t,x,y)\, dx\, dy\\
&+ \sum_{k=1}^{N} \int_0^1 \int_0^1 2\gamma_d(\gamma_d y + \gamma_s) \widetilde{\phi}_k^f(t,x,y)\, dx\, dy,
\end{aligned}
$$

and

$$
M(t) := \sum_{f=1}^{n} M_f(t)
$$

is the global maturity on the ovarian scale.

The parameters γ_s and γ_d are positive constants. $U = U(M(t), t)$ depends only on the global maturity on the ovarian scale. We assume that $u_f > 0$ and $U > 0$ are continuous differentiable, i.e., $u_f \in C^1([0,\infty)^2 \times [0,T])$ and $U \in C^1([0,\infty)\times[0,T])$. For instance, the specific case that motivated our work is presented in section 2.6.1.

For sake of simplicity, we use the simplified notations $u_f(t) := u_f(M_f(t), M(t), t)$, $U(t) := U(M(t), t)$, $\overline{u}_f(t) := u_f(\overline{M}_f(t), \overline{M}(t), t)$ and $\overline{U}(t) := U(\overline{M}(t), t)$ in the whole chapter.

The initial conditions are given by

$$
\begin{aligned}
\vec{\phi}_{f0} :=& \vec{\phi}_f(0,x,y) \\
=& (\overline{\phi}_{10}^f(x,y), \cdots, \overline{\phi}_{N0}^f(x,y),\ \widehat{\phi}_{10}^f(x,y), \cdots, \widehat{\phi}_{N0}^f(x,y),\ \widetilde{\phi}_{10}^f(x,y), \cdots, \widetilde{\phi}_{N0}^f(x,y))^{tr}.
\end{aligned} \tag{2.2}
$$

There is no influx for $\overline{\phi}_1^f$ and $\widetilde{\phi}_1^f$ at $x = 0$ (see figure 2.1), hence

$$
\overline{\phi}_1^f(t,0,y) = \widetilde{\phi}_1^f(t,0,y) = 0, \quad (t,y) \in [0,T]\times[0,1]. \tag{2.3}
$$

The mitosis happens when the cell leaves the previous cycle and goes into the next cycle (see figure 2.1), hence for $k = 2, \cdots, N$

$$\overline{g}_f(u_f(t))\overline{\phi}_k^f(t,0,y) = 2\tau_{gf}\widehat{\phi}_{k-1}^f(t,1,y), \quad (t,y) \in [0,T] \times [0,1]. \tag{2.4}$$

There is no mitosis in phase 3, hence

$$\widetilde{\phi}_k^f(t,0,y) = \widetilde{\phi}_{k-1}^f(t,1,y), \quad (t,y) \in [0,T] \times [0,1]. \tag{2.5}$$

In the same cycle k, $k = 1, \cdots, N$, the dynamics amounts to a transport dynamics from phase 1 to phase 2 (see figure 2.1), hence

$$\tau_{gf}\widehat{\phi}_k^f(t,0,y) = \overline{g}_f(u_f(t))\overline{\phi}_k^f(t,1,y), \quad (t,y) \in [0,T] \times [0,1]. \tag{2.6}$$

There is no influx from the bottom $y = 0$, hence for $k = 1, \cdots, N$

$$\overline{\phi}_k^f(t,x,0) = \widehat{\phi}_k^f(t,x,0) = 0, \quad (t,x) \in [0,T] \times [0,1]. \tag{2.7}$$

We assume that there is only influx from phase 1 to phase 3, and no influx from phase 2 to phase 3 (see figure 2.1), hence for $k = 1, \cdots, N$

$$\widetilde{\phi}_k^f(t,x,0) = \begin{cases} \overline{\phi}_k^f(t,2x,1), & (t,x) \in [0,T] \times [0,\frac{1}{2}], \\ 0, & (t,x) \in [0,T] \times [\frac{1}{2},1]. \end{cases} \tag{2.8}$$

There is no influx from the above $y = 1$ (see figure 2.1), hence for $k = 1, \cdots, N$

$$\widetilde{\phi}_k^f(t,x,1) = 0, \quad (t,x) \in [0,T] \times [0,1]. \tag{2.9}$$

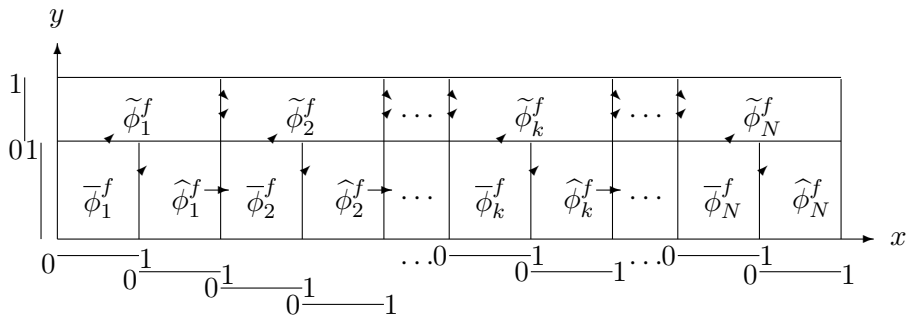


Figure 2.1. Domain of the solution in the reformulated model. For each follicle f, the domain consists of the sequence of N cell cycles. x denotes the age of the cell and y denotes its maturity. The top of the domain corresponds to the differentiation phase and the bottom to the proliferation phase.

The well-posedness problems of the hyperbolic conservation laws have been widely studied. We refer to the works [13, 14, 61, 71, 80] (and the references therein) for weak solutions to systems in conservation laws, and [66, 70] for classical solutions to general quasi-linear

hyperbolic systems. In this chapter, we perform the following mathematical analysis: we prove the existence, uniqueness and regularity of the weak solution to Cauchy problem (2.1)-(2.9) with initial and boundary data in L^∞. Besides the nonlocal velocity, we have to deal with the 2D formulation, the coupling between boundary conditions and the coupling between different follicles in the model. Additionally, we have to deal with source terms and possibly nonpositive velocities. A related work addressed well-posedness for systems of hyperbolic conservation laws with a nonlocal velocity [92]. However, our method of proof and even our definition of solutions are different from the ones given in [92]. In [92], the author used the Schauder fixed point theorem to prove the existence of the solution, while our proof uses the Banach fixed point theorem, which is more useful to compute numerically the solution. Furthermore, the author proved the uniqueness under strong assumptions that the initial data is continuously differentiable, while we get the uniqueness when initial data is in L^∞.

In another related work [75], which was also motivated by [45], the author reduced and simplified the model to a 1D mass-maturity dynamical system of coupled ODEs, basing on the asymptotic properties of the original law. After giving some assumptions on velocities according to biological observations, the model is amenable to analysis by bifurcation theory, that allows one to predict the issue of the selection for one specific follicle amongst the whole population. An associated reachability problem has been tackled in [44], which described the set of microscopic initial conditions leading to the macroscopic phenomenon of either ovulation or atresia in the framework of backwards reachable sets theory. The authors also performed some mathematical analysis on the well-posedness of this model but in a simplified open loop like case, since the authors assumed that the local control u_f and the global control U are given functions of time t. In contrast, we consider both the closed and open loop cases.

In section 2.2 we first give the main results. In section 2.3, after giving some basic notations, we prove that the maturity $\vec{M} := (M_1, \cdots, M_n)$ exists as a fixed point of a map from a continuous function space, and then we construct a local weak solution to Cauchy problem (2.1)-(2.9). In section 2.4 we prove the uniqueness of the weak solution. Finally, in section 2.5 we prove the existence of a global solution. In complement, we introduce in section 2.6.1 the original biological mathematical model proposed by F. Clément [45]. In section 2.6.2 we reformulate this model to the new system (2.1) and we give the equivalence between the original notations and the new ones. In section 2.6.3 we give a basic lemma that is used to prove the existence and uniqueness of the weak solution.

2.2 Main results

We recall from [31, section 2.1], the usual definition of a weak solution to Cauchy problem (2.1)-(2.9).

Definition 2.2.1. Let $T > 0$, $\vec{\phi}_{f0} \in L^\infty((0,1)^2)$ be given. A weak solution of Cauchy problem

(2.1)-(2.9) is a vector function $\vec{\phi}_f \in C^0([0,T];L^1((0,1)^2))$ such that for every $\tau \in [0,T]$ and every vector function $\vec{\varphi} := (\overline{\varphi}_1,\cdots,\overline{\varphi}_N,\widehat{\varphi}_1,\cdots,\widehat{\varphi}_N,\widetilde{\varphi}_1,\cdots,\widetilde{\varphi}_N)^{tr} \in C^1([0,\tau]\times[0,1]^2)$ such that

$$\vec{\varphi}(\tau,x,y) = 0, \quad \forall (x,y) \in [0,1]^2, \tag{2.10}$$

$$\vec{\varphi}(t,1,y) = 0, \quad \forall (t,y) \in [0,\tau]\times[0,1], \tag{2.11}$$

$$\overline{\varphi}_1(t,0,y) = \widetilde{\varphi}_1(t,0,y) = 0, \quad \forall (t,y) \in [0,\tau]\times[0,1], \tag{2.12}$$

$$\overline{\varphi}_k(t,x,0) = \widehat{\varphi}_k(t,x,0) = \overline{\varphi}_k(t,x,1) = \widehat{\varphi}_k(t,x,1) = 0, \quad \forall (t,x) \in [0,\tau]\times[0,1], \tag{2.13}$$

one has

$$\begin{aligned}
&\int_0^\tau\int_0^1\int_0^1 \vec{\phi}_f(t,x,y)\cdot(\vec{\varphi}_t(t,x,y)+A_f\vec{\varphi}_x(t,x,y)+B_f\vec{\varphi}_y(t,x,y)+C\vec{\varphi}(t,x,y))dxdydt\\
&+\int_0^1\int_0^1 \vec{\phi}_{f0}(x,y)\cdot\vec{\varphi}(0,x,y)dxdy+\sum_{k=1}^N\int_0^\tau\int_0^{\frac{1}{2}} \widetilde{h}_f(0,u_f(t))\overline{\phi}_k^f(t,2x,1)\widetilde{\varphi}_k(t,x,0)dxdt\\
&+\sum_{k=2}^N\int_0^\tau\int_0^1 2\tau_{gf}\widehat{\phi}_{k-1}^f(t,1,y)\overline{\varphi}_k(t,0,y)dydt+\sum_{k=2}^N\int_0^\tau\int_0^1 \frac{\tau_{gf}}{2}\widetilde{\phi}_{k-1}^f(t,1,y)\widetilde{\varphi}_k(t,0,y)dydt\\
&+\sum_{k=1}^N\int_0^\tau\int_0^1 \overline{g}_f(u_f(t))\overline{\phi}_k^f(t,1,y)\widehat{\varphi}_k(t,0,y)dydt = 0.
\end{aligned} \tag{2.14}$$

Basing on the definition, we have the main result

Theorem 2.2.1. *Let $T>0$, $\vec{\phi}_{f0} \in L^\infty((0,1)^2)$ be given. Let us further assume that*

$$\begin{aligned}
&\overline{g}_f(u_f) > 0, \quad \forall\ u_f \in [0,\infty),\\
&\overline{h}_f(y,u_f) > 0, \quad \forall\ (y,u_f) \in [0,1]\times[0,\infty),\\
&\widetilde{h}_f(0,u_f) > 0,\ \widetilde{h}_f(1,u_f) < 0, \quad \forall\ u_f \in [0,\infty).
\end{aligned}$$

Then Cauchy problem (2.1)-(2.9) *admits a unique weak solution $\vec{\phi}_f$. Moreover, this weak solution even belongs to $C^0([0,T];L^p((0,1)^2))$ for all $p \in [1,\infty)$.*

The sketch of the proof of Theorem 2.2.1 consists in first proving that the maturity $\vec{M}(t) = (M_1(t),\cdots,M_n(t))$ exists as a fixed point of the map $\vec{M} \mapsto \vec{G}(\vec{M})$ (see section 2.3.1), and then in constructing a (unique) local solution (see section 2.3.2 and section 2.4), before finally proving the existence of a global solution to Cauchy problem (2.1)-(2.9) (see section 2.5).

2.3 Fixed point argument and construction of a local solution to Cauchy problem

In this section, we first derive the contraction mapping function $\vec{G}$ (see section 2.3.1). Given the existence of a fixed point to this contraction mapping function, we can then construct a local solution to Cauchy problem (2.1)-(2.9) (see section 2.3.2).

2.3.1 Fixed point argument

First we introduce some notations. Let us define:

$$\|\overline{\phi}^f_{k0}\| := \|\overline{\phi}^f_{k0}\|_{L^\infty((0,1)^2)} := \operatorname*{ess\,sup}_{(x,y)\in(0,1)^2} |\overline{\phi}^f_{k0}(x,y)|,$$
$$\|\widehat{\phi}^f_{k0}\| := \|\widehat{\phi}^f_{k0}\|_{L^\infty((0,1)^2)} := \operatorname*{ess\,sup}_{(x,y)\in(0,1)^2} |\widehat{\phi}^f_{k0}(x,y)|,$$
$$\|\widetilde{\phi}^f_{k0}\| := \|\widetilde{\phi}^f_{k0}\|_{L^\infty((0,1)^2)} := \operatorname*{ess\,sup}_{(x,y)\in(0,1)^2} |\widetilde{\phi}^f_{k0}(x,y)|.$$

$$K := 2^N(\gamma_s+\gamma_d)^2 \sum_{f=1}^{n}\sum_{k=1}^{N} \Big(\|\overline{\phi}^f_{k0}\|_{L^1((0,1)^2)} + \|\widehat{\phi}^f_{k0}\|_{L^1((0,1)^2)} + \|\widetilde{\phi}^f_{k0}\|_{L^1((0,1)^2)}\Big), \tag{2.15}$$

$$K_1 := \max\Big\{\tau_{gf}, \|\overline{g}_f(u_f(M_f,M,t))\|_{C^1(Q_1)}, \|\overline{h}_f(y,u_f(M_f,M,t))\|_{C^1(Q_2)}, \tag{2.16}$$
$$\|\widetilde{h}_f(y,u_f(M_f,M,t))\|_{C^1(Q_2)}, \|\overline{\lambda}(y,U(M,t))\|_{C^1(Q_3)}, \|\widetilde{\lambda}(y,U(M,t))\|_{C^1(Q_3)}\Big\},$$

$$K_2 := \min\Big\{\inf_{(M_f,M,t)\in Q_1} \overline{g}_f(u_f(M_f,M,t)), \inf_{(y,M_f,M,t)\in Q_2} \overline{h}_f(y,u_f(M_f,M,t))\Big\}, \tag{2.17}$$

$$Q_1 := [0,K]^2\times[0,T],\ Q_2 := [0,1]\times[0,K]^2\times[0,T],\ Q_3 := [0,1]\times[0,K]\times[0,T].$$

For any $\delta>0$, let

$$\Omega_{\delta,K} := \Big\{\vec{M}(t)=(M_1(t),\cdots,M_n(t))\in C^0([0,\delta]) : \|\vec{M}\|_{C^0([0,\delta])} := \max_f \|M_f\|_{C^0([0,\delta])} \leqslant K\Big\},$$

where the constant K is given by (2.15).

In order to derive the expression of the contraction mapping function $\vec{G}$ on $\Omega_{\delta,K}$, we solve the corresponding *linear Cauchy problem* (2.1)-(2.9) with given $\vec{M}\in\Omega_{\delta,K}$.

In phase 1, for any fixed $(x_0,y_0)\in[0,1]^2$, we define the characteristic curve $\overline{\xi} := (\overline{x},\overline{y})$ such that

$$\frac{d\overline{x}}{ds} = \overline{g}_f(u_f(s)), \quad \frac{d\overline{y}}{ds} = \overline{h}_f(\overline{y},u_f)(s), \quad \overline{\xi}(0) = (x_0,y_0). \tag{2.18}$$

In phase 3, for any fixed $(x_0,y_0)\in[0,1]^2$, we define the characteristic curve $\widetilde{\xi} := (\widetilde{x},\widetilde{y})$ such that

$$\frac{d\widetilde{x}}{ds} = \frac{\tau_{gf}}{2}, \quad \frac{d\widetilde{y}}{ds} = \widetilde{h}_f(\widetilde{y},u_f)(s), \quad \widetilde{\xi}(0) = (x_0,y_0). \tag{2.19}$$

Besides, we define a curve $\Gamma(s)$ $(0\leqslant s\leqslant t)$ as

$$\frac{d\Gamma}{ds} = \overline{h}_f(\Gamma,u_f)(s), \quad \Gamma(t) = 1. \tag{2.20}$$

After defining the above characteristics and using Lemma 2.6.1 in section 2.6.3, we are now able to define a map $\vec{G}(\vec{M})(t) := \Big(G_1(M_1,M)(t),\cdots,G_n(M_n,M)(t)\Big)$ for all $t\in[0,\delta]$, where

for each $f = 1, \cdots, n$

$$
\begin{aligned}
G_f(M_f, M)(t) :=& \int_0^{\Gamma(0)} \int_0^{1-\int_0^t \overline{g}_f(u_f(\sigma))\,d\sigma} \gamma_s^2 \overline{y}(t) \sum_{k=1}^{N} \overline{\phi}_{k0}^f(x_0, y_0) e^{-\int_0^t \overline{\lambda}(\overline{y},U)(s)\,ds} dx_0 dy_0 \\
&+ \int_{1-\tau_{gf}t}^1 \int_0^{\Gamma(\frac{1-x_0}{\tau_{gf}})} 2\gamma_s^2 \overline{y}(t) \sum_{k=2}^{N} \widehat{\phi}_{k-1,0}^f(x_0, y_0) e^{-\int_{\frac{1-x_0}{\tau_{gf}}}^t \overline{\lambda}(\overline{y},U)(s)\,ds} dy_0\, dx_0 \\
&+ \int_0^1 \int_0^{1-\tau_{gf}t} \gamma_s^2 y_0 \sum_{k=1}^{N} \widehat{\phi}_{k0}^f(x_0, y_0)\, dx_0\, dy_0 \\
&+ \int_{1-\int_0^t \overline{g}_f(u_f(\sigma))d\sigma}^1 \int_0^{\zeta(x_0)} \gamma_s^2 \overline{y}(\tau_0) \sum_{k=1}^{N} \overline{\phi}_{k0}^f(x_0, y_0) e^{-\int_0^{\tau_0} \overline{\lambda}(\overline{y},U)(s)ds} dy_0 dx_0 \qquad (2.21) \\
&+ \int_0^1 \int_0^1 2\gamma_d(\gamma_d \widetilde{y}(t) + \gamma_s) \sum_{k=1}^{N-1} \widetilde{\phi}_{k0}^f(x_0, y_0) e^{-\int_0^t \widetilde{\lambda}(\widetilde{y},U)(s)\,ds} dx_0 dy_0 \\
&+ \int_0^1 \int_0^{1-\frac{\tau_{gf}}{2}t} 2\gamma_d(\gamma_d \widetilde{y}(t) + \gamma_s) \widetilde{\phi}_{N0}^f(x_0, y_0) e^{-\int_0^t \widetilde{\lambda}(\widetilde{y},U)(s)\,ds} dx_0 dy_0 \\
&+ \int_{\Gamma(0)}^1 \int_0^{\zeta^{-1}(y_0)} \gamma_d(\gamma_d \widetilde{y}(t) + \gamma_s) \sum_{k=1}^{N} \overline{\phi}_{k0}^f(x_0, y_0) e^{-(\int_0^{\overline{y}^{-1}(1)} \overline{\lambda}(\overline{y},U)(s)ds + \int_{\overline{y}^{-1}(1)}^t \widetilde{\lambda}(\widetilde{y},U)(s)ds)} dx_0 dy_0 \\
&+ \int_{1-\tau_{gf}t}^1 \int_{\Gamma(\frac{1-x_0}{\tau_{gf}})}^1 2\gamma_d(\gamma_d \widetilde{y}(t) + \gamma_s) \sum_{k=2}^{N} \widehat{\phi}_{k-1,0}^f(x_0, y_0) e^{-(\int_{\frac{1-x_0}{\tau_{gf}}}^{\overline{y}^{-1}(1)} \overline{\lambda}(\overline{y},U)(s)\,ds + \int_{\overline{y}^{-1}(1)}^t \widetilde{\lambda}(\widetilde{y},U)(s)\,ds)} dy_0 dx_0. \qquad (2.22)
\end{aligned}
$$

In (2.21), τ_0 is defined by

$$1 - x_0 = \int_0^{\tau_0} \overline{g}_f(u_f(\sigma))d\sigma.$$

The curve $y_0 = \zeta(x_0)$ denotes the whole set of points where characteritics passing through the line $x = y = 1$ intersect with the initial time plane (see figure 2.2 (b)), hence $y_0 = \zeta(x_0) := \eta(0, x_0)$ with $\eta(s, x_0)$ given by

$$\frac{d\eta}{ds} = \overline{h}_f(\eta, u_f)(s), \quad \eta(\theta) = 1, \quad 0 \leqslant s \leqslant \theta,$$

with θ defined by $1 - x_0 = \int_0^{\theta} \overline{g}_f(u_f(\sigma))d\sigma$.

Next we prove the following fixed point theorem.

Lemma 2.3.1. *If δ is small enough, $\vec{G}$ is a contraction mapping on $\Omega_{\delta,K}$ with respect to the C^0 norm.*

Proof. It is easy to check that $\vec{G}$ maps into $\Omega_{\delta,K}$ itself if

$$0 < \delta \leqslant \min\{\frac{1}{2K_1}, T\}, \qquad (2.23)$$

where K_1 is defined by (2.16). Let $\vec{M}(t) = (M_1(t), \cdots, M_n(t))$, $\overline{\vec{M}}(t) = (\overline{M}_1(t), \cdots, \overline{M}_n(t)) \in \Omega_{\delta,K}$, and $M = \sum_{f=1}^n M_f$, $\overline{M} = \sum_{f=1}^n \overline{M}_f$. In order to estimate $\|\vec{G}(\overline{\vec{M}}) - \vec{G}(\vec{M})\|_{C^0([0,\delta])}$, we first estimate the norms $\|G_f(\overline{M}_f, \overline{M}) - G_f(M_f, M)\|_{C^0([0,\delta])}$ separately.

Let us recall the simplified notation $\overline{u}_f = u_f(\overline{M}_f, \overline{M}, t)$ and $\overline{U} = U(\overline{M}, t)$. Observing the definition (2.22) of G_f, it is sufficient to estimate $\|\overline{y} - y\|_{C^0([0,\delta])}$, where

$$\begin{aligned} y &= C + \int_\alpha^\beta h_f(y, u_f)(\sigma)d\sigma, \\ \overline{y} &= C + \int_\alpha^\beta h_f(\overline{y}, \overline{u}_f)(\sigma)d\sigma. \end{aligned} \tag{2.24}$$

Here C denotes various constants. y denotes $\overline{y}$ or $\widetilde{y}$, correspondingly, h_f denotes $\overline{h}_f$ or $\widetilde{h}_f$, and $0 \leqslant \alpha \leqslant \beta \leqslant t \leqslant \delta \leqslant \min\{\frac{1}{2K_1}, T\}$. We have

$$\begin{aligned} |\overline{y}(s) - y(s)| &\leqslant \int_\alpha^\beta |h_f(\overline{y}, \overline{u}_f)(\sigma) - h_f(y, u_f)(\sigma)|\, d\sigma \\ &\leqslant tK_1(\|\overline{M}_f - M_f\|_{C^0([0,\delta])} + \|\overline{M} - M\|_{C^0([0,\delta])}) + tK_1\|\overline{y} - y\|_{C^0([\alpha,\beta])}, \end{aligned}$$

hence

$$\|\overline{y} - y\|_{C^0([0,\delta])} \leqslant \frac{tK_1(\|\overline{M}_f - M_f\|_{C^0([0,\delta])} + \|\overline{M} - M\|_{C^0([0,\delta])})}{1 - tK_1}. \tag{2.25}$$

By (2.25), we have

$$\begin{aligned} &\int_\alpha^\beta |h_f(\overline{y}, \overline{u}_f)(\sigma) - h_f(y, u_f)(\sigma)|d\sigma \\ &\leqslant tK_1(\|\overline{M}_f - M_f\|_{C^0([0,\delta])} + \|\overline{M} - M\|_{C^0([0,\delta])}) + tK_1\|\overline{y} - y\|_{C^0([0,\delta])} \\ &\leqslant tK_1(\|\overline{M}_f - M_f\|_{C^0([0,\delta])} + \|\overline{M} - M\|_{C^0([0,\delta])}) + \frac{t^2K_1^2(\|\overline{M}_f - M_f\|_{C^0([0,\delta])} + \|\overline{M} - M\|_{C^0([0,\delta])})}{1 - tK_1} \\ &= \frac{tK_1(\|\overline{M}_f - M_f\|_{C^0([0,\delta])} + \|\overline{M} - M\|_{C^0([0,\delta])})}{1 - tK_1}. \end{aligned} \tag{2.26}$$

Similarly, we have

$$\begin{aligned} &\int_\alpha^\beta |\lambda(\overline{y}, \overline{U})(\sigma) - \lambda(y, U)(\sigma)|d\sigma \\ &\leqslant tK_1\|\overline{M} - M\|_{C^0([0,\delta])} + tK_1\|\overline{y} - y\|_{C^0([0,\delta])} \\ &\leqslant \frac{t^2K_1^2\|\overline{M}_f - M_f\|_{C^0([0,\delta])} + tK_1\|\overline{M} - M\|_{C^0([0,\delta])}}{1 - tK_1}, \end{aligned} \tag{2.27}$$

where λ represents $\overline{\lambda}$ or $\widetilde{\lambda}$, and

$$\int_\alpha^\beta |\overline{g}_f(\overline{u}_f(\sigma)) - \overline{g}_f(u_f(\sigma))|d\sigma \leqslant tK_1(\|\overline{M}_f - M_f\|_{C^0([0,\delta])} + \|\overline{M} - M\|_{C^0([0,\delta])}). \tag{2.28}$$

By (2.25)-(2.28) and the definition (2.22) of G_f, we have

$$\begin{aligned} &\|G_f(\overline{M}_f, \overline{M}) - G_f(M_f, M)\|_{C^0([0,\delta])} \\ \leqslant &tC_1^f\|\overline{M}_f - M_f\|_{C^0([0,\delta])} + tC_2^f\|\overline{M} - M\|_{C^0([0,\delta])}. \end{aligned} \tag{2.29}$$

The expressions of C_1^f and C_2^f are given by (2.123) in section 2.6.3. They depend on $\|\overline{\phi}_{k0}^f\|$, $\|\widehat{\phi}_{k0}^f\|$, $\|\widetilde{\phi}_{k0}^f\|$, K_1 and K_2. Thus for the mapping function $\vec{G}$, we have

$$
\begin{aligned}
&\|\vec{G}(\overline{\vec{M}}) - \vec{G}(\vec{M})\|_{C^0([0,\delta])} \qquad (2.30)\\
=&\Big\| \Big(G_1(\overline{M}_1, \overline{M}) - G_1(M_1, M), \cdots, G_n(\overline{M}_n, \overline{M}) - G_n(M_n, M) \Big) \Big\|_{C^0([0,\delta])}\\
=&\max_f \|G_f(\overline{M}_f, \overline{M}) - G_f(M_f, M)\|_{C^0([0,\delta])}\\
\leqslant&\max_f \Big(tC_1^f \|\overline{M}_f - M_f\|_{C^0([0,\delta])} + tC_2^f \|\overline{M} - M\|_{C^0([0,\delta])} \Big)\\
\leqslant&\max_f \Big(tC_1^f \|\overline{M}_f - M_f\|_{C^0([0,\delta])} + tC_2^f \|\overline{M}_1 - M_1\|_{C^0([0,\delta])} + \cdots + tC_2^f \|\overline{M}_n - M_n\|_{C^0([0,\delta])} \Big)\\
\leqslant&\max_f t(C_1^f + C_2^f) \Big(\|\overline{M}_1 - M_1\|_{C^0([0,\delta])} + \cdots + \|\overline{M}_n - M_n\|_{C^0([0,\delta])} \Big)\\
\leqslant&nt \max_f (C_1^f + C_2^f) \max_f \|\overline{M}_f - M_f\|_{C^0([0,\delta])}.
\end{aligned}
$$

Finally, we get

$$
\|\vec{G}(\overline{\vec{M}}) - \vec{G}(\vec{M})\|_{C^0([0,\delta])} \leqslant nt \max_f (C_1^f + C_2^f) \|\overline{\vec{M}} - \vec{M}\|_{C^0([0,\delta])}. \qquad (2.31)
$$

Hence we can choose δ small enough (depending on $\|\overline{\phi}_{k0}^f\|, \|\widehat{\phi}_{k0}^f\|, \|\widetilde{\phi}_{k0}^f\|, K_1, K_2, T$) so that

$$
\|\vec{G}(\overline{\vec{M}}) - \vec{G}(\vec{M})\|_{C^0([0,\delta])} \leqslant \frac{1}{2} \|\overline{\vec{M}} - \vec{M}\|_{C^0([0,\delta])}. \qquad (2.32)
$$

□

By Lemma 2.3.1 and the contraction mapping principle, there exists a unique fixed point $\vec{M} = \vec{G}(\vec{M})$ in $\Omega_{\delta,K}$.

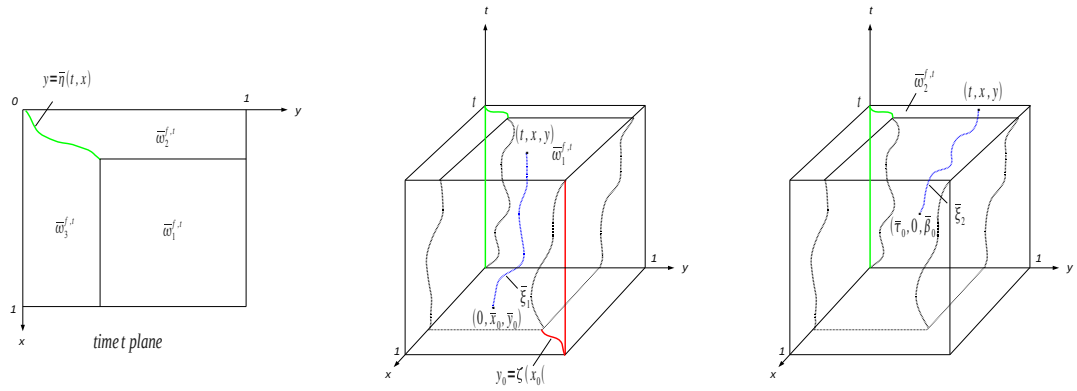
2.3.2 Construction of a local solution to Cauchy problem

Now we show how the fixed point $\vec{M}$ allows us to find a solution to Cauchy problem (2.1)-(2.9) for $t \in [0, \delta]$. For any fixed $(t, x, y) \in [0, \delta] \times [0, 1]^2$, we trace back the density function $\vec{\phi}_f(t, x, y)$ along the characteristics either to the initial or to the boundary data. Hence we divide the time t plane into several parts. In phase 1, the velocities $\overline{h}_f$ are always positive, we introduce three subsets $\overline{\omega}_1^{f,t}$, $\overline{\omega}_2^{f,t}$ and $\overline{\omega}_3^{f,t}$ of $[0, 1]^2$ (see figure 2.2 (a))

$$
\begin{aligned}
\overline{\omega}_1^{f,t} &:= \Big\{ (x, y) |\ \int_0^t \overline{g}_f(u_f(\sigma))\, d\sigma \leqslant x \leqslant 1,\ \overline{\eta}(t, \int_0^t \overline{g}_f(u_f(\sigma))\, d\sigma) \leqslant y \leqslant 1 \Big\},\\
\overline{\omega}_2^{f,t} &:= \Big\{ (x, y) |\ 0 \leqslant x \leqslant \int_0^t \overline{g}_f(u_f(\sigma))\, d\sigma,\ \overline{\eta}(t, x) \leqslant y \leqslant 1 \Big\},\\
\overline{\omega}_3^{f,t} &:= [0, 1]^2 \backslash (\overline{\omega}_1^{f,t} \cup \overline{\omega}_2^{f,t}).
\end{aligned}
$$

Here $y = \overline{\eta}(t, x)$ (see figure 2.2 (a)) satisfies

$$
\frac{d\overline{\eta}}{ds} = \overline{h}_f(\overline{\eta}, u_f)(s), \quad \overline{\eta}(\theta) = 0, \quad \theta \leqslant s \leqslant t, \qquad (2.33)
$$



(a) (b) (c)

Figure 2.2. Backward tracking of the characteristics in phase 1. (a) Time t plane. The green curve denotes the whole set of points where characteristics passing through the line $x = y = 0$ (green in (b)) intersect with time t plane. We divide the time t plane into three parts $\overline{\omega}_1^{f,t}$, $\overline{\omega}_2^{f,t}$ and $\overline{\omega}_3^{f,t}$ according to this boundary curve; (b) If $(t, x, y) \in \overline{\omega}_1^{f,t}$, we trace back $\overline{\phi}_k^f(t, x, y)$ along the characteristic curve $\overline{\xi}_1$ (blue) to the initial data $\overline{\phi}_{k0}^f(\overline{x}_0, \overline{y}_0)$. The curve $y_0 = \zeta(x_0)$ denotes the whole set of points where characteristics passing through the line $x = y = 1$ (red) intersect with the initial plane $t = 0$; (c) If $(t, x, y) \in \overline{\omega}_2^{f,t}$, we trace back $\overline{\phi}_k^f(t, x, y)$ along the characteristic curve $\overline{\xi}_2$ (blue) to the boundary data $\overline{\phi}_k^f(\overline{\tau}_0, 0, \overline{\beta}_0)$.

with θ defined by $x = \displaystyle\int_\theta^t \overline{g}_f(u_f(\sigma))d\sigma$.

If $(x, y) \in \overline{\omega}_1^{f,t}$, we trace back $\overline{\phi}_k^f(t, x, y)$ along the characteristics to the initial data (see figure 2.2 (b)). Hence, we define the characteristics $\overline{\xi}_1 = (\overline{x}_1, \overline{y}_1)$ by

$$\frac{d\overline{x}_1}{ds} = \overline{g}_f(u_f(s)), \quad \frac{d\overline{y}_1}{ds} = \overline{h}_f(\overline{y}_1, u_f)(s), \quad \overline{\xi}_1(t) = (x, y).$$

One has $\overline{\xi}_1(s) \in [0, 1]^2, \ \forall s \in [0, t]$. Let us define

$$(\overline{x}_0, \overline{y}_0) := (\overline{x}_1(0), \overline{y}_1(0)). \tag{2.34}$$

If $(x, y) \in \overline{\omega}_2^{f,t}$, we trace back $\overline{\phi}_k^f(t, x, y)$ along the characteristics to the boundary $x = 0$ (see figure 2.2 (c)). Hence, we define the characteristics $\overline{\xi}_2 = (\overline{x}_2, \overline{y}_2)$ by

$$\frac{d\overline{x}_2}{ds} = \overline{g}_f(u_f(s)), \quad \frac{d\overline{y}_2}{ds} = \overline{h}_f(\overline{y}_2, u_f)(s), \quad \overline{\xi}_2(t) = (x, y).$$

There exists a unique $\overline{\tau}_0 \in [0, t]$ such that $\overline{x}_2(\overline{\tau}_0) = 0$, so that we can define

$$\overline{\beta}_0 := \overline{y}_2(\overline{\tau}_0). \tag{2.35}$$

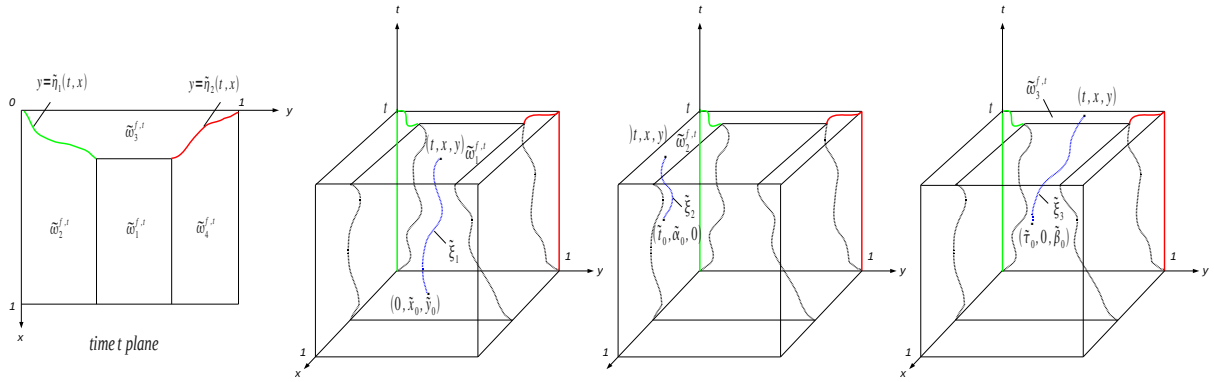
In phase 3, due to the assumption $\widetilde{h}_f(1, u_f) < 0$, we divide the time t plane into four subsets

$\widetilde{\omega}_1^{f,t}$, $\widetilde{\omega}_2^{f,t}$, $\widetilde{\omega}_3^{f,t}$ and $\widetilde{\omega}_4^{f,t}$ of $[0,1]^2$ (see figure 2.3 (a))

$$\widetilde{\omega}_1^{f,t} := \Big\{(x,y)|\frac{\tau_{gf}}{2}t \leqslant x \leqslant 1,\ \widetilde{\eta}_1(t,\frac{\tau_{gf}}{2}t) \leqslant y \leqslant \widetilde{\eta}_2(t,\frac{\tau_{gf}}{2}t)\Big\},$$
$$\widetilde{\omega}_2^{f,t} := \Big\{(x,y)|0 \leqslant x \leqslant \frac{\tau_{gf}}{2}t,\ 0 \leqslant y \leqslant \widetilde{\eta}_1(t,x)\Big\} \cup \Big\{(x,y)|\ \frac{\tau_{gf}}{2}t \leqslant x \leqslant 1, 0 \leqslant y \leqslant \widetilde{\eta}_1(t,\frac{\tau_{gf}}{2}t)\Big\},$$
$$\widetilde{\omega}_3^{f,t} := \Big\{(x,y)|0 \leqslant x \leqslant \frac{\tau_{gf}}{2}t,\ \widetilde{\eta}_1(t,x) \leqslant y \leqslant \widetilde{\eta}_2(t,x)\Big\},$$
$$\widetilde{\omega}_4^{f,t} := [0,1]^2 \backslash (\widetilde{\omega}_1^{f,t} \cup \widetilde{\omega}_2^{f,t} \cup \widetilde{\omega}_3^{f,t}).$$

Here $y = \widetilde{\eta}_1(t,x)$ and $y = \widetilde{\eta}_2(t,x)$ (see figure 2.3 (a)) satisfy

$$\frac{d\widetilde{\eta}_1}{ds} = \widetilde{h}_f(\widetilde{\eta}_1, u_f)(s), \quad \widetilde{\eta}_1(t - \frac{2x}{\tau_{g_f}}) = 0, \quad t - \frac{2x}{\tau_{g_f}} \leqslant s \leqslant t,$$
$$\frac{d\widetilde{\eta}_2}{ds} = \widetilde{h}_f(\widetilde{\eta}_2, u_f)(s), \quad \widetilde{\eta}_2(t - \frac{2x}{\tau_{g_f}}) = 1, \quad t - \frac{2x}{\tau_{g_f}} \leqslant s \leqslant t.$$



(a) (b) (c) (d)

Figure 2.3. Backward tracking of the characteristics in phase 3. (a) Time t plane. The green curve denotes the whole set of points where characteristics passing through the line $x = y = 0$ (green in (b)) intersect with time t plane, the red curve denotes the whole set of points where characteristics passing through the line $x = 0, y = 1$ (red in (b)) intersect with time t plane. We divide the time t plane into four parts $\widetilde{\omega}_1^{f,t}$, $\widetilde{\omega}_2^{f,t}$, $\widetilde{\omega}_3^{f,t}$ and $\widetilde{\omega}_4^{f,t}$ according to these two boundary curves; (b) If $(t,x,y) \in \widetilde{\omega}_1^{f,t}$, we trace back $\widetilde{\phi}_k^f(t,x,y)$ along the characteristic curve $\widetilde{\xi}_1$ (blue) to the initial data $\widetilde{\phi}_{k0}^f(\widetilde{x}_0, \widetilde{y}_0)$; (c) If $(t,x,y) \in \widetilde{\omega}_2^{f,t}$, we trace back $\widetilde{\phi}_k^f(t,x,y)$ along the characteristic curve $\widetilde{\xi}_2$ (blue) to the boundary data $\widetilde{\phi}_k^f(\widetilde{t}_0, \widetilde{\alpha}_0, 0)$; (d) If $(t,x,y) \in \widetilde{\omega}_3^{f,t}$, we trace back $\widetilde{\phi}_k^f(t,x,y)$ along the characteristic curve $\widetilde{\xi}_3$ (blue) to the boundary data $\widetilde{\phi}_k^f(\widetilde{\tau}_0, 0, \widetilde{\beta}_0)$.

If $(x,y) \in \widetilde{\omega}_1^{f,t}$, we trace back $\widetilde{\phi}_k^f(t,x,y)$ along the characteristics to the initial data (see figure 2.3 (b)). Hence, we define the characteristics $\widetilde{\xi}_1 = (\widetilde{x}_1, \widetilde{y}_1)$ by

$$\frac{d\widetilde{x}_1}{ds} = \frac{\tau_{gf}}{2}, \quad \frac{d\widetilde{y}_1}{ds} = \widetilde{h}_f(\widetilde{y}_1, u_f)(s), \quad \widetilde{\xi}_1(t) = (x,y).$$

One has $\widetilde{\xi}_1(s) \in [0,1]^2,\ \forall s \in [0,t]$. Let us define

$$(\widetilde{x}_0, \widetilde{y}_0) := (\widetilde{x}_1(0), \widetilde{y}_1(0)). \tag{2.36}$$

If $(x,y) \in \widetilde{\omega}_2^{f,t}$, we trace back $\widetilde{\phi}_k^f(t,x,y)$ along the characteristics to the boundary $y=0$ (see figure 2.3 (c)). Hence, we define the characteristics $\widetilde{\xi}_2 = (\widetilde{x}_2, \widetilde{y}_2)$ by

$$\frac{d\widetilde{x}_2}{ds} = \frac{\tau_{gf}}{2}, \quad \frac{d\widetilde{y}_2}{ds} = \widetilde{h}_f(\widetilde{y}_2, u_f)(s), \quad \widetilde{\xi}_2(t) = (x,y).$$

There exists a unique $\widetilde{t}_0 \in [0,t]$ such that $\widetilde{y}_2(\widetilde{t}_0) = 0$, so that we can define

$$\widetilde{\alpha}_0 := \widetilde{x}_2(\widetilde{t}_0). \tag{2.37}$$

If $(x,y) \in \widetilde{\omega}_3^{f,t}$, we trace back $\widetilde{\phi}_k^f(t,x,y)$ along the characteristics to the boundary $x=0$ (see figure 2.3 (d)). Hence, we define the characteristics $\widetilde{\xi}_3 = (\widetilde{x}_3, \widetilde{y}_3)$ by

$$\frac{d\widetilde{x}_3}{ds} = \frac{\tau_{gf}}{2}, \quad \frac{d\widetilde{y}_3}{ds} = \widetilde{h}_f(\widetilde{y}_3, u_f)(s), \quad \widetilde{\xi}_3(t) = (x,y).$$

There exists a unique $\widetilde{\tau}_0 \in [0,t]$ such that $\widetilde{x}_3(\widetilde{\tau}_0) = 0$, so that we can define

$$\widetilde{\beta}_0 := \widetilde{y}_3(\widetilde{\tau}_0). \tag{2.38}$$

Given the above defined characteristics, we can now define a solution $\vec{\phi}_f$ by

$$\overline{\phi}_1^f(t,x,y) := \begin{cases} \overline{\phi}_{10}^f(\overline{x}_0, \overline{y}_0) e^{-\int_0^t [\overline{\lambda}(\overline{y}_1, U) + \frac{\partial \overline{h}_f}{\partial y}(\overline{y}_1, u_f)](\sigma)\, d\sigma}, & \text{if } (x,y) \in \overline{\omega}_1^{f,t}, \\ 0, \quad \text{else.} \end{cases} \tag{2.39}$$

For $k = 2, \cdots, N$, we define $\overline{\phi}_k^f(t,x,y)$ by

$$\overline{\phi}_k^f(t,x,y) := \begin{cases} \overline{\phi}_{k0}^f(\overline{x}_0, \overline{y}_0) e^{-\int_0^t [\overline{\lambda}(\overline{y}_1, U) + \frac{\partial \overline{h}_f}{\partial y}(\overline{y}_1, u_f)](\sigma)\, d\sigma}, & \text{if } (x,y) \in \overline{\omega}_1^{f,t}, \\ \dfrac{2\tau_{gf} \widehat{\phi}_{k-1}^f(\overline{\tau}_0, 1, \overline{\beta}_0)}{\overline{g}_f(u_f(\overline{\tau}_0))}\ e^{-\int_{\overline{\tau}_0}^t [\overline{\lambda}(\overline{y}_2, U) + \frac{\partial \overline{h}_f}{\partial y}(\overline{y}_2, u_f)](\sigma)\, d\sigma}, & \text{if } (x,y) \in \overline{\omega}_2^{f,t}, \\ 0, \quad \text{else.} \end{cases} \tag{2.40}$$

Since the dynamics in phase 2 amounts to pure transport equations, we define $\widehat{\phi}_k^f(t,x,y)$, $k = 1, \cdots, N$ by

$$\widehat{\phi}_k^f(t,x,y) := \begin{cases} \widehat{\phi}_{k0}^f(x - \tau_{gf} t, y), & \text{if } (x,y) \in [\tau_{gf} t, 1] \times [0,1], \\ \frac{\overline{g}_f(u_f(t - \frac{x}{\tau_{gf}}))}{\tau_{gf}} \overline{\phi}_k^f(t - \frac{x}{\tau_{gf}}, 1, y), & \text{if } (x,y) \in [0, \tau_{gf} t] \times [0,1]. \end{cases} \tag{2.41}$$

For $k = 1$, we define $\widetilde{\phi}_1^f(t,x,y)$ by

$$\widetilde{\phi}_1^f(t,x,y) := \begin{cases} \widetilde{\phi}_{10}^f(\widetilde{x}_0, \widetilde{y}_0) e^{-\int_0^t [\widetilde{\lambda}(\widetilde{y}_1, U) + \frac{\partial \widetilde{h}_f}{\partial y}(\widetilde{y}_1, u_f)](\sigma)\, d\sigma}, & \text{if } (x,y) \in \widetilde{\omega}_1^{f,t}, \\ \overline{\phi}_1^f(\widetilde{t}_0, 2\widetilde{\alpha}_0, 1) e^{-\int_{\widetilde{t}_0}^t [\widetilde{\lambda}(\widetilde{y}_2, U) + \frac{\partial \widetilde{h}_f}{\partial y}(\widetilde{y}_2, u_f)](\sigma)\, d\sigma}, & \text{if } (x,y) \in \widetilde{\omega}_2^{f,t}, \\ 0, \quad \text{else.} \end{cases} \tag{2.42}$$

For $k=2,\cdots,N$, we define $\widetilde{\phi}_k^f(t,x,y)$ by

$$\widetilde{\phi}_k^f(t,x,y):=\begin{cases}\widetilde{\phi}_{k0}^f(\widetilde{x}_0,\widetilde{y}_0)e^{-\int_0^t[\widetilde{\lambda}(\widetilde{y}_1,U)+\frac{\partial\widetilde{h}_f}{\partial y}(\widetilde{y}_1,u_f)](\sigma)\,d\sigma}, & \text{if } (x,y)\in\widetilde{\omega}_1^{f,t},\\ \overline{\phi}_k^f(\widetilde{t}_0,2\widetilde{\alpha}_0,1)e^{-\int_{\widetilde{t}_0}^t[\widetilde{\lambda}(\widetilde{y}_2,U)+\frac{\partial\widetilde{h}_f}{\partial y}(\widetilde{y}_2,u_f)](\sigma)\,d\sigma}, & \text{if } (x,y)\in\widetilde{\omega}_2^{f,t},\\ \widetilde{\phi}_{k-1}^f(\widetilde{\tau}_0,1,\widetilde{\beta}_0)e^{-\int_{\widetilde{\tau}_0}^t[\widetilde{\lambda}(\widetilde{y}_3,U)+\frac{\partial\widetilde{h}_f}{\partial y}(\widetilde{y}_3,u_f)](\sigma)\,d\sigma}, & \text{if } (x,y)\in\widetilde{\omega}_3^{f,t},\\ 0, \quad \text{else.}\end{cases}\tag{2.43}$$

Next we prove that the function $\vec{\phi}_f$ defined by (2.39)-(2.43) is a weak solution to Cauchy problem (2.1)-(2.9) for $t\in[0,\delta]$. We first prove that $\vec{\phi}_f$ satisfies equality (2.14) of Definition 2.2.1, then we prove that $\vec{\phi}_f\in C^0([0,\delta];L^1((0,1)^2))$.

Let $\tau\in[0,\delta]$. For any vector function $\vec{\varphi}(t,x,y)\in C^1([0,\tau]\times[0,1]^2)$, $\vec{\varphi}:=(\overline{\varphi}_1,\cdots,\overline{\varphi}_N,\widehat{\varphi}_1,\cdots,\widehat{\varphi}_N,\widetilde{\varphi}_1,\cdots,\widetilde{\varphi}_N)^{tr}$ such that (2.10)-(2.13) hold. Using definition (2.39)-(2.43) of $\vec{\phi}_f$, we get

$$\int_0^\tau\int_0^1\int_0^1\vec{\phi}_f(t,x,y)\cdot(\vec{\varphi}_t+A_f\vec{\varphi}_x+B_f\vec{\varphi}_y+C\vec{\varphi})dxdydt:=\sum_{i=1}^7 A_i.\tag{2.44}$$

In (2.44),

$$A_1:=\sum_{k=1}^N\int_0^\tau\iint\limits_{\overline{\omega}_1^{f,t}}\overline{\phi}_{k0}^f(\overline{x}_0,\overline{y}_0)e^{-\int_0^t[\overline{\lambda}(\overline{y}_1,U)+\frac{\partial\overline{h}_f}{\partial y}(\overline{y}_1,u_f)](\sigma)d\sigma}(\overline{\varphi}_{kt}+\overline{g}_f\overline{\varphi}_{kx}+\overline{h}_f\overline{\varphi}_{ky}-\overline{\lambda}\overline{\varphi}_k)dxdydt,$$

$$A_2:=\sum_{k=2}^N\int_0^\tau\iint\limits_{\overline{\omega}_2^{f,t}}\frac{2\tau_{gf}\widehat{\phi}_{k-1}^f(\overline{\tau}_0,1,\overline{\beta}_0)}{\overline{g}_f(u_f(\overline{\tau}_0))}e^{-\int_{\overline{\tau}_0}^t[\overline{\lambda}(\overline{y}_2,U)+\frac{\partial\overline{h}_f}{\partial y}(\overline{y}_2,u_f)](\sigma)d\sigma}(\overline{\varphi}_{kt}+\overline{g}_f\overline{\varphi}_{kx}+\overline{h}_f\overline{\varphi}_{ky}-\overline{\lambda}\overline{\varphi}_k)dxdydt,$$

$$A_3:=\sum_{k=1}^N\int_0^\tau\int_0^1\int_{\tau_{gf}t}^1\widehat{\phi}_{k0}^f(x-\tau_{gf}t,y)(\widehat{\varphi}_{kt}+\tau_{gf}\widehat{\varphi}_{kx})dxdydt,$$

$$A_4:=\sum_{k=1}^N\int_0^\tau\int_0^1\int_0^{\tau_{gf}t}\overline{g}_f(u_f(t-\frac{x}{\tau_{gf}}))\overline{\phi}_k^f(t-\frac{x}{\tau_{gf}},1,y)(\widehat{\varphi}_{kt}+\tau_{gf}\widehat{\varphi}_{kx})dxdydt,$$

$$A_5:=\sum_{k=1}^N\int_0^\tau\iint\limits_{\widetilde{\omega}_1^{f,t}}\widetilde{\phi}_{k0}^f(\widetilde{x}_0,\widetilde{y}_0)e^{-\int_0^t[\widetilde{\lambda}(\widetilde{y}_1,U)+\frac{\partial\widetilde{h}_f}{\partial y}(\widetilde{y}_1,u_f)](\sigma)d\sigma}(\widetilde{\varphi}_{kt}+\frac{\tau_{gf}}{2}\widetilde{\varphi}_{kx}+\widetilde{h}_f\widetilde{\varphi}_{ky}-\widetilde{\lambda}\widetilde{\varphi}_k)dxdydt,$$

$$A_6:=\sum_{k=1}^N\int_0^\tau\iint\limits_{\widetilde{\omega}_2^{f,t}}\overline{\phi}_k^f(\widetilde{t}_0,2\widetilde{\alpha}_0,1)e^{-\int_{\widetilde{t}_0}^t[\widetilde{\lambda}(\widetilde{y}_2,U)+\frac{\partial\widetilde{h}_f}{\partial y}(\widetilde{y}_2,u_f)](\sigma)d\sigma}(\widetilde{\varphi}_{kt}+\frac{\tau_{gf}}{2}\widetilde{\varphi}_{kx}+\widetilde{h}_f\widetilde{\varphi}_{ky}-\widetilde{\lambda}\widetilde{\varphi}_k)dxdydt,$$

$$A_7:=\sum_{k=2}^N\int_0^\tau\iint\limits_{\widetilde{\omega}_3^{f,t}}\widetilde{\phi}_{k-1}^f(\widetilde{\tau}_0,1,\widetilde{\beta}_0)e^{-\int_{\widetilde{\tau}_0}^t[\widetilde{\lambda}(\widetilde{y}_3,U)+\frac{\partial\widetilde{h}_f}{\partial y}(\widetilde{y}_3,u_f)](\sigma)d\sigma}(\widetilde{\varphi}_{kt}+\frac{\tau_{gf}}{2}\widetilde{\varphi}_{kx}+\widetilde{h}_f\widetilde{\varphi}_{ky}-\widetilde{\lambda}\widetilde{\varphi}_k)dxdydt.$$

Next we prove equality (2.14) of Definition 2.2.1 holds by applying the change of variables.

We consider the first term A_1 as an instance. Let us recall the definition of the characteristic curve $\overline{\xi}_1=(\overline{x}_1,\overline{y}_1)$ (see figure 2.4 (a)). Thanks to (2.118) of Lemma 2.6.1 in section

2.6.3, after applying the change of variables $(x,y)\to(x_0,y_0)$, we get

$$A_1=\sum_{k=1}^{N}\int_0^{\tau}\int_0^{\beta}\int_0^{\alpha}\overline{\phi}^f_{k0}(x_0,y_0)e^{-\int_0^t\overline{\lambda}(\overline{y}_1,U)(\sigma)d\sigma}\Big(\overline{\varphi}_{kt}(t,\overline{x}_1(t),\overline{y}_1(t))+\overline{g}_f\overline{\varphi}_{kx}(t,\overline{x}_1(t),\overline{y}_1(t))$$
$$+\overline{h}_f\overline{\varphi}_{ky}(t,\overline{x}_1(t),\overline{y}_1(t))-\overline{\lambda}\overline{\varphi}_k(t,\overline{x}_1(t),\overline{y}_1(t))\Big)dx_0dy_0dt, \tag{2.45}$$

where, for any fixed $t\in[0,\tau]$, α and β are defined as (see figure 2.4 (a))

$$\alpha:=1-\int_0^t\overline{g}_f(u_f(\sigma))\,d\sigma\triangleq f_1(t),\quad \beta:=1-\int_0^t\overline{h}_f(\Gamma,u_f)(\sigma)d\sigma\triangleq g_1(t). \tag{2.46}$$

Clearly, α is a function of β, suppose that $\alpha=h(\beta)$. After changing the order of integration (see figure 2.4 (b)), A_1 can be rewritten as

$$A_1=\sum_{k=1}^{N}\Big\{\int_0^{g_1(\tau)}\int_0^{f_1(\tau)}\int_0^{\tau}+\int_0^{g_1(\tau)}\int_{f_1(\tau)}^1\int_0^{f_1^{-1}(\alpha)}+\int_{g_1(\tau)}^1\int_0^{f_1(\tau)}\int_0^{g_1^{-1}(\beta)}+\int_{g_1(\tau)}^1\int_{h(\beta)}^1\int_0^{f_1^{-1}(\alpha)}$$
$$+\int_{g_1(\tau)}^1\int_{f_1(\tau)}^{h(\beta)}\int_0^{g_1^{-1}(\beta)}\Big\}\overline{\phi}^f_{k0}(x_0,y_0)\frac{d\left(e^{-\int_0^t\overline{\lambda}(\overline{y}_1,U)(\sigma)d\sigma}\overline{\varphi}_k(t,\overline{x}_1(t),\overline{y}_1(t))\right)}{dt}dtdx_0y_0 \tag{2.47}$$

Noting property (2.10) that $\vec{\varphi}(\tau,x,y)\equiv0$, (2.47) becomes

$$\sum_{k=1}^{N}\Big\{\int_0^{g_1(\tau)}\int_{f_1(\tau)}^1\overline{\phi}^f_{k0}(x_0,y_0)e^{-\int_0^{f_1^{-1}(\alpha)}\overline{\lambda}(\overline{y}_1,U)(\sigma)d\sigma}\overline{\varphi}_k(f_1^{-1}(\alpha),\overline{x}_1(f_1^{-1}(\alpha)),\overline{y}_1(f_1^{-1}(\alpha)))dx_0dy_0$$
$$+\int_{g_1(\tau)}^1\int_0^{f_1(\tau)}\overline{\phi}^f_{k0}(x_0,y_0)e^{-\int_0^{g_1^{-1}(\beta)}\overline{\lambda}(\overline{y}_1,U)(\sigma)d\sigma}\overline{\varphi}_k(g_1^{-1}(\beta),\overline{x}_1(g_1^{-1}(\beta)),\overline{y}_1(g_1^{-1}(\beta)))dx_0dy_0$$
$$+\int_{g_1(\tau)}^1\int_{h(\beta)}^1\overline{\phi}^f_{k0}(x_0,y_0)e^{-\int_0^{f_1^{-1}(\alpha)}\overline{\lambda}(\overline{y}_1,U)(\sigma)d\sigma}\overline{\varphi}_k(f_1^{-1}(\alpha),\overline{x}_1(f_1^{-1}(\alpha)),\overline{y}_1(f_1^{-1}(\alpha)))dx_0dy_0$$
$$+\int_{g_1(\tau)}^1\int_{f_1(\tau)}^{h(\beta)}\overline{\phi}^f_{k0}(x_0,y_0)e^{-\int_0^{g_1^{-1}(\beta)}\overline{\lambda}(\overline{y}_1,U)(\sigma)d\sigma}\overline{\varphi}_k(g_1^{-1}(\beta),\overline{x}_1(g_1^{-1}(\beta)),\overline{y}_1(g_1^{-1}(\beta)))dx_0dy_0$$
$$-\int_0^1\int_0^1\overline{\phi}^f_{k0}(x_0,y_0)\overline{\varphi}_k(0,x_0,y_0)dx_0dy_0\Big\}. \tag{2.48}$$

From the boundary condition (2.11) and (2.13), we have

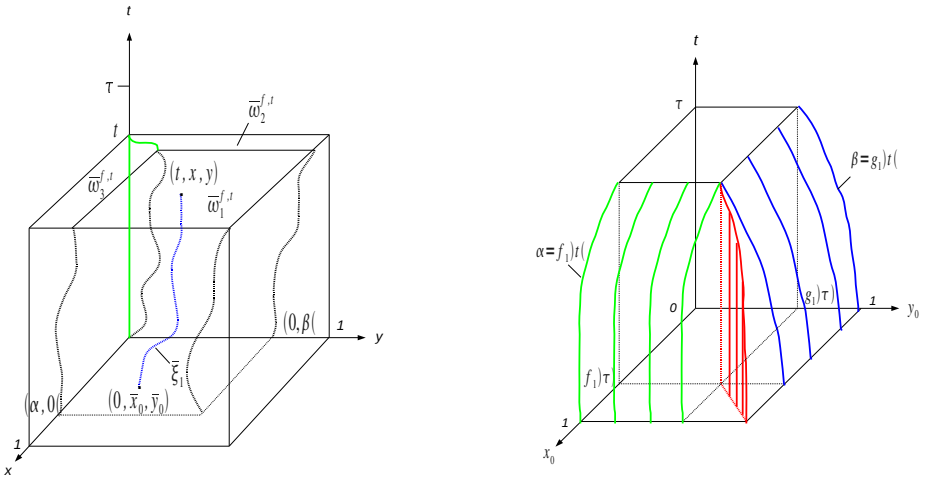
$$\overline{\varphi}_k(t,x,1)\equiv0,\ \forall\ (t,x)\in[0,\tau]\times[0,1], \tag{2.49}$$
$$\overline{\varphi}_k(t,1,y)\equiv0,\ \forall\ (t,y)\in[0,\tau]\times[0,1]. \tag{2.50}$$

Noting that

$$\overline{x}_1(f_1^{-1}(\alpha))=\overline{y}_1(g_1^{-1}(\beta))=1. \tag{2.51}$$

Summarizing (2.48)-(2.51), we get

$$A_1=-\sum_{k=1}^{N}\int_0^1\int_0^1\overline{\phi}^f_{k0}(x_0,y_0)\overline{\varphi}_k(0,x_0,y_0)dx_0dy_0. \tag{2.52}$$



(a) (b)

Figure 2.4. Illustration of the new integral domains after changing the order of some integrals. (a) For any fixed $t \in [0, \tau]$, both the characteristic curve $\overline{\xi}_1$ (blue) and points $(\alpha, 0)$ and $(0, \beta)$ are shown; (b) New integral domain in the x_0, y_0 and τ space after changing the order of integration in term A_1 from dx_0dy_0dt to $dtdx_0dy_0$. The green surface represents $\alpha = f_1(t)$ and the blue surface represents $\beta = g_1(t)$.

Similarly to A_1, we can prove that

$$A_2 = -\sum_{k=2}^{N} \int_0^{\tau} \int_0^1 2\tau_{gf} \widehat{\phi}^f_{k-1}(\tau_0, 1, \beta_0) \overline{\varphi}_k(\tau_0, 0, \beta_0) d\beta_0 d\tau_0, \tag{2.53}$$

$$A_3 = -\sum_{k=1}^{N} \int_0^{1} \int_0^1 \widehat{\phi}^f_{k0}(x_0, y_0) \widehat{\varphi}_k(0, x_0, y_0) dx_0 dy_0, \tag{2.54}$$

$$A_4 = -\sum_{k=1}^{N} \int_0^{\tau} \int_0^1 \overline{g}_f(u_f(\tau_0)) \overline{\phi}^f_k(\tau_0, 1, \beta_0) \widehat{\phi}_k(\tau_0, 0, \beta_0) d\beta_0 d\tau_0, \tag{2.55}$$

$$A_5 = -\sum_{k=1}^{N} \int_0^{1} \int_0^1 \widetilde{\phi}^f_{k0}(x_0, y_0) \widetilde{\varphi}_k(0, x_0, y_0) dx_0 dy_0, \tag{2.56}$$

$$A_6 = -\sum_{k=1}^{N} \int_0^{\tau} \int_0^{\frac{1}{2}} \widetilde{h}_f(0, u_f(t_0)) \overline{\phi}^f_k(t_0, \frac{1}{2}\alpha_0, 1) \widetilde{\varphi}_k(t_0, \alpha_0, 0) d\alpha_0 dt_0, \tag{2.57}$$

$$A_7 = -\sum_{k=2}^{N} \int_0^{\tau} \int_0^1 \frac{\tau_{gf}}{2} \widetilde{\phi}^f_{k-1}(\tau_0, 1, \beta_0) \widetilde{\varphi}_k(\tau_0, 0, \beta_0) d\beta_0 d\tau_0. \tag{2.58}$$

By (2.52)-(2.58), we have proved that the vector function $\vec{\phi}_f$ defined by (2.39)-(2.43) satisfies equality (2.14). Next we prove that $\vec{\phi}_f \in C^0([0, \delta]; L^1((0,1)^2))$. Moreover, we can prove that $\vec{\phi}_f$ even belongs to $C^0([0, \delta]; L^p((0,1)^2))$ for all $p \in [1, \infty)$.

Lemma 2.3.2. *The weak solution $\vec{\phi}_f$ to Cauchy problem (2.1)-(2.9) defined by (2.39)-(2.43) belongs to $C^0([0, \delta]; L^p((0,1)^2))$ for all $p \in [1, \infty)$.*

Proof. From definition (2.39)-(2.43) of $\vec{\phi}_f$, we get easily that $\vec{\phi}_f \in L^\infty((0,\delta)\times(0,1)^2)$. Next we prove that the vector function $\vec{\phi}_f$ belongs to $C^0([0,\delta];L^p((0,1)^2))$ for all $p\in[1,\infty)$, i.e., for every $\widetilde{t},t\in[0,\delta]$ with $\widetilde{t}\geqslant t$ (the case when $\widetilde{t}\leqslant t$ can be treated similarly), we need to prove

$$\|\vec{\phi}_f(\widetilde{t},\cdot)-\vec{\phi}_f(t,\cdot)\|_{L^p((0,1)^2)}\to 0,\quad \text{as}\quad |\widetilde{t}-t|\to 0,\quad \forall p\in[1,\infty).$$

In order to do that, we estimate $\|\overline{\phi}_k^f(\widetilde{t},\cdot)-\overline{\phi}_k^f(t,\cdot)\|_{L^p((0,1)^2)}$, $\|\widehat{\phi}_k^f(\widetilde{t},\cdot)-\widehat{\phi}_k^f(t,\cdot)\|_{L^p((0,1)^2)}$ and $\|\widetilde{\phi}_k^f(\widetilde{t},\cdot)-\widetilde{\phi}_k^f(t,\cdot)\|_{L^p((0,1)^2)}(k=1,\cdots,N)$ separately.

Suppose that the characteristic curve passing through $(t,0,0)$ intersects time $\widetilde{t}$ plane at $(\widetilde{t},q_1,q_2)$ (see figure 2.5 (a)), we have

$$q_1=\int_t^{\widetilde{t}}\overline{g}_f(u_f(\sigma))d\sigma,\quad q_2=\int_t^{\widetilde{t}}\overline{h}_f(y,u_f)(\sigma)d\sigma,$$

where $y(s),t\leqslant s\leqslant\widetilde{t}$ satisfies

$$\frac{dy}{ds}=\overline{h}_f(y,u_f)(s),\quad y(t)=0.$$

We get easily that

$$q_1\leqslant C|\widetilde{t}-t|,\quad q_2\leqslant C|\widetilde{t}-t|. \tag{2.59}$$

Here and hereafter in this section, we denote by C various constants which do not depend on $\widetilde{t}$, t, x and y.

Let $\overline{S}:=[q_1,1]\times[q_2,1]$ (see figure 2.5 (a)). For any fixed $(x,y)\in\overline{S}$, we define a new characteristic curve $\overline{\xi}_3=(\overline{x}_3,\overline{y}_3)$ passing through $(\widetilde{t},x,y)$ that intersects time t plane at $(t,\widetilde{x},\widetilde{y})$. Then we have

$$\begin{aligned}
&|\overline{\phi}_k^f(\widetilde{t},x,y)-\overline{\phi}_k^f(t,x,y)|\\
&=\left|\overline{\phi}_k^f(t,\widetilde{x},\widetilde{y})e^{-\int_t^{\widetilde{t}}[\overline{\lambda}(\overline{y}_3,U)+\frac{\partial\overline{h}_f}{\partial y}(\overline{y}_3,u_f)](\sigma)\,d\sigma}-\overline{\phi}_k^f(t,x,y)\right|\\
&\leqslant|\overline{\phi}_k^f(t,\widetilde{x},\widetilde{y})-\overline{\phi}_k^f(t,x,y)|e^{-\int_t^{\widetilde{t}}[\overline{\lambda}(\overline{y}_3,U)+\frac{\partial\overline{h}_f}{\partial y}(\overline{y}_3,u_f)](\sigma)\,d\sigma}+C|\overline{\phi}_k^f(t,x,y)||\widetilde{t}-t|.
\end{aligned}$$

Furthermore,

$$\widetilde{x}=x-\int_t^{\widetilde{t}}\overline{g}_f(u_f(\sigma))d\sigma,\quad \widetilde{y}=y-\int_t^{\widetilde{t}}\overline{h}_f(\overline{y}_3,u_f)(\sigma)d\sigma.$$

Hence, we get

$$|\widetilde{x}-x|\leqslant C|\widetilde{t}-t|,\quad |\widetilde{y}-y|\leqslant C|\widetilde{t}-t|. \tag{2.60}$$

Since $\overline{\phi}_k^f\in L^\infty((0,\delta)\times(0,1)^2)$, for every $l>0$, there exists C_l such that for every $t\in[0,\delta]$, there exists $\overline{\phi}_k^{fl}(t,\cdot)\in C^1([0,1]^2)$ satisfying

$$\|\overline{\phi}_k^{fl}(t,\cdot)-\overline{\phi}_k^f(t,\cdot)\|_{L^p((0,1)^2)}\leqslant\frac{1}{l},\quad \|\overline{\phi}_k^{fl}(t,\cdot)\|_{C^1([0,1]^2)}\leqslant C_l. \tag{2.61}$$

Here and hereafter in this section, we denote by C_l various constants that may depend on l (the index of the corresponding approximating sequences $\overline{\phi}_k^{fl}(t,\cdot)$, $\widehat{\phi}_k^{fl}(t,\cdot)$ and $\widetilde{\phi}_k^{fl}(t,\cdot)$ but are independent of $0\leqslant t\leqslant\widetilde{t}\leqslant\delta$.

Noting (2.60), we have

$$\begin{aligned}&|\overline{\phi}_k^f(\widetilde{t},x,y)-\overline{\phi}_k^f(t,x,y)|\\ \leqslant&C|\overline{\phi}_k^{fl}(t,\widetilde{x},\widetilde{y})-\overline{\phi}_k^f(t,\widetilde{x},\widetilde{y})|+C|\overline{\phi}_k^{fl}(t,x,y)-\overline{\phi}_k^f(t,x,y)|\\ &+C|\overline{\phi}_k^f(t,x,y)||\widetilde{t}-t|+C_l|\widetilde{t}-t|.\end{aligned}\tag{2.62}$$

By (2.61) and (2.62), we get

$$\iint\limits_{\overline{S}}|\overline{\phi}_k^f(\widetilde{t},x,y)-\overline{\phi}_k^f(t,x,y)|^p dxdy\leqslant\frac{C}{l^p}+C_l|\widetilde{t}-t|^p.\tag{2.63}$$

Noting (2.59), we have

$$\iint\limits_{[0,1]^2\setminus\overline{S}}|\overline{\phi}_k^f(\widetilde{t},x,y)-\overline{\phi}_k^f(t,x,y)|^p dxdy\leqslant C(q_1+q_2)\leqslant C|\widetilde{t}-t|.\tag{2.64}$$

Combining (2.63) with (2.64), we obtain

$$\int_0^1\int_0^1|\overline{\phi}_k^f(\widetilde{t},x,y)-\overline{\phi}_k^f(t,x,y)|^p dxdy\leqslant\frac{C}{l^p}+C_l|\widetilde{t}-t|^p+C|\widetilde{t}-t|.\tag{2.65}$$

Next we estimate $\|\widehat{\phi}_k^f(\widetilde{t},\cdot)-\widehat{\phi}_k^f(t,\cdot)\|_{L^p((0,1)^2)}$. In phase 2, it is easy to get that the characteristic curve passing through $(t,0,0)$ intersects time $\widetilde{t}$ plane at $(\widetilde{t},\tau_{gf}(\widetilde{t}-t),0)$. Let $\widehat{S}:=[\tau_{gf}(\widetilde{t}-t),1]\times[0,1]$ (see figure 2.5 (b)). For any fixed $(x,y)\in\widehat{S}$, we have

$$|\widehat{\phi}_k^f(\widetilde{t},x,y)-\widehat{\phi}_k^f(t,x,y)|=|\widehat{\phi}_k^f(t,\widetilde{x},\widetilde{y})-\widehat{\phi}_k^f(t,x,y)|=|\widehat{\phi}_k^f(t,x-\tau_{gf}(\widetilde{t}-t),y)-\widehat{\phi}_k^f(t,x,y)|.$$

Since $\widehat{\phi}_k^f\in L^\infty((0,\delta)\times(0,1)^2)$, for every $l>0$, there exists C_l such that for every $t\in[0,\delta]$, there exists $\widehat{\phi}_k^{fl}(t,\cdot)\in C^1([0,1]^2)$ satisfying

$$\|\widehat{\phi}_k^{fl}(t,\cdot)-\widehat{\phi}_k^f(t,\cdot)\|_{L^p((0,1)^2)}\leqslant\frac{1}{l},\quad\|\widehat{\phi}_k^{fl}(t,\cdot)\|_{C^1([0,1]^2)}\leqslant C_l.\tag{2.66}$$

Similarly to (2.63), we can prove that

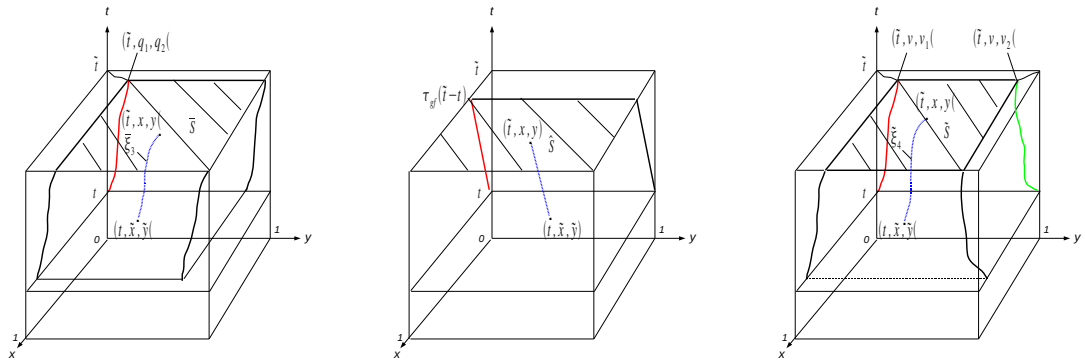
$$\iint\limits_{\widehat{S}}|\widehat{\phi}_k^f(\widetilde{t},x,y)-\widehat{\phi}_k^f(t,x,y)|^p dxdy\leqslant\frac{C}{l^p}+C_l|\widetilde{t}-t|^p.\tag{2.67}$$

It is easy to check that

$$\iint\limits_{[0,1]^2\setminus\widehat{S}}|\widehat{\phi}_k^f(\widetilde{t},x,y)-\widehat{\phi}_k^f(t,x,y)|^p dxdy\leqslant C|\widetilde{t}-t|.\tag{2.68}$$

Combining (2.67) with (2.68), we get

$$\int_0^1\int_0^1|\widehat{\phi}_k^f(\widetilde{t},x,y)-\widehat{\phi}_k^f(t,x,y)|^p dxdy\leqslant\frac{C}{l^p}+C_l|\widetilde{t}-t|^p+C|\widetilde{t}-t|.\tag{2.69}$$



(a) (b) (c)

Figure 2.5. Different time planes corresponding to each cell cycle k: time $\widetilde{t}$ plane and time t plane with $0 \leqslant t \leqslant \widetilde{t} \leqslant \delta$. (a) In phase 1, the characteristic curve $\overline{\xi}_3$ (blue) connects $(\widetilde{t}, x, y)$ with $(t, \widetilde{x}, \widetilde{y})$ and the characteristic curve (red) passing through $(t, 0, 0)$ intersects time $\widetilde{t}$ plane at $(\widetilde{t}, q_1, q_2)$, so that we can define the (shaded) domain $\overline{S}$; (b) In phase 2, the characteristic curve (blue) connects $(\widetilde{t}, x, y)$ with $(t, \widetilde{x}, \widetilde{y})$ and the characteristic curve (red) passing through $(t, 0, 0)$ intersects time $\widetilde{t}$ plane at $(\widetilde{t}, \tau_{gf}(\widetilde{t} - t), 0)$, so that we can define the (shaded) domain $\widehat{S}$; (c) In phase 3, the characteristic curve $\widetilde{\xi}_4$ (blue) connects $(\widetilde{t}, x, y)$ with $(t, \widetilde{x}, \widetilde{y})$ and the characteristic curve (red) passing through $(t, 0, 0)$ intersects time $\widetilde{t}$ plane at $(\widetilde{t}, v, v_1)$ and the characteristic curve (green) passing through $(t, 0, 1)$ intersects time $\widetilde{t}$ plane at $(\widetilde{t}, v, v_2)$, so that we can define the (shaded) domain $\widetilde{S}$.

Finally, we estimate $\|\widetilde{\phi}_k^f(\widetilde{t},\cdot)-\widetilde{\phi}_k^f(t,\cdot)\|_{L^p((0,1)^2)}$. Suppose that the characteristic curve passing through $(t,0,0)$ intersects time $\widetilde{t}$ plane at $(\widetilde{t},v,v_1)$, and the characteristic curve passing through $(t,0,1)$ intersects time $\widetilde{t}$ plane at $(\widetilde{t},v,v_2)$ (see figure 2.5 (c)). Similarly to (2.59), we can prove that

$$v\leqslant C|\widetilde{t}-t|,\quad v_1\leqslant C|\widetilde{t}-t|,\quad 1-v_2\leqslant C|\widetilde{t}-t|. \tag{2.70}$$

Let $\widetilde{S}:=[v,1]\times[v_1,v_2]$ (see figure 2.5 (c)). For any fixed $(x,y)\in\widetilde{S}$, we define the characteristic curve $\widetilde{\xi}_4=(\widetilde{x}_4,\widetilde{y}_4)$ passing through $(\widetilde{t},x,y)$ that intersects time t plane at $(t,\widetilde{x},\widetilde{y})$. Then we have

$$|\widetilde{\phi}_k^f(\widetilde{t},x,y)-\widetilde{\phi}_k^f(t,x,y)|=|\widetilde{\phi}_k^f(t,\widetilde{x},\widetilde{y})e^{-\int_t^{\widetilde{t}}[\widetilde{\lambda}(\widetilde{y}_4,U)+\frac{\partial\widetilde{h}_f}{\partial y}(\widetilde{y}_4,u_f)](\sigma)d\sigma}-\widetilde{\phi}_k^f(t,x,y)|.$$

Similarly to (2.60), we can prove that

$$|\widetilde{x}-x|\leqslant C|\widetilde{t}-t|,\quad |\widetilde{y}-y|\leqslant C|\widetilde{t}-t|.$$

Since $\widetilde{\phi}_k^f\in L^\infty((0,\delta)\times(0,1)^2)$, for every $l>0$, there exists C_l such that for every $t\in[0,\delta]$, there exists $\widetilde{\phi}_k^{fl}(t,\cdot)\in C^1([0,1]^2)$ satisfying

$$\|\widetilde{\phi}_k^{fl}(t,\cdot)-\widetilde{\phi}_k^f(t,\cdot)\|_{L^p((0,1)^2)}\leqslant\frac{1}{l},\quad \|\widetilde{\phi}_k^{fl}(t,\cdot)\|_{C^1([0,1]^2)}\leqslant C_l. \tag{2.71}$$

Similarly to (2.63), we can prove that

$$\iint\limits_{\widetilde{S}}|\widetilde{\phi}_k^f(\widetilde{t},x,y)-\widetilde{\phi}_k^f(t,x,y)|^p dxdy\leqslant\frac{C}{l^p}+C_l|\widetilde{t}-t|^p. \tag{2.72}$$

Noting (2.70), we have

$$\iint\limits_{[0,1]^2\setminus\widetilde{S}}|\widetilde{\phi}_k^f(\widetilde{t},x,y)-\widetilde{\phi}_k^f(t,x,y)|^p dxdy\leqslant C(v+v_1+1-v_2)\leqslant C|\widetilde{t}-t|. \tag{2.73}$$

Combining (2.72) with (2.73), we get

$$\int_0^1\int_0^1|\widetilde{\phi}_k^f(\widetilde{t},x,y)-\widetilde{\phi}_k^f(t,x,y)|^p dxdy\leqslant\frac{C}{l^p}+C_l|\widetilde{t}-t|^p+C|\widetilde{t}-t|. \tag{2.74}$$

Therefore letting l be large enough and then $|\widetilde{t}-t|$ be small enough, the right hand side of (2.65), (2.69) and (2.74) can be arbitrarily small. As a whole, we have proved that the vector function $\vec{\phi}_f$ belongs to $C^0([0,\delta];L^p((0,1)^2))$ for all $p\in[1,\infty)$. □

Let us recall Definition 2.2.1 of a weak solution, we have proved that the vector function $\vec{\phi}_f$ defined by (2.39)-(2.43) is indeed a weak solution to Cauchy problem (2.1)-(2.9).

2.4 Uniqueness of the solution

In this section, we prove the uniqueness of the solution.

Lemma 2.4.1. *The weak solution to Cauchy problem* (2.1)-(2.9) *is unique.*

Proof. Assume that $\vec{\overline{\phi}}_f=(\overline{\overline{\phi}}^f_1,\cdots,\overline{\overline{\phi}}^f_N,\overline{\widetilde{\phi}}^f_1,\cdots,\overline{\widetilde{\phi}}^f_N,\widetilde{\overline{\phi}}^f_1,\cdots,\widetilde{\overline{\phi}}^f_N)^{tr}\in C^0([0,\delta];L^1((0,1)^2))$ is another weak solution to Cauchy problem (2.1)-(2.9). Similarly to Lemma 2.2 in [35, section 2.2], we can prove that for any fixed $t\in[0,\delta]$ and any $\vec{\Phi}(\tau,x,y):=(\overline{\Phi}_1,\cdots,\overline{\Phi}_N,\widehat{\Phi}_1,\cdots,\widehat{\Phi}_N,\widetilde{\Phi}_1,\cdots,\widetilde{\Phi}_N)^{tr}\in C^1([0,t]\times[0,1]^2)$ with

$$\begin{aligned}
&\vec{\Phi}(\tau,1,y)=0,\quad \forall(\tau,y)\in[0,t]\times[0,1],\\
&\overline{\Phi}_1(\tau,0,y)=\widetilde{\Phi}_1(\tau,0,y)=0,\quad \forall(\tau,y)\in[0,t]\times[0,1],\\
&\overline{\Phi}_k(\tau,x,0)=\widehat{\Phi}_k(\tau,x,0)=\overline{\Phi}_k(\tau,x,1)=\widehat{\Phi}_k(\tau,x,1)=0,\quad \forall(\tau,x)\in[0,t]\times[0,1],
\end{aligned}$$

one has

$$\begin{aligned}
&\int_0^t\int_0^1\int_0^1 \vec{\overline{\phi}}_f(\tau,x,y)\cdot(\vec{\Phi}_\tau(\tau,x,y)+\overline{A}_f\vec{\Phi}_x(\tau,x,y)+\overline{B}_f\vec{\Phi}_y(\tau,x,y)+\overline{C}\vec{\Phi}(\tau,x,y))dxdyd\tau\\
&+\int_0^1\int_0^1\vec{\phi}_{f0}(x,y)\cdot\vec{\Phi}(0,x,y)dxdy+\sum_{k=1}^N\int_0^t\int_0^{\frac12}\widetilde{h}_f(0,\overline{u}_f(\tau))\overline{\overline{\phi}}^f_k(\tau,2x,1)\widetilde{\Phi}_k(t,x,0)dxd\tau\\
&+\sum_{k=2}^N\int_0^t\int_0^1 2\tau_{gf}\overline{\widetilde{\phi}}^f_{k-1}(\tau,1,y)\overline{\Phi}_k(\tau,0,y)dyd\tau+\sum_{k=2}^N\int_0^t\int_0^1\frac{\tau_{gf}}{2}\overline{\widetilde{\phi}}^f_{k-1}(\tau,1,y)\widetilde{\Phi}_k(\tau,0,y)dyd\tau\\
&+\sum_{k=1}^N\int_0^t\int_0^1\overline{g}_f(\overline{u}_f(\tau))\overline{\overline{\phi}}^f_k(\tau,1,y)\widehat{\Phi}_k(\tau,0,y)dyd\tau=\int_0^1\int_0^1\vec{\overline{\phi}}_f(t,x,y)\cdot\vec{\Phi}(t,x,y)dxdy.
\end{aligned}\tag{2.75}$$

In (2.75), the velocity matrices $\overline{A}_f$, $\overline{B}_f$ and $\overline{C}$ are defined in the same way as the diagonal matrices A_f, B_f and C, but with $\vec{\overline{\phi}}_f$ instead of $\vec{\phi}_f$.

Let $\vec{\varphi}_0(x,y)=(\overline{\varphi}_{01},\cdots,\overline{\varphi}_{0N},\widehat{\varphi}_{01},\cdots,\widehat{\varphi}_{0N},\widetilde{\varphi}_{01},\cdots,\widetilde{\varphi}_{0N})^{tr}\in C^1_0((0,1)^2)$, and choose the test function as the solution to the following backward linear Cauchy problem

$$\begin{cases}
\vec{\Phi}_\tau+\overline{A}_f\vec{\Phi}_x+\overline{B}_f\vec{\Phi}_y=-\overline{C}\vec{\Phi},\quad 0\leqslant\tau\leqslant t,\quad (x,y)\in[0,1]^2,\\
\vec{\Phi}(t,x,y)=\vec{\varphi}_0(x,y),\quad (x,y)\in[0,1]^2,\\
\vec{\Phi}(\tau,1,y)=0,\quad (\tau,y)\in[0,t]\times[0,1],\\
\overline{\Phi}_1(\tau,0,y)=\widetilde{\Phi}_1(\tau,0,y)=0,\quad (\tau,y)\in[0,t]\times[0,1],\\
\overline{\Phi}_k(\tau,x,0)=\widehat{\Phi}_k(\tau,x,0)=\overline{\Phi}_k(\tau,x,1)=\widehat{\Phi}_k(\tau,x,1)=0,\quad (\tau,x)\in[0,t]\times[0,1].
\end{cases}\tag{2.76}$$

For any fixed $t\in[0,\delta]$, we introduce three new subsets $\overline{\overline{\omega}}^{f,t}_1$, $\overline{\overline{\omega}}^{f,t}_2$ and $\overline{\overline{\omega}}^{f,t}_3$ of $[0,1]^2$

$$\begin{aligned}
&\overline{\overline{\omega}}^{f,t}_1:=\Big\{(x,y)|\ \int_0^t\overline{g}_f(\overline{u}_f(\sigma))\,d\sigma\leqslant x\leqslant 1,\ \overline{\overline{\eta}}(t,\int_0^t\overline{g}_f(\overline{u}_f(\sigma))\,d\sigma)\leqslant y\leqslant 1\Big\},\\
&\overline{\overline{\omega}}^{f,t}_2:=\Big\{(x,y)|\ 0\leqslant x\leqslant\int_0^t\overline{g}_f(\overline{u}_f(\sigma))d\sigma,\ \overline{\overline{\eta}}(t,x)\leqslant y\leqslant 1\Big\},\\
&\overline{\overline{\omega}}^{f,t}_3:=[0,1]^2\backslash(\overline{\overline{\omega}}^{f,t}_1\cup\overline{\overline{\omega}}^{f,t}_2).
\end{aligned}$$

Where $y=\overline{\overline{\eta}}(t,x)$ is difined the same way as $y=\overline{\eta}(t,x)$ in (2.33) but with $\overline{\overline{\vec{\phi}}}_f$ instead of $\vec{\phi}_f$. Let us recall the simplified notation $\overline{u}_f=u_f(\overline{M}_f,\overline{M},t)$, we get

$$\frac{d\overline{\overline{\eta}}}{ds}=\overline{h}_f(\overline{\overline{\eta}},\overline{u}_f)(s),\quad \overline{\overline{\eta}}(\overline{\theta})=0,\quad \overline{\theta}\leqslant s\leqslant t,$$

with $\overline{\theta}$ defined by $x=\displaystyle\int_{\overline{\theta}}^{t}\overline{g}_f(\overline{u}_f(\sigma))d\sigma$.

For any fixed $t\in[0,\delta]$ and $(x,y)\in[0,1]^2$. If $(x,y)\in\overline{\overline{\omega}}_1^{f,t}$, we define $\overline{\overline{\xi}}_1=(\overline{\overline{x}}_1,\overline{\overline{y}}_1)$ by

$$\frac{d\overline{\overline{x}}_1}{ds}=\overline{g}_f(\overline{u}_f(s)),\quad \frac{d\overline{\overline{y}}_1}{ds}=\overline{h}_f(\overline{\overline{y}}_1,\overline{u}_f)(s),\quad \overline{\overline{\xi}}_1(t)=(x,y).$$

Let us then define

$$(\overline{\overline{x}}_0,\overline{\overline{y}}_0):=(\overline{\overline{x}}_1(0),\overline{\overline{y}}_1(0)). \tag{2.77}$$

If $(x,y)\in\overline{\overline{\omega}}_2^{f,t}$, we define $\overline{\overline{\xi}}_2=(\overline{\overline{x}}_2,\overline{\overline{y}}_2)$ by

$$\frac{d\overline{\overline{x}}_2}{ds}=\overline{g}_f(\overline{u}_f(s)),\quad \frac{d\overline{\overline{y}}_2}{ds}=\overline{h}_f(\overline{\overline{y}}_2,\overline{u}_f)(s),\quad \overline{\overline{\xi}}_2(t)=(x,y).$$

There exists a unique $\overline{\overline{\tau}}_0$ such that $\overline{\overline{x}}_2(\overline{\overline{\tau}}_0)=0$, so that we can define

$$\overline{\overline{\beta}}_0:=\overline{\overline{y}}_2(\overline{\overline{\tau}}_0). \tag{2.78}$$

Combining (2.75) with (2.76), we obtain that

$$\begin{aligned}
&\int_0^1\int_0^1\overline{\overline{\vec{\phi}}}_f(t,x,y)\cdot\vec{\Phi}(t,x,y)dxdy=\int_0^1\int_0^1\overline{\overline{\vec{\phi}}}_f(t,x,y)\cdot\vec{\varphi}_0(x,y)dxdy\\
=&\int_0^1\int_0^1\vec{\phi}_{f0}(x,y)\cdot\vec{\Phi}(0,x,y)dxdy+\sum_{k=1}^{N}\int_0^t\int_0^{\frac{1}{2}}\widetilde{h}_f(0,\overline{u}_f(\tau))\overline{\overline{\phi}}_k^f(\tau,2x,1)\widetilde{\Phi}_k(t,x,0)dxd\tau\\
&+\sum_{k=2}^{N}\int_0^t\int_0^1 2\tau_{gf}\overline{\overline{\phi}}_{k-1}^f(\tau,1,y)\overline{\Phi}_k(\tau,0,y)dyd\tau+\sum_{k=2}^{N}\int_0^t\int_0^1\frac{\tau_{gf}}{2}\overline{\overline{\phi}}_{k-1}^f(\tau,1,y)\widetilde{\Phi}_k(\tau,0,y)dyd\tau\\
&+\sum_{k=1}^{N}\int_0^t\int_0^1\overline{g}_f(\overline{u}_f(\tau))\overline{\overline{\phi}}_k^f(\tau,1,y)\widehat{\Phi}_k(\tau,0,y)dyd\tau\triangleq I_1+I_2+I_3+I_4+I_5.
\end{aligned}\tag{2.79}$$

Next we analyze each term $I_i(i=1,\cdots,5)$ in (2.79) by solving the backward linear Cauchy problem (2.76). For the last term I_5, since $\widehat{\Phi}_k$ satisfy pure transport equations, by solving the backward linear Cauchy problem (2.76), it is easy to get

$$\begin{aligned}
I_5=&\sum_{k=1}^{N}\int_0^t\int_0^1\overline{g}_f(\overline{u}_f(\tau))\overline{\overline{\phi}}_k^f(\tau,1,y)\widehat{\Phi}_k(\tau,0,y)dyd\tau\\
=&\sum_{k=1}^{N}\int_0^1\int_0^{\tau_{gf}t}\frac{\overline{g}_f(\overline{u}_f(t-\frac{x}{\tau_{gf}}))}{\tau_{gf}}\overline{\overline{\phi}}_k^f(t-\frac{x}{\tau_{gf}},1,y)\widehat{\varphi}_{0k}(x,y)dxdy.
\end{aligned}\tag{2.80}$$

Let us recall the definition of the characteristic curve $\overline{\overline{\xi}}_1$ and also definition (2.77) of $(\overline{\overline{x}}_0,\overline{\overline{y}}_0)$. By solving the backward linear Cauchy problem (2.76) and noting (2.118) of Lemma 2.6.1 in

section 2.6.3, we have

$$\begin{aligned}
I_1 =& \int_0^1 \int_0^1 \vec{\phi}_{f0}(x,y)\cdot\vec{\Phi}(0,x,y)dxdy\\
=&\sum_{k=1}^{N}\iint\limits_{\overline{\overline{\omega}}_1^{f,t}} \overline{\phi}_{k0}^f(\overline{\overline{x}}_0,\overline{\overline{y}}_0)\overline{\varphi}_{0k}(x,y)e^{-\int_0^t[\overline{\lambda}(\overline{\overline{y}}_1,\overline{U})+\frac{\partial\overline{h}_f}{\partial y}(\overline{\overline{y}}_1,\overline{u}_f)](\sigma)\,d\sigma}dxdy\\
&+\int_0^1\int_t^1 \widehat{\phi}_{k0}^f(x-\tau_{gf}t,y)\widehat{\varphi}_{0k}(x,y)dxdy+\sum_{k=1}^{N}\int_0^1\int_0^1 \widetilde{\phi}_{k0}^f(x,y)\widetilde{\Phi}_k(0,x,y)dxdy.
\end{aligned}\tag{2.81}$$

Since $\vec{\varphi}_0\in C_0^1((0,1)^2)$ and $t\in[0,\delta]$ are both arbitrary, from (2.80) and (2.81), we obtain in $C^0([0,\delta];L^1((0,1)^2))$ that for $k=1,\cdots,N$

$$\overline{\overline{\phi}}_k^f(t,x,y)=\begin{cases}\dfrac{\overline{g}_f(\overline{u}_f(t-\frac{x}{\tau_{gf}}))}{\tau_{gf}}\ \overline{\overline{\phi}}_k^f(t-\dfrac{x}{\tau_{gf}},1,y), & \text{if } (x,y)\in[0,\tau_{gf}t]\times[0,1],\\ \overline{\overline{\phi}}_k^f(t,x,y)=\widehat{\phi}_k^f(t,x,y), & \text{if } (x,y)\in[\tau_{gf}t,1]\times[0,1].\end{cases}\tag{2.82}$$

Let us recall the definition of the characteristic curve $\overline{\overline{\xi}}_2$ and also definition (2.78) of $(\overline{\overline{\tau}}_0,\overline{\overline{\beta}}_0)$. By solving the backward linear Cauchy problem (2.76), noting (2.82) and (2.119) of Lemma 2.6.1 in section 2.6.3, we get

$$\begin{aligned}
I_3=&\sum_{k=2}^{N}\int_0^t\int_0^1 2\tau_{gf}\overline{\overline{\phi}}_{k-1}^f(\tau,1,y)\overline{\Phi}_k(\tau,0,y)dyd\tau\\
=&\sum_{k=2}^{N}\iint\limits_{\overline{\overline{\omega}}_2^{f,t}}\frac{2\tau_{gf}\widehat{\phi}_{k-1}^f(\overline{\overline{\tau}}_0,1,\overline{\overline{\beta}}_0)}{\overline{g}_f(\overline{u}_f(\overline{\overline{\tau}}_0))}\ \overline{\varphi}_{0k}(x,y)e^{-\int_{\overline{\overline{\tau}}_0}^t[\overline{\lambda}(\overline{\overline{y}}_2,\overline{U})+\frac{\partial\overline{h}_f}{\partial y}(\overline{\overline{y}}_2,\overline{u}_f)]}dxdy.
\end{aligned}\tag{2.83}$$

Since $\vec{\varphi}_0\in C_0^1((0,1)^2)$ and $t\in[0,\delta]$ are both arbitrary, from (2.81) and (2.83), we obtain in $C^0([0,\delta];L^1((0,1)^2))$ that for $k=1$

$$\overline{\overline{\phi}}_1^f(t,x,y)=\begin{cases}\overline{\phi}_{10}^f(\overline{\overline{x}}_0,\overline{\overline{y}}_0)e^{-\int_0^t[\overline{\lambda}(\overline{\overline{y}}_1,\overline{U})+\frac{\partial\overline{h}_f}{\partial y}(\overline{\overline{y}}_1,\overline{u}_f)](\sigma)\,d\sigma}, & \text{if } (x,y)\in\overline{\overline{\omega}}_1^{f,t},\\ 0, \quad \text{else.}\end{cases}\tag{2.84}$$

For $k=2,\cdots,N$, we have

$$\overline{\overline{\phi}}_k^f(t,x,y)=\begin{cases}\overline{\phi}_{k0}^f(\overline{\overline{x}}_0,\overline{\overline{y}}_0)e^{-\int_0^t[\overline{\lambda}(\overline{\overline{y}}_1,\overline{U})+\frac{\partial\overline{h}_f}{\partial y}(\overline{\overline{y}}_1,\overline{u}_f)](\sigma)\,d\sigma}, & \text{if } (x,y)\in\overline{\overline{\omega}}_1^{f,t},\\ \dfrac{2\tau_{gf}\widehat{\phi}_{k-1}^f(\overline{\overline{\tau}}_0,1,\overline{\overline{\beta}}_0)}{\overline{g}_f(\overline{u}_f(\overline{\overline{\tau}}_0))}\ e^{-\int_{\overline{\overline{\tau}}_0}^t[\overline{\lambda}(\overline{\overline{y}}_2,\overline{U})+\frac{\partial\overline{h}_f}{\partial y}(\overline{\overline{y}}_2,\overline{u}_f)]}, & \text{if } (x,y)\in\overline{\overline{\omega}}_2^{f,t},\\ 0, \quad \text{else.}\end{cases}\tag{2.85}$$

For any fixed $t\in[0,\delta]$, we introduce four new subsets $\overline{\overline{\omega}}_1^{f,t}$, $\overline{\overline{\omega}}_2^{f,t}$, $\overline{\overline{\omega}}_3^{f,t}$ and $\overline{\overline{\omega}}_4^{f,t}$ of $[0,1]^2$

$$\begin{aligned}
\overline{\overline{\omega}}_1^{f,t}:=&\Big\{(x,y)|\ \frac{\tau_{gf}}{2}t\leqslant x\leqslant 1,\ \overline{\overline{\eta}}_1(t,\frac{\tau_{gf}}{2}t)\leqslant y\leqslant\overline{\overline{\eta}}_2(t,\frac{\tau_{gf}}{2}t)\Big\},\\
\overline{\overline{\omega}}_2^{f,t}:=&\Big\{(x,y)|\ 0\leqslant x\leqslant\frac{\tau_{gf}}{2}t,0\leqslant y\leqslant\overline{\overline{\eta}}_1(t,x)\Big\}\cup\Big\{(x,y)|\ \frac{\tau_{gf}}{2}t\leqslant x\leqslant 1,0\leqslant y\leqslant\overline{\overline{\eta}}_1(t,\frac{\tau_{gf}}{2}t)\Big\},\\
\overline{\overline{\omega}}_3^{f,t}:=&\Big\{(x,y)|\ 0\leqslant x\leqslant\frac{\tau_{gf}}{2}t,\ \overline{\overline{\eta}}_1(t,x)\leqslant y\leqslant\overline{\overline{\eta}}_2(t,x)\Big\},\\
\overline{\overline{\omega}}_4^{f,t}:=&[0,1]^2\backslash(\overline{\overline{\omega}}_1^{f,t}\cup\overline{\overline{\omega}}_2^{f,t}\cup\overline{\overline{\omega}}_3^{f,t}).
\end{aligned}$$

Here $y=\overline{\widetilde{\eta}}_1(t,x)$ and $y=\overline{\widetilde{\eta}}_2(t,x)$ satisfy

$$\frac{d\overline{\widetilde{\eta}}_1}{ds}=\widetilde{h}_f(\overline{\widetilde{\eta}}_1,\overline{u}_f)(s),\quad \overline{\widetilde{\eta}}_1(t-\frac{2x}{\tau_{gf}})=0,\quad t-\frac{2x}{\tau_{gf}}\leqslant s\leqslant t,$$
$$\frac{d\overline{\widetilde{\eta}}_2}{ds}=\widetilde{h}_f(\overline{\widetilde{\eta}}_2,\overline{u}_f)(s),\quad \overline{\widetilde{\eta}}_2(t-\frac{2x}{\tau_{gf}})=1,\quad t-\frac{2x}{\tau_{gf}}\leqslant s\leqslant t.$$

For any fixed $t\in[0,\delta]$ and $(x,y)\in[0,1]^2$. If $(x,y)\in\overline{\widetilde{\omega}}_1^{f,t}$, we define $\overline{\widetilde{\xi}}_1=(\overline{\widetilde{x}}_1,\overline{\widetilde{y}}_1)$ by

$$\frac{d\overline{\widetilde{x}}_1}{ds}=\frac{\tau_{gf}}{2},\quad \frac{d\overline{\widetilde{y}}_1}{ds}=\widetilde{h}_f(\overline{\widetilde{y}}_1,\overline{u}_f)(s),\quad \overline{\widetilde{\xi}}_1(t)=(x,y).$$

Let us then define $(\overline{\widetilde{x}}_0,\overline{\widetilde{y}}_0):=(\overline{\widetilde{x}}_1(0),\overline{\widetilde{y}}_1(0))$. With this definition, we solve the backward linear Cauchy problem (2.76) and use (2.120) of Lemma 2.6.1 in section 2.6.3, the last term of (2.81) can be rewritten as

$$\begin{aligned}&\int_0^1\int_0^1\widetilde{\phi}_{k0}^f(x,y)\widetilde{\Phi}_k(0,x,y)dxdy\\&=\sum_{k=1}^N\iint\limits_{\overline{\widetilde{\omega}}_1^{f,t}}\widetilde{\phi}_{k0}^f(\overline{\widetilde{x}}_0,\overline{\widetilde{y}}_0)\widetilde{\varphi}_{0k}(x,y)e^{-\int_0^t[\overline{\lambda}(\overline{\widetilde{y}}_1,\overline{U})+\frac{\partial\overline{h}_f}{\partial y}(\overline{\widetilde{y}}_1,\overline{u}_f)](\sigma)\,d\sigma}dxdy.\end{aligned}\tag{2.86}$$

If $(x,y)\in\overline{\widetilde{\omega}}_2^{f,t}$, we define $\overline{\widetilde{\xi}}_2=(\overline{\widetilde{x}}_2,\overline{\widetilde{y}}_2)$ by

$$\frac{d\overline{\widetilde{x}}_2}{ds}=\frac{\tau_{gf}}{2},\quad \frac{d\overline{\widetilde{y}}_2}{ds}=\widetilde{h}_f(\overline{\widetilde{y}}_2,\overline{u}_f)(s),\quad \overline{\widetilde{\xi}}_2(t)=(x,y).$$

There exists a unique $\overline{\widetilde{t}}_0$ such that $\overline{\widetilde{y}}_2(\overline{\widetilde{t}}_0)=0$, so that we can define $\overline{\widetilde{\alpha}}_0:=\overline{\widetilde{x}}_2(\overline{\widetilde{t}}_0)$. With this definition, we solve the backward linear Cauchy problem (2.76) and use (2.121) of Lemma 2.6.1 in section 2.6.3, we get

$$\begin{aligned}I_2=&\sum_{k=1}^N\int_0^t\int_0^{\frac{1}{2}}\widetilde{h}_f(0,\overline{u}_f(\tau))\overline{\widetilde{\phi}}_k^f(\tau,2x,1)\widetilde{\Phi}_k(\tau,x,0)dxd\tau\\=&\sum_{k=1}^N\iint\limits_{\overline{\widetilde{\omega}}_2^{f,t}}\overline{\widetilde{\phi}}_k^f(\overline{\widetilde{t}}_0,2\overline{\widetilde{\alpha}}_0,1)\widetilde{\varphi}_{0k}(x,y)e^{-\int_{\overline{\widetilde{t}}_0}^t[\widetilde{\lambda}(\overline{\widetilde{y}}_2,\overline{U})+\frac{\partial\widetilde{h}_f}{\partial y}(\overline{\widetilde{y}}_2,\overline{u}_f)](\sigma)\,d\sigma}dxdy.\end{aligned}\tag{2.87}$$

If $(x,y)\in\overline{\widetilde{\omega}}_3^{f,t}$, we define $\overline{\widetilde{\xi}}_3=(\overline{\widetilde{x}}_3,\overline{\widetilde{y}}_3)$ by

$$\frac{d\overline{\widetilde{x}}_3}{ds}=\frac{\tau_{gf}}{2},\quad \frac{d\overline{\widetilde{y}}_3}{ds}=\widetilde{h}_f(\overline{\widetilde{y}}_3,\overline{u}_f)(s),\quad \overline{\widetilde{\xi}}_3(t)=(x,y).$$

There exists a unique $\overline{\widetilde{\tau}}_0$ such that $\overline{\widetilde{x}}_3(\overline{\widetilde{\tau}}_0)=0$, so that we can define $\overline{\widetilde{\beta}}_0:=\overline{\widetilde{y}}_3(\overline{\widetilde{\tau}}_0)$. With this definition, we solve the backward linear Cauchy problem (2.76) and use (2.122) of Lemma 2.6.1 in section 2.6.3, we get

$$\begin{aligned}I_4=&\sum_{k=2}^N\int_0^t\int_0^1\frac{\tau_{gf}}{2}\overline{\widetilde{\phi}}_{k-1}^f(\tau,1,y)\widetilde{\Phi}_k(\tau,0,y)dyd\tau\\=&\sum_{k=2}^N\iint\limits_{\overline{\widetilde{\omega}}_3^{f,t}}\overline{\widetilde{\phi}}_{k-1}^f(\overline{\widetilde{\tau}}_0,1,\overline{\widetilde{\beta}}_0)\widetilde{\varphi}_{0k}(x,y)e^{-\int_{\overline{\widetilde{\tau}}_0}^t[\widetilde{\lambda}(\overline{\widetilde{y}}_3,\overline{U})+\frac{\partial\widetilde{h}_f}{\partial y}(\overline{\widetilde{y}}_3,\overline{u}_f)](\sigma)\,d\sigma}dxdy.\end{aligned}\tag{2.88}$$

Since $\vec{\varphi}_0 \in C_0^1((0,1)^2)$ and $t \in [0,\delta]$ are both arbitrary, combining (2.81) and (2.86)-(2.88), we obtain in $C^0([0,\delta];L^1((0,1)^2))$ that for $k=1$

$$\overline{\widetilde{\phi}}_1^f(t,x,y)=\begin{cases}\widetilde{\phi}_{10}^f(\overline{\widetilde{x}}_0,\overline{\widetilde{y}}_0)e^{-\int_0^t[\widetilde{\lambda}(\overline{\widetilde{y}}_1,\overline{U})+\frac{\partial\widetilde{h}_f}{\partial y}(\overline{\widetilde{y}}_1,\overline{u}_f)](\sigma)\,d\sigma}, & \text{if } (x,y)\in\overline{\widetilde{\omega}}_1^{f,t},\\ \overline{\widetilde{\phi}}_1^f(\overline{\widetilde{t}}_0,2\overline{\widetilde{\alpha}}_0,1)e^{-\int_{\overline{\widetilde{t}}_0}^t[\widetilde{\lambda}(\overline{\widetilde{y}}_2,\overline{U})+\frac{\partial\widetilde{h}_f}{\partial y}(\overline{\widetilde{y}}_2,\overline{u}_f)](\sigma)\,d\sigma}, & \text{if } (x,y)\in\overline{\widetilde{\omega}}_2^{f,t},\\ 0, \quad \text{else.}\end{cases}\tag{2.89}$$

For $k=2,\cdots,N$, we get

$$\overline{\widetilde{\phi}}_k^f(t,x,y)=\begin{cases}\widetilde{\phi}_{k0}^f(\overline{\widetilde{x}}_0,\overline{\widetilde{y}}_0)e^{-\int_0^t[\widetilde{\lambda}(\overline{\widetilde{y}}_1,\overline{U})+\frac{\partial\widetilde{h}_f}{\partial y}(\overline{\widetilde{y}}_1,\overline{u}_f)](\sigma)\,d\sigma}, & \text{if } (x,y)\in\overline{\widetilde{\omega}}_1^{f,t},\\ \overline{\widetilde{\phi}}_1^f(\overline{\widetilde{t}}_0,2\overline{\widetilde{\alpha}}_0,1)e^{-\int_{\overline{\widetilde{t}}_0}^t[\widetilde{\lambda}(\overline{\widetilde{y}}_2,\overline{U})+\frac{\partial\widetilde{h}_f}{\partial y}(\overline{\widetilde{y}}_2,\overline{u}_f)](\sigma)\,d\sigma}, & \text{if } (x,y)\in\overline{\widetilde{\omega}}_2^{f,t},\\ \overline{\widetilde{\phi}}_{k-1}^f(\overline{\widetilde{\tau}}_0,1,\overline{\widetilde{\beta}}_0)e^{-\int_{\overline{\widetilde{\tau}}_0}^t[\widetilde{\lambda}(\overline{\widetilde{y}}_3,\overline{U})+\frac{\partial\widetilde{h}_f}{\partial y}(\overline{\widetilde{y}}_3,\overline{u}_f)](\sigma)\,d\sigma}, & \text{if } (x,y)\in\overline{\widetilde{\omega}}_3^{f,t},\\ 0, \quad \text{else.}\end{cases}\tag{2.90}$$

By (2.23), we claim that $\overline{\vec{M}}(t)\in\Omega_{\delta,K}$ and $\overline{\vec{M}}(t)$ satisfies the same contraction mapping function $\vec{G}$. Since $\vec{M}$ is the unique fixed point of $\vec{G}$ in $\Omega_{\delta,K}$, therefore we have $\overline{\vec{M}}\equiv\vec{M}$. Consequently, we have $\overline{\overline{\xi}}_i\equiv\overline{\xi}_i(i=1,2)$, $\overline{\widetilde{\xi}}_i=\widetilde{\xi}_i(i=1,2,3)$, $\overline{\overline{\eta}}_i\equiv\overline{\eta}_i(i=1,2)$ and $\overline{\overline{\eta}}\equiv\overline{\eta}$. Obviously, we have then $(\overline{\overline{x}}_0,\overline{\overline{y}}_0)\equiv(\overline{x}_0,\overline{y}_0)$, $(\overline{\widetilde{x}}_0,\overline{\widetilde{y}}_0)\equiv(\widetilde{x}_0,\widetilde{y}_0)$, $(\overline{\widetilde{t}}_0,\overline{\widetilde{\alpha}}_0)\equiv(\widetilde{t}_0,\widetilde{\alpha}_0)$, $(\overline{\overline{\tau}}_0,\overline{\overline{\beta}}_0)\equiv(\overline{\tau}_0,\overline{\beta}_0)$, $(\overline{\widetilde{\tau}}_0,\overline{\widetilde{\beta}}_0)\equiv(\widetilde{\tau}_0,\widetilde{\beta}_0)$, $\overline{\overline{\omega}}_i^{f,t}\equiv\overline{\omega}_i^{f,t}(i=1,2,3)$ and $\overline{\widetilde{\omega}}_i^{f,t}\equiv\widetilde{\omega}_i^{f,t}(i=1,2,3,4)$. Finally, by comparing the definition (2.82), (2.84)-(2.85) and (2.89)-(2.90) of $\overline{\vec{\phi}}_f$ with the definition (2.39)-(2.43) of $\vec{\phi}_f$, we obtain $\overline{\vec{\phi}}_f\equiv\vec{\phi}_f$. This gives us the uniqueness of the weak solution for small time. □

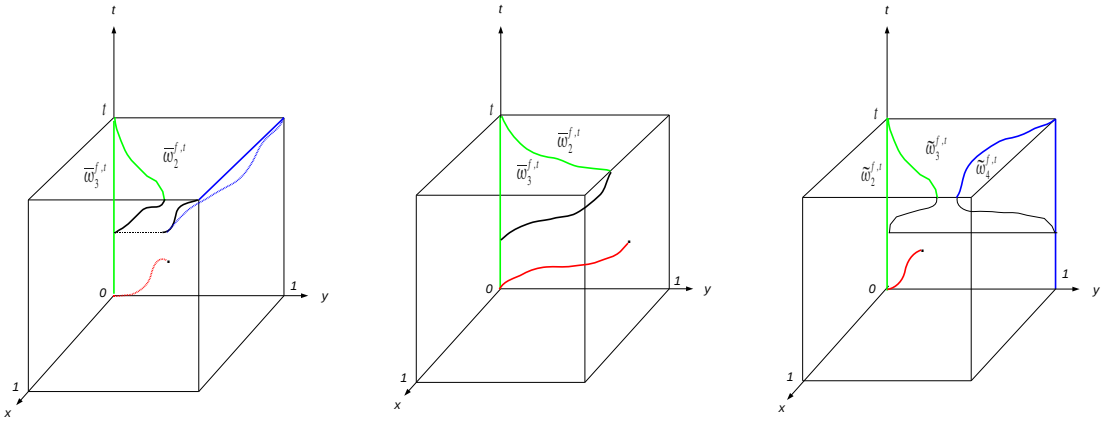
2.5 Proof of the existence of a global solution to Cauchy problem

Let us now prove the existence of global solution to Cauchy problem (2.1)-(2.9). Noting the definition (2.22) of G_f and the definition (2.39)-(2.43) of the local solution $\vec{\phi}_f$, it is easy to check that the following two estimates hold for all $t\in[0,\delta]$

$$0\leqslant M(t)\leqslant K,\tag{2.91}$$

$$\|\vec{\phi}_f(t,\cdot)\|_{L^\infty((0,1)^2)}\leqslant e^{2(N+1)TK_1}\max_k\Big\{(\frac{2K_1}{K_2}+\frac{K_1}{\tau_{gf}})^N\|\overline{\vec{\phi}}_{k0}^f\|,(\frac{2(K_1+\tau_{gf})}{K_2})^N\|\widehat{\phi}_{k0}^f\|,\|\widetilde{\phi}_{k0}^f\|\Big\},\tag{2.92}$$

where K is defined by (2.15), K_1 is defined by (2.16) and K_2 is defined by (2.17). In order to obtain a global solution, we suppose that we have solved Cauchy problem (2.1)-(2.9) up to the moment $\tau\in[0,T]$ with the weak solution $\vec{\phi}_f\in C^0([0,\tau];L^p((0,1)^2))$. From our way to construct the weak solution, we know that for any $0\leqslant t\leqslant\tau$, the weak solution is given as the form defined by (2.39)-(2.43).



(a) (b) (c)

Figure 2.6. Division of the time t plane for each cell cycle k when t is large enough. In phase 1, when t is large, the characteristic curve (red) passing through the origin may encounter two cases: in case (a), it intersects the front face, then go to phase 2; in case (b), it intersects the right face, then go to phase 3. (c) In phase 3, due to the assumption that $\widetilde{h}_f(1, u_f) < 0$, the characteristic curve (red) passing through the origin will definitely intersect the front face, then go to the next cycle $k + 1$.

As time increases, for each cell cycle k ($k = 1, \cdots, N$) in phase 1, the characteristic curve which passes through the origin may encounter two possible cases. It may either intersect with the front face (see figure 2.6 (a)), then go to phase 2 (mitosis). Or it may intersect with the right face (see figure 2.6 (b)), then go to phase 3 (differentiation). For each cell cycle k ($k = 1, \cdots, N$) in phase 3, the characteristic curve which passes through the origin will definitely intersect with the front face due to the assumption that $\widetilde{h}_f(1, u_f) < 0$ (see figure 2.6 (c)). Then it will go further to the next cell cycle. We get in any case that

$$M_f(t) := \sum_{k=1}^{N} \iint\limits_{\overline{\omega}_2^{f,t}} \gamma_s^2 y \overline{\phi}_k^f(t,x,y)dxdy + \sum_{k=1}^{N} \int_0^1 \int_0^1 \gamma_s^2 y \widehat{\phi}_k^f(t,x,y)dxdy$$
$$+ \sum_{k=1}^{N} \iint\limits_{\widetilde{\omega}_2^{f,t} \cup\, \widetilde{\omega}_3^{f,t}} 2\gamma_d(\gamma_d y + \gamma_s)\widetilde{\phi}_k^f(t,x,y)dxdy.$$

Thanks to Lemma 2.6.1 in section 2.6.3, after tracing back $\overline{\phi}_k^f(t,x,y)$, $\widehat{\phi}_k^f(t,x,y)$ and $\widetilde{\phi}_k^f(t,x,y)$ along the characteristics finally to the initial data at most N times, we can prove that estimate (2.91) holds for every $t \in [0,T]$. Moreover, noting definition (2.39)-(2.43) of the global solution, it is easy to check that the uniform a priori estimate (2.92) holds for every $t \in [0,T]$. Hence we can choose $\delta \in [0,T]$ independent of τ. Applying Lemma 2.3.2 and Lemma 2.4.1 again, the weak solution $\vec{\phi}_f \in C^0([0,\tau]; L^p((0,1)^2))$ can be extended to the time interval $[\tau, \tau+\delta] \cap [\tau, T]$. Step by step, we finally obtain a unique global weak solution

$\vec{\phi}_f \in C^0([0,T];L^p((0,1)^2))$ for any $p \in [1,\infty)$. This finishes the proof of the existence of a global solution to Cauchy problem (2.1)-(2.9).

2.6 Appendix

2.6.1 Introduction of the model

In this section, we first recall the systems of equations describing the dynamics of the cell density of ovarian follicles in the model of F. Clément [22, 44, 45]. The cell population in a follicle f is represented by cell density functions $\phi^f_{j,k}(t,a,\gamma)$ defined on each cellular phase $Q^f_{j,k}$ with age a and maturity γ, which satisfy the following conservation laws

$$\frac{\partial \phi^f_{j,k}}{\partial t} + \frac{\partial (g_f(u_f)\phi^f_{j,k})}{\partial a} + \frac{\partial (h_f(\gamma,u_f)\phi^f_{j,k})}{\partial \gamma} = -\lambda(\gamma,U)\phi^f_{j,k} \quad \text{in } Q^f_{j,k}, \tag{2.93}$$

$$\begin{aligned}
&Q^f_{j,k} := \Omega_{j,k} \times [0,T], \text{ for } j = 1,2,3,\ f = 1,\cdots,n, \quad \text{where}\\
&\Omega_{1,k} := [(k-1)a_2, (k-1)a_2 + a_1] \times [0,\gamma_s], \quad \Omega_{2,k} := [(k-1)a_2 + a_1, ka_2] \times [0,\gamma_s],\\
&\Omega_{3,k} := [(k-1)a_2, ka_2] \times [\gamma_s,\gamma_m].
\end{aligned}$$

Here $k = 1,\cdots,N$, and N is the number of consecutive cell cycles (see figure 2.7).

Define the maturity operator M as

$$M(\varphi)(t) := \int_0^{\gamma_m}\int_0^{a_m} \gamma\varphi(t,a,\gamma)\,da d\gamma. \tag{2.94}$$

Then

$$M_f(t) := \sum_{j=1}^{3}\sum_{k=1}^{N} M(\phi^f_{j,k})(t) = \sum_{j=1}^{3}\sum_{k=1}^{N}\int_0^{\gamma_m}\int_0^{a_m} \gamma\phi^f_{j,k}(t,a,\gamma)\,da d\gamma \tag{2.95}$$

is the global follicular maturity on the follicular scale, while

$$M(t) := \sum_{f=1}^{n} M_f(t) = \sum_{f=1}^{n}\sum_{j=1}^{3}\sum_{k=1}^{N}\int_0^{\gamma_m}\int_0^{a_m} \gamma\phi^f_{j,k}(t,a,\gamma)\,da d\gamma \tag{2.96}$$

is the global maturity on the ovarian scale.

In (2.94)-(2.96), γ_m and a_m are maximum of maturity and age. The velocity and source terms are all smooth functions of u_f and U, where u_f is the local control and U is the global control. Here, we consider both closed and open loop problems, that is to say u_f and U are functions of M_f, M and t. As an instance of closed loop problem, the velocity and source

terms are given by the following expressions in [22] (all parameters are positive constants)

$$
\begin{aligned}
&g_f(u_f) = \tau_{gf}(1 - g_1(1 - u_f)), \quad \text{in} \quad \Omega_{1,k},\\
&g_f(u_f) = \tau_{gf}, \quad \text{in} \quad \Omega_{j,k}, \quad j = 2, 3,\\
&h_f(\gamma, u_f) = \tau_{hf}(-\gamma^2 + (c_1\gamma + c_2)(1 - e^{\frac{-u_f}{\bar{u}}})), \quad \text{in} \quad \Omega_{j,k}, \quad j = 1, 3,\\
&h_f(\gamma, u_f) = \lambda(\gamma, U) = 0, \quad \text{in} \quad \Omega_{2,k},\\
&\lambda(\gamma, U) = Ke^{-(\frac{\gamma-\gamma_s}{\bar{\gamma}})^2}(1 - U), \quad \text{in} \quad \Omega_{j,k}, \quad j = 1, 3.\\
&U = S(M) + U_0 = U_0 + U_s + \frac{1 - U_s}{1 + e^{c(M-m)}},\\
&u_f = b(M_f)U = \min\{b_1 + \frac{e^{b_2 M_f}}{b_3}, 1\} \cdot [U_0 + U_s + \frac{1 - U_s}{1 + e^{c(M-m)}}].
\end{aligned}
\tag{2.97}
$$

The initial conditions are given as follows

$$
\phi^f_{j,k}(0, a, \gamma) = \phi^f_{k0}(a, \gamma)|_{\Omega_{j,k}}, \qquad j = 1, 2, 3, \quad k = 1, \cdots, N. \tag{2.98}
$$

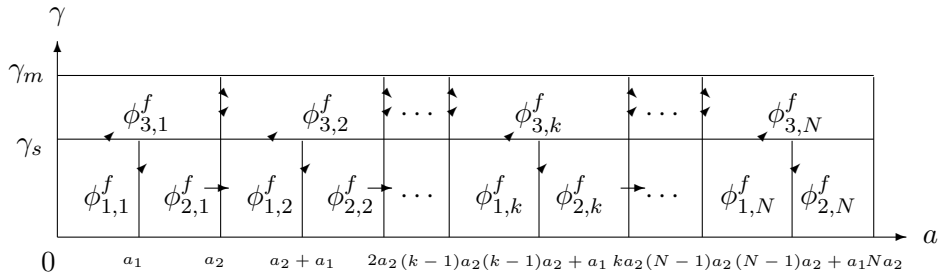


Figure 2.7. Domain of the solution in the original model. For each follicle f, the domain consists of the sequence of N cell cycles. a denotes the age of the cell and γ denotes its maturity. The top of the domain corresponds to the differentiation phase and the bottom to the proliferation phase.

The boundary conditions are given as follows

$$
g_f(u_f)\phi^f_{1,k}(t, (k-1)a_2, \gamma) = \begin{cases} 2\tau_{gf}\phi^f_{2,k-1}(t, (k-1)a_2, \gamma), \text{ for } k \geqslant 2, \\ 0, \quad \text{for } k = 1, \end{cases} \quad \text{for } \gamma \in [0, \gamma_s].
$$

$$
\phi^f_{1,k}(t, a, 0) = 0, \quad \text{for } a \in [(k-1)a_2, (k-1)a_2 + a_1],
$$

$$
\tau_{gf}\phi^f_{2,k}(t, (k-1)a_2 + a_1, \gamma) = g_f(u_f)\phi^f_{1,k}(t, (k-1)a_2 + a_1, \gamma), \quad \text{for } \gamma \in [0, \gamma_s],
$$

$$
\phi^f_{2,k}(t, a, 0) = 0, \quad \text{for } a \in [(k-1)a_2 + a_1, ka_2],
$$

$$
\phi^f_{3,k}(t, (k-1)a_2, \gamma) = \begin{cases} \phi^f_{3,k-1}(t, (k-1)a_2, \gamma), \quad \text{for } k \geqslant 2, \\ 0, \quad \text{for } k = 1, \end{cases} \quad \text{for } \gamma \in [\gamma_s, \gamma_m],
$$

$$
\phi^f_{3,k}(t, a, \gamma_s) = \begin{cases} \phi^f_{1,k}(t, a, \gamma_s), \quad \text{for } a \in [(k-1)a_2, (k-1)a_2 + a_1], \\ 0, \quad \text{for } a \in [(k-1)a_2 + a_1, ka_2]. \end{cases}
$$

2.6.2 Mathematical reformulation

In this section, we perform a mathematical reformulation of the original model introduced in section 2.6.1. One can notice that in system (2.93), all the unknowns are defined on different domains, so that one has to solve the equations successively. Here we transform system (2.93) into a regular one where the unknowns are defined on the same domain $[0,T]\times[0,1]^2$. In phase 1, we denote by $\overline{\phi}_k^f$ the density functions, $\overline{g}_f$ the age velocities and $\overline{h}_f$ the maturity velocities; In phase 2, we denote by $\widehat{\phi}_k^f$ the density functions and $\widehat{g}_f$ the age velocities; In phase 3, we denote by $\widetilde{\phi}_k^f$ the density functions, $\widetilde{g}_f$ the age velocities and $\widetilde{h}_f$ the maturity velocities.

Let

$$\overline{\phi}_k^f(t,x,y) := \phi_{1,k}^f(t,a,\gamma), \quad (a,\gamma)\in\Omega_{1,k}, \tag{2.99}$$

where

$$x := \frac{a-(k-1)a_2}{a_1},\ y := \frac{\gamma}{\gamma_s}, \tag{2.100}$$

so that we get $(a,\gamma)\in\Omega_{1,k} \Longleftrightarrow (x,y)\in[0,1]^2$, and

$$(\overline{\phi}_k^f)_t + (\overline{g}_f\overline{\phi}_k^f)_x + (\overline{h}_f\overline{\phi}_k^f)_y = -\overline{\lambda}\ \overline{\phi}_k^f, \tag{2.101}$$

with

$$\overline{g}_f(u_f) := \frac{g_f(u_f)}{a_1}, \quad \overline{h}_f(y,u_f) := \frac{h_f(\gamma_s y,u_f)}{\gamma_s}, \quad \overline{\lambda}(y,U) := \lambda(\gamma_s y,U). \tag{2.102}$$

Let

$$\widehat{\phi}_k^f(t,x,y) := \phi_{2,k}^f(t,a,\gamma), \quad (a,\gamma)\in\Omega_{2,k}, \tag{2.103}$$

where

$$x := \frac{a-(k-1)a_2-a_1}{a_2-a_1},\ y := \frac{\gamma}{\gamma_s}. \tag{2.104}$$

So that we get $(a,\gamma)\in\Omega_{2,k} \Longleftrightarrow (x,y)\in[0,1]^2$, and

$$(\widehat{\phi}_k^f)_t + \widehat{g}_f(\widehat{\phi}_k^f)_x = 0, \quad \widehat{g}_f := \frac{\tau_{gf}}{a_2-a_1}. \tag{2.105}$$

Let

$$\widetilde{\phi}_k^f(t,x,y) := \phi_{3,k}^f(t,a,\gamma), \quad (a,\gamma)\in\Omega_{3,k}, \tag{2.106}$$

where

$$x := \frac{a-(k-1)a_2}{a_2},\ y := \frac{\gamma-\gamma_s}{\gamma_m-\gamma_s}, \tag{2.107}$$

so that we get $(a,\gamma)\in\Omega_{3,k} \Longleftrightarrow (x,y)\in[0,1]^2$, and

$$(\widetilde{\phi}_k^f)_t + (\widetilde{g}_f\widetilde{\phi}_k^f)_x + (\widetilde{h}_f\widetilde{\phi}_k^f)_y = -\widetilde{\lambda}\widetilde{\phi}_k^f, \tag{2.108}$$

with

$$\widetilde{g}_f := \frac{\tau_{gf}}{a_2}, \widetilde{h}_f(y,u_f) := \frac{h_f((\gamma_m-\gamma_s)y+\gamma_s,u_f)}{\gamma_m-\gamma_s}, \widetilde{\lambda}(y,U) := \lambda((\gamma_m-\gamma_s)y+\gamma_s,U). \tag{2.109}$$

Correspondingly, let us denote the initial conditions (2.98) with new notations by

$$\vec{\phi}_{f0} := (\overline{\phi}^f_{10}(x,y),\cdots,\overline{\phi}^f_{N0}(x,y),\ \widehat{\phi}^f_{10}(x,y),\cdots\widehat{\phi}^f_{N0},\ \widetilde{\phi}^f_{10}(x,y),\cdots,\widetilde{\phi}^f_{N0}(x,y))^{tr}, \tag{2.110}$$

where

$$\overline{\phi}^f_{k0}(x,y) := \phi^f_{1,k}(0,a,\gamma),\ \widehat{\phi}^f_{k0}(x,y) := \phi^f_{2,k}(0,a,\gamma),\ \widetilde{\phi}^f_{k0}(x,y) := \phi^f_{3,k}(0,a,\gamma). \tag{2.111}$$

Let $\vec{\phi}_f := (\overline{\phi}^f_1,\cdots,\overline{\phi}^f_N,\ \widehat{\phi}^f_1,\cdots,\widehat{\phi}^f_N,\ \widetilde{\phi}^f_1,\cdots,\widetilde{\phi}^f_N)^{tr}$, we have

$$\vec{\phi}_f(t,x,y)_t+(A_f\vec{\phi}_f(t,x,y))_x+(B_f\vec{\phi}_f(t,x,y))_y=C\vec{\phi}_f(t,x,y),\ t\geqslant 0,\ (x,y)\in[0,1]^2, \tag{2.112}$$

where

$$\begin{aligned}
A_f :&= \text{diag}\ \{\overbrace{\overline{g}_f,\cdots,\overline{g}_f}^{N},\ \overbrace{\widehat{g}_f,\cdots,\widehat{g}_f}^{N}\ \overbrace{\widetilde{g}_f,\cdots,\widetilde{g}_f}^{N}\},\\
B_f :&= \text{diag}\ \{\overbrace{\overline{h}_f,\cdots,\overline{h}_f}^{N},\ \overbrace{0,\cdots,0}^{N}\ \overbrace{\widetilde{h}_f,\cdots,\widetilde{h}_f}^{N}\},\\
C :&= -\text{diag}\ \{\overbrace{\overline{\lambda},\cdots,\overline{\lambda}}^{N},\ \overbrace{0,\cdots,0}^{N}\ \overbrace{\widetilde{\lambda},\cdots,\widetilde{\lambda}}^{N}\}.
\end{aligned}$$

Without loss of generality, we assume that $a_1 = a_2 - a_1 = 1$ and $\gamma_d = \gamma_m - \gamma_s$ in the whole chapter. Correspondingly, the velocities become

$$\overline{g}_f(u_f) = g_f(u_f),\quad \widehat{g}_f = \tau_{gf},\quad \widetilde{g}_f = \frac{\tau_{gf}}{2}, \tag{2.113}$$

$$\overline{h}_f(y,u_f) = \frac{h_f(\gamma_s y,u_f)}{\gamma_s},\quad \widehat{h}_f = 0,\quad \widetilde{h}_f(y,u_f) = \frac{h_f(\gamma_d y+\gamma_s,u_f)}{\gamma_d}, \tag{2.114}$$

$$\overline{\lambda}(y,U) = \lambda(\gamma_s y,U),\quad \widehat{\lambda} = 0,\quad \widetilde{\lambda}(y,U) = \lambda(\gamma_d y+\gamma_s,U). \tag{2.115}$$

Since

$$\begin{aligned}
M(\phi^f_{1,k})(t) &= \iint_{\Omega_{1,k}} \gamma\phi^f_{1,k}(t,a,\gamma)\,da\,d\gamma = \int_0^1\int_0^1 \gamma_s^2 y\overline{\phi}^f_k(t,x,y)\,dx\,dy,\\
M(\phi^f_{2,k})(t) &= \iint_{\Omega_{2,k}} \gamma\phi^f_{2,k}(t,a,\gamma)\,da\,d\gamma = \int_0^1\int_0^1 \gamma_s^2 y\widehat{\phi}^f_k(t,x,y)\,dx\,dy,\\
M(\phi^f_{3,k})(t) &= \iint_{\Omega_{3,k}} \gamma\phi^f_{3,k}(t,a,\gamma)\,da\,d\gamma = \int_0^1\int_0^1 2\gamma_d(\gamma_d y+\gamma_s)\widetilde{\phi}^f_k(t,x,y)\,dx\,dy.
\end{aligned}$$

We have the maturity on the follicular scale

$$\begin{aligned}
M_f(t) =& \sum_{k=1}^N M(\phi^f_{1,k})(t) + \sum_{k=1}^N M(\phi^f_{2,k})(t) + \sum_{k=1}^N M(\phi^f_{3,k})(t)\\
=& \sum_{k=1}^N \int_0^1\int_0^1 \gamma_s^2 y\overline{\phi}^f_k(t,x,y)dxdy + \sum_{k=1}^N \int_0^1\int_0^1 \gamma_s^2 y\widehat{\phi}^f_k(t,x,y)dxdy\\
&+ \sum_{k=1}^N \int_0^1\int_0^1 2\gamma_d(\gamma_d y+\gamma_s)\widetilde{\phi}^f_k(t,x,y)\,dx\,dy.
\end{aligned} \tag{2.116}$$

Finally, we derive the assumptions on maturity velocities $\overline{h}_f$ and $\widetilde{h}_f$ from view point of biology. From the original expression of $h_f(\gamma, u_f)$ (see (2.97) in section 2.6.1), let us define

$$\gamma_{\pm}(u_f) := \frac{c_1(1-e^{\frac{-u_f}{\overline{u}}}) \pm \sqrt{c_1^2(1-e^{\frac{-u_f}{\overline{u}}})^2 + 4c_2(1-e^{\frac{-u_f}{\overline{u}}})}}{2}.$$

It is easy to see that $\gamma_+(u_f)$ is an increasing function of u_f, and

$$h_f(\gamma, u_f) = \tau_{hf}(\gamma_+(u_f) - \gamma)(\gamma - \gamma_-(u_f)).$$

Hence, when $\gamma = \gamma_+(u_f)$, we have $h_f(\gamma, u_f) = 0$, moreover

$$\begin{aligned} &h_f(\gamma, u_f) > 0, \quad \text{if } 0 \leqslant \gamma < \gamma_+(u_f), \\ &h_f(\gamma, u_f) < 0, \quad \text{if } \gamma > \gamma_+(u_f). \end{aligned}$$

Furthermore, under the assumption that the local control u_f satisfies $\gamma_+(u_f) > \gamma_s$, and

$$0 \leqslant \gamma_+(u_f) \leqslant \gamma_+(1) \simeq (1-e^{\frac{-1}{\overline{u}}})\frac{c_1 + \sqrt{c_1^2 + 4c_2}}{2} < \gamma_m.$$

From the fact that $0 < \gamma \leqslant \gamma_s$ in phase 1 and $\gamma_s \leqslant \gamma \leqslant \gamma_m$ in phase 3, we have

$$\begin{aligned} &h_f(\gamma, u_f) > 0, \quad 0 < \gamma \leqslant \gamma_s, \\ &h_f(\gamma_s, u_f) > 0, \quad h_f(\gamma_m, u_f) < 0. \end{aligned}$$

Corresponding to the new notations, we have assumptions

$$\begin{aligned} &\overline{h}_f(y, u_f) > 0, \quad \forall y \in [0,1], \\ &\widetilde{h}_f(0, u_f) > 0, \quad \widetilde{h}_f(1, u_f) < 0. \end{aligned} \tag{2.117}$$

2.6.3 Basic lemmas

The following lemma is used to prove the existence of the weak solution to Cauchy problem (2.1)-(2.9), when we derive the contraction mapping function $\vec{G}$, change variables in some integrals (see section 2.3) and prove the uniqueness of the solution (see section 2.4).

Lemma 2.6.1. *The characteristic curve $\overline{\xi}_1 = (\overline{x}_1, \overline{y}_1)$ passing through (t, x, y) intersects the bottom face at $(0, \overline{x}_0, \overline{y}_0)$. We have*

$$\frac{\partial(x,y)}{\partial(\overline{x}_0, \overline{y}_0)} = e^{\int_0^t \frac{\partial \overline{h}_f}{\partial y}(\overline{y}_1, u_f)(\sigma)\, d\sigma}. \tag{2.118}$$

The characteristic curve $\overline{\xi}_2 = (\overline{x}_2, \overline{y}_2)$ passing through (t, x, y) intersects the back face at $(\overline{\tau}_0, 0, \overline{\beta}_0)$. We have

$$\frac{\partial(x,y)}{\partial(\overline{\tau}_0, \overline{\beta}_0)} = -\overline{g}_f(u_f(\overline{\tau}_0)) \cdot e^{\int_{\overline{\tau}_0}^t \frac{\partial \overline{h}_f}{\partial y}(\overline{y}_2, u_f)(\sigma)\, d\sigma}. \tag{2.119}$$

The characteristic curve $\widetilde{\xi}_1 = (\widetilde{x}_1, \widetilde{y}_1)$ *passing through* (t, x, y) *intersects the bottom face at* $(0, \widetilde{x}_0, \widetilde{y}_0)$. *We have*

$$\frac{\partial(x,y)}{\partial(\widetilde{x}_0, \widetilde{y}_0)} = e^{\int_0^t \frac{\partial \widetilde{h}_f}{\partial y}(\widetilde{y}_1, u_f)(\sigma)\, d\sigma}. \tag{2.120}$$

The characteristic curve $\widetilde{\xi}_2 = (\widetilde{x}_2, \widetilde{y}_2)$ *passing through* (t, x, y) *intersects the left face at* $(\widetilde{t}_0, \widetilde{\alpha}_0, 0)$. *We have*

$$\frac{\partial(x,y)}{\partial(\widetilde{t}_0, \widetilde{\alpha}_0)} = \widetilde{h}_f(0, u_f(\widetilde{t}_0)) \cdot e^{\int_{\widetilde{t}_0}^t \frac{\partial \widetilde{h}_f}{\partial y}(\widetilde{y}_2, u_f)(\sigma)\, d\sigma}. \tag{2.121}$$

The characteristic curve $\widetilde{\xi}_3 = (\widetilde{x}_3, \widetilde{y}_3)$ *passing through* (t, x, y) *intersects the back face at* $(\widetilde{\tau}_0, 0, \widetilde{\beta}_0)$. *We have*

$$\frac{\partial(x,y)}{\partial(\widetilde{\tau}_0, \widetilde{\beta}_0)} = -\frac{\tau_{gf}}{2} e^{\int_{\widetilde{\tau}_0}^t \frac{\partial \widetilde{h}_f}{\partial y}(\widetilde{y}_3, u_f)(\sigma)\, d\sigma}. \tag{2.122}$$

The proof of this lemma is trivial, and can be found in [70] for 1D case, we omit here.

The expressions of contraction mapping coefficients C_1^f and C_2^f are the following

$$\begin{aligned}
C_1^f :=& \frac{(\gamma_s+\gamma_d)^2(2K_1^2 - tK_1^2 + 3K_1 + tK_1^2K_2 + 9K_1K_2)}{K_2(1-tK_1)} \sum_{k=1}^{N} \|\overline{\phi}_{k0}^f\| \\
&+ \frac{2(\gamma_s+\gamma_d)^2(K_1^2 + 2tK_1^2K_2 + 4K_1K_2)}{K_2(1-tK_1)} \sum_{k=2}^{N} \|\widehat{\phi}_{k0}^f\| + \frac{2(\gamma_s+\gamma_d)^2(2K_1 + 2tK_1^2)}{1-tK_1} \sum_{k=1}^{N} \|\widetilde{\phi}_{k0}^f\|, \\
C_2^f :=& \frac{(\gamma_s+\gamma_d)^2(2K_1^2 + 2K_1 + 12K_1K_2 - 2tK_1^2K_2)}{K_2(1-tK_1)} \sum_{k=1}^{N} \|\overline{\phi}_{k0}^f\| \\
&+ \frac{2(\gamma_s+\gamma_d)^2(K_1^2 + 6K_1K_2)}{K_2(1-tK_1)} \sum_{k=2}^{N} \|\widehat{\phi}_{k0}^f\| + \frac{8(\gamma_s+\gamma_d)^2K_1}{1-tK_1} \|\widetilde{\phi}_{k0}^f\|.
\end{aligned} \tag{2.123}$$

Chapter 3

Optimal control of cell mass and maturity in a model of follicular ovulation

In this chapter, we study optimal control problems associated with the hyperbolic conservation law modeling the development of ovarian follicles. Changes in the age and maturity of follicular cells are described by a 2D conservation law, where the control terms act on the velocities. The control problem consists in optimizing the follicular cell resources so that the follicular maturity reaches a maximal value in fixed time. Using an approximation method, we prove necessary optimality conditions in the form of PMP. Then we derive the optimal strategy and show that there exists at least one optimal bang-bang control with one single switching time. This chapter has been the matter submitted for publication (see [23]).

3.1 Introduction

In this chapter, we denote by $\rho^f_{j,k}(t,x,y)$ the cell population in a follicle f, defined on each cellular phase $Q^f_{j,k}$, where $j=1,2,3$ denotes phase 1, phase 2 and phase 3, $k=1,2,\cdots$ denotes the number of the successive cell cycles (see figure 3.1). We denote by y_s the threshold for cell cycle exit and by y_m the maximal maturity (see figure 3.1). The cell density functions satisfy the following conservation laws:

$$\frac{\partial \rho^f_{j,k}}{\partial t}+\frac{\partial (g_f(u_f)\rho^f_{j,k})}{\partial x}+\frac{\partial (h_f(y,u_f)\rho^f_{j,k})}{\partial y}=-\lambda(y,U)\rho^f_{j,k} \text{ in } Q^f_{j,k}, \tag{3.1}$$

where $Q^f_{j,k}=\Omega^f_{j,k}\times[0,T]$, with

$$\begin{aligned}
\Omega^f_{1,k}&=[(k-1)a_2,(k-1)a_2+a_1]\times[0,y_s],\\
\Omega^f_{2,k}&=[(k-1)a_2+a_1,ka_2]\times[0,y_s],\\
\Omega^f_{3,k}&=[(k-1)a_2,ka_2]\times[y_s,y_m].
\end{aligned}$$

Let us recall that

$$M_f(t) := \sum_{j=1}^{3} \sum_{k=1}^{N} \int_0^{+\infty} \int_0^{+\infty} y\, \rho_{j,k}^f(t,x,y)\, dx\, dy \tag{3.2}$$

is the maturity on the follicle scale, and

$$M(t) := \sum_f M_f(t) \tag{3.3}$$

is the maturity on the ovarian scale.

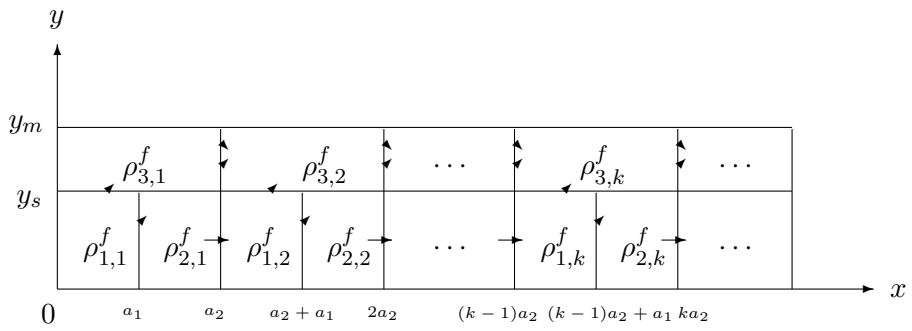


Figure 3.1. Cellular phases on the age-maturity plane for each follicle f. The domain consists of the sequence of $k = 1, 2, \cdots$ cell cycles. The variable x denotes the age of the cell and y denotes its maturity. The number y_s is the threshold value at which cell cycle exit occurs and y_m is the maximal maturity. The top of the domain corresponds to the differentiation phase and the bottom to the proliferation phase.

Two acting controls, $u_f(t, M_f)$ and $U(t, M)$ can be distinguished (see [44]). The global control $U(t, M)$ results from the ovarian feedback onto the pituitary gland and impacts the secretion of FSH. The feedback is responsible for reducing FSH release, leading to the degeneration of all but those follicles selected for ovulation. The local control $u_f(t, M_f)$ is specific to each follicle and accounts for the modulation in FSH bioavailability related to follicular vascularization.

In phase 1 and 3, both a global control U and a local control u_f act on the velocities of aging (g_f function, locally controlled in phase 1), and maturation (h_f function, locally controlled in phase 1 and 3) as well as on the loss term (λ apoptosis rate, globally controlled in phase 1 and 3). Phase 2 is uncontrolled ($g_f = \tau_{gf}$, $h_f = \lambda = 0$) and corresponds to completion of mitosis after a pure delay in age $a_2 - a_1$ (no cells leave the cycle here). The increase in the cell mass occurs through mitosis. At the time of mitosis, a mother cell gives birth to two daughter cells, which results in a local doubling of the flux. Accordingly, the boundary between different cell cycles $k = 1, 2, \cdots$ is expressed as (see figure 3.1)

$$g_f(u_f)\rho_{1,k+1}^f(t, ka_2, y) = 2\tau_{gf}\rho_{2,k}^f(t, ka_2, y), \quad (t, y) \in [0, T] \times [0, y_s].$$

One can refer to [45] for more details on the model.

The aging velocity controls the duration of the cell division cycle. Once the cell age has reached a critical age, the mitosis event is triggered and the two daughter cells enter a new cell cycle. Hence, there are local singularities in the subpart of the domain where $y \leqslant y_s$, that correspond to the flux doubling due to the successive mitosis events. The maturation velocity controls the time needed to reach a threshold maturity y_s, when the cell exits the division cycle definitively. After the exit time, the cell is no more able to contribute to the increase in the follicular cell mass.

Ovulation is triggered when the ovarian maturity reaches a threshold value M_s. The stopping time T_s is defined as

$$T_s := \min \{T \mid M(T) = M_s\}, \tag{3.4}$$

and corresponds on the biological ground to the triggering of a massive secretion of the hypothalamic gonadotropin releasing hormone (GnRH).

As a whole, system (3.1)-(3.3) combined with stopping condition (3.4) defines a multiscale reachability problem. It can be associated to an optimal control problem that consists in minimizing T_s for a given target maturity M_s.

The follicles are then sorted according to their individual maturity. The ovulatory follicles are those whose maturity at time T_s has overpassed a threshold M_{s1} such as $M_{s1} < M_s$. The ovulation rate can then be computed as

$$N_{s,s1} = Card \{f \mid M_f(T_s) \geqslant M_{s1}\}. \tag{3.5}$$

The hormonal control exerted by FSH acts directly on follicular cells to control their commitment towards either proliferation or differentiation. In turn, the hormonal feedback exerted by the ovary on the hypothalamo-pituitary axis ensues from the weighted contribution of all cells distributed amongst all follicles. Hence, a hormone-driven competition process, occurring within the population of simultaneously developing follicles, is intertwined with each cell dynamics process taking place within a given follicle.

A concept central to the understanding of these entangled processes is that of the management of follicular cell resources, both on the follicular (intensity of selection) and ovarian (triggering and chronology of ovulation) scales. There is indeed a finely tuned balance between the production of new cells through proliferation, that increases the whole cell mass, and the maturation of cells, that increases their contribution to hormone secretion.

This concept has already been investigated on a mathematical ground. In [44], the authors studied the characteristics associated with a follicle as an open-loop control problem. They described the sets of microscopic initial conditions compatible with either ovulation or atresia in the framework of backwards reachable set theory. Since these sets were largely overlapping, their results illustrate the prominent impact of cell dynamics control in the model. In [75], the author focused on the issue of the selection process in a game theory approach, where

one follicle plays against all the other ones. Whether the follicle becomes atretic (doomed) or ovulatory (saved) depends on the follicular cell mass reached at the time when all cells stop proliferating.

In this chapter, we study an optimal control problem of follicular cell resources, where the control acts directly on the velocity terms. The controllability of nonlinear hyperbolic equations (or systems) have been widely studied for a long time; for the 1D case, see, for instance [30, 33, 36, 51, 56, 67, 68, 69, 89] for smooth solutions and [2, 15, 50, 59] for BV entropic solutions. In particular, [31] provides a comprehensive survey of controllability of partial differential equations including nonlinear hyperbolic systems. As far as optimal control problems for hyperbolic systems are concerned, one can refer to [52, 53, 54, 86]. However, most of these monographs study the case where the controls are either applied inside the domain or on the boundary. Our control problem is quite different from the problems already studied in the literature, since the control terms appear in the flux. To solve the problem, we make use both of analytical methods based on PMP and numerical computations.

Although bang-bang control has been very well studied for finite dimensional control systems, there are few results available for PDE control systems (see e.g.[46]).

In section 3.2, we set the optimal control problem, together with our simplified assumptions, and we enunciate the main result. In section 3.3, we give some optimal results in the case where Dirac masses are used as a rough approximation of the density. We show that for finite Dirac masses, every measurable optimal control is a bang-bang control with one single switching time. In addition to the theoretical results, we give some numerical illustrations. In section 3.4, we go back to the original PDE formulation of the model, and we show that there exists at least one optimal bang-bang control with one single switching time.

3.2 Problem statement and introductory results

3.2.1 Optimal control problem

We consider the following conservation law on a fixed time horizon:

$$\rho_t + \rho_x + (h(y,u)\rho)_y = c(y)\rho, \quad t \in (t_0, t_1),\, x > 0,\, y > 0, \tag{3.6}$$

where $h(y,u) = a(y) + b(y)u$, with

$$a(y) := -y^2, \quad b(y) := c_1 y + c_2, \tag{3.7}$$

and

$$c(y) := \begin{cases} c_s, & \text{if } y \in [0, y_s), \\ 0, & \text{if } y \in [y_s, \infty), \end{cases} \tag{3.8}$$

with y_s, c_s, c_1 and c_2 being given strictly positive constants. We assume that

$$\frac{y_s^2}{c_1 y_s + c_2} < 1. \tag{3.9}$$

According to the biological background (see chapter 2), to make sure that $h > 0$ in phase 1, the control u is assumed to satisfy the following constraint throughout this chapter

$$u \in [w, 1], \tag{3.10}$$

where w a positive constant such that

$$w \in (\frac{y_s^2}{c_1 y_s + c_2}, 1). \tag{3.11}$$

Hence, from (3.7) and (3.11), we have

$$a(y) + b(y)u > 0, \, \forall y \in [0, y_s], \, \forall u \in [w, 1]. \tag{3.12}$$

Let us define the exit time $\hat{t}_0$ as

$$y(\hat{t}_0) = y_s, \tag{3.13}$$

where $y(t)$ is the solution to the Cauchy problem

$$\dot{y} = a(y) + b(y)w, \quad y(t_0) = 0. \tag{3.14}$$

Let us point out that, by (3.12), there exists one and only one $\hat{t}_0$ satisfying (3.13). Note that it is not guaranteed that the exit time $\hat{t}_0$ occurs before the final time t_1, so that we may have $\hat{t}_0 > t_1$. When $t > \hat{t}_0$, all the cells are in phase 3, i.e. their maturity is larger than the threshold y_s. After time $\hat{t}_0$ the mass will not increase any more due to (3.8).

We assume that there is no outer influx, i.e.

$$\rho(t, 0, y) = \rho(t, x, 0) = 0, \quad \forall t \in (t_0, t_1), \, x > 0, \, y > 0. \tag{3.15}$$

The initial condition is

$$\rho(0, x, y) = \rho_0(x, y), \, x \geqslant 0, \, y \geqslant 0, \tag{3.16}$$

where ρ_0 is a positive Borel measure on $\mathbb{R} \times \mathbb{R}$ with a compact support included in $[0, 1] \times [0, y_s]$.

For any admissible control $u \in L^\infty((t_0, t_1); [w, 1])$, we define the cost function

$$J(u) := -\int_0^{+\infty} \int_0^{+\infty} y \, d\rho(t_1, x, y), \tag{3.17}$$

and we want to study the following optimal control problem:

$$\text{minimize } J(u) \text{ for } u \in L^\infty((t_0, t_1); [w, 1]). \tag{3.18}$$

Due to the fact that c is discontinuous, we cannot apply PMP directly here. The idea is to first consider optimal control problems for Dirac masses (see section 3.3), and then to pass to the limit to get optimal control results for the PDE case (see section 3.4). For "discontinuous" optimal control problems of finite dimension, one cannot derive necessary optimality conditions by applying directly the standard apparatus of the theory of extremal problems

[16, 60, 79]. The first problem where the cost function was an integral functional with discontinuous integrand was dealt in [7]. Later, in [87], the author studied the case of a more general functional that includes both the discontinuous characteristic function and continuous terms. There, the author used approximation methods to prove necessary optimality conditions in the form of PMP. One of the difficulties of our problem is that both the integrand of the cost function and the dynamics are discontinuous.

The main result is the following theorem.

Theorem 3.2.1. *Let us assume that*

$$t_1 > \hat{t}_0, \tag{3.19}$$

$$2y_s - c_1 > 0 \quad \textit{and} \quad c_s > \frac{a(y_s) + b(y_s)}{y_s}. \tag{3.20}$$

Then, among all admissible controls $u \in L^\infty((t_0, t_1); [w, 1])$, there exists an optimal control u_* for the minimization problem (3.18) *such that*

$$\exists\, t_* \in [t_0, t_1] \textit{ such that } u_* = w \textit{ in } (t_0, t_*) \quad \textit{and} \quad u_* = 1 \textit{ in } (t_*, t_1). \tag{3.21}$$

3.2.2 Simplifications with respect to the original model

To make the initial problem tractable, we have made several simplifications on the model dynamics.

A_1. We consider only one developing follicle, i.e. $f = 1$;

A_2. There is no loss term anymore, i.e. $\lambda = 0$;

A_3. The age velocity is uncontrolled, i.e. $g_f \equiv 1$;

A_4. The cell division is represented by a new gain term, i.e. $c(y)$ defined by (3.8);

A_5. The target maturity M_s can always be reached in finite time.

Simplification (A_1) means that, in this problem, we are specially interested in the coupling between the condition needed to trigger the ovulation, on the one hand, and the control of the follicular cell dynamics, on the other hand. We consider this interaction independently of the process of follicle selection, in the sense that we isolate the dynamics of one specific follicle, as if we could ignore the influence of the other growing follicles.

(A_2) to (A_4) allow us to simplify the cell dynamics. In (A_2), we neglect the cell death, which is quite natural when considering only ovulatory trajectories, while, in (A_3), we consider that the cell age evolves as time (so that the cell duration is constant and uncontrolled). Moreover, the cell division process is distributed over ages with (A_4), so that there is a new gain term in the model instead of the former mitosis transfer condition. Even if the way that cell proliferation is represented is less realistic (no real mitosis), this does not impact the dynamics too much as long as the average cell cycle duration is preserved.

Even if it is simplified, the problem studied here still captures the essential question of the compromise between proliferation and differentiation that characterizes terminal follicular development. On the one hand, the follicle can benefit from a strong and quick enlargement of its cell population. On the other hand, this enlargement occurs at the expense of the maturation of individual cells. This compromise was instanced here as a problem of composition of velocities. We chose as control variable the nonlocal variable u_f, which is the most downstream input representing FSH on the follicular level in the original model, since it intervenes directly in the aging and maturation velocities. A relatively high aging velocity tends to favor cell mass production while a relatively high maturation velocity tends to favor an increase in the average cell maturity.

As shown in section 3.2.4, assumptions (A_2) and (A_5) allow us to replace a minimal time criterion by a criterion that consists in maximizing the final maturity. Hence, from the initial, minimal time criterion, we have shifted, for sake of technical simplicity, to an equivalent problem where the final time is fixed and the optimality criterion is the follicular maturity at final time. On the biological ground, this means that for any chosen final time t_1, the resulting maturity at final time $M_f(t_1)$ can be chosen in turn as a maturity target which would be reached in minimal time at time t_1. It can be noticed that in the initial problem (3.4), there might be no optimal solution without assumption (A_5), if the target maturity is higher than the maximal asymptotic reachable maturity.

3.2.3 Solution to Cauchy problem

In this section, we give the definition of a (weak) solution to the Cauchy problem

$$\begin{cases} \rho_t + \rho_x + ((a(y) + b(y)u)\rho)_y = c(y)\rho, \quad t \in (t_0, t_1),\ x > 0,\ y > 0, \\ \rho(t, 0, y) = \rho(t, x, 0) = 0, \quad t \in (t_0, t_1),\ x > 0,\ y > 0, \\ \rho(0, x, y) = \rho_0(x, y), \quad x > 0,\ y > 0, \end{cases} \tag{3.22}$$

where $\rho_0 : [0, 1] \times [0, y_s] \to [0, +\infty)$ is given.

Let us denote by $\bar{y}$ the asymptotic maturity, i.e. the positive root y of $a(y) + b(y)u = 0$ with control $u = 1$. From (3.7), we have

$$\bar{y} = \frac{c_1 + \sqrt{c_1^2 + 4c_2}}{2}. \tag{3.23}$$

Let $u \in L^\infty((t_0, t_1); [w, 1])$. Let us define the map

$$\begin{array}{rcl} \Psi : [t_0, t_1] \times [0, y_s] \times L^\infty((t_0, t_1); [w, 1]) & \to & [0, \bar{y}] \\ (t, y_0, u) & \mapsto & \Psi(t, y_0, u) \end{array}$$

by requiring

$$\begin{cases} \dfrac{\partial \Psi}{\partial t}(t, y_0, u) = a(\Psi(t, y_0, u)) + b(\Psi(t, y_0, u))u(t), \\ \Psi(t_0, y_0, u) = y_0. \end{cases} \tag{3.24}$$

Let ρ_0 be a Borel measure on $\mathbb{R} \times \mathbb{R}$ such that

$$\rho_0 \geqslant 0, \tag{3.25}$$

$$\text{and the support of } \rho_0 \text{ is included in } [0,1] \times [0, y_s]. \tag{3.26}$$

Let $K := [0, t_1 - t_0 + 1] \times [0, \bar{y}]$. Let $M(K)$ be the set of Borel measures on K, i.e. the set of continuous linear maps from $C^0(K)$ into $\mathbb{R}$. The solution to Cauchy problem (3.22) is the function $\rho : [t_0, t_1] \to M(K)$ such that, for every $\varphi \in C^0(K)$,

$$\iint_K \varphi(\alpha, \beta) d\rho(t, \alpha, \beta) = \iint_K \varphi(x_0 + t - t_0, \Psi(t, y_0, u))\, e^{\int_{t_0}^{t} c(\Psi(s, y_0, u))ds}\, d\rho_0(x_0, y_0). \tag{3.27}$$

We take expression (3.27) as a definition. This expression is also justified by the fact that if ρ_0 is a L^∞ function, one recovers the usual notion of weak solutions to Cauchy problem (3.22) studied in [31, 35, 85, 86], as well as by the characteristics method used to solve hyperbolic equations (see figure 3.2).

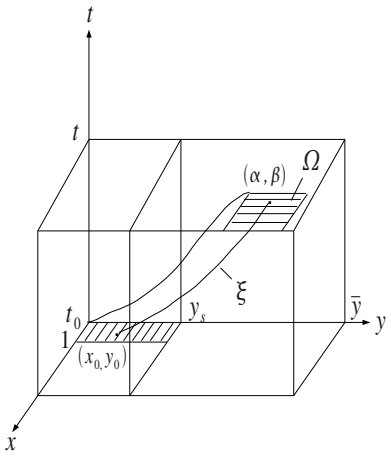


Figure 3.2. Construction of a weak solution by backward tracking of the characteristics. The variables x and y respectively denote the age and the maturity, y_s is the threshold maturity and $\bar{y}$ is the asymptotic maturity. The initial mass concentrates in the shaded area $[0,1] \times [0, y_s]$. The curve $\xi = (x, y)$ is the characteristic curve passing through (t, α, β) that intersects the initial plane $t = t_0$ at (t_0, x_0, y_0).

3.2.4 Minimal time versus maximal maturity

In this section, we show that the two optimal control problems enunciate either as: "minimize the time to achieve a given maturity" or "achieve a maximal maturity at a given time" are equivalent.

Let ρ_0 be a nonzero Borel measure on $\mathbb{R} \times \mathbb{R}$ satisfying (3.25) and (3.26). Let us denote by $M^u(t)$ the maturity at time t for the control $u \in L^\infty((t_0, t_1); [w, 1])$ (and the initial data ρ_0).

A. For fixed target time t_1, suppose that the maximum of the maturity

$$M^u(t_1) := M \tag{3.28}$$

is achieved with an optimal control $u \in L^\infty((t_0, t_1); [w, 1])$. Then we conclude that for this fixed M, the minimal time needed to reach M is t_1 with the same control u. We prove it by contradiction. We assume that there exists another control $\tilde{u} \in L^\infty((t_0, \tilde{t}_1); [w, 1])$ such that

$$M^{\tilde{u}}(\tilde{t}_1) = M, \quad \tilde{t}_1 < t_1. \tag{3.29}$$

We extend $\tilde{u}$ to $[t_0, t_1]$ by requiring $\tilde{u} = 1$ in $(\tilde{t}_1, t_1]$. Let us prove that

$$t \in [\tilde{t}_1, t_1] \to M^{\tilde{u}}(t) \text{ is strictly increasing.} \tag{3.30}$$

Let $\tilde{\rho} : [t_0, t_1] \to M(K)$ be the solution to the Cauchy problem (see section 3.2.3)

$$\begin{cases} \tilde{\rho}_t + \tilde{\rho}_x + ((a(y) + b(y)u)\tilde{\rho})_y = c(y)\tilde{\rho}, \quad t \in (t_0, t_1),\ x > 0,\ y > 0, \\ \tilde{\rho}(t, 0, y) = \tilde{\rho}(t, x, 0) = 0, \quad t \in (t_0, t_1),\ x > 0,\ y > 0, \\ \tilde{\rho}(0, x, y) = \rho_0(x, y), \quad x > 0,\ y > 0. \end{cases}$$

Note that $a(y) + b(y) > 0$ for every $y \in [0, \bar{y})$ and that, for every $t \in [t_0, t_1]$, the support of $\tilde{\rho}(t)$ is included in $[0, t_1 - t_0 + 1] \times [0, y_s)$. Together with (3.27) for $\rho = \tilde{\rho}$ and $\varphi(\alpha, \beta) = \beta$, this proves (3.30). From (3.30) it follows that

$$M^{\tilde{u}}(t_1) > M^{\tilde{u}}(\tilde{t}_1) = M, \tag{3.31}$$

which is a contradiction with the optimality of u.

B. For any fixed target maturity M, suppose that the minimal time needed to reach M is t_1 with control $u \in L^\infty((t_0, t_1); [w, 1])$. Then we conclude that for this fixed target time t_1, the maximal maturity at time t_1 is M with the same control u. We prove it again by contradiction. We assume that there exists another control $\tilde{u} \in L^\infty((t_0, t_1); [w, 1])$ such that

$$M^{\tilde{u}}(t_1) > M. \tag{3.32}$$

Then by the continuity of $M^{\tilde{u}}(t)$ with respect to time t, there exists a time $\tilde{t}_1 < t_1$ such that

$$M^{\tilde{u}}(\tilde{t}_1) = M, \tag{3.33}$$

which is a contradiction with minimal property of t_1. This concludes the proof of the equivalence between the two optimal control problems. ■

3.3 Optimal results for finite Dirac masses

In this section, we give results on the optimal control problem (3.18) when the initial data $\rho_0 \geqslant 0$ is a linear combination of a finite number of Dirac masses. For $(\alpha, \beta)^{\mathrm{tr}} \in \mathbb{R}^2$, we denote

by $\delta_{\alpha,\beta}$ the Dirac mass at $(\alpha,\beta)^{\mathrm{tr}}$. We assume that, for some positive integer N, there exist a sequence $((x_1^{k0},x_2^{k0}))_{k\in\{1,\dots,N\}}$ of elements in $[0,1]\times[0,y_s]$ and a sequence $(x_3^{k0})_{k\in\{1,\dots,N\}}$ of strictly positive real numbers such that

$$\rho_0 := \sum_{k=1}^{N} x_3^{k0}\delta_{x_1^{k0},x_2^{k0}}. \tag{3.34}$$

We consider the following Cauchy problem:

$$\begin{cases} \dot{x}^k = f(x^k,u), \quad u\in L^\infty((t_0,t_1);[w,1]), \quad t\in[t_0,t_1], \\ x^k(t_0) = x^{k0}, \end{cases} \tag{3.35}$$

where

$$f(x^k,u) = \begin{pmatrix} 1 \\ a(x_2^k)+b(x_2^k)\,u \\ c(x_2^k)\,x_3^k \end{pmatrix},\ x^k = \begin{pmatrix} x_1^k \\ x_2^k \\ x_3^k \end{pmatrix},\ x^{k0} = \begin{pmatrix} x_1^{k0} \\ x_2^{k0} \\ x_3^{k0} \end{pmatrix}. \tag{3.36}$$

It is easy to check that the maximal solution to Cauchy problem (3.35) is defined on $[t_0,t_1]$.

One can also easily check that the solution to Cauchy problem (3.22), as defined in section 3.2.3, is

$$\rho(t) = \sum_{k=1}^{N} x_3^k(t)\delta_{x_1^k(t),x_2^k(t)}. \tag{3.37}$$

The cost function J defined in (3.17) now becomes

$$J(u) = \sum_{k=1}^{N} -x_2^k(t_1)\,x_3^k(t_1). \tag{3.38}$$

One of the goals of this section is to prove that there exists an optimal control for this optimal control problem and that, if (3.19) and (3.20) hold, every optimal control is bang-bang with only one switching time. More precisely, we prove the following two theorems.

Theorem 3.3.1. *The optimal control problem* (3.18) *has a solution, i.e., there exists* $u_*\in L^\infty((t_0,t_1);[w,1])$ *such that*

$$J(u_*) = \inf_{u\in L^\infty((t_0,t_1);[w,1])} J(u).$$

Theorem 3.3.2. *Let us assume that* (3.19) *and* (3.20) *hold. Then, for every optimal control* u_* *for the optimal control problem* (3.18)*, there exists* $t_*\in(t_0,t_1)$ *such that*

$$u_* = w \text{ in } (t_0,t_*) \quad \text{and} \quad u_* = 1 \text{ in } (t_*,t_1). \tag{3.39}$$

This section is organized as follows. In subsection 3.3.1 we prove Theorem 3.3.1. In subsection 3.3.2 we prove a PMP (Theorem 3.3.3) for our optimal control problem. In subsection 3.3.3 we show how to deduce Theorem 3.3.2 from Theorem 3.3.3.

3.3.1 Proof of the existence of the optimal control

In this section, we prove Theorem 3.3.1. For sake of simplicity, we give the proof of Theorem 3.3.1 only in the case where $N = 1$. The case where $N > 1$ can be treated similarly, except that the notations are more complicated. To simplify the notations we also delete the $k = 1$ index.

Let $(u^n)_{n\in\mathbb{N}} \subset L^\infty((t_0, t_1); [w, 1])$ be a minimizing sequence of the functional J:

$$\lim_{n\to\infty} J(u^n) = \inf_{u\in L^\infty((t_0,t_1);[w,1])} J(u).$$

We have, using (3.35), (3.36) and (3.38),

$$J(u^n) = -\int_{t_0}^{t_1} \big(a(x_2^n) + b(x_2^n)u^n + c(x_2^n)x_2^n\big)x_3^n \, dt - x_2^0 x_3^0, \tag{3.40}$$

where x_2^n and x_3^n are solutions to the Cauchy problem

$$\dot{x}_2^n = a(x_2^n) + b(x_2^n)u^n, \quad x_2^n(t_0) = x_2^0, \tag{3.41}$$

$$\dot{x}_3^n = c(x_2^n)x_3^n, \quad x_3^n(t_0) = x_3^0. \tag{3.42}$$

Since $(u^n)_{n\in\mathbb{N}}$ are in $L^\infty((t_0, t_1); [w, 1])$, there exists $u_* \in L^\infty((t_0, t_1); [w, 1])$ and a subsequence $(u^{n_k})_{k\in\mathbb{N}}$ such that $u^{n_k} \overset{*}{\rightharpoonup} u_*$ in $L^\infty(t_0, t_1)$ as $k \to +\infty$. For sake of simplicity, we still denote the subsequence by $(u^n)_{n\in\mathbb{N}}$.

Let x_2 and x_3 be the solutions to the Cauchy problem

$$\dot{x}_2 = a(x_2) + b(x_2)u_*, \quad x_2(t_0) = x_2^0, \tag{3.43}$$

$$\dot{x}_3 = c(x_2)x_3, \quad x_3(t_0) = x_3^0. \tag{3.44}$$

Similarly to (3.40), one has

$$J(u_*) = -\int_{t_0}^{t_1} \big(a(x_2) + b(x_2)u_* + c(x_2)x_2\big)x_3 \, dt - x_2^0 x_3^0. \tag{3.45}$$

By (3.7), (3.41) and using the property $w \leqslant u^n \leqslant 1$, there exists a constant C such that

$$\|x_2^n\|_{W^{1,\infty}} \leqslant C, \quad \forall n \in \mathbb{N}. \tag{3.46}$$

In (3.46) and until the end of the proof of Theorem 3.3.1, we denote by C different positive constants which are independent of n. It follows from the Arzelà-Ascoli theorem and (3.46) that there exists $\tilde{x}_2 \in C^0([t_0, t_1])$ and a subsequence $(x_2^{n_l})_{l\in\mathbb{N}}$ such that $x_2^{n_l} \to \tilde{x}_2$ in $C^0([t_0, t_1])$ as $l \to +\infty$. Now, we choose the corresponding subsequence $(u^{n_l})_{l\in\mathbb{N}}$ and again, we write $(u^n)_{n\in\mathbb{N}}$ instead of $(u^{n_l})_{l\in\mathbb{N}}$ and $(x_2^n)_{n\in\mathbb{N}}$ instead of $(x_2^{n_l})_{l\in\mathbb{N}}$. We have

$$u^n \overset{*}{\rightharpoonup} u_* \quad \text{in} \quad L^\infty(t_0, t_1) \quad \text{as} \quad n \to +\infty, \tag{3.47}$$

$$x_2^n \to \tilde{x}_2 \quad \text{in} \quad C^0([t_0, t_1]) \quad \text{as} \quad n \to +\infty. \tag{3.48}$$

By solving (3.41), we have

$$x_2^n(t) = x_2^0 + \int_{t_0}^{t} \big(a(x_2^n) + b(x_2^n)u^n\big)ds, \ \forall t \in [t_0, t_1]. \tag{3.49}$$

Using (3.47) and (3.48) and letting $n \to +\infty$ in (3.49), we obtain

$$\tilde{x}_2(t) = x_2^0 + \int_{t_0}^{t} \big(a(\tilde{x}_2) + b(\tilde{x}_2)u_*\big)ds, \ \forall t \in [t_0, t_1],$$

which together with (3.43) shows that

$$\tilde{x}_2(t) = x_2(t), \quad \forall t \in [t_0, t_1]. \tag{3.50}$$

From (3.48) and (3.50), we have

$$x_2^n \to x_2 \quad \text{in} \quad C^0([t_0, t_1]) \text{ as } n \to +\infty. \tag{3.51}$$

Let us only treat the case where

$$x_2(t_1) > y_s, \tag{3.52}$$

(the case $x_2(t_1) = y_s$ can be treated similarly and the case $x_2(t_1) < y_s$ is simpler). By (3.52), there exists $\hat{t} \in [t_0, t_1)$ such that

$$x_2(\hat{t}\,) = y_s. \tag{3.53}$$

Moreover, by (3.12), this $\hat{t}$ is unique. From (3.51) and (3.52), we have, for n large enough, which will be from now on always assumed,

$$x_2^n(t_1) > y_s. \tag{3.54}$$

Hence, as for x_2, there exists one and only one $\hat{t}_n \in [t_0, t_1)$ such that

$$x_2^n(\hat{t}_n) = y_s. \tag{3.55}$$

Let us prove that

$$\hat{t}_n \to \hat{t} \text{ as } n \to +\infty. \tag{3.56}$$

In order to prove (3.56), we may assume, without loss of generality, the existence of $\tilde{t} \in [t_0, t_1]$ such that

$$\hat{t}_n \to \tilde{t} \text{ as } n \to +\infty. \tag{3.57}$$

Letting $n \to +\infty$ in (3.51), and using (3.55) together with (3.57), we get that

$$x_2(\tilde{t}\,) = y_s. \tag{3.58}$$

Since $\hat{t}$ is characterized by (3.53), (3.56) follows from (3.57) and (3.58).

From (3.8), (3.42) and (3.44), we have

$$x_3^n(t) = x_3^0\, e^{c_s(t-t_0)},\ \forall t \in [t_0, \hat{t}_n] \text{ and } x_3^n(t) = x_3^0\, e^{c_s(\hat{t}_n - t_0)},\ \forall t \in [\hat{t}_n, t_1], \tag{3.59}$$

$$x_3(t) = x_3^0\, e^{c_s(t-t_0)},\ \forall t \in [t_0, \hat{t}\,] \text{ and } x_3(t) = x_3^0\, e^{c_s(\hat{t}-t_0)},\ \forall t \in [\hat{t}, t_1]. \tag{3.60}$$

From (3.56), (3.59) and (3.60), we get that

$$x_3^n \to x_3 \quad \text{in} \quad C^0([t_0, t_1]) \text{ as } n \to +\infty. \tag{3.61}$$

Finally, combining (3.40), (3.45), (3.47), (3.51) and (3.61), we get

$$\lim_{n \to +\infty} J(u^n) = J(u_*),$$

which shows that u_* is an optimal control. This concludes the proof of Theorem 3.3.1. ∎

3.3.2 Pontryagin Maximum Principle

In this section we prove a PMP for our optimal control problem. For sake of simplicity, we denote, from now on,

$$p(x,u) := -(a(x_2) + b(x_2)\, u)\, x_3, \quad q(x) := -c_s\, x_2\, x_3,\ \forall x = (x_1, x_2, x_3)^{\mathrm{tr}} \in \mathbb{R}^3. \tag{3.62}$$

Let us denote by $\chi : \mathbb{R} \to \mathbb{R}$ the characteristic function of $(-\infty, y_s)$, i.e.

$$\chi(x_2) = \begin{cases} 1, & \forall x_2 \in (-\infty, y_s), \\ 0, & \forall x_2 \in [y_s, +\infty). \end{cases} \tag{3.63}$$

Hence, the cost function J for our optimal control problem problem (3.18) is

$$J(u) = \int_{t_0}^{t_1} \big(p(x,u) + q(x)\, \chi(x_2)\big)\, dt - x_2^0 x_3^0. \tag{3.64}$$

Let us define the Hamiltonian

$$\begin{array}{rcl} \mathcal{H} : (\mathbb{R}^3)^N \times \mathbb{R} \times (\mathbb{R}^3)^N & \to & \mathbb{R} \\ (x, u, \psi) = ((x^1, x^2, \dots, x^N), u, (\psi^1, \psi^2, \dots, \psi^N)) & \mapsto & \mathcal{H}(x, u, \psi) \end{array}$$

by

$$\mathcal{H}(x,u,\psi) := \sum_{k=1}^{N} \langle f(x^k, u), \psi^k \rangle - \sum_{k=1}^{N} \big(p(x^k, u) + q(x^k)\chi(x_2^k)\big). \tag{3.65}$$

In (3.65) and in the following $\langle a, b \rangle$ denotes the usual scalar product of $a \in \mathbb{R}^3$ and $b \in \mathbb{R}^3$. Let us also define the Hamilton-Pontryagin function $H : (\mathbb{R}^3)^N \times (\mathbb{R}^3)^N \to \mathbb{R}$ by

$$H(x, \psi) := \max_{u \in [w,1]} \mathcal{H}(x, u, \psi). \tag{3.66}$$

Our goal in this section is to prove the following theorem.

Theorem 3.3.3. *Let $u_* \in L^\infty((t_0,t_1);[w,1])$ be an optimal control for the optimal control problem (3.18). Let $x_*^k = (x_{*1}^k, x_{*2}^k, x_{*3}^k)^{tr}$, $k = 1, \cdots, N$, be the corresponding optimal trajectory, i.e. $x_{*1}^k \in W^{1,\infty}(t_0,t_1)$, $x_{*2}^k \in W^{1,\infty}(t_0,t_1)$, $x_{*3}^k \in W^{1,\infty}(t_0,t_1)$ are solutions to the following Cauchy problems*

$$\dot{x}_{*1}^k = 1, \qquad x_{*1}^k(t_0) = x_1^{k0}, \tag{3.67}$$

$$\dot{x}_{*2}^k = a(x_{*2}^k) + b(x_{*2}^k)\, u_*, \quad x_{*2}^k(t_0) = x_2^{k0}, \tag{3.68}$$

$$\dot{x}_{*3}^k = c(x_{*2}^k)\, x_{*3}^k, \quad x_{*3}^k(t_0) = x_3^{k0}. \tag{3.69}$$

If $y_s \in \big\{x_{*2}^k(t);\, t \in [t_0,t_1]\big\}$, let $\hat{t}_k \in [t_0,t_1]$ be the exit time for the k-th Dirac mass, i.e. the unique time $\hat{t}_k \in [t_0,t_1]$ such that $x_{*2}^k(\hat{t}_k) = y_s$. If $y_s \notin \big\{x_{*2}^k(t);\, t \in (t_0,t_1]\big\}$, let $\hat{t}_k = t_1 + 1$. Then, there exists N vector functions $\psi^k = (\psi_1^k, \psi_2^k, \psi_3^k)^{tr}$, such that $\psi_1^k \in W^{1,\infty}(t_0,t_1)$, $\psi_2^k \in W^{1,\infty}(((t_0,\hat{t}_k) \cup (\hat{t}_k,t_1)) \cap (t_0,t_1))$ and $\psi_3^k \in W^{1,\infty}(t_0,t_1)$ such that

$$\dot{\psi}_1^k = 0, \tag{3.70}$$

$$\begin{aligned}\dot{\psi}_2^k = &-(a'(x_{*2}^k) + b'(x_{*2}^k)u_*)\psi_2^k - (a'(x_{*2}^k) + b'(x_{*2}^k)u_*)x_{*3}^k \\ &- c_s x_{*3}^k \chi(x_{*2}^k) \quad \text{in} \quad ((t_0,\hat{t}_k) \cup (\hat{t}_k,t_1)) \cap (t_0,t_1),\end{aligned} \tag{3.71}$$

$$\dot{\psi}_3^k = -c_s \chi(x_{*2}^k)\, \psi_3^k - (a(x_{*2}^k) + b(x_{*2}^k)u_*) - c_s x_{*2}^k\, \chi(x_{*2}^k), \tag{3.72}$$

$$\psi_1^k(t_1) = \psi_3^k(t_1) = 0, \tag{3.73}$$

and

- *if $\hat{t}_k < t_1$,*

$$\psi_2^k(\hat{t}_k + 0) - \psi_2^k(\hat{t}_k - 0) \in \Big[\frac{c_s\, x_{*3}^k(\hat{t}_k)(y_s + \psi_3^k(\hat{t}_k))}{a(y_s) + b(y_s)}, \frac{c_s\, x_{*3}^k(\hat{t}_k)(y_s + \psi_3^k(\hat{t}_k))}{a(y_s) + b(y_s)\, w}\Big], \tag{3.74}$$

$$\psi_2^k(t_1) = 0, \tag{3.75}$$

- *if $\hat{t}_k = t_1$,*

$$-\psi_2^k(t_1) \in \Big[0, \frac{c_s\, x_{*3}^k(t_1) y_s}{a(y_s) + b(y_s)\, w}\Big]. \tag{3.76}$$

Moreover the following condition holds

$$\mathcal{H}(x_*^k(t), u_*(t), \psi^k(t)) = H(x_*^k(t), \psi^k(t)) \text{ for almost every } t \in (t_0,t_1). \tag{3.77}$$

Proof of Theorem 3.3.3. For sake of simplicity, we give the proof only for one Dirac mass ($N = 1$) and, again, we omit the index $k = 1$. For more than one Dirac mass, the proof is similar. Our proof is inspired from [87].

Step 1. Let $(w_i)_{i\in\mathbb{N}^*}$ be a sequence of elements in $C^\infty(\mathbb{R})$ such that

$$0 \leqslant w_i, \quad \int_{\mathbb{R}} w_i(x)\, dx = 1, \quad \text{support}\, w_i \subset [-1/i, 0], \quad \forall i \in \mathbb{N}^*, \tag{3.78}$$

and, for some $C > 0$,

$$|w_i'(x)| \leqslant Ci^2, \quad \forall x \in \mathbb{R}, \quad \forall i \in \mathbb{N}^*, \tag{3.79}$$

(clearly such a sequence does exist). Then, we define a sequence of functions $(\chi_i)_{i\in\mathbb{N}^*}$ from $\mathbb{R}$ into $\mathbb{R}$ as follows:

$$\chi_i(x) := \int_{\mathbb{R}} \chi(y)\, w_i(x-y)\, dy = \int_{-\infty}^{y_s} w_i(x-y)\, dy = \int_{x-y_s}^{+\infty} w_i(z)\, dz, \ \forall i \in \mathbb{N}^*, \ \forall x \in \mathbb{R}. \tag{3.80}$$

One easily sees that the functions χ_i thus defined possess the following properties (compare to [87, Lemma 1 and Lemma 2]):

$$0 \leqslant \chi_i(x_2) \leqslant \chi(x_2), \quad \forall i \in \mathbb{N}^*, \quad \forall x_2 \in \mathbb{R}, \tag{3.81}$$

$$\chi_i(x_2) \to \chi(x_2) \text{ as } i \to \infty, \quad \forall x_2 \in \mathbb{R}, \tag{3.82}$$

$$0 \leqslant \chi_i(x_2) \leqslant 1, \quad \forall i \in \mathbb{N}^*, \quad \forall x_2 \in \mathbb{R}, \tag{3.83}$$

$$\chi_i = 1 \text{ in } (-\infty, y_s - (1/i)] \text{ and } \chi_i = 0 \text{ in } [y_s, +\infty), \quad \forall i \in \mathbb{N}^*. \tag{3.84}$$

Let u_* be an optimal control for the optimal control problem (3.18) and let x_* be the associated trajectory. Let $(z_i)_{i\in\mathbb{N}^*}$ be a sequence of elements of $C^1([t_0, t_1])$ such that the following conditions hold:

$$z_i \to u_* \text{ in } L^2(t_0, t_1) \text{ as } i \to +\infty, \tag{3.85}$$

$$\sup_{t_0 \leqslant t \leqslant t_1} |z_i(t)| \leqslant 2, \ i = 1, 2, \cdots. \tag{3.86}$$

It is again obvious that such a sequence of functions $(z_i)_{i\in\mathbb{N}^*}$ does exist.

Let us first prove the following lemma which will be used later.

Lemma 3.3.1. *There exists $C > 0$ such that, for every $u \in L^\infty((t_0, t_1); [w, 1])$ and every $x_2^0 \in [0, y_s]$, the following holds*

$$\int_{t_0}^{t_1} (\chi(x_2(t)) - \chi_i(x_2(t)))\, dt \leqslant \frac{C}{i}, \quad \forall i \in \mathbb{N}^*, \tag{3.87}$$

where x_2 is the solution to the following Cauchy problem:

$$\dot{x}_2 = a(x_2) + b(x_2)\, u, \quad x_2(t_0) = x_2^0.$$

Proof of Lemma 3.3.1. The case where $x_2(t_1) < y_s$ is trivial, we treat the case where $x_2(t_1) > y_s$. Then, there exists one and only one $\hat{t} \in [t_0, t_1)$ and one and only one $\bar{t}_i \in [t_0, t_1)$ depending on i such that

$$x_2(\hat{t}\,) = y_s, \quad x_2(\bar{t}_i) = \max(\, y_s - (1/i),\, x_2^0\,). \tag{3.88}$$

Using (3.81) to (3.84), we obtain

$$\int_{t_0}^{t_1} (\chi(x_2(t)) - \chi_i(x_2(t)))\, dt = \int_{\bar{t}_i}^{\hat{t}} (\chi(x_2(t)) - \chi_i(x_2(t)))\, dt \leqslant \hat{t} - \bar{t}_i. \tag{3.89}$$

By (3.88), we have

$$y_s = x_2^0 + \int_{t_0}^{\hat{t}} \big(a(x_2) + b(x_2)u\big)\, dt,$$
$$\max\big(\, y_s - (1/i),\, x_2^0\,\big) = x_2^0 + \int_{t_0}^{\bar{t}_i} \big(a(x_2) + b(x_2)u\big)\, dt,$$

which together give

$$\int_{\bar{t}_i}^{\hat{t}} \big(a(x_2) + b(x_2)u\big)\, dt \leqslant \frac{1}{i}. \tag{3.90}$$

By (3.12), there exists $\sigma > 0$ such that

$$a(x_2) + b(x_2)\, u \geqslant \sigma, \quad \forall x_2 \in [0, y_s],\, \forall u \in [w, 1]. \tag{3.91}$$

From (3.90), by choosing $C = \dfrac{1}{\sigma}$, we get

$$0 < \hat{t} - \bar{t}_i \leqslant \frac{C}{i}, \tag{3.92}$$

which, together with (3.89) concludes the proof of Lemma 3.3.1. ■

Let $f_i : \mathbb{R}^3 \times \mathbb{R} \to \mathbb{R}^3$ be defined by

$$f_i(x, u) := \begin{pmatrix} 1 \\ a(x_2) + b(x_2)\, u \\ c_s \chi_i(x_2)\, x_3 \end{pmatrix}, \quad \forall x = (x_1, x_2, x_3)^{\mathrm{tr}} \in \mathbb{R}^3, \quad \forall u \in \mathbb{R}. \tag{3.93}$$

Let us also define $J_i : L^\infty((t_0, t_1); [w, 1]) \to \mathbb{R}$ by

$$J_i(u) := \int_{t_0}^{t_1} \big(p(x, u) + q(x)\, \chi_i(x_2)\big)\, dt + \frac{1}{\sqrt{i}} \int_{t_0}^{t_1} |u(t) - z_i(t)|^2\, dt - x_2^0 x_3^0, \tag{3.94}$$

where $x : [t_0, t_1] \to \mathbb{R}^3$ is the solution to the Cauchy problem

$$\dot{x} = f_i(x, u),\, x(t_0) = x^0. \tag{3.95}$$

We consider the following optimal control problem

$$\text{minimize } J_i(u) \text{ for } u \in L^\infty((t_0, t_1); [w, 1]). \tag{$\mathcal{P}_i$}$$

For any $i = 1, 2, \cdots$, problem $(\mathcal{P}_i)$ is a "smooth" optimal control problem. By a classical result in optimal control theory (see, e.g., [63, Corollary 2, p. 262]), there exists an optimal control u_i for problem $(\mathcal{P}_i)$. Let x_i be the optimal trajectory corresponding to the control u_i for dynamics (3.95). We have the following lemma.

Lemma 3.3.2. *The following holds as $i \to +\infty$*

$$u_i \to u_* \text{ in } L^2(t_0, t_1), \tag{3.96}$$
$$x_i \to x_* \text{ in } C^0([t_0, t_1]; \mathbb{R}^3), \tag{3.97}$$
$$\chi_i(x_{i2}) \to \chi(x_{*2}) \text{ in } L^1(t_0, t_1). \tag{3.98}$$

Proof of Lemma 3.3.2. Since u_i is an optimal control for the optimal control problem $(\mathcal{P}_i)$ and $u_* \in L^\infty((t_0,t_1);[w,1])$ is an admissible control for this problem, we have

$$J_i(u_i) \leqslant J_i(u_*), \quad \forall i \in \mathbb{N}^*.$$

By (3.94),

$$\begin{aligned}
&\int_{t_0}^{t_1} \big(p(x_i(t),u_i(t)) + q(x_i(t))\,\chi_i(x_{i2}(t))\big)\,dt + \frac{1}{\sqrt{i}}\int_{t_0}^{t_1} |u_i(t)-z_i(t)|^2\,dt \\
&\leqslant \int_{t_0}^{t_1} \big(p(\bar{x}_*(t),u_*(t)) + q(\bar{x}_*(t))\,\chi_i(\bar{x}_{*2}(t))\big)\,dt + \frac{1}{\sqrt{i}}\int_{t_0}^{t_1} |u_*(t)-z_i(t)|^2\,dt,
\end{aligned} \tag{3.99}$$

where $x_i = (x_{i1},x_{i2},x_{i3})^{\mathrm{tr}}$ and $\bar{x}_* = (\bar{x}_{*1},\bar{x}_{*2},\bar{x}_{*3})^{\mathrm{tr}}$ are solutions to the Cauchy problems

$$\dot{x}_i = f_i(x_i,u_i), \quad x_i(t_0) = x^0, \tag{3.100}$$

$$\dot{\bar{x}}_* = f_i(\bar{x}_*,u_*), \quad \bar{x}_*(t_0) = x^0. \tag{3.101}$$

Since u_* is an optimal control for the optimal control problem (3.18) and u_i is an admissible control for this problem, we have, for every $i \in \mathbb{N}^*$,

$$\int_{t_0}^{t_1} \big(p(x_*(t),u_*(t)) + q(x_*(t))\,\chi(x_{*2}(t))\big)\,dt \leqslant \int_{t_0}^{t_1} \big(p(\tilde{x}_i(t),u_i(t)) + q(\tilde{x}_i(t))\,\chi(\tilde{x}_{i2}(t))\big)\,dt, \tag{3.102}$$

where $x_* = (x_{*1},x_{*2},x_{*3})^{\mathrm{tr}}$ and $\tilde{x}_i = (\tilde{x}_{i1},\tilde{x}_{i2},\tilde{x}_{i3})^{\mathrm{tr}}$ are solutions to the Cauchy problems

$$\dot{x}_* = f(x_*,u_*), \quad x_*(t_0) = x^0, \tag{3.103}$$

$$\dot{\tilde{x}}_i = f(\tilde{x}_i,u_i), \quad \tilde{x}_i(t_0) = x^0. \tag{3.104}$$

By (3.81) and note that $q \leqslant 0$, the inequality

$$\int_{t_0}^{t_1} q(\tilde{x}_i(t))\,\chi(\tilde{x}_{i2}(t))\,dt \leqslant \int_{t_0}^{t_1} q(\tilde{x}_i(t))\,\chi_i(\tilde{x}_{i2}(t))\,dt \tag{3.105}$$

holds for every $i \in \mathbb{N}^*$. Combining (3.102) and (3.105), we obtain

$$\begin{aligned}
&\int_{t_0}^{t_1} \big(p(x_*(t),u_*(t)) + q(x_*(t))\,\chi(x_{*2}(t))\big)\,dt \leqslant \\
&\qquad\qquad \int_{t_0}^{t_1} \big(p(\tilde{x}_i(t),u_i(t)) + q(\tilde{x}_i(t))\,\chi_i(\tilde{x}_{i2}(t))\big)\,dt.
\end{aligned} \tag{3.106}$$

By (3.99) and (3.106), we have

$$\begin{aligned}
&\frac{1}{\sqrt{i}}\int_{t_0}^{t_1} |u_i(t)-z_i(t)|^2\,dt \\
&\leqslant \int_{t_0}^{t_1} \big(p(\bar{x}_*(t),u_*(t)) + q(\bar{x}_*(t))\,\chi_i(\bar{x}_{*2}(t))\big)\,dt - \int_{t_0}^{t_1} \big(p(x_*(t),u_*(t)) + q(x_*(t))\,\chi(x_{*2}(t))\big)\,dt \\
&+ \int_{t_0}^{t_1} \big(p(\tilde{x}_i(t),u_i(t)) + q(\tilde{x}_i(t))\,\chi_i(\tilde{x}_{i2}(t))\big)\,dt - \int_{t_0}^{t_1} \big(p(x_i(t),u_i(t)) + q(x_i(t))\,\chi_i(x_{i2}(t))\big)\,dt \\
&\qquad + \frac{1}{\sqrt{i}}\int_{t_0}^{t_1} |u_*(t)-z_i(t)|^2\,dt.
\end{aligned} \tag{3.107}$$

By definition of f and f_i in (3.36) and (3.93), we have

$$\tilde{x}_{i2}(t) = x_{i2}(t) \quad \text{and} \quad \bar{x}_{*2}(t) = x_{*2}(t), \quad \forall t \in [t_0, t_1]. \tag{3.108}$$

Using (3.62), (3.84), (3.107) and (3.108), one has

$$\begin{aligned}\frac{1}{\sqrt{i}} \int_{t_0}^{t_1} |u_i(t) - z_i(t)|^2 \, dt \leqslant C & \int_{t_0}^{t_1} |\bar{x}_{*3}(t) - x_{*3}(t)| \, dt + C \int_{t_0}^{t_1} |\tilde{x}_{i3}(t) - x_{i3}(t)| \, dt \\ & + C \int_{t_0}^{t_1} \big(\chi(x_{*2}(t)) - \chi_i(x_{*2}(t))\big) \, dt \\ & + \frac{1}{\sqrt{i}} \int_{t_0}^{t_1} |u_*(t) - z_i(t)|^2 \, dt. \end{aligned} \tag{3.109}$$

In (3.109) and until the end of the proof of Theorem 3.3.3, we denote by C different positive constants which are independent of i. From (3.81), (3.101), (3.103) and (3.108), we have

$$\begin{aligned}\int_{t_0}^{t_1} |\bar{x}_{*3}(t) - x_{*3}(t)| \, dt &= \int_{t_0}^{t_1} |x_3^0 \, e^{\int_{t_0}^t c_s \chi_i(x_{*2}(s)) \, ds} - x_3^0 \, e^{\int_{t_0}^t c_s \chi(x_{*2}(s)) \, ds}| \, dt \\ &\leqslant C \int_{t_0}^{t_1} \int_{t_0}^{t} \big(\chi(x_{*2}(s)) - \chi_i(x_{*2}(s))\big) \, ds \, dt. \end{aligned} \tag{3.110}$$

Applying Lemma 3.3.1 to (3.110), we get

$$\int_{t_0}^{t_1} |\bar{x}_{*3}(t) - x_{*3}(t)| \, dt \leqslant \frac{C}{i}. \tag{3.111}$$

Similarly, we can prove

$$\int_{t_0}^{t_1} |\tilde{x}_{i3}(t) - x_{i3}(t)| \, dt \leqslant \frac{C}{i}. \tag{3.112}$$

Combining (3.109), (3.111) and (3.112), and noticing (3.85), we get

$$\int_{t_0}^{t_1} |u_i(t) - z_i(t)|^2 \, dt \to 0 \quad \text{as} \quad i \to +\infty. \tag{3.113}$$

From (3.85) and (3.113), we get that

$$\|u_i - u_*\|_{L^2(t_0,t_1)} \to 0 \quad \text{as} \quad i \to +\infty. \tag{3.114}$$

Thus, property (3.96) is proved.

Let us now prove (3.97). Using in particular (3.96), one easily sees that

$$x_{i1}(t) = x_{*1}(t), \quad \forall i \in \mathbb{N}^*, \quad \forall t \in [t_0, t_1], \tag{3.115}$$

$$x_{i2} \to x_{*2} \quad \text{in} \quad \mathrm{C}^0([t_0, t_1]) \quad \text{as} \quad i \to +\infty. \tag{3.116}$$

Moreover, the same proof as that of (3.61) shows that

$$x_{i3} \to x_{*3} \quad \text{in} \quad \mathrm{C}^0([t_0, t_1]) \quad \text{as} \quad i \to +\infty.$$

Finally, let us prove (3.98). From (3.84) and (3.116),

$$(x_{*2}(t) \neq y_s) \Rightarrow \left(\lim_{i \to +\infty} \chi_i(x_{i2}(t)) = \chi(x_{*2}(t)) \right), \quad \forall t \in [t_0, t_1]. \tag{3.117}$$

But, as we have already seen in section 3.3.1, there exists at most one $\hat{t} \in [t_0, t_1]$ such that $x_{*2}(\hat{t}) = y_s$. Property (3.98) follows from (3.81), (3.117) and Lebesgue's dominated convergence theorem. This concludes the proof of Lemma 3.3.2. ∎

Step 2. We now deduce necessary optimality conditions for the optimal control problem (3.18) in the form of PMP. Suppose that x_i and u_i is an optimal pair for problem $(\mathcal{P}_i)$. The Hamiltonian and the Hamilton-Pontryagin function for problem $(\mathcal{P}_i)$ are respectively

$$\mathcal{H}_i(t,x,u,\psi) = \langle f_i(x,u),\psi\rangle - (p(x,u)+q(x)\chi_i(x_2)) - \frac{1}{\sqrt{i}}|u-z_i(t)|^2, \tag{3.118}$$

$$H_i(t,x,\psi) = \max_{u\in[w,1]} \mathcal{H}_i(t,x,u,\psi). \tag{3.119}$$

By the PMP -see, e.g., [63, Theorem 2, p. 319] or [16, Section 6.5]-, there exists an absolutely continuous function $\psi_i : [t_0,t_1] \to \mathbb{R}^3$ such that

$$\dot{\psi}_i \overset{a.e.}{=} -\Big[\frac{\partial f_i}{\partial x}(x_i(t),u_i(t))\Big]^{\mathrm{tr}} \psi_i + \frac{\partial}{\partial x}\left(p(x_i,u)+q(x_i)\chi_i(x_{i2})\right), \tag{3.120}$$

$$\psi_i(t_1) = 0, \tag{3.121}$$

and

$$\mathcal{H}_i(t,x_i(t),u_i(t),\psi_i(t)) = H_i(t,x_i(t),\psi_i(t)) \text{ for almost every } t\in(t_0,t_1). \tag{3.122}$$

Let us denote $\psi_i = (\psi_{i1},\psi_{i2},\psi_{i3})^{\mathrm{tr}}$. From (3.62), (3.93), (3.120) and (3.121), we have

$$\dot{\psi}_{i1} = 0, \tag{3.123}$$

$$\dot{\psi}_{i2} = -(a'(x_{i2})+b'(x_{i2})\,u_i)\,\psi_{i2} - c_s\,\chi_i'(x_{i2})\,x_{i3}\,\psi_{i3} - (a'(x_{i2})+b'(x_{i2})\,u_i)\,x_{i3} - c_s\,\chi_i(x_{i2})\,x_{i3} - c_s\,x_{i2}\chi_i'(x_{i2})\,x_{i3}, \tag{3.124}$$

$$\dot{\psi}_{i3} = -c_s\,\chi_i(x_{i2})\,\psi_{i3} - (a(x_{i2})+b(x_{i2})u_i) - c_s\,x_{i2}\,\chi_i(x_{i2}), \tag{3.125}$$

$$\psi_{i1}(t_1) = \psi_{i2}(t_1) = \psi_{i3}(t_1) = 0. \tag{3.126}$$

Let $\psi_1 : [t_0,t_1] \to \mathbb{R}$ be defined by

$$\psi_1(t) = 0, \quad \forall t\in[t_0,t_1]. \tag{3.127}$$

From (3.123), (3.126) and (3.127), one has

$$\psi_{i1}(t) = \psi_1(t), \quad \forall t\in[t_0,t_1]. \tag{3.128}$$

Let $\psi_3 \in W^{1,\infty}(t_0,t_1)$ be the solution to the following Cauchy problem:

$$\dot{\psi}_3 = -c_s\chi(x_{*2})\,\psi_3 - (a(x_{*2})+b(x_{*2})u_*) - c_s x_{*2}\,\chi(x_{*2}), \quad \psi_3(t_1) = 0. \tag{3.129}$$

From (3.96), (3.97), (3.98), (3.125), (3.126) and (3.129), one easily gets that

$$\psi_{i3} \to \psi_3 \text{ in } C^0([t_0,t_1]) \text{ as } i\to+\infty. \tag{3.130}$$

We now deal with ψ_{i2}. By (3.78) and (3.80), we have

$$\text{support } \chi_i' \subset [y_s-(1/i),y_s]. \tag{3.131}$$

Moreover, from (3.78), (3.79) and (3.80), we obtain

$$|\chi_i'(x_2)| \leqslant Ci, \quad \forall x_2 \in [y_s - (1/i), y_s], \tag{3.132}$$

Theorem 3.3.3 in the case where $x_{*2}(t_0) = x_2^0 = y_s$ or $x_{*2}(t_1) < y_s$ follows directly from the standard PMP. Hence, we may assume that

$$x_{*2}(t_0) < y_s \leqslant x_{*2}(t_1). \tag{3.133}$$

Let us first treat the case where

$$x_{*2}(t_0) < y_s < x_{*2}(t_1). \tag{3.134}$$

Then, again, there exists one and only one $\hat{t} \in (t_0, t_1)$ such that

$$x_{*2}(\hat{t}\,) = y_s. \tag{3.135}$$

Using (3.97) and (3.135), one also gets that, at least if i is large enough, which, from now on, will always be assumed, there exists one and only one $\hat{t}_i \in (t_0, t_1)$ and one and only one $\bar{t}_i \in (t_0, t_1)$ such that

$$x_{i2}(\hat{t}_i) = y_s, \quad x_{i2}(\bar{t}_i) = y_s - (1/i). \tag{3.136}$$

Using (3.96) and (3.97), and proceeding as in the proof of (3.56), one has

$$\hat{t}_i \to \hat{t} \text{ and } \bar{t}_i \to \hat{t} \text{ as } i \to +\infty. \tag{3.137}$$

From (3.132) and (3.136), we get

$$|\chi_i'(x_{i2}(t))| \leqslant Ci, \quad \forall t \in [\bar{t}_i, \hat{t}_i]. \tag{3.138}$$

From (3.131) and (3.136), we have

$$\chi_i'(x_{i2}(t)) = 0, \quad t \in [t_0, t_1] \setminus [\bar{t}_i, \hat{t}_i]. \tag{3.139}$$

Proceeding as in the proof of Lemma 3.3.1, one has

$$0 < \hat{t}_i - \bar{t}_i \leqslant \frac{C}{i}. \tag{3.140}$$

From (3.97), (3.124), (3.126), (3.130), (3.138), (3.139) and (3.140), we get

$$\|\dot{\psi}_{i2}\|_{L^\infty((t_0,\bar{t}_i)\cup(\hat{t}_i,t_1))} \leqslant C, \tag{3.141}$$

$$\|\psi_{i2}\|_{L^\infty(t_0,t_1)} \leqslant C. \tag{3.142}$$

From (3.141) and (3.142), and extracting if necessary a subsequence, we get the existence of $\psi_2 \in W^{1,\infty}((t_0, \hat{t}\,) \cup (\hat{t}, t_1))$, such that, as $i \to +\infty$,

$$\psi_{i2} \to \psi_2 \quad \text{in} \quad C^0([t_0, \hat{t} - \varepsilon] \cup [\hat{t} + \varepsilon, t_1]), \quad \forall \varepsilon > 0. \tag{3.143}$$

Letting $i \to +\infty$ in (3.124), one gets, using (3.96), (3.97), (3.131), (3.139) and (3.143),

$$\dot{\psi}_2 = -\big(a'(x_{*2}) + b'(x_{*2})u_*\big)\psi_2 - (a'(x_{*2}) + b'(x_{*2})u_*)x_{*3} \\ - c_s x_{*3}\chi(x_{*2}) \quad \text{in} \quad (t_0, t_1) \setminus \{\hat{t}\}. \tag{3.144}$$

Moreover, from (3.126) and (3.143), we have

$$\psi_2(t_1) = 0. \tag{3.145}$$

We now prove the gap condition (3.74). Let us integrate (3.124) from $\bar{t}_i$ to $\hat{t}_i$, we get

$$\psi_{i2}(\hat{t}_i) - \psi_{i2}(\bar{t}_i) = A(i) + B(i), \tag{3.146}$$

with

$$A(i) := -\int_{\bar{t}_i}^{\hat{t}_i} ((a'(x_{i2}) + b'(x_{i2})\, u_i)\, (\psi_{i2} + x_{i3}) + c_s\, \chi_i(x_{i2})\, x_{i3})\, dt, \tag{3.147}$$

$$B(i) := -\int_{\bar{t}_i}^{\hat{t}_i} c_s\, x_{i3}\, (x_{i2} + \psi_{i3})\, \chi_i'(x_{i2})\, dt. \tag{3.148}$$

From (3.97), (3.137), (3.141), (3.142) and (3.147), one gets that

$$A(i) \to 0 \text{ as } i \to +\infty. \tag{3.149}$$

For $B(i)$, we perform the change of variable $\tau = x_{i2}(t)$. Using (3.136) and (3.148), we get

$$B(i) = -\int_{y_s-(1/i)}^{y_s} \frac{c_s\, x_{i3}(x_{i2}^{-1}(\tau))\, (\tau + \psi_{i3}(x_{i2}^{-1}(\tau)))}{a(\tau) + b(\tau)u(x_{i2}^{-1}(\tau))}\, \chi_i'(\tau)\, d\tau. \tag{3.150}$$

Let us point out that, from (3.78), (3.80) and (3.84), one has

$$\int_{y_s-(1/i)}^{y_s} \chi_i'(\tau)\, d\tau = -1, \quad \chi_i' \leqslant 0. \tag{3.151}$$

From (3.91), (3.97), (3.130), (3.150) and (3.151), one gets that

$$\frac{c_s\, x_{*3}(\hat{t})(y_s + \psi_3(\hat{t}))}{a(y_s) + b(y_s)} \leqslant \liminf_{i\to+\infty} B(i) \leqslant \limsup_{i\to+\infty} B(i) \leqslant \frac{c_s\, x_{*3}(\hat{t})(y_s + \psi_3(\hat{t}))}{a(y_s) + b(y_s)w},$$

which, together with (3.137), (3.141), (3.143), (3.146) and (3.149), gives (3.74).

Let us now treat the case where

$$x_{*2}(t_1) = y_s. \tag{3.152}$$

One adapts the proof given above in the following way.

- If, for some $i \to +\infty$, $x_{i2}(t_1) \leqslant y_s - (1/i)$, then one gets $\psi_2(t_1) = 0$.
- If, for some $i \to +\infty$, $x_{i2}(t_1) > y_s$, then, proceeding as above, one gets

$$-\psi_2(t_1) \in \left[\frac{c_s\, x_{*3}(\hat{t})y_s}{a(y_s) + b(y_s)}, \frac{c_s\, x_{*3}(\hat{t})y_s}{a(y_s) + b(y_s)\, w}\right]. \tag{3.153}$$

- If, for some $i \to +\infty$, $y_s - (1/i) < x_{i2}(t_1) \leqslant y_s$, one just need to replace $\bar{t}_i$ by t_1 in the above proof. Then, one replaces (3.151) by

$$\int_{y_s-(1/i)}^{x_{i2}(t_1)} \chi_i'(\tau)\, d\tau \leqslant -1, \quad \chi_i' \leqslant 0,$$

  and one gets (3.153).

Let us now prove the maximum condition (3.77). By (3.96), extracting if necessary a subsequence of the u_i's and still denoting by $(u_i)_{i\in\mathbb{N}^*}$ the extracted sequence, there exists a Borel subset $\mathcal{N}_0$ of (t_0, t_1) of Lebesgue measure 0 such that

$$\lim_{i\to+\infty} u_i(t) = u_*(t), \quad \forall t \in (t_0, t_1) \setminus \mathcal{N}_0. \tag{3.154}$$

Let $i \in \mathbb{N}^*$. By (3.122), there exists a Borel subset $\mathcal{N}_i$ of (t_0, t_1) of Lebesgue measure 0 such that

$$\mathcal{H}_i(t, x_i(t), u_i(t), \psi_i(t)) = H_i(t, x_i(t), \psi_i(t)), \quad \forall t \in (t_0, t_1) \setminus \mathcal{N}_i. \tag{3.155}$$

Let

$$\mathcal{N} := \{\hat{t}\,\} \cup (\cup_{i\in\mathbb{N}^*}\mathcal{N}_i)\,.$$

Then $\mathcal{N}$ is a Borel subset of (t_0, t_1) of Lebesgue measure 0. Let $u \in [w, 1]$. By (3.155),

$$\mathcal{H}_i(t, x_i(t), u_i(t), \psi_i(t)) \geqslant \mathcal{H}_i(t, x_i(t), u, \psi_i(t)), \quad \forall i \in \mathbb{N}^*, \quad \forall t \in (t_0, t_1) \setminus \mathcal{N}. \tag{3.156}$$

Let $\psi := (\psi_1, \psi_2, \psi_3)^{\mathrm{tr}}$. Letting $i \to +\infty$ in (3.156) and using (3.86), (3.97), (3.117), (3.118), (3.128), (3.130), (3.143) and (3.154), one gets that

$$\mathcal{H}(x_*(t), u_*(t), \psi(t)) \geqslant \mathcal{H}(x_*(t), u, \psi(t)), \quad \forall t \in (t_0, t_1) \setminus \mathcal{N},$$

which gives (3.77). This concludes the proof of Theorem 3.3.3. ∎

3.3.3 Proof of the bang-bang property of the optimal control

In this section, we use the necessary optimality conditions given in Theorem 3.3.3 in order to prove Theorem 3.3.2. From now on, we assume that the target time t_1 satisfies $t_1 > \hat{t}_0$ so that all the cells will exit from phase 1 into phase 3 before time t_1. We give a proof of Theorem 3.3.2 first in the case where $N = 1$, then we study the case where $N > 1$, in this case we need additionally to analyze the dynamics between different exit times $\hat{t}_k$, $k = 1, 2, \cdots, N$, to obtain that there exists one and only one switching time and that the optimal switching direction is from $u = w$ to $u = 1$. In both cases $N = 1$ or $N > 1$, we give some numerical illustrations in this section.

Proof of Theorem 3.3.2 in the case $N = 1$

The Hamiltonian (3.65) becomes

$$\begin{aligned}\mathcal{H}(x,u,\psi) &= \psi_1 + (a(x_2)+b(x_2)u)\psi_2 + c(x_2)x_3\psi_3 + (a(x_2)+b(x_2)u)x_3 + c(x_2)x_2x_3 \\ &= (a(x_2)+c(x_2)x_2)\,x_3 + \psi_1 + a(x_2)\psi_2 + c(x_2)x_3\,\psi_3 + b(x_2)(x_3+\psi_2)\,u. \quad (3.157)\end{aligned}$$

Let u be an optimal control for the optimal control problem (3.18) and let $x = (x_1, x_2, x_3)^{\mathrm{tr}}$ be the corresponding trajectory. Note that, by (3.7), $b(x_2) > 0$. Then, by (3.66), (3.77) and (3.157), one has, for almost every $t \in (t_0, t_1)$,

$$u(t) = 1 \quad \text{if} \quad x_3(t) + \psi_2(t) > 0, \tag{3.158}$$

$$u(t) = w \quad \text{if} \quad x_3(t) + \psi_2(t) < 0. \tag{3.159}$$

Let us recall that, under assumption (3.19) of Theorem 3.3.2, there exists one and only one $\hat{t} \in [t_0, t_1)$ such that

$$x_2(\hat{t}\,) = y_s. \tag{3.160}$$

Then

$$x_2(t) > y_s, \quad \forall t \in (\hat{t}, t_1]. \tag{3.161}$$

We study the case where $\hat{t} > t_0$, the case $\hat{t} = t_0$ being obvious. Thanks to (3.74), we get

$$(x_3+\psi_2)(\hat{t}+0) - (x_3+\psi_2)(\hat{t}-0) \geqslant c_s\, x_3(\hat{t}\,)\,\frac{y_s + \psi_3(\hat{t}\,)}{a(y_s)+b(y_s)}. \tag{3.162}$$

By (3.68) and (3.72), we get

$$\frac{d(x_2+\psi_3)}{dt} = -(x_2+\psi_3)\,c_s\chi(x_2), \tag{3.163}$$

and then, using also (3.63), (3.73), (3.160) and (3.161), we obtain

$$y_s + \psi_3(\hat{t}\,) = (x_2+\psi_3)(\hat{t}\,) = (x_2+\psi_3)(t_1) \geqslant y_s. \tag{3.164}$$

Combining (3.162) with (3.164), we get

$$(x_3+\psi_2)(\hat{t}-0) \leqslant (x_3+\psi_2)(\hat{t}+0) - c_s\, x_3(\hat{t}\,)\frac{y_s}{a(y_s)+b(y_s)}. \tag{3.165}$$

When $t \neq \hat{t}$, from (3.8), (3.63), (3.69) and (3.71), we obtain

$$\frac{d(x_3+\psi_2)}{dt} = -(a'(x_2)+b'(x_2)u)\,(x_3+\psi_2). \tag{3.166}$$

Hence, using also (3.7), we have

$$(x_3+\psi_2)(\hat{t}+0) = (x_3+\psi_2)(t_1)\,e^{-\int_{\hat{t}}^{t_1}(2x_2(s)-c_1u(s))\,ds}. \tag{3.167}$$

Using the first inequality of (3.20), (3.75), (3.161) and (3.167), we get

$$(x_3 + \psi_2)(\hat{t} + 0) \leqslant x_3(t_1). \tag{3.168}$$

Noticing that $x_3(\hat{t} + 0) = x_3(t_1)$ and using (3.165) and (3.168), we get

$$(x_3 + \psi_2)(\hat{t} - 0) \leqslant x_3(t_1)(1 - c_s \frac{y_s}{a(y_s) + b(y_s)}). \tag{3.169}$$

From the second inequality of (3.20) and (3.169), we get

$$(x_3 + \psi_2)(\hat{t} - 0) < 0. \tag{3.170}$$

which, together with (3.166), gives us

$$(x_3 + \psi_2)(t) < 0, \quad t \in [t_0, \hat{t}\,). \tag{3.171}$$

Moreover, by (3.75), we have

$$(x_3 + \psi_2)(t_1) = x_3(t_1) > 0,$$

which together with (3.166), gives

$$(x_3 + \psi_2)(t) > 0, \quad t \in (\hat{t}, t_1]. \tag{3.172}$$

Taking $t_* = \hat{t}$ and combining (3.171) and (3.172), with (3.158) and (3.159), we conclude the proof of Theorem 3.3.2 in the case where $N = 1$. ■

Numerical illustration in the case $N = 1$

For one Dirac mass, the optimal switching time is unique. Assumption (3.20) is not necessary to guarantee that the optimal control is a bang-bang control with only one switching time. It is only used to guarantee that the optimal switching time coincides with the exit time. We give a numerical example to show that when c_s is "small", there is no switch at all and the optimal control is constant ($u = 1$), while when c_s is "large", there is a switch occuring at the exit time (see figure 3.3).

The default parameter values are specified in Table 3.1 for the numerical studies.

Proof of Theorem 3.3.2 in the case $N > 1$

Now, the Hamiltonian (3.65) becomes

$$\mathcal{H}(x, u, \psi) = \sum_{k=1}^{N} \big((a(x_2^k) + c(x_2^k)x_2^k)x_3^k + \psi_1^k + a(x_2^k)\psi_2^k + c(x_2^k)x_3^k\psi_3^k + b(x_2^k)(x_3^k + \psi_2^k)u\big). \tag{3.173}$$

t_0	initial time	0.0
t_1	final time	17.0
c_1	slope in the $b(y)$ function	11.892
c_2	origin ordinate in the $b(y)$ function	2.288
y_s	threshold maturity	6.0
w	minimal bound of the control	0.5

Table 3.1. Default parameter values

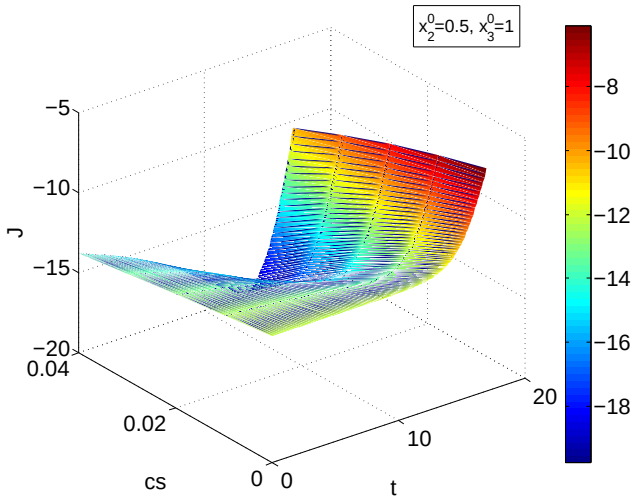


Figure 3.3. Value of the cost function J with respect to the switching time (t) and c_s parameter in the case of one Dirac mass. When c_s is "small", there is no switching time ($t = 0$) and the optimal control is constant ($u = 1$), while, when c_s is "large", the optimal control strategy consists in switching from $u = w$ to $u = 1$ at a time coinciding with the exit time. The initial values are specified in the insert.

Reordering if necessary the x^k's, we may assume, without loss of generality, that

$$x_2^{10} < x_2^{20} < \ldots < x_2^{k0} < \ldots < x_2^{N0}. \tag{3.174}$$

Let u be an optimal control for the optimal control problem (3.18) and let $x = (x^1, \ldots, x^k, \ldots x^N)$, with $x^k = (x_1^k, x_2^k, x_3^k)^{\mathrm{tr}}$, be the corresponding trajectory. From (3.174), we have

$$\hat{t}_N < \hat{t}_{N-1} < \ldots \hat{t}_k < \ldots < \hat{t}_1. \tag{3.175}$$

Let $\Phi : [t_0, t_1] \to \mathbb{R}$ be defined by

$$\Phi(t) := \sum_{k=1}^{N} b(x_2^k(t))(x_3^k(t) + \psi_2^k(t)). \tag{3.176}$$

Noticing that $b(x_2^k) > 0$, by (3.66), (3.77), (3.173) and (3.176), one has, for almost every $t \in (t_0, t_1)$,

$$u = w, \quad \text{if} \quad \Phi(t) < 0, \tag{3.177}$$

$$u = 1, \quad \text{if} \quad \Phi(t) > 0. \tag{3.178}$$

We take the time-derivative of (3.176) when $t \neq \hat{t}_k$, $k = 1, \cdots, N$. From (3.7), we obtain

$$\dot{\Phi}(t) = \sum_{k=1}^{N} (c_1 (x_2^k)^2 + 2c_2 x_2^k)(x_3^k + \psi_2^k). \tag{3.179}$$

Similarly to the above proof for one Dirac mass, we can prove that, under assumption (3.20), we have, for each $k = 1, \cdots, N$,

$$(x_3^k + \psi_2^k)(t) < 0, \quad \text{when } t \in (t_0, \hat{t}_k), \tag{3.180}$$

$$(x_3^k + \psi_2^k)(t) > 0, \quad \text{when } t \in (\hat{t}_k, t_1). \tag{3.181}$$

By (3.175), (3.176), (3.180) and (3.181), and note that $b(x_2^k) > 0$, we get

$$\Phi(t) < 0, \quad \text{when} \quad t \in (t_0, \hat{t}_N), \tag{3.182}$$

$$\Phi(t) > 0, \quad \text{when} \quad t \in (\hat{t}_1, t_1). \tag{3.183}$$

The key point now is to study the dynamics of Φ between different exit times $\hat{t}_k$. Let $k \in \{1, \cdots, N-1\}$ and let us assume that

$$\Phi(t) = 0, \quad \text{for some} \quad t \in (\hat{t}_{k+1}, \hat{t}_k). \tag{3.184}$$

From (3.176) and (3.184), we get

$$x_3^k(t) + \psi_2^k(t) = -\sum_{i \neq k} \frac{b(x_2^i(t))}{b(x_2^k(t))} (x_3^i(t) + \psi_2^i(t)). \tag{3.185}$$

From (3.180) and (3.181), for every $t \in (\hat{t}_{k+1}, \hat{t}_k)$,

$$x_3^i(t) + \psi_2^i(t) < 0, \quad \text{when} \quad i \leqslant k-1, \tag{3.186}$$

$$x_3^i(t) + \psi_2^i(t) > 0, \quad \text{when} \quad i \geqslant k+1. \tag{3.187}$$

From (3.7), (3.179) and (3.185), we get

$$\begin{aligned}\dot{\Phi}(t) = &\sum_{i \leqslant k-1} \frac{x_3^i + \psi_2^i}{b(x_2^k)} \big(c_1^2 x_2^i x_2^k + 2c_2^2 + c_1 c_2 (x_2^i + x_2^k)\big)(x_2^i - x_2^k) \\ &+ \sum_{i \geqslant k+1} \frac{x_3^i + \psi_2^i}{b(x_2^k)} \big(c_1^2 x_2^i x_2^k + 2c_2^2 + c_1 c_2 (x_2^i + x_2^k)\big)(x_2^i - x_2^k). \end{aligned} \tag{3.188}$$

From (3.174), we get

$$x_2^i(t) - x_2^k(t) < 0, \quad \text{when} \quad i \leqslant k-1, \tag{3.189}$$

$$x_2^i(t) - x_2^k(t) > 0, \quad \text{when} \quad i \geqslant k+1. \tag{3.190}$$

Using (3.186) to (3.190), we get

$$\dot{\Phi}(t) > 0 \quad \text{whenever} \quad \Phi(t) = 0, \quad \forall t \in (\hat{t}_{k+1}, \hat{t}_k). \tag{3.191}$$

Combining (3.177), (3.178), (3.182), (3.183) and (3.191) together, we get the existence of $t_* \in (t_0, t_1)$ such that

$$u_* = w \quad \text{in} \quad (t_0, t_*) \quad \text{and} \quad u_* = 1 \quad \text{in} \quad (t_*, t_1).$$

This concludes the proof of Theorem 3.3.2. ∎

Numerical illustration in the case $N > 1$

The optimal control is not unique for more than one Dirac mass. Let us consider the case of two Dirac masses as an example. The optimal switching time may happen either at the first exit time or at the second exit time (see figure 3.4), or between the two exit times (see figure 3.5).

3.4 Optimal control in the PDE case

In this section, we study the optimal control in the PDE case. We give the proof of Theorem 3.2.1. We first give an explicit expression for the cost function J defined in (3.17).

Let us define a new map

$$\begin{array}{rcl} e : [0, y_s] \times L^\infty((t_0, t_1); [w, 1]) & \to & [t_0, t_1] \\ (y_0, u) & \mapsto & e(y_0, u) \end{array}$$

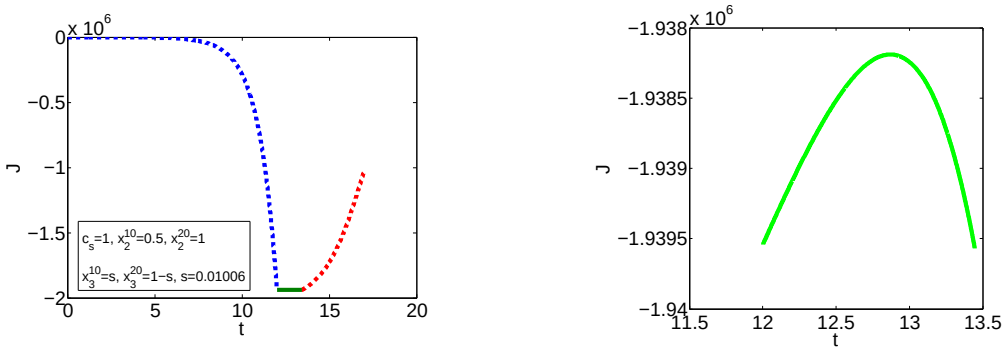


Figure 3.4. Value of the cost function J with respect to the switching time (t) in the case of two Dirac masses and a "large" value of c_s (c_s =1.0). In the left panel, the three-part curve represents the value of the cost function obtained after switching from $u = w$ to $u = 1$ at time t. Blue dashed curve: switching time occurring before the first exit time; green solid curve: switching time occurring in between the two exit times; red dashed curve: switching time occurring after the second exit time. The initial values are specified in the insert. The right panel is a zoom on the green solid curve displayed on the left panel. There are two optimal switching times which coincide with the two exit times.

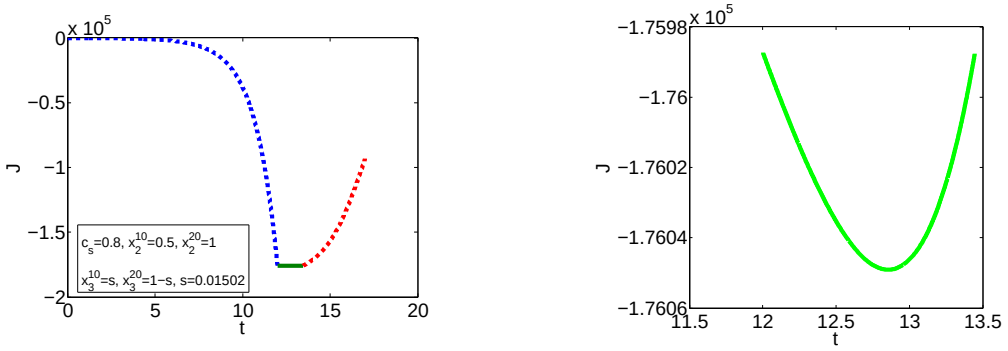


Figure 3.5. Value of the cost function J with respect to the switching time (t) in the case of two Dirac masses and a "large" value of c_s (c_s =0.8). In the left panel, the three-part curve represents the value of the cost function obtained after switching from $u = w$ to $u = 1$ at time t. Blue dashed curve: switching time occurring before the first exit time; green solid curve: switching time occurring in between the two exit times; red dashed curve: switching time occurring after the second exit time. The initial values are specified in the insert. The right panel is a zoom on the green solid curve displayed on the left panel. There is one single optimal switching time, which occurs in between the two exit times.

by requiring

$$\Psi(e(y_0,u),y_0,u)=y_s, \tag{3.192}$$

where Ψ is defined by (3.24). Note that, under assumption (3.19), one has, for every $y_0 \in [0,y_s]$, the existence of $t \in [t_0,t_1]$ such that

$$\Psi(t,y_0,u)=y_s. \tag{3.193}$$

Again, (3.91) implies that there exists at most one $t \in [t_0,t_1]$ such that (3.193) holds. This shows that e is well defined. Moreover, proceeding as in the proof of (3.56) and using standard results on ordinary differential equations together with (3.91) gives the following lemma.

Lemma 3.4.1. *Let $(y_0^n)_{n\in\mathbb{N}}$ be a sequence of elements in $[0,y_s]$ and $(u^n)_{n\in\mathbb{N}}$ be a sequence of elements in $L^\infty((t_0,t_1);[w,1])$. Let us assume that, for some $y_0 \in [0,y_s]$ and for some $u \in L^\infty((t_0,t_1);[w,1])$,*

$$y_0^n \to y_0 \text{ as } n \to +\infty,$$
$$u^n \overset{*}{\rightharpoonup} u \text{ in } L^\infty(t_0,t_1) \text{ as } n \to +\infty.$$

Then

$$e(y_0^n,u^n) \to e(y_0,u) \text{ as } n \to +\infty.$$

Let now ρ_0 be a Borel measure on $\mathbb{R}\times\mathbb{R}$ such that (3.25) and (3.26) hold. Using (3.27), (3.17) becomes

$$J(u)=-\iint_{[0,1]\times[0,y_s]} \Psi(t_1,y_0,u)\, e^{c_s e(y_0,u)}\, d\rho_0(x_0,y_0). \tag{3.194}$$

In order to emphasize the dependence of J on the initial data ρ_0, from now on we write $J(\rho_0,u)$ for $J(u)$.

It is well known that there exists a sequence $((x_0^{i,n},y_0^{i,n},\lambda_0^{i,n}))_{1\leqslant i\leqslant n,\, n\in\mathbb{N}}$ of elements in $[0,1]\times[0,y_s]\times(0,+\infty)$ such that, if

$$\rho_0^n := \sum_{i=1}^n \lambda_0^{i,n}\delta_{x_0^{i,n},y_0^{i,n}}, \tag{3.195}$$

then

$$\lim_{n\to+\infty}\iint_{[0,1]\times[0,y_s]} \varphi(x_0,y_0)\, d\rho_0^n(x_0,y_0) = \iint_{[0,1]\times[0,y_s]} \varphi(x_0,y_0)d\rho_0(x_0,y_0),\ \forall\varphi\in C^0([0,1]\times[0,y_s]). \tag{3.196}$$

From Theorem 3.3.1 and Theorem 3.3.2, there exists $t_*^n \in [t_0,t_1]$ such that, if $u_*^n : [t_0,t_1] \to [w,1]$ is defined by

$$u_*^n = w \text{ in } [t_0,t_*^n) \text{ and } u_*^n = 1 \text{ in } (t_*^n,t_1], \tag{3.197}$$

then

$$J(\rho_0^n, u_*^n) \leqslant J(\rho_0^n, u), \quad \forall u \in L^\infty((t_0, t_1); [w, 1]). \tag{3.198}$$

Extracting a subsequence if necessary, we may assume without loss of generality the existence of $t_* \in [t_0, t_1]$ such that

$$\lim_{n \to +\infty} t_*^n = t_*. \tag{3.199}$$

Let us define $u_* : [t_0, t_1] \to [w, 1]$ by

$$u_* = w \text{ in } [t_0, t_*) \text{ and } u_* = 1 \text{ in } (t_*, t_1]. \tag{3.200}$$

Then, using (3.197), (3.199) and (3.200), one gets

$$\Psi(t_1, \cdot, u_*^n) \to \Psi(t_1, \cdot, u_*) \text{ in } C^0([0, y_s]) \text{ as } n \to +\infty. \tag{3.201}$$

Moreover, from (3.197), (3.199) and (3.200), one has

$$u_*^n \overset{*}{\rightharpoonup} u_* \text{ in } L^\infty(t_0, t_1) \text{ as } n \to +\infty. \tag{3.202}$$

From Lemma 3.4.1 and (3.202), one gets

$$e(\cdot, u_*^n) \to e(\cdot, u_*) \text{ in } C^0([0, y_s]) \text{ as } n \to +\infty. \tag{3.203}$$

From (3.194), (3.196), (3.201) and (3.203) and a classical theorem on the weak topology (see, e.g., [17, (iv) of Proposition 3.13, p. 63]), one has

$$J(\rho_0^n, u_*^n) \to J(\rho_0, u_*) \text{ as } n \to +\infty. \tag{3.204}$$

Let now $u \in L^\infty((t_0, t_1); [w, 1])$. From Lemma 3.4.1, (3.194) and (3.196), one gets

$$J(\rho_0^n, u) \to J(\rho_0, u) \text{ as } n \to +\infty. \tag{3.205}$$

Finally, letting $n \to +\infty$ in (3.198) and using (3.204) together with (3.205), one has

$$J(\rho_0, u_*) \leqslant J(\rho_0, u),$$

which concludes the proof of Theorem 3.2.1. ■

Chapter 4

Some numerical results

In chapter 3, we have proved that under some reseasonable assumptions, there exists an optimal bang-bang control that maximizes the maturity for a fixed target time. Based on this, in this chapter, we mainly use numerically resolvent to compute the mass and the maturity for the very original model with mitosis boundary. After comparing with constant control case, we conclude that bang-bang control is indeed better than constant control. We also give some biological outputs in this chapter.

4.1 Notations and some assumptions

First, let us recall in chapter 3 that under some simplifying assumptions (see section 3.2.2 in chapter 3), we study an optimal control problem where the final time is fixed and the optimality criterion is the follicular maturity at final time. After applying PMP, we show that there exists an optimal bang-bang control with one single switching time.

Based on the result we obtained in chapter 3, in this chapter, we study the optimal control problem by both analytical method and also numerical resolvent. We made the same assumptions as in chapter 3 except that we keep the mitosis boundary as in the original model. Let us recall the assumptions made in chapter 3

A_1. We consider only one developing follicle, i.e. $f = 1$;

A_2. There is no loss term anymore, i.e. $\lambda = 0$;

A_3. The age velocity is uncontrolled, i.e. $g_f \equiv 1$;

A_4. The target maturity M_s can always be reached in finite time.

Furthermore, for simplicity of numerical computation, we assume that

A_5. The duration of phase 1 is equal to the duration of phase 2, i.e. $a_1 = a_2 - a_1 = 1$.

Since we consider only one follicle, for sake of simplicity, in this chapter, we denote by $\phi_{j,k}(t, x, y)$ the density function defined on each cellular phase $Q_{j,k}$ where x is the age variable

and y is the maturity variable. The changes in the density satisfies the following conservation laws

$$\frac{\partial \phi_{j,k}}{\partial t} + \frac{\partial \phi_{j,k}}{\partial x} + \frac{\partial (h(y,u)\phi_{j,k})}{\partial y} = 0, \quad \text{in } Q_{j,k}, \tag{4.1}$$

$$\begin{aligned} Q_{j,k} &:= \Omega_{j,k} \times [0,T], \text{ with } (x,y) \in \Omega_{j,k}, \text{ where} \\ \Omega_{1,k} &:= [(k-1)a_2, (k-1)a_2 + a_1] \times [0, y_s], \\ \Omega_{2,k} &:= [(k-1)a_2 + a_1, ka_2] \times [0, y_s], \\ \Omega_{3,k} &:= [(k-1)a_2, ka_2] \times [y_s, y_m]. \end{aligned}$$

Here $j = 1, 2, 3$ and $k = 1, \cdots, N$ with N the number of consecutive cell cycles (see figure 4.1).

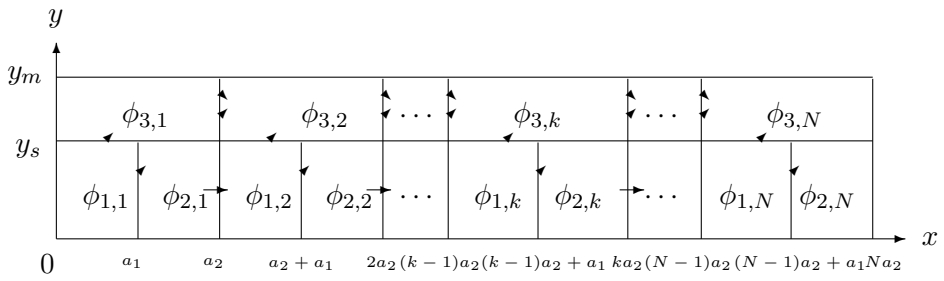


Figure 4.1. Sketch of the domain, x denotes the age and y denotes the maturity. The bottom of the domain is composed of N cell cycles, it corresponds to the proliferation phase. The top of the domain corresponds to the differentiation phase when cells have exited the cell cycle.

The initial conditions are given as follows

$$\phi_{j,k}(0,x,y) = \phi^0_{j,k}(x,y) \text{ in } \Omega_{j,k}, \quad j = 1,2,3, \quad k = 1, \cdots, N. \tag{4.2}$$

Let us recall the boundary conditions. There is no influx for phase 1 and phase 3 in the first cell cycle (see figure 4.1), hence

$$\phi_{1,1}(t,0,y) = \phi_{3,1}(t,0,y) = 0, \quad (t,y) \in [0,T] \times [0, y_s].$$

The mitosis happens when the cell leaves the previous cycle and goes into the next cycle (see figure 4.1), hence for $k = 2, \cdots, N$

$$\phi_{1,k}(t,(k-1)a_2,y) = 2\phi_{2,k-1}(t,(k-1)a_2,y), \quad (t,y) \in [0,T] \times [0,y_s].$$

There is no mitosis in phase 3, hence

$$\phi_{3,k}(t,(k-1)a_2,y) = \phi_{3,k-1}(t,(k-1)a_2,y), \quad (t,y) \in [0,T] \times [0,y_s].$$

In the same cycle k, $k = 1, \cdots, N$, the dynamics amounts to a transport dynamics from phase 1 to phase 2 (see figure 4.1), hence

$$\phi_{2,k}(t,(k-1)a_2 + a_1,y) = \phi_{1,k}(t,(k-1)a_2 + a_1,y), \quad (t,y) \in [0,T] \times [0,y_s].$$

There is no influx from the bottom $y = 0$ (see figure 4.1), hence for $k = 1, \cdots, N$

$$\phi_{1,k}(t, x, 0) = 0, \quad (t, x) \in [0, T] \times [(k-1)a_2, (k-1)a_2 + a_1],$$
$$\phi_{2,k}(t, x, 0) = 0, \quad (t, x) \in [0, T] \times [(k-1)a_2 + a_1, ka_2].$$

There is only influx from phase 1 to phase 3, and no influx from phase 2 to phase 3 (see figure 4.1), hence for $k = 1, \cdots, N$

$$\phi_{3,k}(t, x, y_s) = \begin{cases} \phi_{1,k}(t, x, y_s), & (t, x) \in [0, T] \times [(k-1)a_2, (k-1)a_2 + a_1], \\ 0, & (t, x) \in [0, T] \times [(k-1)a_2 + a_1, ka_2]. \end{cases}$$

There is no influx from the above $y = y_m$ (see figure 4.1), hence for $k = 1, \cdots, N$

$$\phi_{3,k}(t, x, y_m) = 0, \quad (t, x) \in [0, T] \times [(k-1)a_2, ka_2]. \tag{4.3}$$

Let us recall that the zero-order moment $M^0(t)$ is defined as

$$M^0(t) := \sum_{j=1}^{3} \sum_{k=1}^{N} \int_0^{y_m} \int_0^{a_m} \phi_{j,k}(t, x, y)\, dxdy \tag{4.4}$$

and the first-order moment $M(t)$ is defined as

$$M(t) := \sum_{j=1}^{3} \sum_{k=1}^{N} \int_0^{y_m} \int_0^{a_m} y\phi_{j,k}(t, x, y)\, dxdy. \tag{4.5}$$

We study the same optimal control problem presented in chapter 3, i.e. for fixed target time $t_1 > 0$, try to find optimal control that maximizes $M(t_1)$.

In section 4.1 we introduce some notations and give some assumptions for simplification of numerical study. In section 4.2 we first study the case where the control is given as a constant and show that the optimal one is always the saturing values (the bounds of the admissible controls) discriminated by a threshold final time t_s. In section 4.3 we then study the bang-bang control case, after comparing with constant control case, we conclude that bang-bang control is indeed better than constant control. Furthermore, we prove that switching from a to b is better than switching from b to a given that $a < b$ in the set of admissible controls. We show that the optimal bang-bang control are also saturing values. At last, we show that the optimal control consists in applying bang-bang control with one single switching time.

For simplicity of numerical computation, we consider the initial conditions for $k = 1, \cdots, N$ cycles as

$$\phi^0_{1,1}(x, y) \equiv 1, \quad \phi^0_{j,k}(x, y) \equiv 0, \quad j \neq 1,\ k \neq 1, \tag{4.6}$$

which means that the initial density is concentrated into phase 1. The case where the initial density is spread along the whole cell cycle (phase 1 and 2) can be treated similarly, except that the computation will be complicated (see remark 4.2.1 in section 4.2.2).

4.2 Constant control

The control u is assumed to satisfy the same constraint (3.10) (see chapter 3) throughout this chapter, i.e.

$$u \in [w, 1], \tag{4.7}$$

where w a positive constant such that

$$w \in (\frac{y_s^2}{c_1 y_s + c_2}, 1) \triangleq I. \tag{4.8}$$

In this section we study the case where the control is given as a constant. In section 4.2.1 we introduce the computation of the zero-order moment $M^0(t)$ with constant control $w \in I$, and we prove that for any fixed $t \in [0, t_1]$, $M^0(t)$ increases as w decreases. In section 4.2.2 we compute the asymptotic maximal maturity M_w with respect to constant control $w \in I$. In section 4.2.3 we study the behaviour of $M(t)$ without control, i.e. $w = 0$. Finally, in section 4.2.4, we give the results on optimal constant control case.

4.2.1 Computation of the zero-order moment

For any given constant control $w \in I$, we introduce the computation of the zero-order moment by tracing all the cells along the characteristics back to the initial plane.

Assume that $y_k(t)$, $k \in \mathbb{Z}^+$ are solutions to the following ODE

$$\begin{cases} \dot{y}_k = \tau_h(-y_k^2 + (c_1 y_k + c_2)w), \\ y_k(k - x_0) = y_s. \end{cases} \tag{4.9}$$

Solving (4.9), we define

$$y_k(x_0) = y_k(0). \tag{4.10}$$

For any fixed $t \in [0, 1]$, we divide the initial plane into different parts (see figure 4.2), where

$$\Sigma_1 := \Big\{(x_0, y_0)|\ 0 \leqslant x_0 \leqslant 1 - t,\ 0 \leqslant y_0 \leqslant \hat{y}\Big\}, \tag{4.11}$$

$$\Sigma_2 := \Big\{(x_0, y_0)|\ 1 - t \leqslant x_0 \leqslant 1,\ 0 \leqslant y_0 \leqslant y_1(x_0)\Big\}, \tag{4.12}$$

$$\Sigma_3 := [0, 1] \times [0, y_s] \backslash (\Sigma_1 \cup \Sigma_2), \tag{4.13}$$

with $y_1(x_0)$ defined by (4.10) in the case where $k = 1$ and $\hat{y}$ satisfies

$$\begin{cases} \dot{\hat{y}} = \tau_h(-\hat{y}^2 + (c_1 \hat{y} + c_2)w), \\ \hat{y}(t) = y_s. \end{cases} \tag{4.14}$$

From assumptions A_3, A_5 and the initial condition (4.6), we have

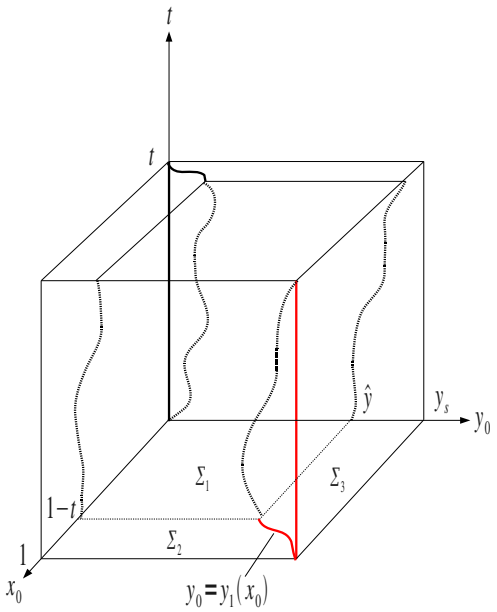


Figure 4.2. Division of the initial plane for any fixed $t \in [0,1]$.

$$\begin{aligned}&\phi_{1,1}(t,x,y) \neq 0,\ \phi_{2,1}(t,x,y) \neq 0,\ \phi_{3,1}(t,x,y) \neq 0,\\ &\phi_{j,k}(t,x,y) \equiv 0 \quad \text{for } j=1,2,3,\ k=2,\cdots,N.\end{aligned} \tag{4.15}$$

By definition of the zero-order moment in (4.4) and (4.15), after applying Lemma 2.6.3 in chapter 2, we obtain that for any fixed $t \in [0,1]$

$$\begin{aligned}M^0(t) =& M^0(\phi_{1,1})(t) + M^0(\phi_{2,1})(t) + M^0(\phi_{3,1})(t)\\ =& \int_0^1 \int_0^{y_s} \phi_{1,1}(t,x,y)\ dx\ dy + \int_1^2 \int_0^{y_s} \phi_{2,1}(t,x,y)\ dx\ dy\\ &+ \int_0^2 \int_{y_s}^{y_m} \phi_1(t,x,y)\ dx\ dy\\ =& \iint_{\Sigma_1} \phi^0_{1,1}(x_0,y_0)\ dx_0\ dy_0 + \iint_{\Sigma_2} \phi^0_{1,1}(x_0,y_0)\ dx_0\ dy_0\\ &+ \iint_{\Sigma_3} \phi^0_{1,1}(x_0,y_0)\ dx_0\ dy_0.\end{aligned} \tag{4.16}$$

Noting initial condition (4.6), (4.16) can be rewritten as

$$M^0(t) = \int_0^1 \int_0^{y_s} \phi^0_{1,1}(x_0,y_0)\ dx_0\ dy_0 = y_s. \tag{4.17}$$

We can also conclude from (4.17) that, for any fixed $t \in [0,1]$, the mass is conserved.

For any fixed $t \in [1,2]$, we divide the initial plane into different parts (see figure 4.3),

where

$$\Sigma_1 := \Big\{(x_0, y_0)|\ 0 \leqslant x_0 \leqslant 2 - t,\ 0 \leqslant y_0 \leqslant y_1(x_0)\Big\}, \tag{4.18}$$

$$\Sigma_2 := \Big\{(x_0, y_0)|\ 2 - t \leqslant x_0 \leqslant 1,\ 0 \leqslant y_0 \leqslant y_1(x_0)\Big\}, \tag{4.19}$$

$$\Sigma_3 := [0, 1] \times [0, y_s]\backslash(\Sigma_1 \cup \Sigma_2), \tag{4.20}$$

with $y_1(x_0)$ defined by (4.10) in the case where $k = 1$.

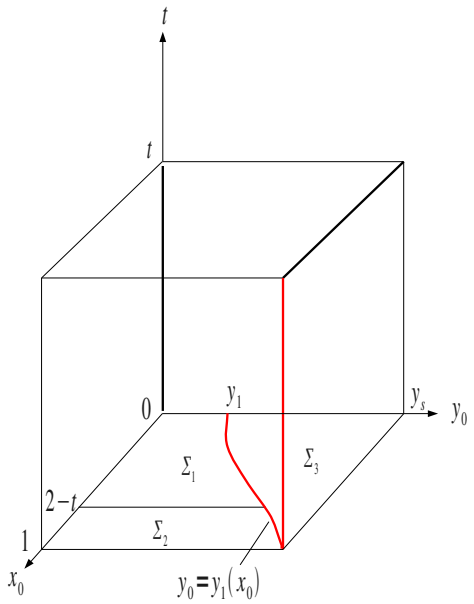


Figure 4.3. Division of the initial plane for any fixed $t \in [1, 2]$.

From assumptions A_3, A_5 and initial data (4.6), we obtain

$$\begin{aligned}&\phi_{1,1}(t, x, y) \equiv 0,\ \phi_{2,1}(t, x, y) \neq 0,\ \phi_{1,2}(t, x, y) \neq 0,\ \phi_{3,1}(t, x, y) \neq 0,\ \phi_{3,2}(t, x, y) \neq 0,\\ &\phi_{j,k}(t, x, y) \equiv 0,\ \text{else.}\end{aligned} \tag{4.21}$$

Noting (4.21), by definition of the zero-order moment (4.4) and applying Lemma 2.6.3 in chapter 2, we obtain that for any fixed $t \in [1, 2]$

$$\begin{aligned}M^0(t) =& M^0(\phi_{2,1})(t) + M^0(\phi_{1,2})(t) + M^0(\phi_{3,1})(t) + M^0(\phi_{3,2})(t)\\ =& \int_1^2 \int_0^{y_s} \phi_{2,1}(t, x, y)\ dx\ dy + \int_2^3 \int_0^{y_s} \phi_{1,2}(t, x, y)\ dx\ dy\\ &+ \int_0^2 \int_{y_s}^{y_m} \phi_{3,1}(t, x, y)\ dx\ dy + \int_2^4 \int_{y_s}^{y_m} \phi_{3,2}(t, x, y)\ dx\ dy\\ =& \iint_{\Sigma_1} \phi^0_{1,1}(x_0, y_0)\ dx_0\ dy_0 + 2 \iint_{\Sigma_2} \phi^0_{1,1}(x_0, y_0)\ dx_0\ dy_0\\ &+ \iint_{\Sigma_3} \phi^0_{1,1}(x_0, y_0)\ dx_0\ dy_0.\end{aligned} \tag{4.22}$$

Noting initial condition (4.6), (4.22) can be rewritten as

$$\begin{aligned} M^0(t) =& \int_0^{2-t} y_1(x_0)\ dx_0 + 2\int_{2-t}^1 y_1(x_0)\ dx_0 + \int_0^1 (y_s - y_1(x_0))\ dx_0 \\ =& y_s + \int_{2-t}^1 y_1(x_0)\ dx_0. \end{aligned} \tag{4.23}$$

Similarly, we can compute $M^0(t)$ for any $t \in [2, \infty)$.

Lemma 4.2.1. *For any fixed $t \in [0, \infty)$, the zero-order moment $M^0(t)$ is increasing as the constant control w decreases.*

Proof. From (4.17), we conclude that when $t \in [0, 1]$, the mass is conserved since $M^0(t) \equiv y_s$. Next, we compute $M^0(t)$ when $t \in [1, 2]$. In order to emphasize the dependence of $y_1(x_0)$ on the constant control w, we replace $y_1(x_0)$ by $y(x_0, w)$ in (4.23), we obtain

$$M^0(t) = y_s + \int_{2-t}^1 y(x_0, w)\ dx_0, \tag{4.24}$$

where $y(x_0, w) = y(0, w)$ with $y(t, w)$ satisfying

$$\begin{cases} \dot{y} = \tau_h(-y^2 + (c_1 y + c_2)w), \\ y(1 - x_0) = y_s. \end{cases} \tag{4.25}$$

Noting (4.24), we only have to prove that $y(x_0, w)$ increases as w decreases. Assume that $w_1 \leqslant w_2 \in I$ and $y^i(t, w_i)$ $(i = 1, 2)$ are solutions to

$$\begin{cases} \dot{y^i} = \tau_h(-y^2 + (c_1 y + c_2)w_i), \\ y^i(1 - x_0) = y_s. \end{cases} \tag{4.26}$$

We now prove that $y^1(0, w_1) \geqslant y^2(0, w_2)$. Otherwise, if $y^1(0, w_1) < y^2(0, w_2)$, noting (4.26), we have $\dot{y}^1 \leqslant \dot{y}^2$, hence it is easy to get

$$y^1(t, w_1) < y^2(t, w_2), \quad \forall t \in [0, \infty).$$

Especially when $t = 1 - x_0$, we have $y^1(1 - x_0, w_1) < y^2(1 - x_0, w_2)$, which is a contradiction.

Similarly, we can prove for any $t \in [2, \infty)$. This concludes the proof of Lemma 4.2.1. □

4.2.2 Computation of the asymptotic maximal maturity

The default parameter values we used here and hereafter are specified in Table 4.1 (see [44]) for the numerical studies.

For any constant control $w \in I$, let us denote by t_w the first time when a cell starting from the origin enters phase 3, i.e. t_w satisfies

$$y(t_w) = y_s, \tag{4.27}$$

t_0	initial time	0.0
c_1	slope in the h function	11.892
c_2	origin ordinate in the h function	2.288
y_s	threshold maturity	3.0
τ_h	time scale parameter	0.07

Table 4.1. Default parameter values

where $y(t)$ is the solution to the following ODE

$$\begin{cases} \dot{y} = \tau_h(-y^2 + (c_1 y + c_2)w), \\ y(0) = 0. \end{cases} \tag{4.28}$$

To compute the asymptotic maximal maturity M_w, we first compute the maximum of the zero-order moment. The idea is to first judge how many cycles the cells will go through by computing the exit time t_w (the time when the cell starting from the origin exit the cell cycle). Then we compute the maximum mass M^0 by tracing all the cells along the characteristics back to the initial plane. Now we take an example to show how to compute the asymptotic maximal maturity. For sake of simplicity, let us fix a constant control value w such that, correspondingly the exit time $t_w = 7$. Noting that under the assumption A_5 that the duration of each cell cycle is 2. That means we choose a constant control w such that the cell starting from the origin will progress four cell cycles before going into the differentiation phase 3. Hence, w satisfies

$$\begin{cases} \dot{y} = \tau_h(-y^2 + (c_1 y + c_2)w), \\ y(0) = 0, \quad y(7) = y_s. \end{cases} \tag{4.29}$$

Furthermore, from assumptions A_3, A_5 and initial condition (4.6), it is easy to see that when $t \geqslant 8$, all the cells have exited the proliferation phases 1 and 2 and entered the differentiation phase 3.

We have the following theorem

Theorem 4.2.1. *For any time $t \geqslant 8$, the total (maximum) mass M^0 is constant and is given by*

$$M^0(t) = y_s + \sum_{k=1}^{4} 2^{k-1} \int_0^1 y_k(x_0)\, dx_0. \tag{4.30}$$

Proof. By definition (4.4) of the zero-order moment and using Lemma 2.6.3 in chapter 2, we have

$$\begin{aligned} M^0(t) :=& \sum_{j=1}^{3} \sum_{k=1}^{N} \int_0^{y_m} \int_0^{a_m} \phi_{j,k}(t, x, y)\, dx\, dy \\ =& \Sigma_1 + 2\Sigma_2 + 2^2\Sigma_3 + 2^3\Sigma_4 + 2^4\Sigma_5, \end{aligned} \tag{4.31}$$

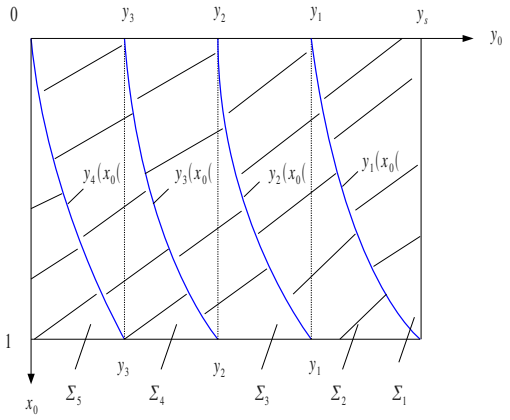


Figure 4.4. Division of the initial plane according to 4 cell cycles undergone before going to phase 3.

where $\Sigma_1, \cdots, \Sigma_5$ are the areas of the domains $\Sigma_1, \cdots, \Sigma_5$ (see figure 4.4)

$$\begin{aligned}
\Sigma_1 &:= \{(x_0, y_0) | 0 \leqslant x_0 \leqslant 1,\ y_1(x_0) \leqslant y_0 \leqslant y_s\},\\
\Sigma_2 &:= \{(x_0, y_0) | 0 \leqslant x_0 \leqslant 1,\ y_2(x_0) \leqslant y_0 \leqslant y_1(x_0)\},\\
\Sigma_3 &:= \{(x_0, y_0) | 0 \leqslant x_0 \leqslant 1,\ y_3(x_0) \leqslant y_0 \leqslant y_2(x_0)\},\\
\Sigma_4 &:= \{(x_0, y_0) | 0 \leqslant x_0 \leqslant 1,\ y_4(x_0) \leqslant y_0 \leqslant y_3(x_0)\},\\
\Sigma_5 &:= \{(x_0, y_0) | 0 \leqslant x_0 \leqslant 1,\ 0 \leqslant y \leqslant y_4(x_0)\},
\end{aligned}$$

with $y_k(x_0)$ $(k = 1, \cdots, 4)$ defined by (4.10). Hence, from (4.31), we get

$$\begin{aligned}
M^0(t) =& \int_0^1 \int_{y_1(x_0)}^{y_s} dy_0\ dx_0 + 2\int_0^1 \int_{y_2(x_0)}^{y_1(x_0)} dy_0\ dx_0 + 2^2 \int_0^1 \int_{y_3(x_0)}^{y_2(x_0)} dy_0\ dx_0\\
&+ 2^3 \int_0^1 \int_{y_4(x_0)}^{y_3(x_0)} dy_0\ dx_0 + 2^4 \int_0^1 \int_0^{y_4(x_0)} dy_0\ dx_0\\
=& y_s + \sum_{k=1}^{4} 2^{k-1} \int_0^1 y_k(x_0)\ dx_0. \qquad (4.32)
\end{aligned}$$

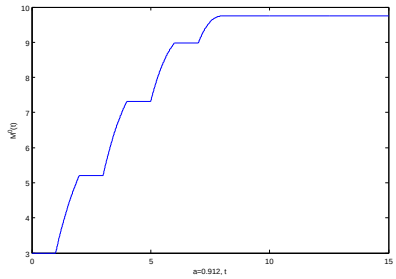
This concludes the proof of Theorem 4.2.1. □

Let us denote by $\gamma_w := \dfrac{wc_1 + \sqrt{w^2c_1^2 + 4wc_2}}{2}$ the asymptotic maximal maturity corresponding to constant control w (the non trivial root of $h(y, w) = 0$), then the asymptotic

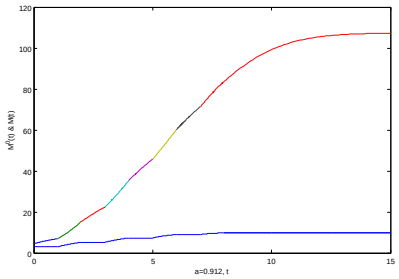
maturity M_w is given by

$$\begin{aligned} M_w :=& \gamma_w \cdot M^0 \\ =& \gamma_w (y_s + \sum_{k=1}^{4} 2^{k-1} \int_0^1 y_k(x_0)\, dx_0). \end{aligned} \tag{4.33}$$

See figure 4.5 for numerical results. From panel (a) of figure 4.5, we can see that when $t \in [2k, 2k+1]$, $k \in \mathbb{N}$, there is no more mitosis, so that the zero-order moment remains constant. When $t \in [2k+1, 2k+2]$, $k \in \mathbb{N}$, the cells progress through mitosis, so that the zero-order moment increases as time increases. When time $t \geqslant 8$, $M^0(t)$ is constant and we can see from panel (a) of figure 4.5 that the maximal mass $M^0 \simeq 9.8$. Hence the asymtotic maximal maturity $M = \gamma_{\hat{a}ss} \cdot M^0 \simeq 108$. We can also see from panel (b) of figure 4.5 the asymptotic phenomena.



(a) The x axis represents the time t, the y axis represents the zero-order moment $M^0(t)$ with constant control $w = 0.912$.



(b) The zero-order moment $M^0(t)$ (blue curve) is displayed together with the first-order moment $M(t)$ with constant control $w = 0.912$.

Figure 4.5. Changes in the mass and maturity when initial density is concentrated into the first phase.

Remark 4.2.1. For sake of simplicity, the initialisation of the cell density has been simplified as (4.6), i.e. instead of being spread along the whole cell cycle, the initial density is concentrated into the first phase ($\phi^0_{1,1}(x, y) \equiv 1$ and $\phi^0_{2,1}(x, y) \equiv 0$). The drawback of this choice is to introduce an artificial synchronisation between cells (although we know from biology that they are fully desynchronised) which brings about steep changes in the slope of the computed $M^0(t)$. However, we can use the same method to deal with desynchronised case, except that the computation will be complicated. See figure 4.6 for desynchronised case where the inital condition is given as $\phi^0_{1,1}(x, y) = \phi^0_{2,1}(x, y) = \dfrac{1}{2}$.

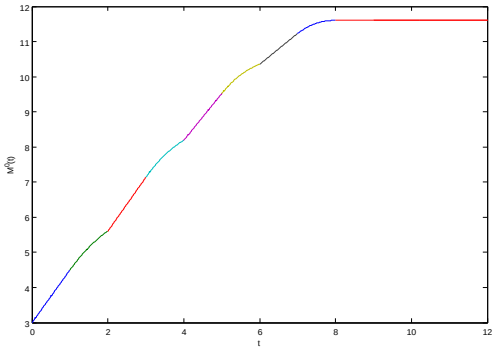


Figure 4.6. Changes in the mass when the initial density is spread along the whole cell cycle. The x axis denotes the time t, the y axis denotes the mass $M^0(t)$ with constant control $w = 0.912$ given the initial data $\phi^0_{1,1}(x,y) \equiv \phi^0_{2,1}(x,y) \equiv \dfrac{1}{2}$ spreading along the whole cell cycle.

Next we study the behaviour of total maturity $M(t)$. First we study a special case where $w = 0$ to see the influence of the maturity y on the total maturity $M(t)$.

4.2.3 The behaviour of the maturity $M(t)$ when the control $u = 0$

Here we study the behaviour of the maturity $M(t)$ numerically when $w = 0$ (see figure 4.7).

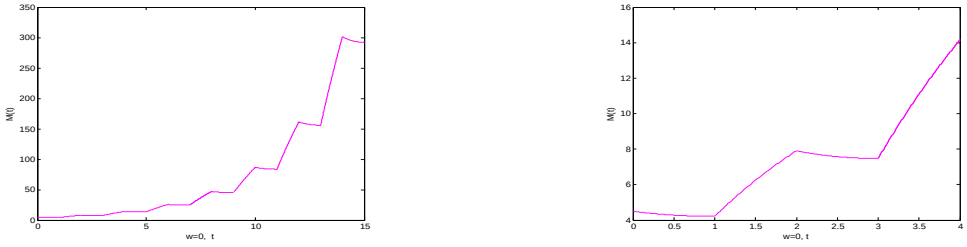
- When $t \in [0,1]$, we observe from figure 4.7 that the maturity decreases as t increases. Indeed, when $w = 0$, the velocity of the maturity is $\dot{y} = h = -\tau_h \cdot y^2 < 0$. Furthermore, the mass will not increase since there is no mitosis as long as $t \in [0,1]$. Hence, the total maturity decreases as time t increases (see panel (b) of figure 4.7).

- When $t \in [1,2]$, we find that the maturity $M(t)$ increases quickly despite the decreasing of the maturity y (see panel (b) of figure 4.7). That is due to the mitosis phenomenon.

- When $t \in [2,3]$, the maturity $M(t)$ decreases again due to the decrease of y, and there is no mitosis during this period.

- When $t \in [3,4]$, the maturity $M(t)$ increases more quickly due to the fact that more and more cells process through mitosis during this time interval.

Those above phenomena happen periodically with a unit time of one cycle duration (see panel (a) of figure 4.7). More precisely, when $t \in [2k, 2k+1]$, $k \in \mathbb{N}$, the maturity decreases as t increases, while when $t \in [2k+1, 2k+2]$, $k \in \mathbb{N}$, the maturity increases as t increases.



(a) (b)

Figure 4.7. The behaviour of the maturity when constant control $w = 0$. The x axis denotes time $0 \leqslant t \leqslant 15$, the y axis denotes the maturity. Panel (b) is a zoom on panel (a) when $0 \leqslant t \leqslant 4$.

4.2.4 Results on optimal constant control

When t is "small", the increase of maturity y contributes more to the maturity $M(t)$, see figure 4.8 that before a threshold time $t_s = 7.8$, i.e. for any fixed final time $t_1 < t_s$, the optimal constant control is the right bounday $w = 1$ of admissible controls. But when final time t_1 is "large" enough, the mitosis contributes more to the maturity $M(t)$, see figure 4.8 that the maturity increases very fast in the later cell cycles. Hence, for any fixed final time $t_1 > t_s$, the optimal constant control is the left boundary $w = \dfrac{y_s^2}{c_1 y_s + c_2} \simeq 0.237$ of the admissible controls.

Hence the optimal constant control is whatever the target time t_1 is, the optimal constant controls are always the saturing values (see figure 4.8), i,e.

$$w = \begin{cases} 0.237, \text{ when } t_1 \in [t_s, \infty), \\ 1, \text{ when } t_1 \in [0, t_s]. \end{cases} \tag{4.34}$$

Remark 4.2.2. We remark here that although the optimal constant control are always the saturing values, the intersection of the maturity with two different constant controls are complicated before the threshold time $t_s = 7.8$. We denote by $M_w(t)$ the maturity at time t when applying constant control $w \in I$.

- See panel (b) of figure 4.9 that the curve $M_{w=0.237}(t)$ intersects with the curve $M_{w=0.45}(t)$ three times, which means that the maturity $M_{w=0.237}(t)$ will first catch up with the

maturity $M_{w=0.45}$ due to the fact that there are more cells process mitosis when applying constant control $w = 0.237$ than applying constant control $w = 0.45$, but after a while, the maturity $M_{w=0.45}(t)$ will catch up with the maturity $M_{w=0.237}(t)$ due to the growth of maturity y. After $t = 7.1$, the curve of maturity $M_{w=0.237}(t)$ is always above the curve of maturity $M_{w=0.45}(t)$ (see panel (a) of figure 4.9).

- We observe from panel (b) of figure 4.10 that the curve of maturity $M_{w=0.237}(t)$ intersects with the curve of maturity $M_{w=0.35}(t)$ only one time, which means that with constant control $w = 0.35$, even if the maturity increases faster, it is not yet enough to catch up with the maturity constant control $w = 0.237$. After $t = 5.4$, the curve of maturity $M_{w=0.237}(t)$ is always above the curve of maturity $M_{w=0.35}(t)$ (see panel (a) of figure 4.10).

- Furthermore, we conclude that whatever the number of intersection points between the $M_{w_1}(t)$ and $M_{w_2}(t)$ curves (see figure 4.9 and figure 4.10), there always exists a threshold time t_{fs} such that for any two constants $w_1 \leqslant w_2 \in I$ we have

$$M_{w_1}(t) \geqslant M_{w_2}(t), \quad \forall\, t \geqslant t_{fs}. \tag{4.35}$$

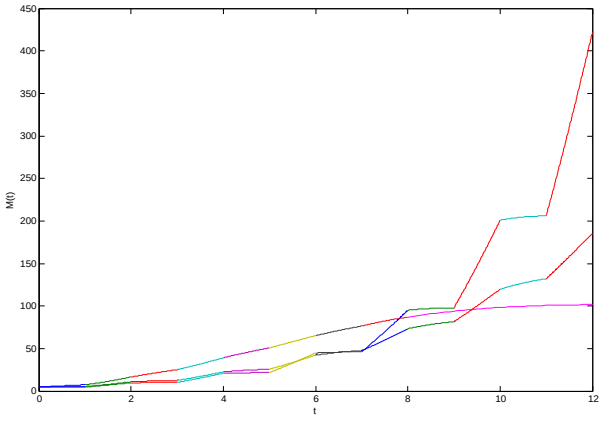
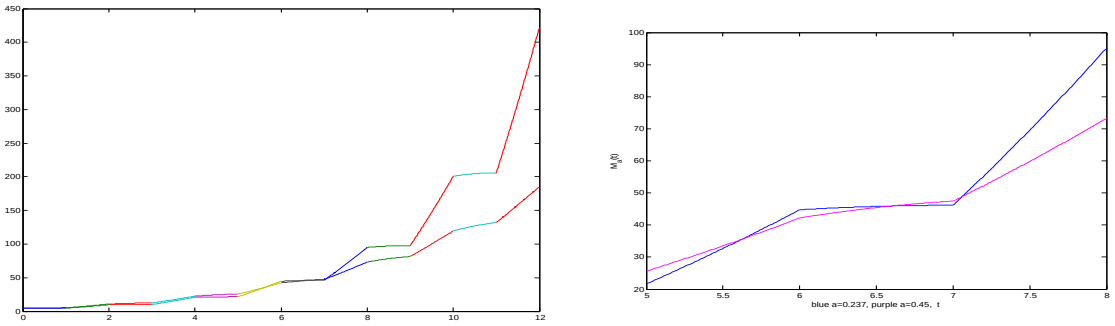
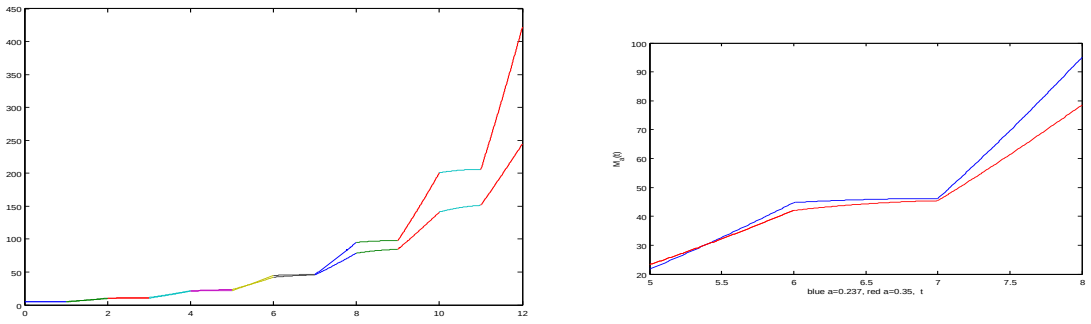


Figure 4.8. The illustration of maturity when applying different constant controls. The x axis represents time t, the y axis represents maturity $M(t)$. From the above to the bottom, the curves represent the maturity when applying $w = 0.237$, $w = 0.45$ and $w = 1$ respectively.



(a) (b)

Figure 4.9. The intersection of the maturity when applying different constant controls. The x axis represents the time $0 \leqslant t \leqslant 12$, the y axis represents the maturity $M(t)$. Panel (b) is a zoom on panel (a) of the intersection part, the blue curve represents the maturity $M_{w=0.237}(t)$, the purple curve represents the maturity $M_{w=0.45}(t)$.



(a) (b)

Figure 4.10. The intersection of the maturity when applying different constant controls. The x axis represents the time $0 \leqslant t \leqslant 12$, the y axis represents the maturity $M(t)$. Panel (b) is a zoom on panel (a) of the intersection part, the blue curve represents the maturity $M_{w=0.237}(t)$, the red curve represents the maturity $M_{w=0.35}(t)$.

4.3 Bang-bang control

From now on, we denote by t_0 the switching time in this section. We mainly study the bang-bang control case and compare it with the constant control case. First in section 4.3.1 we introduce some notations and some possible control strategies. In section 4.3.2 we prove that switching from a to b ($a \to b$) is better than switching from b to a ($b \to a$) given that $a < b$ in the set of admissible controls and that the target time t_1 is large enough. We then compare in section 4.3.3 bang-bang control with constant control on the numerical ground, we give the optimal combination (t_0^*, a^*, b^*) that maximizes maturity $M(t_1)$ at a given target time t_1 chosen according to biological knowledges. We also show that bang-bang control with one single switching time is optimal.

4.3.1 Some notations and possible control strategies

For any given switching time t_0, target time t_1 and $a < b \in I$, we denote by $M_{ab}^{t_0}(t_1)$ the maturity at time t_1 when applying bang-bang control

$$w = \begin{cases} a, & \text{for} \quad 0 < t \leqslant t_0, \\ b, & \text{for} \quad t_0 < t < t_1, \end{cases} \tag{4.36}$$

and by $M_{ba}^{t_0}(t_1)$ the maturity at time t_1 when applying bang-bang control

$$w = \begin{cases} b, & \text{for} \quad 0 < t \leqslant t_0, \\ a, & \text{for} \quad t_0 < t < t_1. \end{cases} \tag{4.37}$$

4.3.2 Optimal switching direction for bang-bang control

In this subsection, we will show that bang-bang control (4.36) is better than bang-bang control (4.37) provided that both the switching time t_0 and the target time t_1 are "large" enough. More precisely, we have the following theorem:

Theorem 4.3.1. *There exists $\hat{t}_0$ and $\hat{t}$, such that when $t_0 > \hat{t}_0$ and $t_1 > \hat{t}$, we have $M_{ab}^{t_0}(t_1) > M_{ba}^{t_0}(t_1)$.*

Proof. From (4.7), we compute numerically that a cell starting from the origin will go through at least three cell cycles before entering phase 3 (i.e. it will enter phase 3 in the fourth cell cycle). For sake of simplicity, we choose constant control $w = 0.745$ such that a cell starting from the origin will go through five cell cycles before entering phase 3, we choose any b such that $\dfrac{y_s^2}{c_1 y_s + c_2} < a < b \leqslant 1$. When $t \geqslant t_a = 10$, all the cells have entered phase 3. We trace all the cells back into the initial plane, by dividing it into several parts (see figure 4.11). For any given switching time $t_0 \in [0, \infty)$, we denote by $S_{ab}(t_0)$ a weighted sum of the areas of the different parts of the initial plane, where the weights are related to the number of cell cycles

performed by cells originating from any parts of the initial plane when applying bang-bang control (4.36). Similarly, we denote by $S_{ba}(t_0)$ the opposite case, i.e. a weighted sum of the areas of the different parts of the initial plane when applying bang-bang control (4.37).

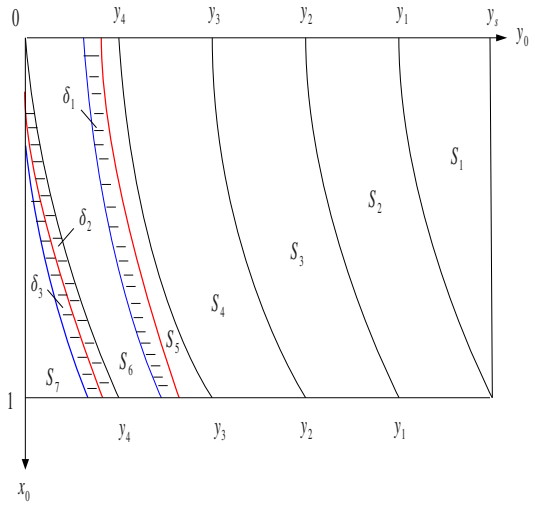


Figure 4.11. Division of the initial plane corresponding to two different switching times (the blue curve corresponding to switching time t_{01}, the red curve corresponding to swiching time t_{02} with $t_{01} < t_{02}$).

For sake of simplicity, we still denote by S_i $(i = 1, \cdots, 7)$ the areas with respect to domain S_i. Then we have

$$S_{ab}(t_{01}) := S_1 + 2S_2 + 2^2S_3 + 2^3S_4 + 2^4S_5 + 2^4\delta_1 + 2^5S_6 + 2^5\delta_2 + 2^5\delta_3 + 2^6S_7, \tag{4.38}$$

$$S_{ab}(t_{02}) := S_1 + 2S_2 + 2^2S_3 + 2^3S_4 + 2^4S_5 + 2^5\delta_1 + 2^5S_6 + 2^5\delta_2 + 2^6\delta_3 + 2^6S_7. \tag{4.39}$$

Comparing (4.38) and (4.39), we get

$$S_{ab}(t_{01}) < S_{ab}(t_{02}).$$

. This gives us the idea that $S_{ab}(t_0)$ increases as t_0 increases. Correspondingly, $S_{ba}(t_0)$ decreases as t_0 increases.

Let us define γ_{ass} and γ_{bss} as the asymptotic maturities with respect to constant control a and b.

$$\gamma_{ass} = \frac{ac_1 + \sqrt{a^2c_1^2 + 4ac_2}}{2}, \quad \gamma_{bss} = \frac{bc_1 + \sqrt{b^2c_1^2 + 4bc_2}}{2}. \tag{4.40}$$

Then we get

$$\gamma_{bss} \cdot S_{ab}(t_0) = \lim_{t\to\infty} M_{ab}^{t_0}(t), \quad \gamma_{ass} \cdot S_{ba}(t_0) = \lim_{t\to\infty} M_{ba}^{t_0}(t). \tag{4.41}$$

Let us then define

$$S(t_0) := \frac{S_{ab}(t_0)}{S_{ba}(t_0)}. \tag{4.42}$$

It is easy to check that $S(t_0) \in C^0[0, \infty)$. Furthermore, $S(t_0)$ increases as t_0 increases (see figure 4.12).

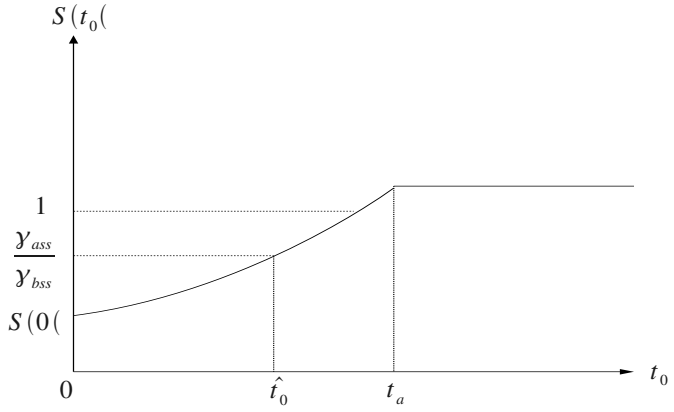


Figure 4.12. The illustration of $S(t_0)$ function.

Then we have

$$S(0) = \frac{S_{ab}(0)}{S_{ba}(0)} < 1, \quad S(t_a) = \frac{S_{ab}(t_a)}{S_{ba}(t_a)} > 1, \quad S(0) \cdot S(t_a) = 1, \tag{4.43}$$

with t_a the exit time defined by (4.27) when applying constant control $w = a$. Given that $a < b$, we get $\gamma_{ass} < \gamma_{bss}$, hence we have

$$\frac{\gamma_{ass}}{\gamma_{bss}} < 1.$$

Noting (4.43), there exists one and only one $\hat{t}_0 < t_a$ such that

$$S(\hat{t}_0) = \frac{S_{ab}(\hat{t}_0)}{S_{ba}(\hat{t}_0)} = \frac{\gamma_{ass}}{\gamma_{bss}}. \tag{4.44}$$

Due to the fact that $S(t_0)$ increases as t_0 increases, when $t_0 > \hat{t}_0$, we have

$$S(t_0) = \frac{S_{ab}(t_0)}{S_{ba}(t_0)} > S(\hat{t}_0) = \frac{S_{ab}(\hat{t}_0)}{S_{ba}(\hat{t}_0)} = \frac{\gamma_{ass}}{\gamma_{bss}}. \tag{4.45}$$

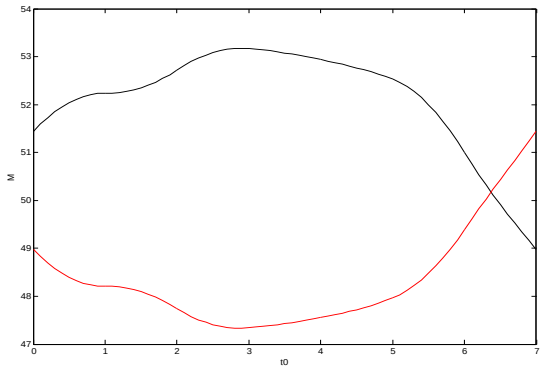
From (4.45), we get

$$\gamma_{bss} \cdot S_{ab}(t_0) > \gamma_{ass} \cdot S_{ba}(t_0). \tag{4.46}$$

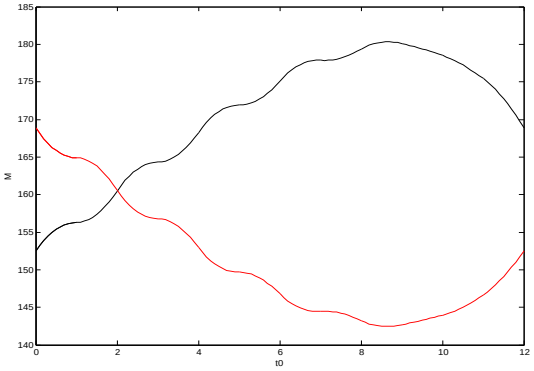
By (4.41) and (4.46), there exists $\hat{t}$ such that

$$M_{ab}^{t_0}(t_1) > M_{ba}^{t_0}(t_1) \quad \text{for all} \quad t_1 > \hat{t}. \tag{4.47}$$

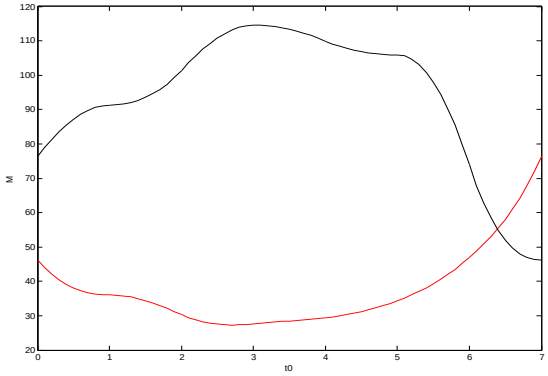
As a whole, we prove that there exists $\hat{t}_0$ and $\hat{t}$ such that when $t_0 > \hat{t}_0$ and $t_1 > \hat{t}$, we have $M_{ab}^{t_0}(t_1) > M_{ba}^{t_0}(t_1)$. This concludes the proof of Theorem 4.3.1. □



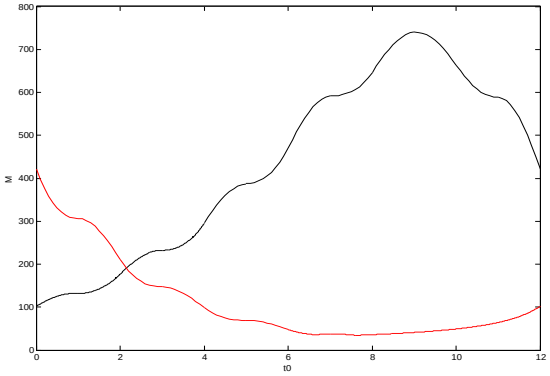
(a) $t_1 = 7$, $a = 0.495$, $b = 0.555$



(b) $t_1 = 12$, $a = 0.495$, $b = 0.555$



(c) $t_1 = 7$, $a = 0.237$, $b = 1$



(d) $t_1 = 12$, $a = 0.237$, $b = 1$

Figure 4.13. Comparison of the final maturity as a function of switching time t_0 when applying different control strategies. The x axis represents the switching time $0 \leqslant t_0 \leqslant t_1$. Black curve: $M_{ab}^{t_0}(t_1)$, i.e. the final maturity when switching from a to b at t_0; Red curve: $M_{ba}^{t_0}(t_1)$, i.e. the final maturity when switching from b to a at t_0. (a) $a = 0.495$, $b = 0.555$ with target time given as $t_1 = 7$; (b) $a = 0.495$, $b = 0.555$ with target time given as $t_1 = 12$; (c) $a = 0.237$, $b = 1$ with target time given as $t_1 = 7$; (d) $a = 0.237$, $b = 1$ with target time given as $t_1 = 12$.

Remark 4.3.1. We give a numerical illustration to support Theorem 4.3.1 (see figure 4.13). We see from panel (a) and (c) of figure 4.13 that with a "small" target time $t_1 = 7$, even if the switching time t_0 is very large, switching from b to a is better than switching from a to b. From panel (b) and (d) of figure 4.13, we see that with a "large" target time $t_1 = 12$, switching from a to b is better than switching from b to a as soon as the switching time $t_0 > 3$.

4.3.3 Optimal control

In this section, we compare constant control with bang-bang control with a given target time t_1. To determine the choice of target time t_1, we refer to the zero-order moment from biological background.

First let us introduce the growth fraction GF. The cell population is divided into proliferating cells and differentiated ones, through what is known as the growth fraction GF defined as

$$GF(t) := \frac{\sum_{j=1}^{2}\sum_{k=1}^{N}\int_0^{y_s}\int_0^{a_m}\phi_{j,k}(t,x,y)\,dx\,dy}{M^0(t)}. \tag{4.48}$$

The most reliable information concerns the total cell number M^0 at initial and final times. The ratio of increase between $M^0(0)$ and $M^0(t_1)$ can be targeted to a range of 20 to 30 (see [21], [24], [78]). With a constant growth fraction $GF = 1$, which means that there are no differentiated cells, this duration roughly corresponds to the cells progressing through 4 to 5 cell cycles. This is the case when we choose constant control as the left boundary $w = \dfrac{y_s^2}{c_1 y_s + c_2}$, which means cells will never go to phase 3, i.e. $GF \equiv 1$. It is easy to get $M^0(0) = 3$ according to initial condition (4.6), hence, to guaranteen that $\frac{M^0(t_1)}{M^0(0)} \in (20, 30)$, we have to choose a target time t_1 such that $M^0(t_1) \in (60, 90)$. From our numerical computation (see figure 4.14), we conclude that $t_1 \in (9, 10)$, which coincides with biological consideration that the cells will progress through 4 to 5 cell cycles.

However, the growth fraction will decrease ($GF < 1$) as the time increases, hence, the time elapsed from the beginning to the final time is longer. Based on biological consideration, a duration equivalent to 6 (or possibly 7) cell cycles can be chosen as a starting point (see [78]). Hence, we choose a target time $t_1 = 12$ in the following.

With the given target time, see panel (b) of figure 4.16 in the case where we fix $a = 0.237$ and let b change. See panel (a) of figure 4.16 that $M_{0.237}(12) \simeq 425$ and $M_1(12) \simeq 100$. However we observe from the red curve in panel (b) of figure 4.16 that the maturity $M \geqslant 425$ with any switching time $t_0 \in [7, 12]$. This means that bang-bang control is better than constant control. We conlude also from panel (b) of figure 4.16 that the optimal strategy is

$$(t_0^*, a^*, b^*) := (9, \frac{y_s^2}{c_1 y_s + c_2}, 1). \tag{4.49}$$

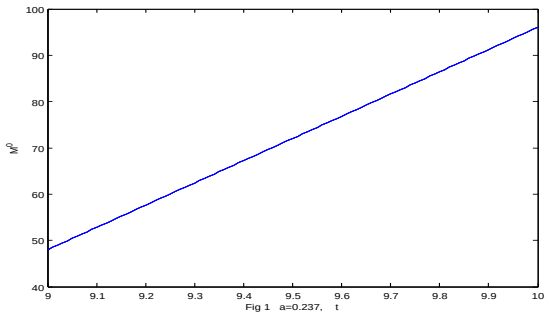


Figure 4.14. The illustration of the zero-order moment $M^0(t)$ for determination of target time t_1. The x axis represents time t, the y axis represents M^0 with constant control $w = 0.237$.

Furthermore, we conclude that for fixed $a = \dfrac{y_s^2}{c_1 y_s + c_2} \simeq 0.237$, the optimal switching time $t_0 = 9$ is also the optimal switching time for any $b \geqslant 0.67$ (see panel (b) of figure 4.16). When $b = 0.67$, the optimal switching time is not unique, there are two optimal switching times $t_0 = 9$ and $t_0 = 11$ (see figure 4.15). When $b > 0.67$, the optimal switching time is shifted to the right $t_0 = 11$ until this curve becomes to a horizontal when $a = b \simeq 0.237$ (see panel (b) of figure 4.16).

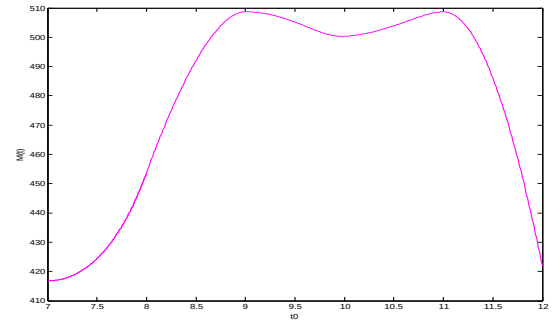
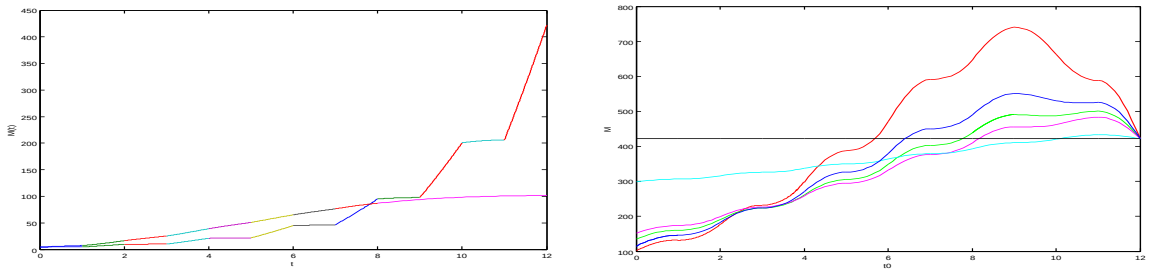


Figure 4.15. The illustration of the case where the optimal switching time is not unique when switching from $a = 0.237$ to $b = 0.67$ (there exist two optimal switching times $t_0 = 9$ and $t_0 = 11$). The x axis represents switching time $0 \leqslant t_0 \leqslant t_1 = 12$, the y axis represents the final maturity $M_{ab}^{t_0}(t_1)$.



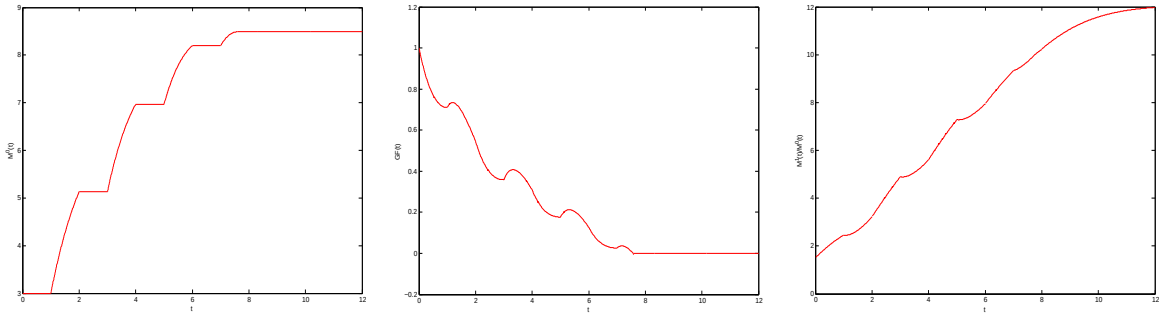
(a) (b)

Figure 4.16. Changes in the maturity for different constant or bang-bang control strategies. (a) The x axis represents the time $0 \leqslant t \leqslant 12$, the y axis represents the maturity $M(t)$. The above curve represents constant control $w = 0.237$, the bottom curve represents constant control $w = 1$. (b) The x axis represents the switching time $0 \leqslant t_0 \leqslant 12$, the y axis represents the maturity $M(t_1)$ at target time $t_1 = 12$, we fix $a = 0.237$, let b change. Red curve: $b = 1$; Blue curve: $b = 0.745$; Green curve: $b = 0.635$; Purple curve: $b = 0.555$; Cyan curve: $b = 0.3$; Black curve: $b = 0.237$.

In the following, we give some biological outputs. See figure 4.17 and figure 4.18 for indices $GF(t)$, $M^0(t)$ and $\dfrac{M^1}{M^0}(t)$ with saturing values. Comparing to those in figure 4.19 when applying optimal bang-bang control, i.e. switching from $a = 0.237$ to $b = 1$ at $t_0 = 9$.

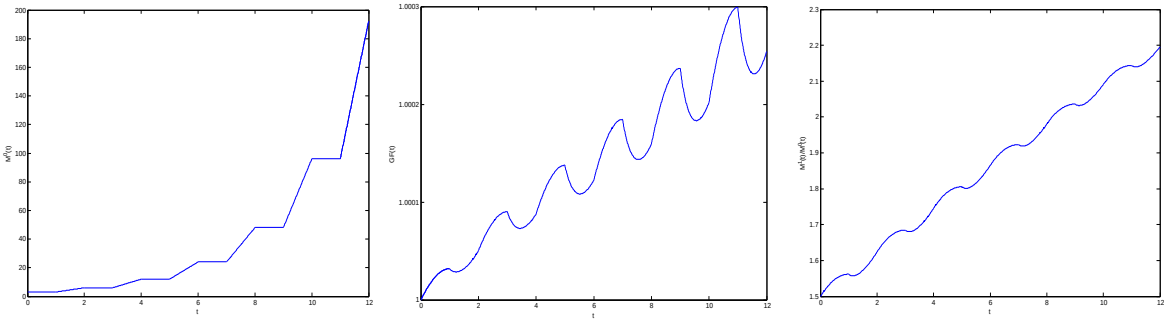
See figure 4.20 for comparison of indices $GF(t)$, $M^0(t)$ and $\dfrac{M^1}{M^0}(t)$ with three different switching times. We get

- When switching at $t_0 = 8$, the growth fraction is the lowest because we switch too early, but the average maturity is the biggest due to the maturity velocity is bigger after switching (see the blue curves of figure 4.20).
- When switching at $t_0 = 10$, the growth fraction is the biggest, but the average maturity is the lowest because we switch too late (see the green curves of figure 4.20).
- When switching at $t_0 = 9$, the two indices are both moderate and thus generates the maximum of the maturity at target $t_1 = 12$ (see the red curves of figure 4.20).



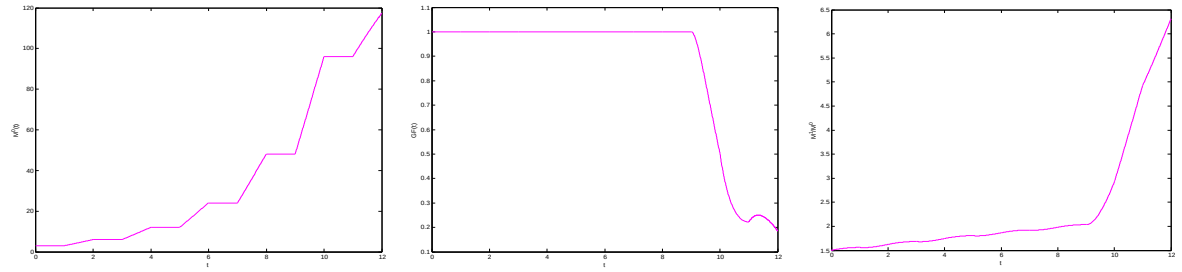
(a) the cell mass $M^0(t)$ (b) the growth fraction $GF(t)$ (c) the average maturity $\frac{M^1}{M^0}(t)$

Figure 4.17. Changes in the cell mass, growth fraction and average maturity when applying constant control $w = 1$. The x axis represents the time $0 \leqslant t \leqslant 12$. In panel (a), the y axis represents the mass $M^0(t)$; In panel (b), the y axis represents the growth fraction $GF(t)$; In panel (c), the y axis represents the average maturity $\frac{M^1}{M^0}(t)$.



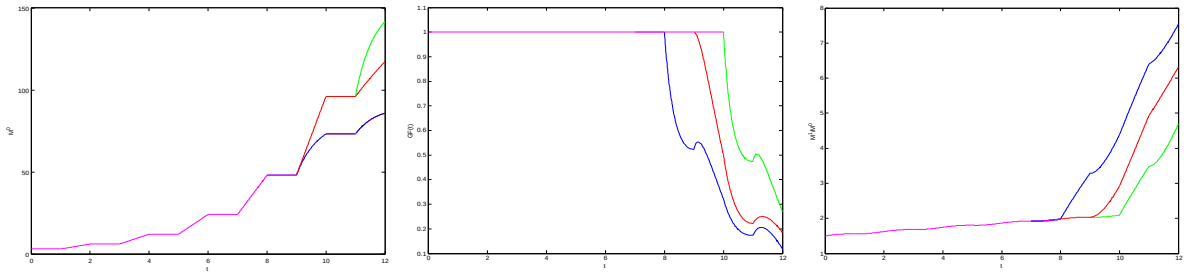
(a) the cell mass $M^0(t)$ (b) the growth fraction $GF(t)$ (c) the average maturity $\frac{M^1}{M^0}(t)$

Figure 4.18. Changes in the cell mass, growth fraction and average maturity when applying constant control $w = 0.237$. The x axis represents the time $0 \leqslant t \leqslant 12$. In panel (a), the y axis represents the mass $M^0(t)$; In panel (b), the y axis represents the growth fraction $GF(t)$; In panel (c), the y axis represents the average maturity $\frac{M^1}{M^0}(t)$.



(a) the cell mass $M^0(t)$ (b) the growth fraction $GF(t)$ (c) the average maturity $\frac{M^1}{M^0}(t)$

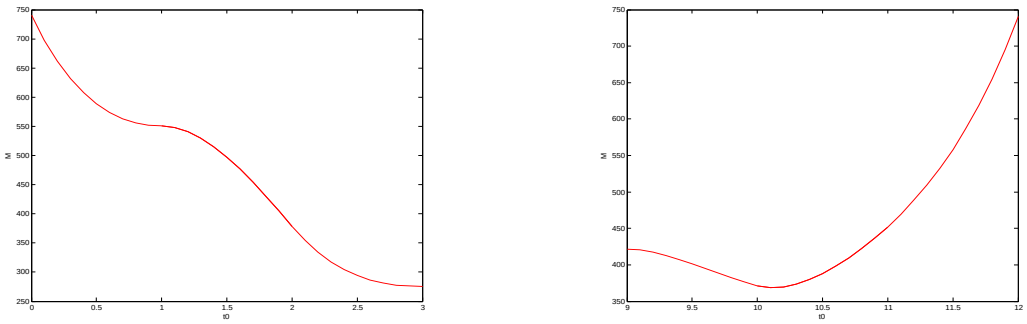
Figure 4.19. Changes in the cell mass, growth fraction and average maturity when applying the optimal bang-bang control, i.e. we switch from $a = 0.237$ to $b = 1$ at $t_0 = 9$. The x axis represents the time $0 \leqslant t \leqslant 12$. In panel (a), the y axis represents the mass $M^0(t)$; In panel (b), the y axis represents the growth fraction $GF(t)$; In panel (c), the y axis represents the average maturity $\frac{M^1}{M^0}(t)$.



(a) the cell mass $M^0(t)$ (b) the growth fraction $GF(t)$ (c) the average maturity $\frac{M^1}{M^0}(t)$

Figure 4.20. Comparison of cell mass, growth fraction and average maturity when switching from $a = 0.237$ to $b = 1$ at different switching times. The x axis represents the time $0 \leqslant t \leqslant 12$. Blue curve: switching at $t_0 = 8$; Red curve: switching at $t_0 = 9$; Green curve: switching at $t_0 = 10$. In panel (a), the y axis represents the mass $M^0(t)$; In panel (b), the y axis represents the growth fraction $GF(t)$; In panel (c), the y axis represents the average maturity $\frac{M^1}{M^0}(t)$.

At last, we show that switching only one time is optimal. To to that, we choose the optimal combination (4.49), i.e. $a = 0.237$ and $b = 1$. We denote by t_{01} the first switching time and by t_{02} the second switching time. First, we consider the case where we switch from b to a at t_{01}, and then from a to b at t_{02} (see panel (a) of figure 4.21). We observe that the case where $t_{01} = 0$ and $t_{02} = 9$ is optimal, which means that we should always give constant control $a = 0.237$ when $t \in [0, 9]$ and then give constant control $b = 1$ when $t \in [9, 12]$. Then we study the case where we switch from a to b at t_{01}, and then from b to a at t_{02} (see panel (b) of figure 4.21). We observe that the case where $t_{01} = 9$ and $t_{02} = 12$ is optimal, which means that we should always give constant control $a = 0.237$ when $t \in [0, 9]$ and then give constant control $b = 1$ when $t \in [9, 12]$.



(a) (b)

Figure 4.21. The illustration of the maturity when switching twice. We fix one switching time and change the other switching time. (a) $b \to a \to b$ case, we fix the second switching time $t_{02} = 9$ and change the first switching time t_{01}. The x axis represents the first switching time $0 \leqslant t_{01} \leqslant 3$, the y axis represents the final maturity $M_{bab}(t_1)$. (b) $a \to b \to a$ case, we fix the first switching time $t_{01} = 9$ and change the second switching time t_{02}. The x axis represents the second switching time $9 \leqslant t_{02} \leqslant 12$, the y axis represents the final maturity $M_{aba}(t_1)$.

Chapter 5

Optimization of an Amplification Protocol for Misfolded Proteins by using Relaxed Control

Abstract. This part of work arises from the optimal control of protocol of protein misfolded cyclic amplification (PMCA). In this work, we mainly studied optimal strategy to maximize a criterion to detect misfolded proteins. We have proved that the optimal controls are relaxed controls which are localized in the admissible domain.

5.1 Introduction

Transmissible Spongifrom Encephalopathies (TSE) are fatal, infectious, neurodegenerative diseases. They include bovine spongiform encephalopathies (BSE) in cattle, scrapie in sheep and Creutzfeldt-Jakob disease (CJD) in human. During the so-called "mad-cow crisis" in the 90's, people were infected by a variant of BSE by ingesting contaminated pieces of beef. More recently, CJD was transmitted between humans via blood or growth hormones. Because of the long incubation times (some decades), TSE still represent an important public health risk. Indeed, there is no *ante mortem* diagnosis currently available to detect infected individuals and prevent possible contaminations. A promising tool to design a diagnosis test is the PMCA technique [65].

The PMCA principle is based on the "protein-only hypothesis". According to this widely accepted hypothesis, the infectious agent of TSE, known as prions, may consist in misfolded proteins called PrPsc (for Prion Protein scrapie). The PrPsc replicates in a self-propagating process, by converting the normal form of PrPc (called PrPc for Prion Protein cellular) into PrPsc. The PMCA enabled to consolidate the idea of an autocatalytic replication of PrPsc by nucleated polymerization [19, 90, 91]. In this model, PrPsc is considered to be a polymeric form of PrPc. Polymers can lengthen by addition of PrPc monomers, and they can replicate

by splitting into smaller fragments. The PrPc is mainly expressed by the cells of the central nervous system, so PrPsc concentrates in this zone. The amount of PrPsc in tissues like blood is very small and this is why it is very difficult to diagnose an infected individual.

The PMCA mimics the nucleation/polymerization mechanism occurring *in vivo* with the aim to quickly amplify polymers present in minute amount in an infected sample. It is a cyclic process, where each cycle consists in two phases:

- *phase 1 - Incubation*: Minute amount of PrPsc are incubated with a large excess of PrPc, to induce the growing of PrPsc polymers.
- *phase 2 - Sonication*: The samples are subjected to ultrasounds in order to break down the polymers, and therefore, to multiply the number of aggregates.

This technique could allow to detect PrPsc in samples of blood for instance. But for now it is not efficient enough to do so. Mathematical modeling and optimization tools can help to optimize the PMCA protocol.

Masel *et al.* [72] proposed a mathematical model for the nucleated polymerziation. We start from it and introduce a *sonication* parameter to model the PMCA. In the PMCA protocol, the monomers of PrPc are in large excess, so their quantity varies little during the experiment. We assume that this variation is small enough to be neglected and the quantity of monomers is supposed to be constant in time. Let us denote by $x_i(t)$ the density of polymers composed of $i \in \mathbb{N}$ PrPsc proteins at time t. Then the evolution of the quantity of polymers is given by the coupled system of ODEs

$$\frac{dx_i}{dt} = -r(u(t))(\tau_i x_i - \tau_{i-1} x_{i-1}) - u(t)\beta_i x_i + 2u(t) \sum_{j=i+1}^{n} \beta_j \, \kappa_{i,j} \, x_j, \quad \text{for } 1 \leqslant i \leqslant n \ . \tag{5.1}$$

The polymers of size i split into smaller aggregates with the rate β_i. This rate is modulated by the *sonication* parameter $u(t)$ which reflects the intensity of ultrasounds *sonication*. We impose the condition $\beta_1 = 0$ since a polymer composed of only one protein cannot divide. The size repartition of the formed fragments is provided by the fragmentation kernel $\kappa_{i,j}$. During the fragmentation process, the quantity of PrPsc is conserved. This conservation requires the assumption

$$\sum_{i=1}^{j-1} i \, \kappa_{ij} = \frac{j}{2}. \tag{5.2}$$

We also assume that the fragmentation of a polymer gives two smaller polymers and this leads to the assumption

$$\sum_{i=1}^{j-1} \kappa_{ij} = 1. \tag{5.3}$$

The polymers of size i have the ability to attach a monomer with the rate τ_i to produce a polymer of size $i+1$. The function $r(u)$ represents the influence of the *sonication* on the

polymerization process. It is assumed to be positive, bounded, continuous and decreasing. The maximal size n represents the longest polymer observed during the experiment. Then we can assume that the polymerization coefficient $\tau_n = 0$.

We write this problem under a matrix form

$$\begin{cases} \dot{X}(t) = M(u(t))\, X(t), \qquad t > 0, \\ \\ X(0) = X^0, \end{cases} \tag{5.4}$$

where $X(t) = (x_i(t))_{1 \leqslant i \leqslant n}^{tr}$ is the size-distribution of polymers and $M(u) := uF + r(u)G$ with G the growth matrix

$$G = \begin{pmatrix} -\tau_1 & & & & \\ \tau_1 & -\tau_2 & & & \\ & \ddots & \ddots & & \\ & & & & \\ & & \tau_{n-2} & -\tau_{n-1} & \\ & & & \tau_{n-1} & 0 \end{pmatrix}, \tag{5.5}$$

and F the fragmentation matrix

$$F = \begin{pmatrix} 0 & & & \\ & -\beta_2 & & (2\kappa_{ij}\beta_j)_{i<j} \\ & & \ddots & \\ & 0 & & \\ & & & -\beta_n \end{pmatrix}. \tag{5.6}$$

The coefficients of these matrices are assumed to be positive

$$\forall i \in [1, n-1], \qquad \tau_i > 0 \quad \text{and} \quad \beta_{i+1} > 0. \tag{5.7}$$

Then the optimization problem we are interested in is to find a control $u(t)$ which maximizes the final quantity of PrPsc $\sum_{i=1}^{n} i\, x_i(T)$ for a given final time of experiment T. Indeed the presence of PrPsc can be detected experimentally (by Western Blot, see [65] for more details) only if this quantity is greater than a critical threshold. First we define the set of admissible controls

$$\mathcal{W} := \{u(\cdot) \,:\, [0, \infty) \to [u_{min}, u_{max}] \mid u(\cdot) \text{ measurable}\},$$

where u_{max} represents the maximal power of the *sonicator* and u_{min} the absence of sonication. Then we define the payoff which corresponds to the quantity we want to optimize

$$c[u(\cdot)] := \psi(X(T)) := \sum_{i=1}^{n} i\, x_i(T), \tag{5.8}$$

where $X(\cdot)$ is the solution of (5.4) with control $u(\cdot)$ and for a given initial data X^0. Finally, the optimal control problem writes

$$\text{find } u^* \in \mathcal{W} \text{ which maximizes } c[u(\cdot)]. \tag{5.9}$$

5.2 The Eigenvalue Problem

For a constant control $u(t) \equiv u \in \mathbb{R}^+$, the Perron-Frobenius theorem ensures that $M(u)$ has a first eigenvalue $\lambda_1(u)$, which is simple, associated with a positive right eigenvector $V_1(u)$ and a positive left eigenvector $\phi_1(u)$

$$\begin{cases} M(u)V_1 = \lambda_1 V_1, \quad V_1 > 0, \\ \phi_1 M(u) = \lambda_1 \phi_1, \quad \phi_1 > 0. \end{cases} \tag{5.10}$$

We normalize these two vectors such that

$$\|V_1(u)\| = 1, \qquad \phi_1(u)V_1(u) = 1,$$

so that they are now uniquely defined. Such eigenelements also exist for the continuous growth-fragmentation equation where the size $i \in \mathbb{N}$ is replaced by the variable $x \in \mathbb{R}^+$ (see [41] for instance), and their dependency on parameters is investigated in [49].

The link between the eigenvalue problem and the optimal control problem is investigated in [18] when the function r is a constant. In this case there exists an optimal control $u^*(t)$ which is essentially equal to the best constant $u^\bullet$ of the Perron optimization problem (see chapter 5 in [49] for numerical simulations).

When r is nonlinear, the velocity set

$$\mathcal{V}(X) := \{(uF + r(u)G)X,\ u \in [u_{min}, u_{max}]\}$$

is not convex, and we cannot ensure the existence of an optimal control. Nevertheless, we can solve a so-called *optimal relaxed control problem* (see [63, section 4.2]). To explain this, we rewrite our original optimal control problem as follows: find

$$(u_1^*(t), u_2^*(t)) \in \Omega := \{(u_1, u_2) \mid u_2 = r(u_1)\}$$

which maximizes $\psi(X(T))$ with X solution to

$$\begin{cases} \dot{X}(t) = \big(u_1(t)F + u_2(t)G\big)\, X(t), \qquad t > 0, \\ \\ X(t=0) = X^0. \end{cases} \tag{5.11}$$

In this case, the relaxed control problem consists in finding $(u_1^*(t), u_2^*(t))$ in the convex hull $H(\Omega)$ of Ω (see figure 5.1), which maximizes the payoff $\psi(X(T))$. For this convexified

problem, the velocity set is given by the convex hull $H(\mathcal{V}(X))$ of $\mathcal{V}(X)$ and is thus convex. So there exists an optimal (relaxed) control and moreover the response $X^*(t)$ to this control is the uniform limit of responses to classical controls (see [63, section 4.2]). As a consequence, it is of interest to solve the optimal relaxed control problem. Based on the case where r is a const, we look at the Perron eigenvalue optimization problem on the convex hull $H(\Omega)$. We want to find the optimum $(u_1^\bullet, u_2^\bullet)$ which maximizes the principal eigenvalue $\lambda_1(u_1, u_2)$ of $M(u_1, u_2) := u_1F + u_2G$ on $H(\Omega)$, and compare the optimal control (u_1^*, u_2^*) to this optimum.

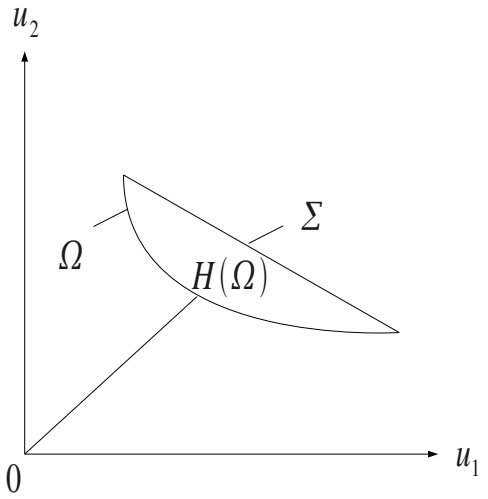


Figure 5.1. The convex hull $H(\Omega)$ of Ω in the case where r is decreasing and convex.

5.3 Pontryagin Maximum Principle

We consider the relaxed optimal control problem in Mayer form

$$\max_{U\in\mathcal{U}} \psi(X(T,U)) := \max_{U\in\mathcal{U}} \sum_{i=1}^{n} i x_i(T), \tag{5.12}$$

subject to

$$\dot{X}(t) = \big(u_1(t)F + u_2(t)G\big)X(t), \quad t \in [0,T], \tag{5.13}$$

$$X(0) = X^0, \tag{5.14}$$

with T a given final time. The state $X := (x_1, \cdots, x_n)^{tr} \in \mathbb{R}^n$. For a given set $H(\Omega) \in \mathbb{R}^2$, the family of admissible control functions is defined as

$$\mathcal{U} := \{U := (u_1, u_2) : [0,T] \to H(\Omega),\, U \,\text{measurable}\}. \tag{5.15}$$

We have the following theorem

Theorem 5.3.1. *(Pontryagin Maximum Principle) Consider the optimal control problem* (5.12)-(5.15)*, let* $U^*(\cdot) = (u_1^*(\cdot), u_2^*(\cdot))$ *be a bounded admissible control whose corresponding trajectory* $X^*(\cdot) = X(\cdot, U^*)$ *is optimal. Call* $P : [0,T] \to \mathbb{R}^n$ *the solution of the adjoint linear equation*

$$\dot{P}(t) = -P(t)(u_1^* F + u_2^* G), \quad P(T) = \nabla\psi(X^*(T)). \tag{5.16}$$

Let us define the Hamiltonian as

$$H(X, P, U) := P(u_1 F + u_2 G)X. \tag{5.17}$$

Then the maximality condition

$$H(X^*, P, U^*) = \max_{U \in \mathcal{U}} H(X^*, P, U). \tag{5.18}$$

holds for almost every time $t \in [0,T]$.

5.3.1 Modified cost function

In a special case where we modify the cost function (5.12) as

$$\max_{U \in\, \mathcal{U}} \psi(X(T,U)) := \max_{U \in\, \mathcal{U}} \phi_1 \cdot X(T). \tag{5.19}$$

Suppose that the initial condition is given by

$$X(0) = V_1. \tag{5.20}$$

At first, we look for a constant control $\bar{U} := (\bar{u}_1, \bar{u}_2) \in H(\Omega)$ and associated responses $(X(t), P(t))$ such that (5.18) holds.

We assume that $\bar{U} = (\bar{u}_1, \bar{u}_2)$ is a pair which maximizes the Perron eigenvalue λ_1, and (V_1, ϕ_1, λ_1) is solution to the Perron eigenvalue problem

$$\begin{cases} \lambda_1 V_1 = (\bar{u}_1 F + \bar{u}_2 G)V_1, \\ \lambda_1 \phi_1 = \phi_1(\bar{u}_1 F + \bar{u}_2 G), \\ \lambda_1 > 0, \quad \phi_1 V_1 = 1, \end{cases} \tag{5.21}$$

Next, we prove that $(\bar{u}_1, \bar{u}_2)$ satisfies the maximality condition (5.18), i.e.

$$H(X, P, \bar{U})) := P(\bar{u}_1 F + \bar{u}_2 G)X = \max_{(u_1,u_2)\in H(\Omega)} \Big\{ P(u_1 F + u_2 G)X \Big\}$$

We know that

$$X(t) := V_1 e^{\lambda_1 t} \tag{5.22}$$

is the unique solution to the system

$$\begin{cases} \dot{X} = (\bar{u}_1 F + \bar{u}_2 G)X, \\ X(0) = V_1, \end{cases}$$

while

$$P(t) := \phi_1 e^{\lambda_1(T-t)} \tag{5.23}$$

is the unique solution to the adjoint system

$$\begin{cases} \dot{P} = -P(\bar{u}_1 F + \bar{u}_2 G), \\ P(T) = \phi_1. \end{cases}$$

To emphasize the dependence of H on $U = (u_1, u_2)$, we denote from now on by $H(\bar{u}_1, \bar{u}_2)$ the Hamiltonian $H(X, P, \bar{U})$ in this section. From (5.22) and (5.23), we have

$$H(\bar{u}_1, \bar{u}_2) = e^{\lambda_1 T} \lambda(\bar{u}_1, \bar{u}_2).$$

For any $(u_1, u_2) \in H(\Omega)$, we have

$$\begin{aligned} H(u_1, u_2) =& P(u_1 F + u_2 G)X && (5.24)\\ =& P(\bar{u}_1 F + \bar{u}_2 G)X + P\big((u_1 - \bar{u}_1)F + (u_2 - \bar{u}_2)G\big)X && (5.25)\\ =& H(\bar{u}_1, \bar{u}_2) + P\big((u_1 - \bar{u}_1)F + (u_2 - \bar{u}_2)G\big)X. && (5.26) \end{aligned}$$

By (5.22) and (5.23), we obtain

$$\begin{aligned} H(u_1, u_2) =& H(\bar{u}_1, \bar{u}_2) + P\big((u_1 - \bar{u}_1)F + (u_2 - \bar{u}_2)G\big)X \\ =& H(\bar{u}_1, \bar{u}_2) + e^{\lambda_1 T}\phi_1\big((u_1 - \bar{u}_1)F + (u_2 - \bar{u}_2)G\big)V_1 && (5.27) \end{aligned}$$

We denote by $\lambda(u_1, u_2)$ the Perron eigenvalue with constant $(u_1, u_2) \in H(\Omega)$, i.e.

$$\begin{cases} \lambda(u_1, u_2)V = (u_1 F + u_2 G)V, \\ \lambda(u_1, u_2)\phi = \phi(u_1 F + u_2 G), \\ \lambda > 0, \quad \phi V = 1, \end{cases} \tag{5.28}$$

Testing against the adjoint eigenvector ϕ to (5.28), we have

$$\lambda(u_1, u_2) = \phi(u_1 F + u_2 G)V. \tag{5.29}$$

From (5.29), we get

$$\begin{aligned} \frac{\partial \lambda}{\partial u_1} &= \frac{\partial \phi}{\partial u_1}(u_1 F + u_2 G)V + \phi F V + \phi(u_1 F + u_2 G)\frac{\partial V}{\partial u_1} \\ &= \lambda(u_1, u_2)\frac{\partial \phi}{\partial u_1}V + \phi F V + \lambda(u_1, u_2)\phi\frac{\partial V}{\partial u_1} \\ &= \lambda(u_1, u_2)\frac{\partial(\phi V)}{\partial u_1} + \phi F V \\ &= \phi F V. \end{aligned} \tag{5.30}$$

Similarly, we can prove that

$$\frac{\partial \lambda}{\partial u_2} = \phi G V. \tag{5.31}$$

Hence, (5.27) becomes

$$H(u_1,u_2)=H(\bar{u}_1,\bar{u}_2)+e^{\lambda_1 T}\begin{pmatrix} u_1-\bar{u}_1 \\ u_2-\bar{u}_2 \end{pmatrix}\cdot\nabla\lambda(\bar{u}_1,\bar{u}_2). \tag{5.32}$$

Since $(\bar{u}_1,\bar{u}_2)$ lies on $\Omega\cup\Sigma$, using lagrangian multipliers, we get that

$$\begin{pmatrix} u_1-\bar{u}_1 \\ u_2-\bar{u}_2 \end{pmatrix}\cdot\nabla\lambda(\bar{u}_1,\bar{u}_2)\leqslant 0$$

holds for any $(u_1,u_2)\in H(\Omega)$. Hence, we have proved that $(\bar{u}_1,\bar{u}_2)$ satisfies maximality condition (5.18).

5.3.2 Original cost function

Small dimensional case - 2D case

We define Lie bracket

$$[F,G]:=GF-FG. \tag{5.33}$$

We denote $\mathcal{A}$ the Lie algebra, i.e. the smallest linear set of matrices generated by Lie brackets, a.e.

$$M\in\mathcal{A},\ N\in\mathcal{A}\Rightarrow[M,N]\in\mathcal{A}. \tag{5.34}$$

Here,

$$F=\begin{pmatrix} 0 & 2\beta_2 \\ 0 & -\beta_2 \end{pmatrix},\quad G=\begin{pmatrix} -\tau_1 & 0 \\ \tau_1 & 0 \end{pmatrix} \tag{5.35}$$

It is easy to check that for all $x\in S:=\{x:\ x_i>0\}$ with $S\subset\mathbb{R}^2$, we have

$$\{Ax;\ A\in\mathcal{A}\}:=\mathbb{R}^2. \tag{5.36}$$

By (5.16) and noting that the diagnal of matrices u_1F+u_2G are strictly negative, it is easy to prove that

$$p_i>0,\quad \forall i=1,\cdots,n,$$

For any fixed $u_1\in[u_{\min},u_{\max}]$

$$r(u_1)\leqslant u_2\leqslant\theta u_1+\zeta, \tag{5.37}$$

where

$$\theta=\frac{r(u_{max})-r(u_{min})}{u_{max}-u_{min}},\quad \zeta=\frac{u_{max}r(u_{min})-u_{min}r(u_{max})}{u_{max}-u_{min}}. \tag{5.38}$$

From (5.35), we get

$$PG=\big((p_2-p_1)\tau_1,0\big),\quad PF=\big(0,(2p_1-p_2)\beta_2\big). \tag{5.39}$$

Let us now prove that for any fixed $X\in\mathbb{R}^2_+$,

$$PGX>0. \tag{5.40}$$

We define new variables

$$Q := (q_1, q_2)^{tr} := \begin{pmatrix} p_2 - p_1 \\ 2p_1 - p_2 \end{pmatrix}.$$

From dynamics (5.16), we have

$$\begin{cases} \dot{p}_1 = u_2\tau_1(p_1 - p_2), \\ \dot{p}_2 = -u_1\beta_2(2p_1 - p_2). \end{cases} \tag{5.41}$$

By (5.41), we obtain

$$\dot{Q} = -\begin{pmatrix} -u_2\tau_1 & u_1\beta_2 \\ 2u_2\tau_1 & -u_1\beta_2 \end{pmatrix} Q.$$

Since the extra-diagonal terms are nonnegative and $q_1(T) = 1 > 0$, $q_2(T) = 0$, we conclude that $Q(t) > 0$ for all $t \in [0, T]$, i.e.

$$(2p_1 - p_2)(t) > 0 \quad \text{and} \quad (p_2 - p_1)(t) > 0, \quad \forall\, t \in [0, T], \tag{5.42}$$

which together with (5.39) gives (5.40). Hence, combining (5.17), (5.37) with (5.40), we conclude that the optimal control (u_1, u_2) will lie on Σ, i.e.

$$u_2 = \theta u_1 + \zeta, \tag{5.43}$$

with θ and ζ defined by (5.38). In this case, Hamiltonian (5.17) becomes

$$\begin{aligned} H(X, P, U) &= P\big(u_1 F + (\theta u_1 + \zeta)G\big)\, X, \\ &= u_1 P(F + \theta G)X + \zeta PGX. \end{aligned} \tag{5.44}$$

We denote

$$\Phi := P(F + \theta G)X. \tag{5.45}$$

Suppose that there exist $t_1 < t_2 \in [0, T]$ such that

$$\Phi = P(F + \theta G)X = 0, \quad t \in [t_1, t_2],$$

i. e.

$$p_1(-\theta\tau_1 x_1 + 2\beta_2 x_2) + p_2(\theta\tau_1 x_1 - \beta_2 x_2) = 0, \quad t \in [t_1, t_2]. \tag{5.46}$$

By (5.13) and (5.16), we have

$$\begin{aligned} \dot{\Phi} &= -P(u_1 F + u_2 G)FX + PF(u_1 F + u_2 G)X + \theta\big(-P(u_1 F + u_2 G)GX + PG(u_1 F + u_2 G)X\big) \\ &= (u_2 - \theta u_1)P(FG - GF)X \\ &= \zeta P(FG - GF)X. \end{aligned} \tag{5.47}$$

From (5.35), we have

$$FG - GF = \tau_1\beta_2 \begin{pmatrix} 2 & 2 \\ -1 & -2 \end{pmatrix}.$$

Hence, (5.47) becomes

$$\dot{\Phi} = \zeta\tau_1\beta_2\big(x_1(2p_1 - p_2) + 2x_2(p_1 - p_2)\big) = 0, \quad t \in [t_1, t_2]. \tag{5.48}$$

Take derivative w.r.t t again in (5.47), we get

$$\ddot{\Phi} = -\zeta\frac{d(P[F,G]X)}{dt} = -\zeta\big(u_1 P([[F,G],F])X + u_2 P([[F,G],G])X\big) = 0. \tag{5.49}$$

By (5.43), we get

$$u_1\big(P([\,[F,G],F\,])X + \theta P([\,[F,G],G\,])X\big) + \zeta P([\,[F,G],G\,])X = 0. \tag{5.50}$$

By (5.35), we get

$$[\,[F,G],F\,] = \tau_1\beta_2^2\begin{pmatrix} 2 & 6 \\ -1 & -2 \end{pmatrix}, \quad [\,[F,G],G\,] = \tau_1^2\beta_2\begin{pmatrix} 2 & 2 \\ -3 & -2 \end{pmatrix}$$

By (5.48), we get

$$P([\,[F,G],F\,])X = 4\tau_1\beta_2^2 p_1 x_2, \tag{5.51}$$

$$P([\,[F,G],G\,])X = -2\tau_1^2\beta_2 p_2 x_1. \tag{5.52}$$

Hence,

$$P([\,[F,G],F\,])X + \theta P([\,[F,G],G\,])X \neq 0.$$

Otherwise, from (5.50), we have

$$P([\,[F,G],F\,])X = 0,$$

which is a contradiction with (5.51). We get

$$\begin{aligned} u_1 &= \frac{-\zeta P([\,[F,G],G\,])X}{P([\,[F,G],F\,])X + \theta P([\,[F,G],G\,])X} \\ &= \frac{\zeta\tau_1 p_2 x_1}{2\beta_2 p_1 x_2 - \theta\tau_1 p_2 x_1}. \end{aligned} \tag{5.53}$$

Since p_1 and p_2 can not be equal to 0 at the same time. If they are both equal to 0 at some time, they will always remain equal to 0, which leads to a contradiction with (5.16). Hence, from (5.46) and (5.48), we get that the determinant has to be equal to 0, which gives

$$\theta\tau_1 x_1^2 + 2\beta_2 x_2^2 = 0. \tag{5.54}$$

Since $\theta < 0$, we get from (5.54) that

$$x_1 = \sqrt{\frac{-2\beta_2}{\theta\tau_1}}x_2. \tag{5.55}$$

By (5.55), (5.53) now becomes

$$u_1 = \frac{\zeta\tau_1 p_2}{\sqrt{-2\theta\tau_1\beta_2}p_1 - \theta\tau_1 p_2}. \tag{5.56}$$

Similarly, x_1 and x_2 can not be equal to 0 at the same time, hence, from (5.46) and (5.48), noting the determinant has to be equal to 0, we get

$$\beta_2(2p_1 - p_2)^2 = -2\theta\tau_1(p_1 - p_2)^2. \tag{5.57}$$

By (5.57) and noting (5.42), we obtain

$$2p_1 - p_2 = \sqrt{\frac{-2\theta\tau_1}{\beta_2}}(p_2 - p_1). \tag{5.58}$$

Hence,

$$\frac{p_1}{p_2} = \frac{\sqrt{\beta_2} + \sqrt{-2\theta\tau_1}}{2\sqrt{\beta_2} + \sqrt{-2\theta\tau_1}}. \tag{5.59}$$

Combining (5.53) and (5.59), we get

$$\tilde{u}_1 \triangleq \frac{\zeta\tau_1(2\sqrt{\beta_2} + \sqrt{-2\theta\tau_1})}{\sqrt{-2\theta\tau_1\beta_2^2} - 4\theta\tau_1\sqrt{\beta_2} - \theta\tau_1\sqrt{-2\theta\tau_1}} = \frac{\zeta\tau_1}{\sqrt{-2\theta\tau_1\beta_2}} \frac{2\beta_2 + \sqrt{-2\theta\tau_1\beta_2}}{\beta_2 + 2\sqrt{-2\theta\tau_1\beta_2} - \theta\tau_1}. \tag{5.60}$$

Hence, we conclude that the optimal control u_1 satisfies

$$u_1 \in \{u_{min}, u_{max}, \tilde{u}_1\}. \tag{5.61}$$

Furthermore, by (5.16), we get

$$\Phi(T) = P(T)(F + \theta G)X(T) = \theta\tau x_1(p_2 - p_1)(T) + \beta x_2(2p_1 - p_2)(T) = \theta\tau x_1(T) < 0.$$

Hence, there exists $\epsilon > 0$ such that

$$\Phi(t) < 0, \quad t \in (T - \epsilon, T].$$

By (5.18), we have

$$(u_1, u_2) = (u_{min}, r(u_{min})), \quad t \in (T - \epsilon, T].$$

Remark 5.3.1. For any given $0 \leqslant u_{min} < u_{max} \leqslant \frac{\zeta}{-\theta}$, it may happen that $\tilde{u}_1 \notin [u_{min}, u_{max}]$. In this case, the optimal control are always the saturing values, i.e.

$$u_1^* \in \{u_{min}, u_{max}\}.$$

Now we want to check that $\tilde{u}_1$ is the value which maximizes the Perron eigenvalue. Denote $\bar{u}_1$ the value such that $(\bar{u}_1, \theta\bar{u}_1 + \zeta)$ maximizes the Perron eigenvalue, we have the following proposition:

Proposition 5.3.1.

$$\tilde{u}_1 = \bar{u}_1.$$

Proof. For the sake of clarity, we denote in the proof τ_1 by τ, β_2 by β and u_1 by u. The characteristic polynomial of $uF + (\theta u + \zeta)G$ writes

$$\chi = X^2 + \big((\theta u + \zeta)\tau + u\beta\big)X - u(\theta u + \zeta)\beta\tau.$$

The discriminant is

$$\begin{aligned}\Delta &= (\theta u + \zeta)^2\tau^2 + u^2\beta^2 + 6u(\theta u + \zeta)\beta\tau \\ &= (\theta^2\tau^2 + \beta^2 + 6\theta\beta\tau)u^2 + 2\zeta\tau(\theta\tau + 3\beta)u + \zeta^2\tau^2.\end{aligned}$$

Since r is a positive function, we have $0 \leqslant u \leqslant \frac{\zeta}{-\theta}$, hence $\Delta > 0$. For the sequel, we define new relevant parameters

$$A := \theta\tau + \beta, \qquad B := \sqrt{-2\theta\beta\tau}, \qquad C := \theta\tau + 3\beta \qquad \text{and} \qquad D := \zeta\tau.$$

With these notations, the discriminant writes

$$\Delta = (A^2 - 2B^2)u^2 + 2CDu + D^2,$$

and the first eigenvalue of $uF + (\theta u + \zeta)G$ is

$$\lambda_1(u) = \frac{1}{2}\left(-Au - D + \sqrt{\Delta}\right).$$

The optimal value $\bar{u}$ satisfies $\lambda_1'(\bar{u}) = 0$, with

$$\lambda_1'(u) = \frac{1}{2}\left(\frac{\Delta'}{2\sqrt{\Delta}} - A\right).$$

To obtain $\bar{u}$, we solve the equation

$$\big(\Delta'\big)^2 = 4A^2\Delta, \tag{5.62}$$

which writes

$$-2B^2(A^2 - 2B^2)u^2 - 4B^2CDu + D^2(C^2 - A^2) = 0.$$

The discriminant of this binomial is

$$\mathfrak{D} = 8\,A^2B^2D^2(C^2 + 2B^2 - A^2) = 64\,A^2B^2D^2\beta^2,$$

and the roots are

$$u^{\pm} = \frac{D}{B}\,\frac{BC \pm 2\beta A}{2B^2 - A^2}.$$

A solution to $\lambda_1'(u) = 0$ is a solution to Equation (5.62) which satisfies $\dfrac{\Delta'}{A} > 0$. The computations give

$$\frac{\Delta'(u^-)}{A} = 4\beta\frac{D}{B} > 0 \qquad \text{and} \qquad \frac{\Delta'(u^+)}{A} = -4\beta\frac{D}{B} < 0.$$

Hence, $\lambda_1'(u) = 0$ has a unique solution given by

$$\bar{u} = u^- = \frac{D}{B}\,\frac{BC - 2\beta A}{2B^2 - A^2}.$$

Finally we compute from (5.60)

$$\begin{aligned}\tilde{u} &:= \frac{D}{B}\frac{2\beta+B}{C-2A+2B}\\ &= \frac{D}{B}\frac{(2\beta+B)(C-2A-2B)}{(C-2A)^2-4B^2}\\ &= \frac{D}{B}\frac{2\beta A-BC}{A^2-2B^2}\\ &= u^- = \bar{u}.\end{aligned}$$

This concludes the proof of Proposition 5.3.1. □

Small dimensional case - 3D case

In this case

$$F = \begin{pmatrix} 0 & 2\beta_2 & \beta_3 \\ 0 & -\beta_2 & \beta_3 \\ 0 & 0 & -\beta_3 \end{pmatrix}, \quad G = \begin{pmatrix} -\tau_1 & 0 & 0 \\ \tau_1 & -\tau_2 & 0 \\ 0 & \tau_2 & 0 \end{pmatrix} \tag{5.63}$$

Hence, we get

$$PG = \Big((p_2-p_1)\tau_1 \quad , \quad (p_3-p_2)\tau_2 \quad , \quad 0\Big),$$

and

$$PF = \Big(0 \quad , \quad (2p_1-p_2)\beta_2 \quad , \quad (p_1+p_2-p_3)\beta_3\Big).$$

We define

$$Q := (q_1,q_2,q_3)^{\mathrm{tr}} := \begin{pmatrix} p_1 \\ p_2-p_1 \\ p_3-p_2 \end{pmatrix}.$$

By (5.16), we obtain

$$\begin{cases} \dot{p}_1 = -\tau_1 u_2 (p_2-p_1), \\ \dot{p}_2 = -\beta_2 u_1 (2p_1-p_2) - \tau_2 u_2 (p_3-p_2), \\ \dot{p}_3 = -\beta_3 u_1 (p_1+p_2-p_3). \end{cases} \tag{5.64}$$

Hence, we obtain

$$\dot{Q} = -\begin{pmatrix} 0 & \tau_1 u_2 & 0 \\ \beta_2 u_1 & -\tau_1 u_2 - \beta_2 u_1 & \tau_2 u_2 \\ (\beta_3-\beta_2)u_1 & \beta_2 u_1 & -\tau_2 u_2 - \beta_3 u_1 \end{pmatrix} Q.$$

Noticing that $\beta_3 > \beta_2$, the extra-diagonal terms are nonnegative. From (5.16), we get $q_1(T) > 0$, $q_2(T) > 0$ and $q_3(T) > 0$. Thus, we conclude that $Q(t) > 0$ for all $t \in [0,T]$, i.e.

$$(p_3-p_2)(t) > 0 \quad \text{and} \quad (p_2-p_1)(t) > 0, \quad \forall\, t \in [0,T]. \tag{5.65}$$

Hence, for any $X > 0$, we have

$$PGX > 0. \tag{5.66}$$

Noting (5.17), we conclude that the optimal control will lie on Σ.

Bibliography

[1] M. Adimy and L. Pujo-Menjouet. Asymptotic behaviour of a singular transport equation modelling cell division. *Dis. Cont. Dyn. Sys. Ser. B*, 3(3):439–456, 2003.

[2] Fabio Ancona and Andrea Marson. On the attainable set for scalar nonlinear conservation laws with boundary control. *SIAM J. Control Optim.*, 36(1):290–312 (electronic), 1998.

[3] Fabio Ancona and Andrea Marson. Asymptotic stabilization of systems of conservation laws by controls acting at a single boundary point. In *Control methods in PDE-dynamical systems*, volume 426 of *Contemp. Math.*, pages 1–43. Amer. Math. Soc., Providence, RI, 2007.

[4] D. Armbruster, P. Degond, and C. Ringhofer. A model for the dynamics of large queuing networks and supply chains. *SIAM J. Appl. Math.*, 66(3):896–920 (electronic), 2006.

[5] D. Armbruster, D. Marthaler, C. Ringhofer, K. Kempf, and T.-C. Jo. A continuum model for a re-entrant factory. *Oper. Res.*, 54(3):933–950, 2006.

[6] A. V. Arutyunov. Perturbations of extremal problems with constraints, and necessary conditions for optimality. In *Mathematical analysis, Vol. 27 (Russian)*, Itogi Nauki i Tekhniki, pages 147–235, 237. Akad. Nauk SSSR Vsesoyuz. Inst. Nauchn. i Tekhn. Inform., Moscow, 1989. Translated in J. Soviet Math. **5**4 (1991), no. 6, 1342–1400.

[7] Aram V. Arutyunov. On necessary optimality conditions in a problem with phase constraints. *Sov. Math., Dokl*, 31(174–177), 1985.

[8] S. M. Aseev. Methods of regularization in nonsmooth problems of dynamic optimization. *J. Math. Sci. (New York)*, 94(3):1366–1393, 1999. Dynamical systems, 6.

[9] B. Basse, B.C. Baguley, E.S. Marshall, W.R. Joseph, B. van Brunt, G. Wake, and D. J. N. Wall. A mathematical model for analysis of the cell cycle in cell lines derived from human tumors. *J. Math. Biol.*, 47(4):295–312, 2003.

[10] F. Bekkal Brikci, J. Clairambault, and B. Perthame. Analysis of a molecular structured population model with possible polynomial growth for the cell division cycle. *Math. Comput. Modelling*, 47(7-8):699–713, 2008.

[11] F. Bekkal Brikci, J. Clairambault, B. Ribba, and B. Perthame. An age-and-cyclin-structured cell population model for healthy and tumoral tissues. *J. Math. Biol.*, 57(1):91–110, 2008.

[12] Bachir Ben Moussa and Anders Szepessy. Scalar conservation laws with boundary conditions and rough data measure solutions. *Methods Appl. Anal.*, 9(4):579–598, 2002.

[13] Stefano Bianchini and Alberto Bressan. Vanishing viscosity solutions of nonlinear hyperbolic systems. *Ann. of Math. (2)*, 161(1):223–342, 2005.

[14] Alberto Bressan. *Hyperbolic systems of conservation laws*, volume 20 of *Oxford Lecture Series in Mathematics and its Applications*. Oxford University Press, Oxford, 2000. The one-dimensional Cauchy problem.

[15] Alberto Bressan and Giuseppe Maria Coclite. On the boundary control of systems of conservation laws. *SIAM J. Control Optim.*, 41(2):607–622, 2002.

[16] Alberto Bressan and Benedetto Piccoli. *Introduction to the mathematical theory of control*, volume 2 of *AIMS Series on Applied Mathematics*. American Institute of Mathematical Sciences (AIMS), Springfield, MO, 2007.

[17] Haim Brezis. *Functional analysis, Sobolev spaces and partial differential equations*. Universitext. Springer, New York, 2011.

[18] Vincent Calvez and Pierre Gabriel. Optimal growth for linear processes with affine control. preprint, arXiv:1203.5189.

[19] J. Castilla, P. Saá, C. Hetz, and C. Soto. In vitro generation of infectious scrapie prions. *Cell*, 121(2):195–206, 2005.

[20] Frédérique Clément. *Modélisation de la cinétique cellulaire au sein de la granulosa des follicules ovariens au cours de leur développement terminal*. PhD thesis, Paris 7, 1997.

[21] Frédérique Clément. Optimal control of the cell dynamics in the granulosa of ovulatory follicles. *Math. Biosci*, 6(123–142), 1998.

[22] Frédérique Clément. Multiscale modelling of endocrine systems: new insight on the gonadotrope axis. In *CANUM 2008*, volume 27 of *ESAIM Proc.*, pages 209–226. EDP Sci., Les Ulis, 2009.

[23] Frédérique Clément, Jean-Michel Coron, and Peipei Shang. Optimal control of cell mass and maturity in a model of follicular ovulation. arXiv:1202.1940, 2012.

[24] Frédérique Clément, M-A Gruet, P Monget, M Terqui, E Jolivet, and Danielle Monniaux. Growth kinetics of the granulosa cell population in ovarian follicles: an approach by mathematical modelling. *Cell Prolif.*, 30:255–270, 1997.

[25] G. M. Coclite, M. Garavello, and B. Piccoli. Traffic flow on a road network. *SIAM J. Math. Anal.*, 36(6):1862–1886 (electronic), 2005.

[26] R. M. Colombo, M. Herty, and M. Mercier. Control of the continuity equation with a non local flow. *ESAIM: COCV*, 17(353–479), 2011.

[27] Rinaldo M. Colombo, Michael Herty, and Magali Mercier. Control of the continuity equation with a non local flow. *ESAIM Control Optim. Calc. Var.*, 17(2):353–379, 2011.

[28] Rinaldo M. Colombo and Massimiliano D. Rosini. Existence of nonclassical solutions in a pedestrian flow model. *Nonlinear Anal. Real World Appl.*, 10(5):2716–2728, 2009.

[29] P. Constantin, P. D. Lax, and A. Majda. A simple one-dimensional model for the three-dimensional vorticity equation. *Comm. Pure Appl. Math.*, 38(6):715–724, 1985.

[30] Jean-Michel Coron. Local controllability of a 1-D tank containing a fluid modeled by the shallow water equations. *ESAIM Control Optim. Calc. Var.*, 8:513–554 (electronic), 2002. A tribute to J. L. Lions.

[31] Jean-Michel Coron. *Control and nonlinearity*, volume 136 of *Mathematical Surveys and Monographs*. American Mathematical Society, Providence, RI, 2007.

[32] Jean-Michel Coron, Brigitte d'Andréa Novel, and Georges Bastin. A strict Lyapunov function for boundary control of hyperbolic systems of conservation laws. *IEEE Trans. Automat. Control*, 52(1):2–11, 2007.

[33] Jean-Michel Coron, Oliver Glass, and Zhiqiang Wang. Exact boundary controllability for 1-D quasilinear hyperbolic systems with a vanishing characteristic speed. *SIAM J. Control Optim.*, 48(5):3105–3122, 2009/10.

[34] Jean-Michel Coron and Sergio Guerrero. Null controllability of the N-dimensional Stokes system with $N-1$ scalar controls. *J. Differential Equations*, 246(7):2908–2921, 2009.

[35] Jean-Michel Coron, Matthias Kawski, and Zhiqiang Wang. Analysis of a conservation law modeling a highly re-entrant manufacturing system. *Discrete Contin. Dyn. Syst. Ser. B*, 14(4):1337–1359, 2010.

[36] Jean-Michel Coron and Zhiqiang Wang. Controllability for a scalar conservation law with nonlocal velocity. *J. Differential Equations*, 252(2):181–201, 2012.

[37] V. Coscia and C. Canavesio. First-order macroscopic modelling of human crowd dynamics. *Math. Models Methods Appl. Sci.*, 18(suppl.):1217–1247, 2008.

[38] Hongjie Dong. Well-posedness for a transport equation with nonlocal velocity. *J. Funct. Anal.*, 255(11):3070–3097, 2008.

[39] V. Dos Santos, G. Bastin, J.-M. Coron, and B. d'Andréa Novel. Boundary control with integral action for hyperbolic systems of conservation laws: stability and experiments. *Automatica J. IFAC*, 44(5):1310–1318, 2008.

[40] M. Doumic. Analysis of a population model structured by the cells molecular content. *Math. Model. Nat. Phenom.*, 2(3):121–152, 2007.

[41] M. Doumic Jauffret and P. Gabriel. Eigenelements of a general aggregation-fragmentation model. *Math. Models Methods Appl. Sci.*, 20(5):757–783, 2010.

[42] Marie Doumic Jauffret and Pierre Gabriel. Eigenelements of a general aggregation-fragmentation model. *Math. Modles. Methods Appl.*, 20(5):757–783, 2010.

[43] Nki Echenim. *Modélisation et contrôle multi-échelles du processus de sélection des follicules ovulatoires.* PhD thesis, Paris 11, 2006.

[44] Nki Echenim, Frédérique Clément, and Michel Sorine. Multiscale modeling of follicular ovulation as a reachability problem. *Multiscale Model. Simul.*, 6(3):895–912, 2007.

[45] Nki Echenim, Danielle Monniaux, Michel Sorine, and Frédérique Clément. Multi-scale modeling of the follicle selection process in the ovary. *Math. Biosci.*, 198(1):57–79, 2005.

[46] Caroline Fabre, Jean-Pierre Puel, and Enrike Zuazua. Approximate controllability of the semilinear heat equation. *Proc. Roy. Soc. Edinburgh Sect. A*, 125(1):31–61, 1995.

[47] Thomas I. Seidman Falk M. Hante, Günter Leugering. Modeling and analysis of modal switching in networked transport systems. *Appl Math Optim.*

[48] Joszef Z. Farkas. Stability conditions for a nonlinear size-structured model. *Nonlin. Anal. Real World Appl.*, 6:962–969, 2005.

[49] Pierre Gabriel. *Équations de transport-fragmentation et applications aux maladies à prions [Transport-fragmentation equations and applications to prion diseases].* PhD thesis, Paris, 2011.

[50] Olivier Glass. On the controllability of the 1-D isentropic Euler equation. *J. Eur. Math. Soc. (JEMS)*, 9(3):427–486, 2007.

[51] Martin Gugat. Boundary controllability between sub- and supercritical flow. *SIAM J. Control Optim.*, 42(3):1056–1070, 2003.

[52] Martin Gugat. Optimal switching boundary control of a string to rest in finite time. *Z. Angew. Math. Mech.*, 88(4):283–305, 2008.

[53] Martin Gugat, Michael Herty, Axel Klar, and Günter Leugering. Optimal control for traffic flow networks. *J. Optim. Theory Appl.*, 126(3):589–616, 2005.

[54] Martin Gugat, Michael Herty, and Veronika Schleper. Flow control in gas networks: exact controllability to a given demand. *Math. Methods Appl. Sci.*, 34(7):745–757, 2011.

[55] Martin Gugat and Günter Leugering. Global boundary controllability of the de St. Venant equations between steady states. *Ann. Inst. H. Poincaré Anal. Non Linéaire*, 20(1):1–11, 2003.

[56] Martin Gugat and Günter Leugering. Global boundary controllability of the Saint-Venant system for sloped canals with friction. *Ann. Inst. H. Poincaré Anal. Non Linéaire*, 26(1):257–270, 2009.

[57] M. Gyllenberg and Glenn F. Webb. A nonlinear structured population model of tumor growth with quiescence. *J. Math. Biol*, 28:671–694, 1990.

[58] M. Herty, A. Klar, and B. Piccoli. Existence of solutions for supply chain models based on partial differential equations. *SIAM J. Math. Anal.*, 39(1):160–173, 2007.

[59] T. Horsin. On the controllability of the Burgers equation. *ESAIM Control Optim. Calc. Var.*, 3:83–95 (electronic), 1998.

[60] Alexander D. Ioffe and Vladimir M. Tikhomirov. *Theory of extremal problems*, volume 6 of *Studies in Mathematics and its Applications*. North-Holland Publishing Co., Amsterdam, 1979. Translated from the Russian by Karol Makowski.

[61] S. N. Kružkov. First order quasilinear equations in several independent variables. *Sb. Math*, 10(217–243), 1970.

[62] Michael La Marca, Dieter Armbruster, Michael Herty, and Christian Ringhofer. Control of continuum models of production systems. *IEEE Trans. Automat. Control*, 55(11):2511–2526, 2010.

[63] Ernest Bruce Lee and Lawrence Markus. *Foundations of optimal control theory*. Robert E. Krieger Publishing Co. Inc., Melbourne, FL, second edition, 1986.

[64] Philippe G. LeFloch. *Hyperbolic systems of conservation laws*. Lectures in Mathematics ETH Zürich. Birkhäuser Verlag, Basel, 2002. The theory of classical and nonclassical shock waves.

[65] N. Lenuzza. *Modélisation de la réplication des Prions: implication de la dépendance en taille des agrégats de PrP et de l'hétérogénéité des populations cellulaires*. PhD thesis, Paris, 2009.

[66] Tatsien Li. *Global classical solutions for quasilinear hyperbolic systems*. Research in Applied Mathematics **32**, John Wiley & Sons, Chichester, 1994.

[67] Tatsien Li. *Controllability and observability for quasilinear hyperbolic systems*, volume 3 of *AIMS Series on Applied Mathematics*. American Institute of Mathematical Sciences (AIMS), Springfield, MO, 2010.

[68] Tatsien Li and Bopeng Rao. Exact boundary controllability for quasi-linear hyperbolic systems. *SIAM J. Control Optim.*, 41(6):1748–1755 (electronic), 2003.

[69] Tatsien Li, Bopeng Rao, and Zhiqiang Wang. Exact boundary controllability and observability for first order quasilinear hyperbolic systems with a kind of nonlocal boundary conditions. *Discrete Contin. Dyn. Syst.*, 28(1):243–257, 2010.

[70] Tatsien Li and Wenci Yu. *Boundary value problems for quasilinear hyperbolic systems*. Duke University Mathematics Series, V. Duke University Mathematics Department, Durham, NC, 1985.

[71] Taiping Liu and Tong Yang. Well-posedness theory for hyperbolic conservation laws. *Comm. Pure Appl. Math.*, 52(12):1553–1586, 1999.

[72] J. Masel, V.A.A. Jansen, and M.A. Nowak. Quantifying the kinetic parameters of prion replication. *Biophysical Chemistry*, 77(2-3):139 – 152, 1999.

[73] Elizabeth A. McGee and Aaron J. Hsueh. Initial and cyclic recruitment of ovarian follicles. *Endocr. Rev*, 21(200–214), 2009.

[74] J. A. J. Metz and O. Diekmann, editors. *The dynamics of physiologically structured populations*, volume 68 of *Lecture Notes in Biomathematics*. Springer-Verlag, Berlin, 1986. Papers from the colloquium held in Amsterdam, 1983.

[75] Philippe Michel. Multiscale modeling of follicular ovulation as a mass and maturity dynamical system. *Multiscale Model. Simul.*, 9(1):282–313, 2011.

[76] Boris S. Mordukhovich and Jean-Pierre Raymond. Optimal boundary control of hyperbolic equations with pointwise state constraints. *Nonlinear Anal.*, 63(5-7):823–830, 2005.

[77] B. Perthame and T.M. Touaoula. Analysis of a cell system with finite divisions. *Boletín SEMA*, (44):55–79, 2008.

[78] C. Pisselet, F. Clément, and D. Monniaux. Fraction of proliferating cells in granulosa during terminal development in high and low prolific sheep breeds. *Reprod. Nutr. Dev.*, 40:295–304, 2000.

[79] Lev S. Pontryagin, Vladimir G. Boltyanskii, Revaz V. Gamkrelidze, and Evgenii Frolovich Mishchenko. *The mathematical theory of optimal processes*. Translated from the Russian by K. N. Trirogoff; edited by L. W. Neustadt. Interscience Publishers John Wiley & Sons, Inc. New York-London, 1962.

[80] A. Poretta and J. Vovelle. l^1 solutions to first order hyperbolic equations in bounded domains. *Commun. Part Diff Eq*, 28(381–408), 2003.

[81] B. N. Pshenichnyi. *Necessary Conditions for an Extremum*. "Nauka", Moscow, 1982.

[82] B. N. Pshenichnyi and S. Ochilov. On the problem of the optimal passage through a given domain. *Kibernet. i Vychisl. Tekhn.*, (99):3–8, 1993.

[83] B. N. Pshenichnyi and S. Ochilov. On a special time-optimality problem. *Kibernet. i Vychisl. Tekhn.*, (101):11–15, 1994.

[84] David L. Russell. Controllability and stabilizability theory for linear partial differential equations: recent progress and open questions. *SIAM Rev.*, 20(4):639–739, 1978.

[85] Peipei Shang. Cauchy problem for multiscale conservation laws: application to structured cell populations, arXiv:1010.2132, 2011.

[86] Peipei Shang and Zhiqiang Wang. Analysis and control of a scalar conservation law modeling a highly re-entrant manufacturing system. *J. Differential Equations*, 250(2):949–982, 2011.

[87] Alexey I. Smirnov. Necessary optimality conditions for a class of optimal control problems with a discontinuous integrand. *Tr. Mat. Inst. Steklova*, 262(Optim. Upr.):222–239, 2008.

[88] Findlay J. Tsonis C., Carson R. Relationships between aromatase activity, follicular fluid oestradiol 17β and testosterone concentrations, and diameter and atresia of individual ovarian follicles. *J. Reprod. Fertil.*, 72(1):153–163, 1984.

[89] Zhiqiang Wang. Exact controllability for nonautonomous first order quasilinear hyperbolic systems. *Chinese Ann. Math. Ser. B*, 27(6):643–656, 2006.

[90] Petra Weber, Armin Giese, Niklas Piening, Gerda Mitteregger, Achim Thomzig, Michael Beekes, and Hans A. Kretzschmar. Cell-free formation of misfolded prion protein with authentic prion infectivity. *Proc. Natl. Acad. Sci. USA*, 103(43):15818–15823, 2006.

[91] Petra Weber, Armin Giese, Niklas Piening, Gerda Mitteregger, Achim Thomzig, Michael Beekes, and Hans A. Kretzschmar. Generation of genuine prion infectivity by serial pmca. *Veterinary Microbiology*, 123(4):346 – 357, 2007.

[92] J. P. Zhang. A nonlinear nonlocal multi-dimensional conservation law. *J. Math. Anal. Appl*, 204(353–388), 1996.

[93] Kevin Zumbrun. On a nonlocal dispersive equation modeling particle suspensions. *Quart. Appl. Math.*, 57(3):573–600, 1999.

Résumé

Dans cette thèse, on a surtout étudié le caractère bien posé pour des équations aux dérivées partielles et des problèmes de contrôle optimal. On a étudié les problèmes de Cauchy associés à des lois de conservation hyperboliques avec des vitesses non-locales, pour un modèle 1D (système de fabrication industrielle), puis 2D (processus de sélection folliculaire). Dans les deux cas, on montre l'existence et l'unicité de solutions des problèmes de Cauchy, en utilisant le théorème du point fixe de Banach. On a étudié par la suite des problèmes de contrôle optimal, d'abord sur le modèle 2D, puis sur un modèle basé sur des équations differentielles ordinaires (amplification de protéines mal repliées). Dans le premier modèle, on montre que les contrôles optimaux sont bang-bang avec un seul instant de commutation. Dans le seconde modèle, les contrôles optimaux sont relaxés, nous déterminons leur positionnement dans l'espace des contrôles admissibles.

Mots-clés: lois de conservation, vitesses non-locales, biomathématiques, multi-échelle, contrôle optimal, le principe de maximum de Pontryagin.

Abstract

In this thesis, the well-posedness of partial differential equations and optimal control problems are studied. The Cauchy problems associated with hyperbolic conservation laws with nonlocal velocities are studied first for a 1D model (manufacturing system) and then for a 2D model (process of follicular selection). In both cases, the existence and uniqueness of the solutions to the Cauchy problems are proved by Banach fixed point theorem. Optimal control problems on the 2D model and on an ODE - based model (amplification of misfolded proteins) are then studied. In the first model, optimal controls are shown to be bang-bang with one single switching time. In the second model, the optimal controls are relaxed controls which are localized on the admissible domain.

Keywords: conservation laws, nonlocal velocities, biomathematics, multiscale model, optimal control, Pontryagin maximum principle.